Immunogenicity and protective efficacy of a new generation of bacterial whole-cell vaccines auxotrophic for D-glutamate

Maria Clara Póvoa Cabral

Doctoral Thesis

2015

Director: Germán Bou Arévalo, PhD

Advisor: Isaac Fuentes Boquete, PhD

Programa Oficial de Doctorado en Ciencias de la Salud

UNIVERSIDADE DA CORUÑA

El director de esta tesis doctoral, D. Germán Bou Arévalo, Doctor en Ciencias Biológicas, Jefe del Servicio de Microbiología del Complejo Hospitalario Universitario A Coruña (CHUAC), Director del área de Microbiología del Instituto de Investigación Biomédica de A Coruña (INIBIC) y Profesor Asociado de Microbiología de la Universidad de Santiago de Compostela (USC),

CERTIFICA:

Que Doña Maria Clara Póvoa Cabral, Licenciada en *Biologia Celular e Molecular* por la *Faculdade de Ciências e Tecnologia* de la *Universidade Nova de Lisboa* (FCT – UNL), Portugal, ha realizado en el Servicio de Microbiología y en el Instituto de Investigación Biomédica (INIBIC) del Complejo Hospitalario Universitario A Coruña, bajo su dirección y tutela el trabajo **"*Immunogenicity and protective efficacy of a new generation of bacterial whole-cell vaccines auxotrophic for D-glutamate*"**, el cual reúne todas las condiciones para ser presentado como Tesis Doctoral.

Y para que así conste, y surta los efectos oportunos, firmo el presente certificado en A Coruña, 21 de Septiembre de 2015.

Dr. Germán Bou Arévalo

Director

D. Isaac Fuentes Boquete, profesor del Departamento de Medicina de la Facultad de Ciencias de la Salud, en la Universidad de A Coruña,

CERTIFICA:

Que Doña Maria Clara Póvoa Cabral, Licenciada en *Biologia Celular e Molecular* por la *Faculdade de Ciências e Tecnologia* de la *Universidade Nova de Lisboa* (FCT – UNL), Portugal, ha realizado en el Servicio de Microbiología y en el Instituto de Investigación Biomédica (INIBIC) del Complejo Hospitalario Universitario A Coruña, bajo su tutela el trabajo **"*Immunogenicity and protective efficacy of a new generation of bacterial whole-cell vaccines auxotrophic for D-glutamate*"**, el cual reúne todas las condiciones para ser presentado como Tesis Doctoral.

Y para que así conste, y surta los efectos oportunos, firmo el presente certificado en A Coruña, 21 de Septiembre de 2015.

Dr. Isaac Fuentes Boquete

Tutor

inibic
instituto de
investigación biomédica
de a coruña

UNIVERSIDADE DA CORUÑA

Yo, Doña Maria Clara Póvoa Cabral, Licenciada en *Biologia Celular e Molecular* por la *Faculdade de Ciências e Tecnologia* de la *Universidade Nova de Lisboa* (FCT – UNL), Portugal,

DECLARO:

Haber realizado en el Servicio de Microbiología y en el Instituto de Investigación Biomédica (INIBIC) del Complejo Hospitalario Universitario A Coruña, la Tesis Doctoral titulada: **"*Immunogenicity and protective efficacy of a new generation of bacterial whole-cell vaccines auxotrophic for D-glutamate*".**

Y para que así conste para su depósito, y surta los efectos oportunos, firmo el presente documento en A Coruña, 21 de Septiembre de 2015.

Maria Clara Póvoa Cabral

Doctorando

Ao meu querido avô João

Agradecimientos

En primer lugar, agradecer a mi director de tesis, Germán Bou Arévalo, la oportunidad que me ha dado de iniciarme en la carrera de investigador científico, por motivarme y por exigir siempre lo mejor de mí a lo largo de estos años.

Especial reconocimiento merece también Nelson Soares, por aportarme muchos de los conocimientos en las herramientas de laboratorio que me servirían más adelante para desarrollar esta tesis. También a mi tutor, Isaac, por su ayuda en los trámites universitarios.

Agradecer a la *Fundação para a Ciência e a Tecnologia*, del *Ministério da Educação e Ciência*, Portugal, por la beca de doctorado y la financiación concedidas durante la práctica totalidad de mi tesis.

Quisiera hacer extensiva mi gratitud al SERGAS, a la Fundación Profesor Novoa Santos y al Centro Tecnológico de Formación de la Xerencia de Xestión Integrada A Coruña, especialmente a Patricia Rey, Graciela Fernández, Alberto Centeno y a todo el personal del animalario, por facilitar todos los recursos humanos y soporte logístico al osado proyecto de las vacunas.

A Susana Torrente e Gustavo Fúster, por ayudarme a "navegar" en el mundo de las patentes y de la propiedad intelectual.

A todo el personal del Servicio de Microbiología del CHUAC y del INIBIC, especialmente a Begoña Fernández, por su colaboración en el suministro de cepas.

A todos mis compañeros de laboratorio, antiguos y recientes, Álex, Patricia G., Patricia R., Zé, Maricuchi, Astrid, Carlos, Mariqui, Mirian, Carmen, Anita, Raquel, Silvia, Jesús, Marta, Juan V., Juan C., Lucía, Laura A., Laura F., José A, José P., Marga, Susi, Soraya, Meri, Eva y María L. Compañeros de aprendizaje, de viaje, de pádel y de muchas aventuras.

Mención especial a Patricia García por ser incansable y enseñarme a proseguir. Y por nunca quitarse la bata.

A todos los amigos de la pandilla de Porriño, especialmente a los "Cucas" Vanessa, Xela, Domingo, Tomás, Emma y Jesús por esos fines de semana de conciertos, festivales, excursiones, outlets, rastrexos y mil cañas, que me ayudaron a desconectar del trabajo y a llegar agotada los lunes a Coruña.

A todos los miembros del clan Patiño, especialmente a Teresita, por sus dosis semanales de cariño, croquetas y ensaladilla.

A Iván, por su buena disposición, infinita paciencia y dedicación. Y por estar siempre a mi lado.

Finalmente, a toda mi familia, especialmente a mi madre, mi padre y mis dos hermanos, a los cuales debo todo lo que soy.

Index

Resumo

A multirresistencia bacteriana é unha ameaza para a humanidade debido á falta de opcións terapéuticas; o desenvolvemento de vacinas para prever as enfermidades bacterianas é unha prioridade na saúde pública e veterinaria.

As vacinas vivas son eficientes, inducindo respostas inmunes de tipo humoral e celular. Con todo, só unhas poucas están licenciadas debido a inexistencia de mecanismos universais de atenuación da virulencia.

A síntese de D-glutamato é un mecanismo conservado nas bacterias e é esencial para a formación do peptidoglicano.

Aquí se describe unha plataforma tecnolóxica para a produción de vacinas bacterianas vivas auxótrofas para D-glutamato, o cal foi aplicado con éxito contra os patóxenos multirresistentes *Acinetobacter baumannii*, *Pseudomonas aeruginosa* e *Staphylococcus aureus*.

Cando foron administradas *in vivo*, as cepas das vacinas presentaron atenuación da virulencia e un crecemento auto-limitado, sen causar enfermidade. Ademais, desencadearon a produción de anticorpos específicos e con reactividades cruzadas e a liberación de citocinas.

Estas vacinas demostraron unha eficacia protectora nos ratos de 80-100% contra clons multirresistentes, virulentos e de alto risco, como *A. baumannii* AbH12O-A2, Ab307-0294, *P. aeruginosa* PA14 y *S. aureus* USA300LAC.

Esta estratexia innovadora pode resolver os problemas de atenuación da virulencia bacteriana, representando unha nova xeración de vacinas eficaces e seguras.

Resumen

La multirresistencia bacteriana constituye una amenaza para la humanidad debido a la falta de opciones terapéuticas; el desarrollo de vacunas para prevenir las enfermedades bacterianas es una prioridad en salud pública y veterinaria.

Las vacunas vivas son eficientes, induciendo una respuesta inmunitaria humoral y celular. Sin embargo, pocas están licenciadas debido a la inexistencia de mecanismos universales de atenuación de la virulencia.

La síntesis de D-glutamato es un mecanismo conservado en las bacterias y esencial para la formación del peptidoglicano.

Aquí se describe una plataforma tecnológica para la obtención de vacunas bacterianas vivas auxótrofas para D-glutamato, que se aplicó con éxito contra los patógenos multirresistentes *Acinetobacter baumannii*, *Pseudomonas aeruginosa* y *Staphylococcus aureus*.

Cuando administradas *in vivo*, las cepas vacunales mostraron atenuación de la virulencia y un crecimiento autolimitado, sin causar enfermedad. Además, desencadenaron la producción de anticuerpos con reactividades específicas y cruzadas y la liberación de citoquinas.

Estas vacunas demostraron una eficacia protectora en ratones de 80-100% frente a clones multirresistentes, virulentos y de alto riesgo, como *A. baumannii* AbH12O-A2, Ab307-0294, *P. aeruginosa* PA14 y *S. aureus* USA300LAC.

Esta estrategia innovadora puede solucionar las dificultades de atenuación de la virulencia bacteriana, representando una nueva generación de vacunas eficaces y seguras.

Abstract

Multidrug resistance in bacteria is a major threat to humanity due to the lack of therapeutic options; thus, vaccine development is a priority for global human and animal health.

Bacterial live vaccines induce antibody- and cell-mediated immunity and result in efficient immunizations, however, only few are licensed and there is no universal strategy for attenuation.

D-glutamate synthesis is a universal key step in bacterial cell wall formation.

Here we present a strategic platform for generating effective bacterial whole-cell vaccines auxotrophic for D-glutamate. This strategy was successfully applied to generate three independent vaccines against the major multidrug-resistant pathogens, *Acinetobacter baumannii*, *Pseudomonas aeruginosa* and *Staphylococcus aureus*.

These vaccine strains showed virulence attenuation and self-limited growth *in vivo* without risk of disease. Immunization with these whole-cell vaccines elicited high levels of specific and cross-reactive antibodies and stimulated cytokine secretion. Furthermore, immune responses correlated with 80-100% mice protection against the genetically unrelated, multidrug-resistant, virulent and high-risk clones *A. baumannii* AbH12O-A2, Ab307-0294, *P. aeruginosa* PA14, and *S. aureus* USA300LAC using an acute lethal infection model.

This innovative approach overcomes the classical difficulties so far encountered in obtaining virulence attenuation and represents a new generation of effective, safe and universal bacterial vaccines for the future.

Preface

D-glutamate (D-Glu) is an essential component of the bacterial cell wall. Glutamate racemase (MurI), enzyme that converts L-glutamate (L-Glu) to D-Glu is present in all species of bacteria and its essential role in peptidoglycan biosynthesis has been confirmed in species spanning the bacterial kingdom, including Gram-positive bacteria that encode the D-amino acid transaminases (Dat) for D-Glu production.

Here it is described a novel platform for the generation of effective live attenuated bacterial vaccines composed of D-Glu auxotrophic strains, which can be obtained through the inactivation of the gene (or genes) encoding MurI and also the gene (or genes) coding for Dat, capable of catalysing the interconversion of D-alanine (D-Ala) to D-Glu.

Hence, we took advantage of this technology to create three prototypes of experimental vaccines against *Acinetobacter baumannii*, *Pseudomonas aeruginosa* and *Staphylococcus aureus*, composed of D-Glu auxotrophic strains. Once obtained, we demonstrated their reliable efficacy as live vaccines in a mouse model of acute lethal infection. More importantly, this strategy has potential application to any bacterial pathogen, overcoming the classical difficulties in obtaining virulence attenuation and represents a new generation of effective bacterial vaccines for the future.

In this Doctoral Thesis, the following objectives were established:

- Obtain MurI$^-$ mutants of *A. baumannii* and *P. aeruginosa*, auxotrophic for D-Glu;
- Obtain a MurI$^-$Dat$^-$ mutant of *S. aureus,* auxotrophic for D-Glu;
- Characterize MurI$^-$ or MurI$^-$Dat$^-$ mutants of *A. baumannii*, *P. aeruginosa* and *S. aureus* at the phenotypic and ultrastructural level;
- Optimize and implement models of acute lethal infection for testing wild-type *A. baumannii*, *P. aeruginosa* and *S. aureus* strains, in BALB/c and C57BL/6 mice;
- Estimate the level of attenuation of MurI$^-$ or MurI$^-$Dat$^-$ mutants using the previously optimized model of acute lethal infection;

- Determine the immunogenic potential of MurI^{-} or MurI^{-}Dat^{-} mutants used as vaccines, by measuring IgM and IgG immunoglobulins and exploring the nature of T cell responses generated in the vaccinated individuals;

- Examine the cross-reactivity of IgG antibodies produced against heterologous strains not included in the vaccine compositions;

- Determine anti-*A. baumannii*, -*P. aeruginosa* and -*S. aureus* vaccine efficacy against acute lethal infection by challenging vaccinated mice with several genetically and epidemiologically unrelated bacterial isolates, including multidrug-resistant, virulent and high-risk clones such as *S. aureus* USA300LAC;

- Evaluate the protection conferred by the passive transfer of antibodies to naïve mice, obtained from mice administered these vaccines;

- Exploit alternative routes of vaccine administration;

- Assess *in vivo* safety of D-Glu auxotrophic bacterial vaccines through monitoring blood clearance of MurI^{-} or MurI^{-}Dat^{-} mutants once administered to mice;

- Assess environmental safety of D-Glu auxotrophic bacterial vaccines through evaluation of phenotypic stability and persistence of MurI^{-} or MurI^{-}Dat^{-} mutants, when compared to their wild-type homologues.

INDEX OF FIGURES

INDEX OF TABLES

ACRONYMS

Ala: Alanine
APC: antigen-presenting cell
Asp: Aspartate
Ata: Trimeric autotransporter protein
ATCC: American Type Culture Collection
BAP: Biofilm-associated protein
Bbp: Bone-binding protein
BCG: Bacille Calmette-Guérin
BCR: B cell receptor
BP: *Bordetella pertussis*
bp: Base pairs
CD: Cluster of differentiation
CECT: Spanish Type Culture Collection
CF: Cystic fibrosis
CFU: Colony-forming units
CHIPS: Chemotaxis inhibitory protein of *Staphylococcus aureus*
Clf: Clumping factor
Cna: Collagen-binding protein
CoA: Coagulase
CP: Capsular polysaccharide
CT: Cholera toxin
Dat: D-amino acid transaminase
DCs: Dendritic cells
DIM: Dimycocerosates
DNA: Deoxyribonucleic acid
DNECs: Desquamated nasal epithelial cells
DTPw: Diphtheria-tetanus-pertussis vaccine, killed whole-cells of the pertussis component (Pw).
Eap: Extracellular adherence proteins
EbpS: Elastin-binding protein
Efb: Extracellular fibrinogen-binding protein
Emp: Extracellular matrix-binding protein
Eno: Enolase (laminin-binding protein)
ESKAPE: *Enterococcus faecium*, *Staphylococcus aureus*, *Klebsiella pneumoniae*, *Acinetobacter baumannii*, *Pseudomonas aeruginosa* and *Enterobacter* species
Fab: Fragment antigen binding region
FBS: Fetal bovine serum
Fc: Fragment crystallizable region
Fep: Cefepime
FnBP: Fibronectin-binding protein
FPR: Formyl peptide receptor
G-CSF: Granulocyte-colony stimulating factor
Gln: Glutamine
Glu: Glutamate
Gly: Glycine
GMO: Genetically modified organism
hHb: Human hemoglobin
His: Histidine

HIV: Human immunodeficiency virus
HLA: Human leukocyte antigens
HNECs: Human nasal epithelial cells
ICU: Intensive care unit
IDSA: Infectious Disease Society of America
IFN-γ: Interferon-gamma
Ig: Immunoglobulin
IL: Interleukin
IM: Inner membrane
IM: Intramuscular
IP: Intraperitoneal
Isd: Iron-regulated surface determinant
JTTR: Joint Theater Trauma Registry
KLH: Keyhole limpet hemocyanin
LB: Luria-Bertani broth
LD: Lethal dose
LPS: Lipopolysaccharide
M: Cytoplasmic membrane
mAb: Monoclonal antibody
MCS: Multiple cloning site
MDR: Multidrug-resistant
MEM: Meropenem
MEP: Mucoid exopolysaccharide
MH: Mueller Hinton
MHC: Major histocompatibility complex
MRSA: Methicillin-resistant-*Staphylococcus aureus*
MSCRAMMs: Microbial surface component recognizing adhesive matrix molecules
MTBVAC: *Mycobacterium tuberculosis* vaccine
MurI: Glutamate racemase
MV: Mechanical ventilation
NK: Natural killer
OM: Outer membrane
Omp: Outer membrane protein
oriT: Origin of transfer
Pa: Pertussis acellular
PAMPs: pathogen-associated molecular patterns
PCR: Polymerase chain reaction
PDIM: Phthiocerol dimycocerosate
PG: Peptidoglycan
PGE2: Prostaglandin E2
PGL: Phenol glycolipid
Phe: Phenylalanine
PMA: Polymannuronic acid
PMNs: Polymorphonuclear leukocytes
PNAG: Poly-N-acetyl-glucosamine
Pro: Proline
PRRs: Pattern recognition receptors
PSM: Phenol soluble modulin
PT: Pertussis toxin
PVL: Panton-Valentine leucocidin
Pw: Whole-cell pertussis vaccine
qRT-PCR: Quantitative real-time reverse transcription PCR

RD: Region of Difference
RNA: Ribonucleic acid
RNS: Reactive nitrogen species
ROS: Reactive oxygen species
SAK: Staphylokinase
SasG: *Staphylococcus aureus* surface protein G
Sbi: Second immunoglobulin-binding protein of *S. aureus*
SCID: Severe combined immunodeficiency
SCIN: Staphylococcal complement inhibitor
Sdr: Serine-aspartic acid repeat protein
SE: Staphylococcal enterotoxin
SEA: Staphylococcal enterotoxin A
SEB: Staphylococcal enterotoxin B
SEM: Scanning electron microscopy
SER: Serine
SNP: Single nucleotide polymorphism
SOD: Superoxide dismutase
Spa: Protein A
SPF: Specific pathogen-free
SPURR: Spurr's epoxy embedding medium
TB: Tuberculosis
TCR: T cell receptor
TEM: Transmission electron microscopy
Tfh: Follicular T helper cells
Th cells: helper T cells
Thr: Threonine
TLR: Toll-like receptor
TMB: Tetramethylbenzidine
TNF: Tumour necrosis factor
TSB: Tryptic Soy Broth
TSST: Toxic shock syndrome toxin
Ty: Typhoid
T3SS: Type III secretion system
UDP-GlcNAc: UDP-N-acetylglucosamine
UDP-MurNAc: UDP-N-acetyl muramic acid
Val: Valine
VAP: Ventilator-associated pneumonia
vWF: Von willebrand factor adhesion
WHO: World Health Organization
WTA: Wall teichoic acids
XDR: Extensively drug-resistant
X-Gal: 5-bromo-4-chloro-3-indolyl β-D-galactopyranoside

1. BACKGROUND

1. BACKGROUND

1.1. Immune response to bacterial pathogens and vaccinology

1.1.1. The innate immune system

Invading pathogens are detected by the innate immune system through molecular-sensing surveillance mechanisms. These mechanisms include detection of pathogens via pattern recognition receptors (PRRs), expressed by cells of the innate immune system, which can be secreted, or expressed on the cell surface, or are present in intracellular compartments (e.g. DNA/RNA sensors). Examples of PRRs are the transmembrane Toll-like receptors (TLRs). Examples of mammalian TLRs that act as bacterial receptors are TLR1, TLR2, TLR4, TLR5, and TLR9. PRRs are able to bind to molecules (such as bacterial membrane components) that are shared by several pathogens (e.g. all Gram-negative bacteria express lipopolysaccharide [LPS]), enabling the innate immune system to sense the occurrence of an infectious event. Recently, dendritic cells (DCs) and macrophages have been shown to react to signals released by damaged cells, indicating that the immune system can react to both the presence of infectious microbes (via pathogen-associated molecular patterns [PAMPs]) and to the consequences of an infectious event. Specialized chemical messengers, including cytokines and chemokines, are secreted by stressed/damaged cells and innate immune cells to attract other resident and circulating innate cells to the site of infection. Cells dying due to infection also release other small molecules, such as urea, which alert DCs.

Signalling through PRRs triggers intracellular signalling pathways to tailor the profile of gene expression. Redundancy exists in pathogens detection systems, as multiple receptors may recognize the same pathogenic structure and, conversely, a single receptor may be capable of delivering more than one signal to the host cell. Overall, the integration of these signals by antigen-presenting cells (APCs) leads to their activation. This enables them to act as messengers to precisely define the nature of the perceived danger and convey this information to the secondary lymphoid organs, where they interact with, and specifically activate, the relevant adaptive immune response.

Under some circumstances, pathogen clearance may be achieved by innate immune effectors without activation of an adaptive immune response. Activated innate cells act as phagocytes, engulfing and destroying the pathogen within intracellular vesicles

containing digestive enzymes. To be efficient, this response requires both the recruitment and activation of phagocytes at the site of infection, a process often referred to as the inflammatory response. Cells residing in proximity to the infection site are activated upon recognition of PAMPs, and secrete a large array of soluble mediators, including chemokines and cytokines. Chemokines behave as chemoattractants, favouring the recruitment of innate immune cells to the site of infection, while cytokines (including tumour necrosis factor and interferons) act by increasing the phagocytic activity of cells. Innate immune cells also produce a series of soluble chemical factors (such as peptides) that are able to directly target the invading microbes. Additionally, antigens are taken up by innate cells, with immature DCs the most specialized among them. The antigen is subsequently processed and the DC differentiates into an APC. Antigen-carrying APCs then migrate to the draining lymph node and provide the link between the innate and adaptive immune responses.

Another component of the innate immune system is the complement system. The complement system consists of approximately 25 proteins that work together to "complement" the action of the adaptive immune response in destroying bacteria. Complement proteins circulate in the blood in an inactive form. Once activated, complement components serve several effector roles including the recruitment of phagocytes, the opsonization of pathogens to promote phagocytosis, the removal of antibody-antigen complexes and the lysis of antibody-coated cells.

1.1.2. The adaptive immune system

Innate immune system alerts the adaptive immune system, whereby lymphocytes with antigen-specific receptors are activated and proliferate to fight the pathogen. Their antigen receptors evolved in response to the selection pressure of different pathogens and therefore have very diverse characteristics. Lymphocytes can be found circulating in the blood/lymph and residing within secondary lymphoid organs, such as the lymph nodes and spleen. There are two main subsets of lymphocytes involved in adaptive immune responses, whose nomenclature reflects the site of their development – B cells develop in the bone marrow and T cells develop in the thymus. The adaptive immune system essentially functions via the production of three key types of effector: antibodies (produced from B cells), cytokines and cytolytic molecules (produced by T cells).

Professional APCs, typified by DCs, can ingest pathogen-derived proteins, partially digest, process and transport the peptide products to the cell surface, rather than targeting

them for complete destruction. These pathogen-derived peptide antigens are bound by a specialized set of receptors known as human leukocyte antigens (HLA) that act as "antigen-presenting" molecules. These molecules are encoded by a gene family called the major histocompatibility complex (MHC). DCs displaying pathogen-derived antigen on the cell surface leave the infected site and migrate towards the nearest lymph node, where they are destined to activate pathogen-specific T cells. T cells do not directly recognize whole pathogens, but are only specifically activated by DCs transformed into APCs which present molecular fragments in association with MHC molecules at the cell surface. Naïve lymphocytes are therefore "blind" to live microorganisms and need the help of APCs to adequately react to an invading pathogen. Cells activated by antigen-bearing DCs express the cluster of differentiation (CD)4 cell-surface protein, and are referred to as $CD4^+$ T cells. These cells acts primarily by secreting soluble factors (cytokines) that are able to exert direct antimicrobial properties and affect the behaviour of other immune cells. In most cases, $CD4^+$ cells help other immune cells perform their task and are, therefore, referred to as helper T cells (Th).

Activation of $CD4^+$ cells represents a key step in setting in motion an adaptive immune response. The adaptive immune response is frequently characterized by two effector cell populations, the CD8-expressing cytolytic T cells and the antibody-secreting B cells. $CD8^+$ T cells exploit the TCR (T cell receptor)/MHC interaction around pathogen-derived peptides to detect and fight intracellular pathogens. In contrast to classically defined APCs, which display antigenic fragments in association with MHC class II molecules, non-immune cells use a closely related set of molecules to display peptides derived from the cytoplasm – the MHC class I molecules. This complex mechanism of antigen presentation allows $CD8^+$ T cells to scan proteins from within the cell, while preserving the integrity of the membrane. $CD8^+$ T cells have the ability to secrete cytotoxic factors in addition to cytokines. These factors enable these cells to kill cells displaying pathogen-derived peptides presented by MHC class I molecules. Optimal proliferation of $CD8^+$ T cells and acquisition of full cytolytic potential is best achieved in the presence of cytokines produced by $CD4^+$ T helper cells.

Antibodies represent a highly diverse set of soluble proteins secreted by the subset of lymphocytes referred to as B cells. B cells develop in the bone marrow before undergoing a process of differentiation and maturation in the spleen. As with T lymphocytes, each B lymphocyte expresses a unique antigen receptor (B cell receptor [BCR]) enabling the cells to react to a specific antigen. In marked contrast to TCRs, BCRs can

directly bind to molecules expressed by pathogens, with no need for previous internalization and presentation by APCs or other innate immune cells. Upon antigen encounter, B cells expressing the cognate BCR are induced to proliferate and differentiate into plasma cells, which can secrete large amounts of a soluble form of the BCR that we know as an antibody. This soluble protein is thus released in the blood and other body fluids enabling them to fight infections at distant sites.

Antibodies consist of a fragment crystallizable region (Fc), a structural feature common to all antibodies of a given isotype, and a fragment antigen binding region (Fab), which includes the portion that gives the antigen specificity (or antigen-binding characteristics) of the antibody. The variable region of the antibody can exist in a huge number of molecular configurations, and an individual's BCR repertoire is generated to maximize capability to produce antibodies that are useful against diverse potential pathogenic threats. The constant part of the molecule exists in five different forms (isotypes) (Immunoglobulin [Ig]A, IgD, IgE, IgG and IgM) that determine the ability of an antibody class to localize to particular body sites and target specific types of infection, and to recruit the optimal local effector cells. IgG is the most abundant antibody in normal human serum and consists of four human subclasses (IgG1, IgG2, IgG3 and IgG4) each containing a different Fc region. As a result, the different subclasses have different effector functions, both in terms of triggering IgG-Fc receptor-expressing cells, resulting in phagocytosis or antibody-dependent cell-mediated cytotoxicity, and activating complement [1]. In mice, the IgG isotype is divided into five subclasses (IgG1, IgG2a, IgG2b, IgG2c and IgG3). Subclass nomenclature has arisen independently for each species and so there is no general relationship between the subclasses from each species.

In most cases, direct activation of B cells by an antigen is observed in response to repetitive antigenic structures, such as carbohydrates found in bacterial walls. These T cell-independent responses are characterized by the secretion of low-affinity antibodies of the IgM type. This type of response is often stereotyped in nature, lacking the typical memory response upon re-exposure to the same antigen. In most cases, optimal B cell activation and differentiation into antibody-secreting plasma cells is only observed when both B and T cells are simultaneously activated by the same pathogen. In these instances, $CD4^+$ T cells differentiate into follicular T helper cells (Tfh) that are able to provide a helper signal to B cells. Tfh cells have been defined by secretion of IL-21, a cytokine though to favour the secretion of antibodies by antigen-specific B cells. T cell-dependent B cell responses are characterized by the secretion of high-affinity antibodies and a large spectrum of isotypes

(in particular IgG), and are typical associated with immunity resulting from natural exposure.

Th1 cells and IFN-γ

One subset of Th cells, the Th1 cells, appear to secrete mainly interferon-gamma (IFN-γ), an important immunoregulatory cytokine known to limit pathogen survival and spreading. It is also known to promote the differentiation of cytolytic cells that are able to destroy cells infected with intracellular pathogens. Indeed, IFN-γ was originally identified through its anti-viral activity [2]. It plays key roles in host defense by exerting anti-viral, anti-proliferative and immunoregulatory activities [3-5]. IFN-γ induces the production of cytokines and upregulates the expression of various membrane proteins including class I and II MHC antigens. IFN-γ is a potent activator of macrophage effector functions. It potentiates the secretion of immunoglobulins by B cells and affects isotype switching. IFN-γ also influences T helper cell phenotype determination by inhibiting Th2 differentiation and stabilizing Th1 cells [3-5]. IFN-γ is produced primarily by activated natural killer (NK) cells, activated Th1 cells and activated $CD8^+$ cytotoxic cells [3-5]. Additional cell types that produce IFN-γ include macrophages [6], DCs [7,8] and mast cells [9]. Mouse IFN-γ shares approximately 40% amino acid (aa) sequence identity with human IFN-γ and does not have cross-species activity [3-5]. Th1 cells are therefore, considered important for inducing immune responses involved in the clearance of intracellular pathogens.

Th2 cells and IL-4

Another subset of T helper cells, the Th2 cells, are key in organizing host defense against extracellular pathogens and in helping B cells to produce antibodies. These cells produce cytokines (interleukins [IL] IL-4, IL-5, IL-13) that appear particularly important at activating innate cells (eosinophils, mast cells). IL-4 was originally described in 1982 as a B cell stimulatory factor [10] and is now known to regulate a myriad of immune functions including Ig isotype switching, class II MHC expression by B cells, and the differentiation fate of certain T cell subsets [11]. Mouse IL-4 is a 20 kDa single chain glycoprotein that shares 56% and 61% aa identity with mature human and rat IL-4, respectively [12-15]. Mouse IL-4 is species specific and is inactive on both human and rat cells [16,17]. Mouse cells known to express IL-4 following activation include $CD4^+$ Th2 cells [18,19], $CD4^+$ $NK1.1^+$ and $NK1.1^-$ T cells [20], DCs [21], mast cells [22], eosinophils [23], and basophils [24]. In mice, IL-4 promotes the synthesis of IgE plus the anaphylactic form of IgG1 [25,26]. On monocytes, IL-4 inhibits the LPS-induced production of tumour necrosis factor (TNF)-α, IL-1β, IL-6, and

prostaglandin E2 (PGE2), thus suppressing the creation of a proinflammatory environment [11,27]. IL-4 also blocks IFN-γ production during T cell differentiation, driving $CD4^+$ T cells towards a Th2 phenotype [28].

Th17 cells and IL-17

A third subset of effector T helper cells, called Th17, produce IL-17 and are important in clearing pathogens during host defense reactions [29]. Functionally, IL-17 is best known for its participation in the recruitment and survival of neutrophils [30-32]. Its induction is believed to be the result of antigen stimulation of DCs, resulting in IL-23 secretion. In a TCR-independent event, IL-23 can induce T cell production of IL-17 [30]. In the tissues, IL-17 appears to promote neutrophil extravasation, principally through its effects on macrophages and endothelial cells. On macrophages, IL-17 induces TNF-α, IL-1β and IL-6 production [33]. TNF-α and IL-1β then act on local endothelial cells to induce granulocyte-colony stimulating factor (G-CSF) secretion, an effect that is potentiated by IL-17 [34]. IL-17 further contributes to polymorphonuclear leukocyte influx by inducing endothelial cells to release chemokines and nitric oxide production, which may increase vascular permeability [30,35]. Several groups have now also demonstrated the formation of Th17 memory in response to vaccination in mice. Generation of immunity to the pulmonary pathogen *Klebsiella pneumoniae* by mucosal vaccination with heat-killed *Klebsiella* bacteria required Th17 cells [36]. The memory response generated afforded protection against multiple different clades of the *K. pneumoniae* species, including much more virulent or multidrug-resistant strains. In a *Mycobacterium tuberculosis* vaccine model, protection was also found to be dependent on Th17 cells acting as a first-line of defense in the lung before Th1 cells arrived [37,38]. Mouse IL-17 is a 30-35 kDa variably glycosylated homodimeric protein that belongs to a unique family of cysteine-knot related proteins [30,39,40]. Mature mouse IL-17 shares 61% and 89% aa sequence identity to human and rat IL-17, respectively [41,42]. While rodent and human mature sequences show modest aa sequence identity, human IL-17 is active on both mouse and rat cells [35,43]. Th17 cells also produce IL-22, an interleukin that acts cooperatively with IL-17 to enhance expression of antimicrobial peptides associated with host defense [44]. Recently, Th17 cells were also shown to function as B cell helpers, triggering antibody production *in vivo* [45].

Figure 1 summarizes the main aspects of the human immune response to pathogens.

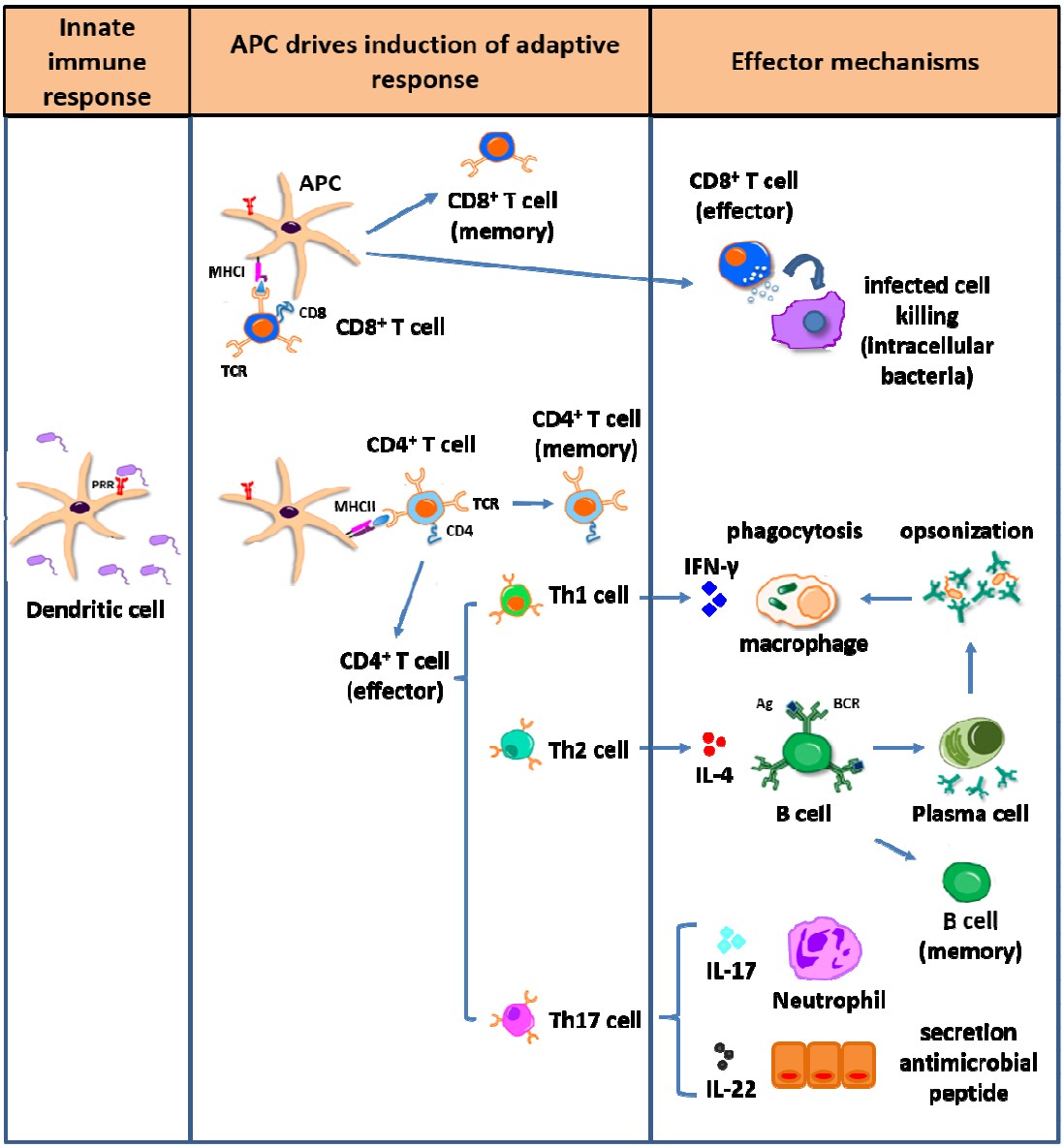

Figure 1 | An overview of the human immune response. Innate immune cells begin to mature and differentiate after detection of invading pathogens, while migrating to the lymph nodes. APCs induce the adaptive immune response including activation of T cells into effector cells and differentiation of T cells into memory cells. $CD8^+$ T cells can directly kill infected tissue/cells via molecular and chemical signaling and induce infected cells/phagocytes to kill intracellular pathogens, or inhibit pathogen replication. Naïve B cells differentiate into antibody-secreting plasma cells and memory B cells following activation by IL-4-secreting Th2 cells. IFN-γ-secreting-Th1 cells activate tissue-resident macrophages. Antibodies can enhance the effector functions of innate cells and neutralize pathogens directly. IL-17 produced by Th17 cells acts by recruiting neutrophils to the site of infection. IL-22 enhances expression of antimicrobial peptides. Partially adapted from [46].

Immunological memory

Upon differentiation, naïve T and B cells, each expressing a unique TCR and BCR, migrate to the blood and peripheral lymphoid organs. Some of these cells will differentiate into effector cells (such as cytokine-producing T cells or antibody-secreting plasma cells), while others will become memory cells, able to survive for a long period of time within the host. Exposure to an antigen (pathogen or vaccine) therefore leads to a long-term (and sometimes permanent) modification of the cellular repertoire, such that the relative frequency of T and B cells specific for an individual antigen is increased in antigen-exposed individuals compared with naïve individuals **(Fig. 2)**.

In addition to their increased frequency, memory T and B lymphocytes also display novel functional properties, enabling them to develop secondary (recall) responses on re-encounter with their specific antigen, or a closely related antigen. The adaptive response on secondary exposure leads to a rapid expansion and differentiation of memory T and B cells into effector cells, and the production of high levels of antibodies. A higher proportion of IgG and other isotypes of antibodies compared with the level of IgM characterizes memory antibody responses.

By definition, all effective vaccines lead to the development of immune memory, by mimicking the threat of an infection and providing antigens derived from the specific pathogen. The ability to generate immune memory is the key attribute of the adaptive immune system, which is crucial for the long-term protection of individuals and populations. Generating immune memory depends on a high degree of interaction among many different cell types, which maintains higher numbers of T and B cells that were selected as the most useful in the primary immune response. However, while the relative contribution of clonal memory cells to protection can be inferred from the molecules they express and their functional behaviour, the presence of memory cells *per se* is not indicative of absolute protection against disease.

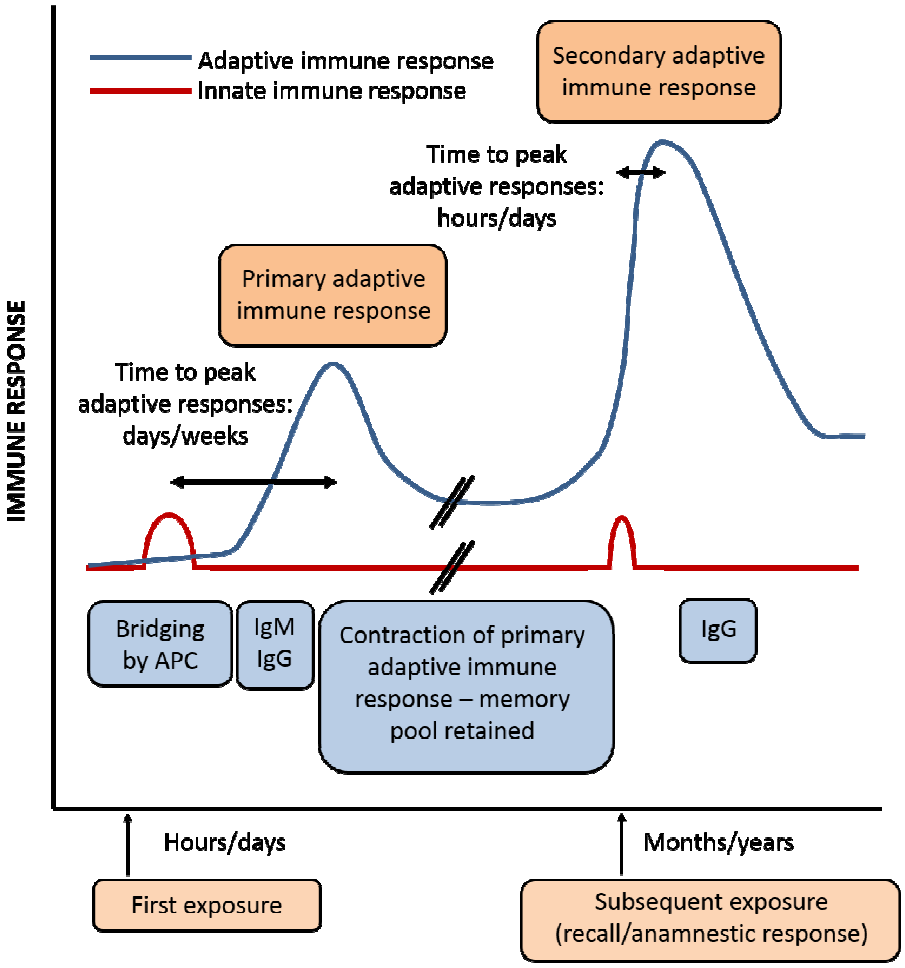

Figure 2 | The kinetics of primary and recall (memory) immune responses. On first exposure to a pathogen or antigen (referred to as "priming" in vaccination), the innate immune system must detect, process and translate the threat into a form that can be understood by the adaptive immune system. This occurs via the bridging actions of APCs and takes days/weeks. Following resolution of the challenge, a specialized "memory" cell population remains, and is maintained for a long time (months/years), remaining within the host for the rest of its life. On subsequent exposure to the same antigen (referred to as "boosting" in vaccination), the innate immune response is triggered as before but now the memory cell populations are able to mount a greater and more rapid response as they do not need to undergo the same activation process as naïve cells. From [46].

1.1.3. Immunological requirements of a vaccine and vaccine development challenges

Vaccines aim to prevent the disease symptoms that are the consequences of a pathogenic infection. In most cases, this does not occur by completely preventing infection but by limiting the consequences of the infection. Vaccines developed from pathogens can vary in the complexity of the pathogen-derived material they contain. The requirement for

more than the presence of a “foreign” antigen to elicit an immune response must always be considered in vaccine design. Highly refined subunit antigen formulations, and some inactivated whole pathogens, do not contain many of the molecular features and defensive triggers that are required to alert the innate immune system. These type of antigen are designed to minimize excessive inflammatory responses but, as a result, may be sub-optimally immunogenic. Under these circumstances, adjuvants are often added to the vaccines compositions. The induction of $CD4^+$ T cells is essentially controlled by the nature of this inflammatory response.

The dominant immune response to a given pathogen or antigen may not necessarily be the optimum response for inducing protection. Antibody titers are often considered to represent adequate indicators of immune protection but may not be the actual mechanism by which optimal protection is achieved. Useful specific so-called immune correlates of immunity/protection may be unknown or incompletely characterized. Therefore, modern vaccine design still looks to clinical trials to provide information about clinical efficacy and, if possible, the immunological profiles of protected individuals.

Immunogenicity is assessed by laboratory measurements of immune effectors, typically antibodies. Increasingly, however, specific T cell activation is included in the parameters assessed, as adequate T cell immunity may be essential for recovery from some infections. Other important consideration in vaccine immunology include the phenomena of immune tolerance and immunological/antigenic interference, which can supress or prevent development of adequate immune responses following vaccination. Immune tolerance refers to the induction of immunological non-responsiveness by repeated exposure to similar antigens, such as polysaccharide antigens; this effect is dose-dependent and may be limited in time as increasing the interval between subsequent doses can partially restore responsiveness.

This text was partially adapted from [46].

1.2. Bacterial vaccines

Vaccines are attenuated, inactivated organisms or purified products derived from them. There are several types of bacterial vaccines in use and actually licensed worldwide **(Fig. 3)**.

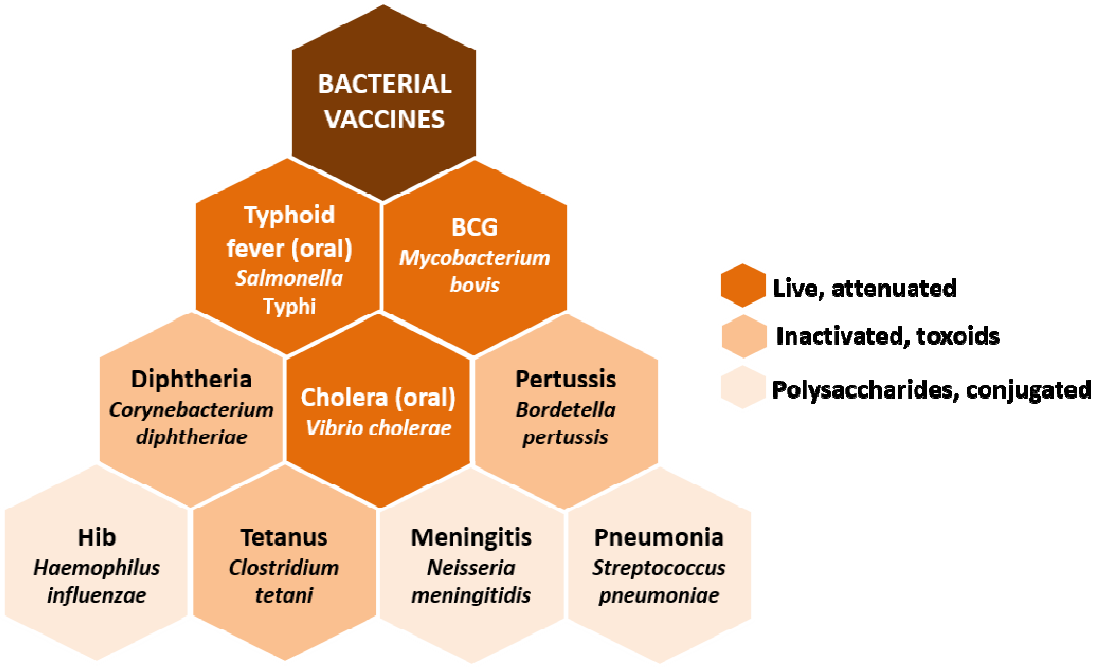

Figure 3 | Major classification of bacterial vaccines licensed for immunization and distribution worldwide.

These vaccines represent different strategies used to try to reduce risk of illness, while retaining the ability to induce a beneficial immune response. Some of these vaccines contain inactivated, but previously virulent bacteria that have been inactivated, or its components. The whole-cell pertussis vaccine (Pw) is a suspension of the entire *Bordetella pertussis* organism that has been inactivated, usually with formalin. Examples of toxoid-based vaccines include *Clostridium tetani* and *Corynebacterium diphtheria*. Conjugated vaccines include *Haemophilus influenzae* b, *Neisseria meningitidis* and *Streptococcus pneumoniae* and are composed of polysaccharides linked to more immunogenic proteins. Live, attenuated bacterial vaccines include *Salmonella* Typhi, *Mycobacterium bovis* and *Vibrio cholerae* and will be discussed in detail.

1.3. Live vaccines and mechanisms of virulence attenuation

Bacterial live vaccines are highly efficient because they are harmless versions of disease causing pathogenic bacteria and mimic the natural infection. These live attenuated vaccines that use the complete pathogen induce both cell-mediated and antibody-mediated immunity, resulting in efficient immunizations and a lessened need for booster injections. This typically provokes more durable immunological responses, being the

preferred vaccine type for healthy adults. These vaccines have been used extensively for decades to prevent respiratory or enteric pathogens that cause severe disease and epidemics in humans [47-49], and the most frequent infections of herd animals [50-57]. Advantages of live bacterial vaccines include their mimicry of a natural infection, intrinsic adjuvant properties and their possibility to be administered orally.

However, pathogenic bacteria demands for attenuation to weaken its virulence. Traditionally, attenuation of virulence was achieved through natural selection by multiple passages of the microorganism on growth medium, random mutagenesis or more recently, genetic modification of target genes particularly suited to inducing virulence attenuation. Moreover, they may not be safe for use in immunocompromised individuals, and may rarely revert to a virulent form and cause disease.

With the increased knowledge of mucosal immunity and the availability of genetic tools for heterologous gene expression, the concept of live vaccine vehicles gains renewed interest. Indeed, the use of live bacteria to induce an immune response to itself or to a carried vaccine component is an attractive vaccine strategy. The actual use of genetic modified bacteria as vaccines and vaccine delivery vehicles implies construction of recombinant strains that contains the gene cassette encoding the antigen. However, vaccination using recombinant bacteria require particular attention regarding their safety as they may propagate in the host and be released into the environment by the vaccines [58]. This places these vaccines in the debate on application of genetically modified organisms.

1.3.1. Typhoid fever (oral)

Typhoid infections, caused by *Salmonella enterica* serovar Typhi, are major killers responsible for over 200,000 deaths yearly [59]. This organism can infect humans and other higher primates but no other animal reservoir has been recognized. This suggests that it may be possible to eliminate typhoid through the use of vaccination and other public health measures. The death toll from typhoid would be higher except for the availability of vaccines. The two well-tolerated vaccines in use in humans provide partial and temporally limited protection and are quite distinct [60-62].

Ty21a live attenuated oral vaccine

One of the two well-tolerated vaccines is the live-attenuated typhoid bacterium-strain Ty21a. Ty21a is safe and protective as live oral vaccine and was developed in the early 1970s by chemical mutagenesis of a pathogenic *S.* Typhi strain [63]. The characteristic mutations in this strain include an inactivation of the *galE* gene, so Ty21a has an impaired capacity to synthetize LPS O-chain, and also inability to express the capsular polysaccharide (CP) Vi antigen, both considered major targets of protective antibody [63]. However, approximately two dozen additional mutations are also present in Ty21a [63] **(Table 1)**.

Table 1| Mutations identified in strain Ty21a compared to Ty2. Adapted from [64].

Gene	Genotype	Phenotype
galE	Base change at pos. 367 TCC → CCC leads to Ser → Pro	No galactose epimerase activity [63]
	Base deletion at pos. 444 leads to frame shift	No production of smooth type LPS without galactose. Only possible in presence of galactose in nutrient medium. Lysis if galactose is in excess in the nutrient medium. Blue when growing on a galactose containing brom-thymol-blue indicator agar **(Fig. 4)** [65]
galT	No mutation	Reduced activity: 35%, independent from the nutrient medium [63]
alK	Base change at pos. 86 GTC → GCC leads to Val → Ala	Reduced activity: 15%, independent from the nutrient medium [63]
galP	No mutation	Activity depends on the nutrient medium
rpoS	Insertion of G at pos. 933 in Ty2 and Ty21a compared to *S. typhimurium* strains → frame shift that modifies the amino acid sequence of the C-terminal part of σ^S	Mutated stress response
ilvD	Base exchange at pos. 1525 GCG → ACG leads to Ala → Thr	Isoleucine and valine auxotrophy test in minimal medium: no growth without these two amino acids
	Base exchange at pos. 1607 GGC → GAC leads to Gly → Asp	
rcsC	Base exchange at pos. 1541 TCC → TTC leads to Ser → Phe	
tviC	Base exchange at pos. 996 CAG → CAA leads to Gln → Gln	
tviE	Base exchange at pos. 803 GGC → GAC leads to Gly → Asp	
tviE	Base exchange at pos. 1699 GGA → AGA leads to Gly → Arg	
vexD	Base exchange at pos. 1205 CGC → CAC leads to Arg → His	No Vi polysaccharide synthesized: no agglutination with Vi antiserum
vexE	Base exchange at pos. 893 GGT → GAT leads to Gly → Asp	
	Base exchange at pos. 1111 GCG → ACG leads to Ala → Thr	

Table 1 (cont.)| Mutations identified in strain Ty21a compared to Ty2. Adapted from [64].

Gene	Genotype	Phenotype
vexE	Base exchange at pos. 1552 GGC → AGC leads to Gly → Ser	

Figure 4 | Growth of *S.* Typhi Ty21a and Ty2 on agar medium containing galactose. Ty21a bacteria produce small grey-bluish colonies, and the wild-type strain Ty2 generates large yellow colonies (From R. Germanier).

Ty21a is the main constituent of Vivotif [66], the only licensed oral vaccine against typhoid fever. Although Ty21a has proven to be remarkably well tolerated in placebo-controlled clinical trials [67], it is not clear precisely what mutations in addition to inactivation of *galE* and of Vi synthesis are most responsible for the stable, impressive attenuation of this vaccine, thus, how this attenuated bacterium confers protection is not fully understood. The importance of antibody to Vi is evidenced by the use of purified Vi antigen as a stand-alone vaccine. Vi antigen is made of repeating units (1-4)-2-deoxy-2-N-acetyl galacturonic acid encoded within the viaB locus from *S.* Typhi [68]. Immunization provides protection against typhoid at levels comparable to Ty21a in adults and older children in the first two years post-immunization [60,61]. The protection conferred by immunization with Vi antigen is likely to be mediated via systemic antibody as it has not been found to induce pronounced mucosal antibody responses, nor have a requirement for T cell involvement [69,70]. Therefore, understanding the nature of antibody responses to Vi antigen and other vaccines based on CP is likely to be important in understanding the basis of immunity to many pathogens and improving vaccines that target them.

1.3.2. Cholera (oral)

Vibrio cholerae is a Gram-negative bacillus that causes cholera, a severe, dehydrating diarrheal illness of humans. Two O serogroups of *V. cholerae*, O1 and O139, can cause epidemics of cholera gravis. *V. cholerae* O1 is by far the more important as O139 infections are found in just a few areas of Asia (where they are responsible for only a few percent of cases) and O139 has not been reported from Africa. Two biotypes of *V. cholerae*

O1 exist, El Tor and classical, although presently only El Tor strains are prevalent. Recently, highly virulent El Tor strains have emerged that produce classical biotype cholera enterotoxin. Within each biotype of O1 are found two main serotypes, Inaba and Ogawa.

For a cholera vaccine to be a useful public health tool, it must protect against both serotypes and biotypes. Live, orally administered, attenuated vaccine strains of *V. cholerae* have many theoretical advantages over killed vaccines. A single oral inoculation could result in intestinal colonization, obviating the need for repetitive dosing. Live *V. cholerae* organisms can also respond to the intestinal environment and immunological exposure to *in vivo*-expressed bacterial products could result in better immunological protection against wild-type *V. cholerae* infection. Attenuated *V. cholerae* have been developed using recombinant molecular biology techniques [71]. Attempts were made to further lessen reactogenicity of obtained strains, by decreasing the ability of attenuated *V. cholerae* vaccine strains to colonize the intestinal surface and by further attenuating vaccine strains by removing various purported toxic elements.

CVD 103-HgR

A σ*ctxA* derivative of classical strain *V. cholerae* 569B (CVD 103) was found to be immunogenic and minimally reactogenic [47]. To facilitate identification of the vaccine strain, a mercury-resistance gene (*hgR*) was inserted into the hemolysis A gene (hlyA) to generate CVD 103-HgR [47,72]. In North American adults, a single oral dose of about 5×10^8 CFU of CVD 103-HgR elicits significant (four-fold or greater) rises in serum vibriocidal antibody (that is, seroconversion) in over 90% of those vaccinated, and vaccine organisms are excreted by about 25% [73]. A single dose of CVD 103-HgR significantly protects North Americans against cholera caused by *V. cholerae* O1 of either classical or El Tor biotype and either Inaba or Ogawa serotype [47,74,75].

Peru-15

A live, oral, attenuated *V. cholerae* O1 El Tor Inaba C6709 cholera vaccine strain was constructed in the 1990s by deleting the entire cholera toxin (CT) genetic element and *attRS1* sites, inserting the gene for the B subunit of CT into *recA*, and screening for a non-motile derivative, to derive the vaccine strain Peru-15 [76]. Peru-15 is well tolerated and immunogenic (90-100% vibriocidal seroconversion rate) as a single dose in volunteer studies [76,77]. Peru-15 was studied in a staged double-blind, randomized, placebo-controlled Phase I/II field trial in Bangladesh. The vaccine was safe and well tolerated.

Vibriocidal antibody responses were seen in 30 out of 40 (75%) vaccine recipients [78]. Studies in toddlers and infants demonstrated 84 and 70% vibriocidal response rates, respectively, with an overall vibriocidal response rate of 77% in children less than 5 years of age [79].

V. cholerae vaccine 638

In the 1990s, a live, oral, attenuated El Tor Ogawa cholera vaccine was constructed by deleting the entire CT genetic element, CTXΦ, from *V. cholerae* O1 El Tor Ogawa strain C7258 and by insertion of the *Clostridium thermocellum* endoglucanase A gene (*celA*) into the hemagglutinin/protease *hapA* gene. The *celA*::*hapA* modification does not affect immunogenicity or colonization of the vaccine strain in animals [80]; but does permit rapid identification of the strain through assessment of β-(1–4) endoglucanase activity encoded by *celA* in carboxymethylcellulose indicator agar stained with Congo red, in which the vaccine strain appears as a red colony [80]. In a double-blind, placebo-controlled study in Cuba, *V. cholerae* 638 was examined preliminary for safety and immunogenicity [80] and no significant adverse reactions were observed in volunteers immunized. *V. cholerae* 638 was further evaluated for protective efficacy in a randomized, double-blind, placebo-controlled in a trial also in Cuba [81]. Among 24 of the vaccinees, 96% developed vibriocidal responses, and 50% developed an anti-LPS IgA response in serum [81]. At 1 month after vaccination, 12 vaccinees and 9 placebo recipients were challenged with 7×10^5 CFU of virulent strain *V. cholerae* 3008 [81]. None of the 12 vaccinees, but 7 volunteers from the placebo group, had diarrhea; two of the latter developed severe cholera [81].

Other live oral cholera vaccines

Other live oral attenuated *V. cholerae* O1 strains have been developed, including VA1.3 in India [82] and IEM108 in China [83]. These strains have been immunogenic in animals, but no human studies have yet been reported.

This text was adapted from [84]**.**

1.3.3. BCG and MTBVAC

BCG

Tuberculosis (TB) caused by *Mycobacterium tuberculosis*, remains a global health emergency. Additional threats to TB control include the spread of multidrug-resistant TB

(MDR-TB), the appearance of extensively drug-resistant TB (XDR-TB), and the destructive impact of TB/HIV coinfection. Bacille Calmette-Guérin (BCG), an attenuated strain of *Mycobacterium bovis*, is currently the only available vaccine against TB. Since 1974, BCG vaccination has been included in the WHO Expanded Program of Immunization [85]. It is estimated that more than 3 billion individuals have been immunized with BCG and over 100 million doses of BCG are administered annually, making it the most widely used vaccine in humans [85]. Meta-analysis studies have confirmed that BCG protects children, providing >80% efficacy against severe forms of TB, including tuberculous meningitis and military TB. In contrast, evidence for protection against pulmonary TB in adolescents and adults remains contentious as efficacy estimates from clinical trials, observational case control studies and contact studies range from 0 to 80% [49]. Although it is generally considered safe and has been used as a human vaccine since the 1920s, the mechanisms of BCG attenuation remain largely unknown. Moreover, BCG strains also exhibit differences in residual virulence level. Recent studies have provided direct evidence that the distribution of major mycobacterial virulence factors varies among BCG lineages [86,87], and suggests that different BCG substrains have different mechanisms of attenuation.

BCG originated with “lait Nocard”, a virulent strain of *M. bovis* isolated from the milk of a cow suffering from tuberculosis mastitis. Around 1901, this strain was brought to the Institute Pasteur in France, and used by Albert Calmette and Camille Guérin for studies of bovine tuberculosis. Calmette added ox bile to the glycerol-soaked potato slices on which the *M. bovis* was cultured in order to minimize bacterial clumping and optimize animal infection experiments. Within a few months, an isolate with unusual colony morphology and reduced virulence in guinea pigs appeared. After 13 years of serial *in vitro* passaging of this *M. bovis* strain (1908-1921) and different animal models experiments, the first human trial occurred. In July 1921, an infant was given three doses (~2.4×10^8 CFU in total) by the oral route [88]. This child did not develop TB even though the infant’s mother had died of TB shortly after giving birth. As early as 1924, cultures of BCG were distributed to laboratories around the world and dozens of distinct daughter strains emerged, including four that are currently in major use: BCG-Pasteur (1173P2), BCG-Japan (Tokyo-172), BCG-Danish (Copenhagen-1331) and BCG-Glaxo (1077).

Mechanisms of BCG attenuation

BCG strains have undergone two phases of attenuation. The initial phase (1908-1921) comprises the 230 *in vitro* passages conducted by Calmette and Guérin to produce

the original vaccine. The second phase starts circa 1924 with widespread use and distribution of BCG. It ends several decades, and hundreds of passages, later with the establishment of frozen seed lots. Due to the initial phase, it is expected that BCG strains should share a set of common attenuating mutations, whereas the second phase should give rise to additional mutations, specific to individual BCG strains and lineages. A molecular phylogeny based on various studies has been established **(Fig. 5)** and is generally consistent with the historical records of BCG dissemination.

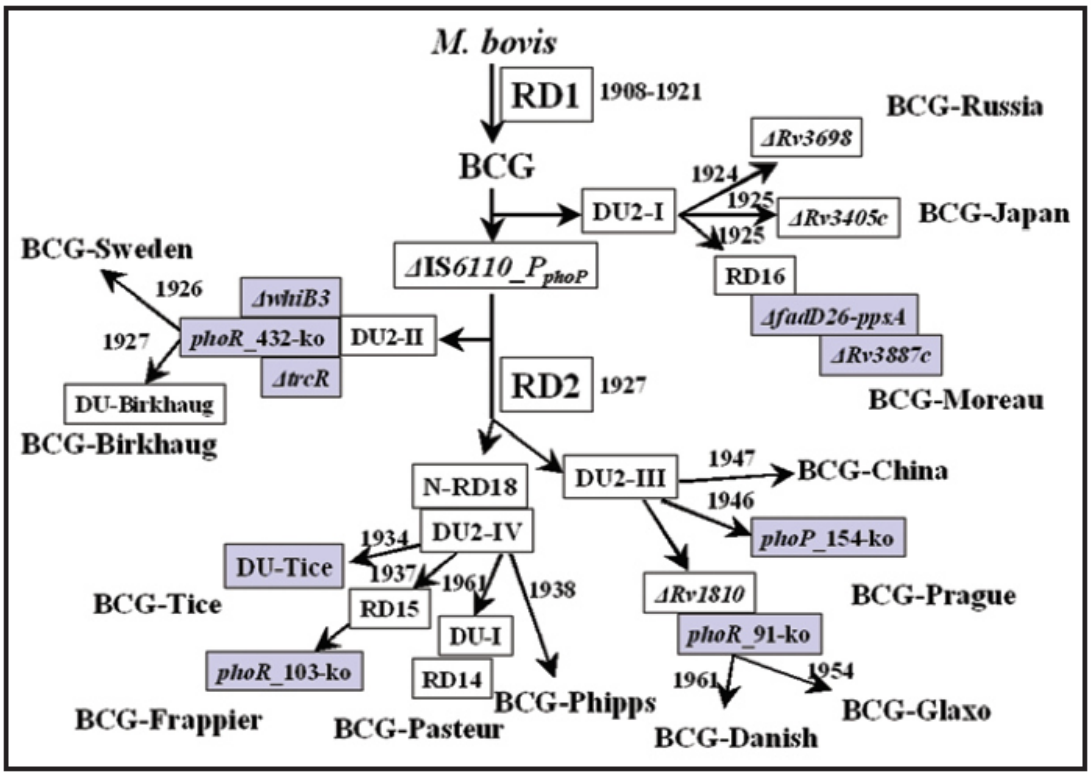

Figure 5 | Genealogy of BCG vaccines. Polymorphisms that affect known virulence genes are highlighted. From [49].

Attenuation of BCG between 1908-1921

A Region of Difference-1 (RD1) that is deleted in all BCG strains but present in virulent strains of *M. tuberculosis* and *M. bovis* was identified [89,90]. RD1 encodes the ESX-1 protein secretion system, which is one of the five type-VII secretion systems found in the *M. tuberculosis* genome [91]. Since it is common to all BCG strains, the loss of RD1 likely occurred in the initial stage of BCG attenuation. However, reintroduction of ESX-1 into BCG does not restore full virulence [92] and the RD1 deletion mutant of *M. tuberculosis* is still more virulent than BCG in long-term murine infections experiments [93]. Posterior studies indicate additional single nucleotide polymorphisms (SNPs) between different BCG strains

[94]. This suggests that loss of virulence during the initial 230 *in vitro* passages of BCG involved both the loss of RD1 and the accumulation of attenuating SNPs.

Attenuation of BCG after 1924

The dissemination of BCG to various parts of the world began in 1924. With different methods of propagation of the vaccine strains, BCG substrains emerged. Not until 1966, with the introduction of the "seed-lot system", was lyophilization of BCG strains started and the process of *in vitro* evolution halted. The deletion of RD2, accounts for the lack of MPB64 in the strains acquired after 1927.

The direct evidence that BCG strains differ in established virulence factors first came from the comparative biochemical analysis of phthiocerol dimycocerosates (PDIMs) and phenol glycolipids (PGLs) [87]. PDIMs and PGLs are structurally related, methyl-branched fatty acid-containing complex lipids of mycobacterial cell wall and are considered exclusive to pathogenic mycobacteria. Analysis of 12 BCG strains reveals that BCG-Japan, BCG-Moreau and BCG-Glaxo do not produce PDIMs and PGLs, whereas the other BCG strains do [87]. In BCG-Moreau, the PDIM and PGL defect is likely due to a 975 bp deletion that affects *fadD26* and *ppsA* [86], which are part of the biosynthetic locus of PDIMs and PGLs [86,95].

Furthermore, strains with defects in the PhoP regulon, such as *phoP* mutant in *M. tuberculosis*, are more attenuated than BCG-Pasteur in SCID mice infections [96]. Other studies have also demonstrated that the PhoP-PhoR system, particularly PhoP, plays an essential role in *M. tuberculosis* virulence [97-99]. A frame-shift mutation whitin the *phoP* gene of BCG-Prague makes this strain a natural *phoP* mutant [86]. The PhoP-PhoR system is one of 11 two component systems found in the *M. tuberculosis* genome [100]. The PhoR protein is a transmembrane histidine kinase that transmits signals from the environment. Autophosphorylation of PhoR is followed by transfer of the phosphoryl group to PhoP, a response regulator that mediates expression of multiple genes [97].

BCG-Sweden and BCG-Birkhaug contain deletions in *whiB3* and *trcR*, that are not present on other BCG strains [86]. Evidence obtained thus far suggest that WhiB proteins are transcriptional factors involved in the regulation of important mycobacterial cellular processes, including cell division, pathogenesis, oxidative stress responses and antibiotic resistance [101-103]. Specifically, deletion of *whiB3* attenuates *in vivo* growth of *M. bovis* in guinea pigs [104] and WhiB3 is known to maintain the redox homeostasis to modulate

macrophage response [105]. TrcR is the response regulator of the TcrR-TrcS two-component system. Deletion of *trcS* from *M. tuberculosis* generates a hypervirulent phenotype such that the strains exhibits increased lethality in SCID mice [106].

Deletions affecting other genes with potential impact on virulence have also been found in certain BCG strains. The *M. tuberculosis* genome contains four *mce* operons, each containing 9-12 genes that encode membrane permease subunits of ABC transporters and putative secreted or cell-surface proteins [107]. The *mce4C* and *mce4D* genes are deleted in BCG-Frappier [108]. Recently, it was shown that the *mce4* operon of *M. tuberculosis* encodes a cholesterol import system, which appears to be important for persistence infection [109,110].

Finally, BCG strains can be viewed as two major groups that differ significantly in virulence level, the more virulent ones represented by BCG-Russia, -Sweden, -Danish and –Pasteur, and the less virulent group including BCG-Japan, -Moreau, -Glaxo and –Prague. Deletions identified in some of these strains that affect vaccine properties as manifested in animal and clinical studies are listed in **Table 2**.

Table 2 | Deletions identified in BCG strains that affect currently known virulence factors.

Deletions	BCG strains affected
fadD26-ppsA	BCG-Moreau
whiB3, trcR	BCG-Birkhaug, BCG-Sweden
phoP	BCG-Prague
phoR	BCG-Sweden, -Birkhaug, -Danish, -Glaxo, -Frappier
mce4	BCG-Frappier

All BCG strains contain the RD1 deletion, which contribute partially their attenuation. Additional deletions that may affect virulence levels of specific BCG strains are listed here. Adapted from [49].

This text was adapted from [49].

MTBVAC

BCG confers protection against severe forms of TB (meningitis and miliary TB) in children but lacks consistency in preventing pulmonary disease, the most common form responsible for transmission by respiratory route [111]. Thus, very substantial efforts have been made over the past decade to develop new vaccines against TB. MTBVAC, a live attenuated *M. tuberculosis* vaccine, is based on the prototype SO2 (which has a safety and efficacy profile) and is genetically engineered to fulfil the Geneva consensus requirements for progressing new live mycobacterial vaccines into Phase 1 clinical trials, demanding the

presence of two stable independent mutations without antibiotic resistance markers for *M. tuberculosis*-based candidates. Indeed, this vaccine has two independent stable deletion mutations without antibiotic resistance markers in the virulence genes *phoP*, coding for a transcription factor key for the regulation of *M. tuberculosis* virulence, and *fadD26*, essential for the synthesis of DIM, one of the major mycobacterial virulence factors **(Fig. 6)**.

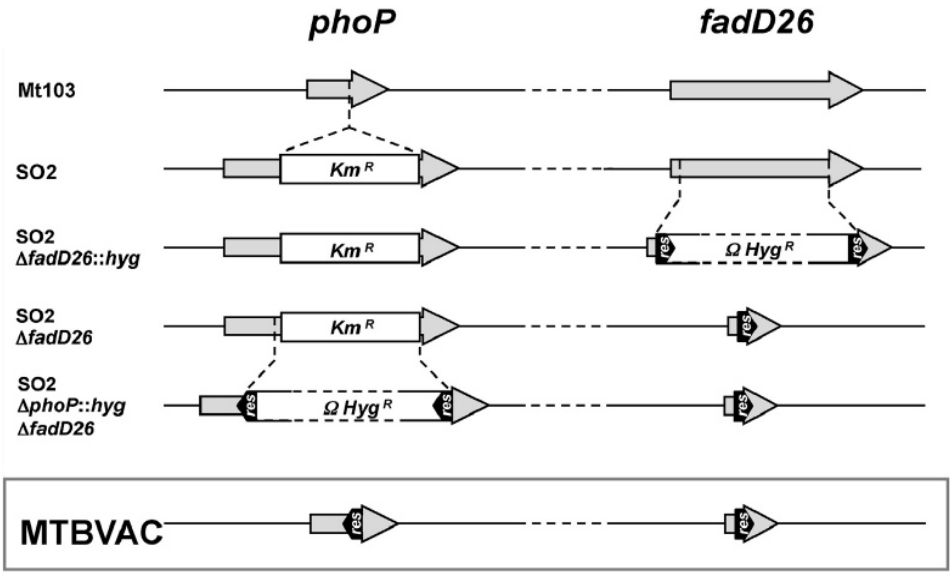

Figure 6 | Step-by-step construction of MTBVAC from SO2. Deletions in *fadD26* and *phoP* genes were genetically engineered in SO2 strain. The final strain MTBVAC is a DIM-deficient *phoP* mutant which provides better assurance of genetic stability and has no antibiotic-resistace markers. *phoP* and *fadD26* genes are represented as grey arrows, white rectangles illustrate antibiotic-resistance markers and black arrow-heads depicts *res* sites [112]. Vertical discontinuous lines indicate the position of restriction sites used for strain construction and horizontal discontinuous lines depict DNA regions that are not to scale. From [113].

MTBVAC exhibits equivalent safety and biodistribution profiles **(Fig. 7)** as the reference licensed strain BCG Danish 1331, used in the clinic, and confers superior protection with mouse model **(Fig. 8)** and other preclinical studies. As a result, MTBVAC is the first vaccine of this kind to enter human clinical trials, in January 2013 [113].

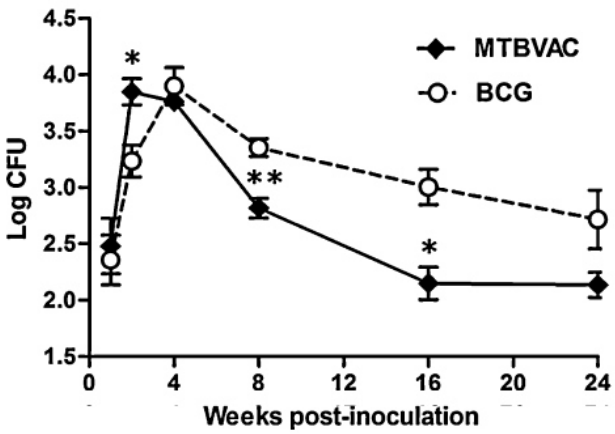

Figure 7 | MTBVAC biodistribution profile. BALB/c mice were intradermally inoculated with MTBVAC (black diamonds) or BGC Danish 1331 (white circles) and bacterial load in lymph nodes was determined. A similar clearance profile was obtained for both strains (mean ± s.e.m.). **P*<0.05 ***P*<0.01, unpaired Student's t test. From [113].

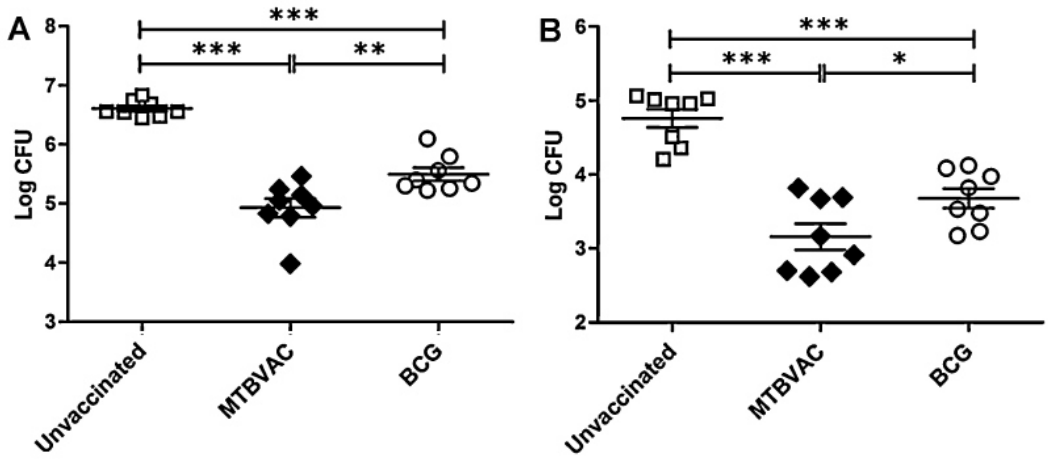

Figure 8 | Protective efficacy of MTBVAC in mice. C57BL/6 mice received a subcutaneous administration of MTBVAC (black diamonds) or BCG Danish 1331 (white circles), or were not vaccinated (white squares), followed by an intranasal challenge with virulent H37Rv. At 4 weeks post-challenge, bacterial burden (mean ± s.e.m.) was assessed in **A,** lungs and **B,** spleen. Significant CFU reduction was observed in MTBVAC vaccinated animals compared to BCG. **P*<0.05, ***P*<0.01, ****P*<0.001, unpaired Student's t test. From [113].

1.3.4. *Bordetella pertussis* BPZE1

Since the 1940s and 1950s, Pw's have been combined with diphtheria and tetanus toxoids in formulations called diphtheria-tetanus-pertussis (DTPw) vaccines and are now sometimes combined in addition with hepatitis B, inactivated polio and/or *H. influenzae* b vaccines. These were produced and used in many countries and are today still the most widely childhood formulations to protect simultaneously against diphtheria, tetanus and pertussis. There is little difference between production procedures of Pw vaccines. All

contain whole *B. pertussis* bacteria that have been inactivated by heat, formaldehyde treatment or other chemical procedures.

The effectiveness of Pw vaccination to prevent pertussis in children has been documented through numerous efficacy trials, starting with those conducted by the British Medical Council in the 1940s, and long-term epidemiological studies. However, not all Pw vaccines showed equal efficacy, leading to substantial differences in quality between the manufacturers. Although Pw vaccines have been administered to millions of children worldwide and have prevented hundreds of thousands of deaths, adverse events have resulted in decreased confidence in Pw vaccines during the 1970s and 1980s.

The first attempts to develop live attenuated *B. pertussis* vaccines date back to the 1980s, when [114] developed an *aroA* mutant of *B. pertussis*. This mutant strain was highly attenuated, but it failed to efficiently colonize the respiratory tract of mice. Therefore, repeated nasal immunizations of high doses were required to obtain significant protective effects using this strain. More recently, [115] have developed an attenuated vaccine strain, based on the knowledge of the specific molecular mechanisms of pertussis pathogenesis. This vaccine strain, BPZE1, contains genetic alterations that eliminate or inactivate three different *B. pertussis* toxins. The dermonecrotic toxin gene was deleted, and the PT (pertussis toxin) gene was genetically modified by altering two different codons, so that the enzymatic ADP-ribosyltransferase activity of the toxin was abolished, yielding a fully inactive protein. Finally, the *B. pertussis ampG* gene was replaced by *E. coli ampG*, which resulted in virtual absence of the tracheal cytotoxin. This strain was found to be nonpathogenic in mouse models and caused no pulmonary inflammation, yet it is able to colonize the mouse respiratory tract nearly as long as the virulent parent strain. A single nasal administration of BPZE1 induces full protection against challenge with virulent *B. pertussis* in mice [116]. Protection against challenge is dose dependent and is directly related to the ability of the vaccine strain to colonize the respiratory tract and to induce both anti-*B. pertussis* antibodies and IFN-γ-secreting cells. Moreover, in preclinical mouse studies, BPZE1 induced long-lasting protection [117]. For up to at least 1 year, a single nasal administration of BPZE1 to adult or infant mice provided total protection against nasal challenge with virulent *B. pertussis*, whereas immunity induced by two administrations of Pa (pertussis acellular) vaccine started to wane at 6 months after the last immunization. In addition to *B. pertussis*, BPZE1 vaccination also protects mice against *B. parapertussis* [115-117] and *B. bronchiseptica* infection [118].

The excellent safety profile of BPZE1 has allowed it to be classified from a safety level 2 to a safety level 1 organism in several countries. Together with its immunoprotective properties in preclinical models, this has allowed BPZE1 to be tested in phase I clinical safety trials in human volunteers. A placebo-controlled, double-blind, dose-escalating safety trial was performed and volunteers were followed up for safety and immunogenicity for 6 months [119]. Twelve subjects per dose received $\times 10^3$, $\times 10^5$ or $\times 10^7$ CFU as droplets with half of the dose in each nostril. Twelve controls received the diluent. Nasopharyngeal colonization with BPZE1 of five subjects were seen in the high dose group. Significant increases in immune responses against pertussis antigens were seen in all colonized subjects. Adverse events occurred with similar frequency in the placebo and vaccine groups and were considered trivial. It was concluded that BPZE1 is safe in healthy adults and able to transiently colonize the nasopharynx and can thus undergo further clinical development (Trial Registration: ClinicalTrials.gov, NCT01188512). Similar to the Bacille Calmette-Guérin, the only available vaccine against tuberculosis, the target population of this vaccine is the newborns in order to provide earlier protection against the most severe forms of the disease and to prime anti-pertussis immunity to be boosted later in life by Pa vaccines [120].

1.4. The background for vaccines against “ESKAPE” bacteria

Further, the emergence of MDR or even pandrug-resistant bacteria, such as MDR-*Acinetobacter baumannii*, MDR-*Pseudomonas aeruginosa* and methicillin-resistant-*Staphylococcus aureus* (MRSA) and the lack of licensed vaccines against these pathogens has resulted in significantly increased mortality rates with limited or no options for therapeutic interventions, especially for Gram-negative bacilli. Moreover, the Infectious Disease Society of America (IDSA) reported the emergence and spread of six highly dangerous pathogens named “ESKAPE” [121]: *Enterococcus faecium*, *Staphylococcus aureus*, *Klebsiella pneumoniae*, *Acinetobacter baumannii*, *Pseudomonas aeruginosa* and *Enterobacter* species, for which therapeutic options are so extremely limited. IDSA issued a “Call to Action for the Medical Community” in the hope of raising awareness [122]. Despite ongoing efforts by governments and some successes, only few new antimicrobial drugs had been approved in recent years and novel strategies for controlling “ESKAPE” bacteria are urgently needed.

1.4.1. The background for a vaccine against *A. baumannii*

A. baumannii is a Gram-negative, strictly aerobic, catalase-positive, oxidase-negative, nonfermenting, nonfastidious, rod-shaped (coccobacillus) bacterium. Bacteria of this genus lacks flagella, but exhibit twitching or swarming motility. This bacterium grows well on solid media that is used routinely in microbiology laboratories, such as sheep blood agar or tryptic soy agar, at a 37 ºC incubation temperature. These organisms form smooth, sometime mucoid, grayish white colonies; these present a colony diameter of 1.5 to 3 mm after overnight culture [123].

Nosocomial infections caused by *A. baumannii* have become a serious public health problem. This has become especially apparent due to the global emergence of MDR strains of *A. baumannii*. MDR *A. baumannii* is resistant to antibiotics from multiple classes, making the clinical management of infections caused by these strains increasingly difficult [124,125]. Moreover, the ability of *A. baumannii* to cause infections in various anatomic sites, ranging from the central nervous system and urinary tracts in hospitalized patients with invasive devices, to severe respiratory and skin and soft tissues infections, suggests the presence of diverse virulence factors [126,127].

In this context, the implementation of prophylactic vaccination, both active and passive, for the prevention of infections caused by *A. baumannii* may represent a cost-effective approach for reducing the clinical and economic burden of infectious caused by this pathogen. Moreover, using this approach, the emergence of new resistance phenotypes would be avoided, since this strategy does not rely on the use of antibiotics. Although community-acquired infections have been reported, infections caused by *A. baumannii* are mostly acquired in the hospital setting. This is a critical point when considering which populations would benefit from prophylaxis, as the targeted vaccination of hospitalized patients or patients at risk of being hospitalized who have risk factors for acquiring infections by *A. baumannii* would likely be the most cost-effective approach. Based on this idea, four patient populations at-risk for the acquisition of *A. baumannii* infection are proposed for targeted vaccination **(Fig. 9).**

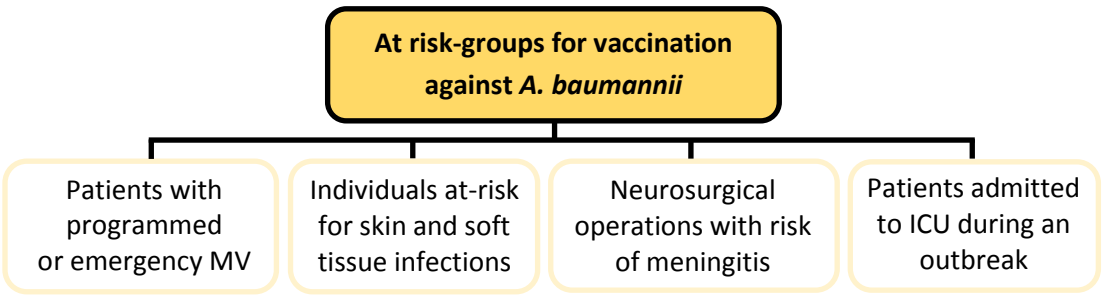

Figure 9 | Proposed high-risk population for targeted vaccination against *A. baumannii.* From [128].

As *A. baumannii* is a frequent cause of ventilator-associated pneumonia (VAP), patients who require mechanical ventilation (MV) at the time of the presentation and patients who have a high likelihood of needing MV during their clinical course are potential targets for vaccination. This includes patients who undergo programmed surgical procedures, such as cardiac, neurologic and pulmonary operations, for which MV is a part of routine post-operative care. In addition, individuals admitted urgently who may require mechanical ventilation are also at-risk for *A. baumannii* VAP. A second group of patients that may benefit form vaccination are those at risk for acquiring nosocomial skin and soft tissue infections caused by *A. baumannii*. Individuals at risk for this type of infection include patients that have sustained extensive burn injury, patients undergoing complex abdominal surgical procedures, and military personnel sustaining war-related trauma and hospitalization.

Extensive surgery, severe trauma, burn injury and war have been associated with *A. baumannii* infection, making patients with these conditions candidates for a vaccine against *A. baumannii*. After severe trauma and burn injury the immune system suffers profound alterations with simultaneous increased expression of classical inflammatory, anti-inflammatory and adaptive immunity genes [129]. Additionally, physical injury related to these events may increase the expression of Th2 lymphocytes which cause impaired cell mediated immunity and may disable critical components of protection against *A. baumannii* [130]. Macrophage activation may suffer, impairing the host defense against *A. baumannii* infection through decreased phagocytosis and secretion of cytokines, which in turn may limit the recruitment of neutrophils to the site of infection and impair the clearance of *A. baumannii* [131,132].

A third target population for immunization is patients who are at risk for *A. baumannii* meningitis. These infections are primarily associated with neurosurgical

operations, raising the possibility that patients with undergoing both programmed and emergent neurosurgical procedures in situations where *A. baumannii* infection could occur may benefit from vaccination. A final possibility is the vaccination of patients admitted to an intensive care unit in the context of an outbreak of a difficult-to-treat clone of *A. baumannii*.

Once at-risk patient populations have been identified, it must be determined when and how these patients should be vaccinated. A key factor is whether an active or passive immunization schedule would be more appropriate given the clinical scenario. Individuals for whom the risk of acquiring an infection caused by *A. baumannii* can be foreseen could be actively immunized with enough time to allow for a protective immune response to be elicited before that individual is exposed to *A. baumannii*. This would include patients undergoing programmed surgical procedures and military personnel. Patients for whom the risk of exposure cannot be foreseen, such as patients sustaining traumatic injuries or patients undergoing emergent surgery, the use of passive immunization is a more logical approach. Although passive immunization has the potential to provide almost instantaneous protective immunity, its ability to prevent bacterial diseases in the clinical setting has yet to be determined.

Experimental vaccines against *A. baumannii*

Due to the fact that some of the target populations for vaccination include critically ill patients with weakened immune systems, a crucial issue will be the ability of a vaccine to elicit an effective response in this context. Patients vulnerable to *A. baumannii* are often elderly, suffer multiple comorbidities, and are functionally impaired. Chronic inflammation and putative deficiencies in antigen presentation, humoral and cellular immunity may lead to poor vaccine responses [133]. Also, as *A. baumannii* produces a diversity of infection types, an ideal vaccine would be capable of protecting against all *A. baumannii* infections. Given the infections described above, this may require that the vaccine produces both a systemic and a mucosal response. In addition, the contributions of the cellular and humoral arms of the immune response have yet to be fully characterized. Studies performed in experimental models of *A. baumannii* infections has shown that the passive transfer of serum raised against *A. baumannii* antigens is sufficient for providing protection against infection [134-139]. Moreover, since in many cases the risk for exposure to *A. baumannii* cannot be foreseen, an ideal vaccine would induce protective immunity shortly after a single administration. This may be less problematic when passive immunization approaches

are employed, however for active vaccination a vaccine that requires a lengthy administration regimen or is slow to induce protective immunity may not be effective in cases that require the rapid elicitation of protective immunity.

Another consideration is the selection of an appropriate strategy for the design of a vaccine for active or passive immunizations. An ideal vaccine should contain antigens that are present on the bacterial cell surface, expressed during human infection, present in the majority of the *A. baumannii* strains and highly conserved at the amino acid level, if the antigen is a protein. The experimental vaccines against *A. baumannii* produced and studied so far are summarized in **Table 3.**

Table 3| Experimental vaccines against *A. baumannii*.

Antigen	Results	References
Purified antigens		
Trimeric autotransporter protein (Ata)	Passive intravenous immunization, opsonophagocytosis of *A. baumannii* with antisera, complement-dependent bactericidal activity of antisera, reduction in tissue bacterial loads after passive immunization in a mouse model of pneumonia	[134]
K1 capsular polysaccharide	Subcutaneous passive immunization in a mouse soft tissue infection model, decrease in tissue bacterial loads	[138]
Outer membrane protein A (OmpA)	Subcutaneous vaccination with an aluminium hydroxide adjuvant, protection in a diabetic mouse model of sepsis, opsonophagocytosis of *A. baumannii* with antisera, protection after passive immunization	[140]
Poly-N-acetyl-β-(1-6)-glucosamine (PNAG)	Passive intranasal/intravenous immunization, opsonophagocytosis of *A. baumannii* with antisera, reduction in tissue bacterial loads after passive immunization in a mouse model of pneumonia	[134]
Biofilm-associated protein (Bap)	Freund's adjuvant, reduction in post-infection tissue bacterial loads, protection in a mouse model of sepsis	[141]
Outer membrane protein W (OmpW)	Subcutaneous vaccination of fusion protein thioredoxin-OmpW with aluminium-based adjuvant, reduction in post-infection tissue bacterial loads, protection in a mouse model of sepsis	[142]
Multicomponent		
Outer membrane vesicles	Intramuscular vaccination with an aluminium-based adjuvant, reduction in post-infection tissue bacterial loads in mouse models of pneumonia and sepsis, protection in a mouse model of sepsis.	[137,143]
Outer membrane complexes	Intramuscular vaccination with an aluminium-based adjuvant, reduction in post-infection tissue bacterial loads, protection in mouse model of sepsis, passive protection using antisera, treatment of infected mice with antisera	[139]

Table 3 (cont.) | Experimental vaccines against *A. baumannii*.

Antigen	Results	References
Multicomponent		
Formalin-inactivated whole-cells	Intramuscular/intranasal vaccination with or without an aluminium-based adjuvant, reduction in post-infection tissue bacterial loads, protection in a mouse model of sepsis and pneumonia, passive protection using antisera.	[136,144,145]
Lipopolysaccharide-deficient whole-cells	Formalin inactivated whole-cell vaccine, intramuscular vaccination with aluminium-based adjuvant, reduction in post-infection tissue bacterial loads, protection in a mouse model of sepsis	[146]

The experimental vaccines that have been described for *A. baumannii* can be classified into two broad groups, vaccines that consist of a single purified antigen, and multicomponent vaccines. Within the first group, the outer membrane protein OmpA [140], the biofilm-associated protein Bap [141], the membrane transporter Ata [135], the K1 capsular polysaccharide [138], the membrane associated polysaccharide poly-N-acetylb-(1–6)-glucosamine [134] and the outer membrane protein OmpW [142] have been reported as good candidates due to their ability to elicit specific immune response. However, survival experiments after active immunization have only been reported for OmpA, OmpW and Bap, whose expression in strains that do not form biofilms is unclear. These vaccines present the limitation of stimulating antibodies only against injected antigens, rather than whole-cells.

The strategies employing multicomponent vaccines have included outer membrane complexes [139], outer membrane vesicles [137,143] and formalin-inactivated whole-cells [136,144,145]. Recently, a formalin-inactivated vaccine containing an LPS-deficient strain of *A. baumannii* was described [146]. This strain has a large deletion in *lpxD* and completely lacks lipopolysaccharide. LPS consists of the O-antigen, a core polysaccharide and lipid A, the moiety responsible for the endotoxin activity of LPS. Thus, this strain had extremely low levels of endotoxin activity. Multicomponent vaccines induced not only a potent immune response but also provided high levels of protection against *A. baumannii* infections in a murine model of acute lethal infection and pneumonia, some of each using both parental strains and clinical isolates.

Considering the presence of diverse virulence factors in *A. baumannii*, as well as the MDR phenotype, it is apparent that its genome readily participates in horizontal gene transfer [147]. Therefore, protection from a single component vaccine targeting resistance

or virulence determinants may be transient and elusive, and effectiveness may vary according to strain type and genotype. Nevertheless, a vaccine that targets even a limited number of *A. baumannii* strains may still prove useful.

In summary, vaccine development for *A. baumannii* has already begun, highlightening the importance of defining characteristics of the target patient populations and the desired immune response that can be used to guide effective vaccine design.

This text was adapted from [128,148].

1.4.2 The background for a vaccine against *P. aeruginosa*

P. aeruginosa belongs to the Pseudomonadaceae family, members of the Gram-negative γ-proteobacteria class, which also includes the Enterobacteriaceae and Vibrionaceae groups of bacteria. *P. aeruginosa* is a Gram-negative rod measuring 0.5-0.8 µm by 1.5-3.0 µm and possesses a polar flagellum providing motility; interestingly, loss of this flagellum may be associated with increased virulence because the flagellum activates host immunity [149]. *P. aeruginosa* is a ubiquitous organism able to survive in inanimate and animate environments. It is commonly found in soil and water but has the ability to survive using a wide variety of nutrients. In humans, it is an opportunistic pathogen, rarely causing disease in healthy individuals but colonizing and then infecting patients with compromised immune system function. Knowledge of the structure and physiology of *P. aeruginosa* is important to understand its high virulence and intrinsic ability to develop resistance to antimicrobial agents and to help develop preventive treatments.

Despite the recognition of *P. aeruginosa* is an opportunistic pathogen, no vaccine against this bacteria have come to market. *P. aeruginosa* causes serious infections in humans, particularly in the critically ill [150], the immunocompromised [151,152], those with burn wounds, or combat-related wound infections [153,154], and those with cystic fibrosis (CF) [155]. It is also one of the most frequently isolated pathogens from contact lenses-associated bacterial keratitis [156]. The multitude of intrinsic and acquired resistance mechanisms contributes to the intractable nature of many of these infections. A recent population-based study of *P. aeruginosa* bacteremia in Canada shed light on the overall incidence of serious *P. aeruginosa* infections [157]. This study reported an exponential increased risk of bacteremia after age 60, with a remarkable high annual incidence (per 100,000) of 10 in ages 60-69, 20 in ages 70-79 and 35 in ages >80, and an overall mortality rate of 29%. About a third of these cases of bacteremia were classified as

having a pulmonary source. This incidence is on par with that of invasive MRSA infections in the US in 2011, which was recently estimated to be 26 per 100,000 [158].

Pulmonary infections caused by *P. aeruginosa* generally dichotomize between acute pneumonia, usually associated with mechanical ventilation (ventilator-associated pneumonia [VAP]) and the chronic pneumonia of CF. Based on the data from the National Healthcare Safety Network from 2009-2010 [159], *P. aeruginosa* was the most commonly isolated Gram-negative pathogen and the second most common pathogen overall in the setting of VAP, accounting for 11% of cases. Of the *P. aeruginosa* VAP isolates, 33% were fluoroquinolone-resistant, 30% were carbapenem-resistant, and 18% were multidrug-resistant [159]. Notably, VAP due to *P. aeruginosa* has a particularly high attributable mortality [160].

P. aeruginosa is also a major cause of combat-related wound infections. A recent review of the Joint Theater Trauma Registry (JTTR) for infections among more than 16,000 Iraq and Afghanistan combat casualties noted that infections were mostly due to Gram-negative bacteria (48%), most commonly involving wounds (27%) or lungs (15%), and 25% of the Gram-negatives were *P. aeruginosa* [153]. In a review of all trauma casualties evacuated from the Iraqi theatre to a U.S. Navy hospital ship in 2003, there was high antibitioic resistance in *P. aeruginosa* strains causing infections, with 56% being tobramycin-resistant and 37% ceftazidime-resistant [154]. These and other similar studies suggest that *P. aeruginosa* is a major cause of combat-related wound infections that are difficult to treat due to high antibiotic resistance and also associated with high morbidity.

CF is an autosomal-recessive genetic disorder, with about 1,000 new cases diagnosed each year. Although there are approximately 30,000 patients suffering from its complications in the U.S. alone, chronic lung infection with *P. aeruginosa* accounts for most of the morbidity and mortality associated with the disease [161].

Candidates to immunization with *P. aeruginosa* vaccine would be relatively easy to identify. While some obvious populations can be identified (preoperative patients schedules for major surgery, soldiers, police, firefighters, wearers of extended-use contact lenses, CF patients), it might be reasonable to consider clinical trials involving vaccination of everyone over 60. An effective vaccine given to individuals with an increased risk for hospitalization due merely to age, and vaccinating adults soon after admission to ICUs (which is predicated on rapid immune responses) could be very cost effective.

Overall, considering the problem of hospital-acquired infections, the prominent role of *P. aeruginosa* in this setting, the problem of antibiotic resistance, and an aging population, a vaccine against *P. aeruginosa* is urgently needed.

Experimental vaccines against *P. aeruginosa*

LPS-based vaccines

LPS, the major component of the outer membrane of *P. aeruginosa*, is composed of lipid A, relatively conserved inner and outer core oligosaccharides and highly variable peripheral long chain polysaccharides (O-antigen). The differences in chemical structure of O-antigens and hence the variation in immunological reactivity of *P. aeruginosa* isolates forms the basis of its classification into more than 20 heterogeneous serotypes, with each serotype possessing subtype strains having subtle variations, leading to over 30 subtypes [162]. It is well established from animal studies that antibodies to the LPS O antigen mediate high-level immunity to *P. aeruginosa* infections [163]. However, for many of the O antigens, protective epitopes are poorly immunogenic, while non-protective O antigen epitopes often elicit the best immune responses after active vaccination [164]. To counter the O-antigen heterogeneity, multivalent vaccines have been developed to target a broader range of clinically active *P. aeruginosa* serotypes. A heptavalent O antigen vaccine prepared from LPS of seven different serotypes called Pseudogen (Parke Davis and Co.) showed efficacy in nonrandomized trials among adult cancer and burn patients in preventing fatal *P. aeruginosa* infections [165,166], but this vaccine was limited by toxicity, and studies in patients with leukemia and CF showed no benefit [167,168]. An improved LPS-based polyvalent vaccine (16 strains) was investigated in CF patients prior to *P. aeruginosa* colonization [169]. However, the vaccine failed to reduce the rate of Pseudomonas colonization when compared with the non-vaccinated control group [170]. Despite these and other efforts for more than 40 years, realization of clinically applicable LPS or O-polysaccharide-based vaccines remain elusive. Extensive serological heterogeneity, LPS-associated toxicity, cost and complexity of development of lipid free multivalent-conjugates are the major obstacles in vaccine development. Another concern for the usefulness of LPS-based vaccine is the observed inconsistency in immune responses in different species [171] that makes it difficult to predict the vaccine performance in humans. Furthermore, vaccination with a multivalent LPS O-antigen vaccine composed of antigens from serologically distinct strains within the same overall serogroup showed interference in the immunogenicity of the individual components [172].

MEP-based vaccines

Chronic infection with *P. aeruginosa* in the respiratory tract of CF patients is characterized by the conversion of the non-mucoid to the mucoid phenotype due to overproduction of mucoid exopolysaccharide (MEP; also known as alginate). The early, non-mucoid isolates are LPS-smooth and serologically typeable while the late, mucoid isolates are LPS-rough and non-typeable [173]. LPS-rough strains lack the O antigen polysaccharide (also known as O side chain) attached to the LPS core. Unlike LPS, MEP is relatively conserved between strains, which makes it an attractive vaccine antigen. The detection of higher levels of serum anti-MEP opsonophagocytic antibody titers in older CF patients that remained free of *P. aeruginosa* infection rationalized the development of MEP-based vaccines more than 20 years ago [174]. To improve immunogenicity, MEPs have been conjugated to various carrier proteins such as exotoxin A, tetanus toxoid or keyhole limpet hemocyanin (KLH) [175-177]. In mice and rabbits, these vaccine preparations successfully enhanced the MEP-specific immune responses and elicited opsonizing antibodies against heterologous MEPs. The preservation of O-acetyl groups and preventing depolymerization of MEP during the conjugate vaccine preparation resulted in broader cross-reactivity among heterologous strains [177]. Interestingly, an engineered human IgG1 monoclonal antibody to the mannuronic acid epitopes of alginate was recently shown to protect mice against acute lethal pneumonia caused by non-mucoid, LPS-smooth strains [178]. It seems MEP-based vaccines may still hold potential, though, for the chronically infected CF population.

Live attenuated vaccines

P. aeruginosa mutants having a deletion of the *aroA* gene, PAO1Δ*aroA* and PA14Δ*aroA*, which is required for the synthesis of aromatic amino acids, have proven to be highly attenuated and immunogenic in animal models [179-181]. These mutants are unable to synthesize aromatic amino acids and cannot efficiently acquire them from the host and hence can survive at detectable levels only up to 3-4 days following administration. Nasal immunization of mice with live attenuated *P. aeruginosa* PAO1Δ*aroA* (*aroA* deletion) is highly protective against acute lethal pneumonia caused by *P. aeruginosa* strains having the same LPS O antigen as the vaccine (called serotype-homologous strains); passive transfer did not protect against a less virulent strain, while active immunization did, thus suggesting that cellular immunity also played a prominent role in protective immunity [180]. Interestingly, in a murine corneal infection model, active immunization with PAO1Δ*aroA* or

passive immunotherapy with rabbit antiserum raised against PAO1Δ*aroA* protected against corneal infections caused by heterologous serogroups of *P. aeruginosa* [182]. Outer membrane antigens, but not the LPS O-antigen, were the protective component of the vaccine in this setting. PA14Δ*aroA* vaccine strain protected mice against acute lethal pneumonia caused by LPS-heterologous *P. aeruginosa* strains in the absence of serum opsonic antibodies, suggesting a T cell effect. Depletion of IL-17 before challenge of immunized mice, or absence of the IL-17 receptor, abrogated the protective efficacy of the vaccine [181]. Mucosal vaccination with a multivalent vaccine composed of live-attenuated *P. aeruginosa* strains (Δ*aroA*) induced multifactorial immune responses against diverse bacterial antigens and protected against acute fatal lung infection [183]. Effector $CD4^+$ T cells as well as opsonic antibodies directed not only against multiple O antigens but also against the more conserved LPS core and bacterial surface proteins, were generated. Furthermore, the use of multivalent live attenuated did not generate immunological interference in opsonic-antibody responses which had been observed with multivalent purified O-antigen vaccines. Thus, live attenuated vaccines provide an easy, safe and efficacious method to induce anti-*P. aeruginosa* immunity against broad range of antigens. Development of additional means to attenuated virulence while maintaining immunogenicity will further facilitate clinical realization of such vaccines.

Live-attenuated *Salmonella* strains for *P. aeruginosa* antigen delivery

Oral immunization of mice with attenuated *Salmonella enterica* serovar Typhimurium SL3261 expressing *P. aeruginosa* O11 O-antigen resulted in enhanced pulmonary bacterial clearance and increased survival time after intranasal challenge with homologous, but not heterologous, *P. aeruginosa* strains [184]. Intranasal administration of this vaccine was more effective against acute pneumonia and could also protect against *P. aeruginosa* infections after burns or eye injury [185] and against pneumonia in immunocompromised mice made leukopenic [186]. Strains in O11 serotype are common clinically and have a high prevalence of cytotoxicity so are associated with a high mortality rate [187]. Another *Salmonella* strain SL3261-based live attenuated vaccine that expressed pseudomonas outer membrane fusion protein OprF-OpRI, induced specific IgG and IgA antibodies in the respiratory mucosa after oral and systemic vaccination [188]. In a clinical trial enrolling healthy volunteers, systemic and mucosal immunization with this vaccine induced comparable levels of OprF-OprI-specific serum antibody titers. However, IgG and IgA in the lower airways were only induced following nasal or oral administration [189].

Overall, the use of *Salmonella* vaccines may be an efficient means to generate mucosal immunity.

Outer membrane proteins, flagella, pili, type III secretion system, extracellular toxins and proteases

P. aeruginosa vaccine strategies have focused on the outer membrane proteins (OMPs) OprF and OprI, which are antigenically related among all serotypes, as well as OprF/I fusion proteins. Recombinant OprI [190,191] and an OprF/I fusion protein [192] have been shown to be well tolerated in human trials. The OprF/I fusion protein vaccine [193] is currently in phase II/III clinical trials (clinicaltrials.gov, NCT01563263) in which adults are vaccinated soon after admission to ICUs. This OprF/I vaccine induces opsonic antibodies [193] as well as antibodies that inhibit IFN-γ binding to *P. aeruginosa* [194] (interfering with a virulence mechanism).

Among vaccines tested in patients with CF, there is a bivalent flagella vaccine, which showed a small but statistically significant (P=0.05) reduction in *P. aeruginosa* infection in a large randomized trial [195]. *P. aeruginosa* flagella is essential for motility, chemotaxis, invasiveness and adhesion [196-198]. The vaccine clearly seemed to work, as only strains with flagella types not included in the vaccine were isolated from patients after vaccination. It was therefore suggested that the inclusion of additional *P. aeruginosa* flagella types in future vaccine preparations may improve the efficacy of a flagella vaccine in CF patients. Unfortunately, the company involved in preparation of this vaccine (IMMUNO, Vienna, Austria) stopped production before the end of the trial [199]. A conjugate vaccine of flagellin coupled to polymannuronic acid (PMA, which contains an epitope recognized by the opsonic monoclonal antibody to alginate) elicited opsonic antibodies against mucoid but not nonmucoid strains of *P. aeruginosa*, and rabbit antisera to this PMA-flagellin vaccine showed improved clearance of both mucoid and nonmucoid strains in a murine respiratory model [200]. Importantly, antibodies elicited by the PMA-flagellin vaccine did not neutralize the TLR5-activating activity of flagellin, an important part of innate immunity flagellated microbial pathogens.

As other Gram-negative bacteria, *P. aeruginosa* expresses pili on their surface, which are polymeric assemblies of the pilin protein that assists in bacterial adhesion, biofilm formation and twitching motility. Pilin-based vaccines have shown variable efficacies to reduce bacterial adherence. Pilus antigens are serologically heterogeneous [201], and pillin alleles among CF and non-CF human isolates showed marked distinction in

allele distribution [202]. This serological heterogeneity and the hidden conserved binding site complicates the further development of pilin-based vaccines. So far there have been no human studies with pilin vaccines.

P. aeruginosa employs the type III secretion system (T3SS) to deliver effector proteins responsible for virulence, tissue injury and cytotoxicity to the cytosol of host cells. PcrV protein, a component of T3SS is located on the bacterial surface and is required for translocation of these effector proteins. Immunization with a vaccine targeting PcrV induced protective immunity in mice, decreased lung inflammation and injury in a murine lung infection model [203] and a burn mouse model [204]. A multivalent T3SS-based protein vaccine, including *P. aeruginosa* PcrV and needle tip proteins for four other Gram-negative bacteria also showed to be immunogenic [205].

Exotoxin A, an ADP-ribosyl transferase that inhibits host protein synthesis, is the most toxic virulence factor of *P. aeruginosa*. Immunization with a truncated exotoxin A subunit or DNA vaccine elicited specific antibodies and protected mice from the lethal challenge with lethal doses of wild-type exotoxin A [206-208].

Elastase and alkaline proteases interfere with the host immune system by cleaving immunoglobulins [209,210] inhibiting cytokines [211,212] and interfering with the immune cell functions [213-215]. Immunization with elastase and alkaline protease toxoids were effective in *P. aeruginosa* infection models of hemorrhagic pneumonia in minks [216], corneal ulcers [217] and burns in mice [218]. In a mouse model of *P. aeruginosa* gut derived sepsis, immunization with alkaline protease, elastase and exotoxin A provided protection when all three were used combined, but failed when each component was used alone [219].

Overall, immunization against PcrV and extracellular toxins seems efficient to block the inflammatory and cytotoxic effects induced by *P. aeruginosa* and they may thus be useful as part of multicomponent vaccines. However, none of these vaccines has yet been tested in humans.

In summary, despite intense efforts over the past few decades a marketable vaccine against *P. aeruginosa* has not yet evolved. The medical community is still waiting a vaccine to delay or prevent initial pulmonary infection in individuals with CF, as this would have significant impact and may be accomplished in the future.

This text was adapted from [220] and [221].

Passive immunotherapy with multifunctional bispecific antibodies

Increasing drug resistance to virtually all antibiotic classes, particularly within ESKAPE pathogens, is stimulating a renewed interest in pathogen-specific strategies including monoclonal antibody (mAb) technology for the most problematic microorganisms. Although mAbs offer considerable potential, *P. aeruginosa* is a challenging target for a single mAb approach. Multifunctional bispecific antibodies targeting persistence factor PsI exopolysaccharide and the serotype-independent T3SS virulence factor PcrV, designated BiS4αPa, were recently constructed [222]. This new bispecific antibody platform exhibited superior synergistic protection against *P. aeruginosa*-induced murine pneumonia compared to parent mAb combinations or other available bispecific antibody structures and supported this molecule (designated MEDI3902) as a promising clinical candidate for the prophylaxis or adjunctive treatment of *P. aeruginosa* infections. MEDI3902 completed a Phase I trial in healthy volunteers for the prevention of nosocomial pneumonia in USA (NCT02255760) on April 2015.

1.4.3 The background for a vaccine against *S. aureus*

S. aureus is a Gram-positive, catalase-positive, oxidase-negative, facultative anaerobe, perfectly spherical bacterium about 1 µm in diameter that occur in microscopic clusters resembling grapes. It forms a fairly large yellow colony on rich medium and is often hemolytic on blood agar. *S. aureus* can grow at a temperature range of 15-45 ºC and at NaCl concentrations as high as 15%. The staphylococci grow in clusters because the cells divide successively in three perpendicular planes with the sister cells remaining attached to one another following each successive division. Since the exact point of attachment of sister cells may not be within the divisional plane, and the cells may change position slightly while remaining attached, the result is formation of an irregular cluster of cells [223].

Many vaccinologists would place the need for a highly effective vaccine against *S. aureus* in the top 3-5 public health essentials. This organism is among the most frequent causes of infections in virtually all human and many animal tissues [224,225] causing considerable morbidity and mortality [226-229] and community-acquired infections in otherwise healthy people. Invasive disease is associated with 20% and higher mortality [230-233] due to a combination of rapidly evolving resistance to antibiotics [228,234-236] and multiple virulence factors **(Fig. 10).**

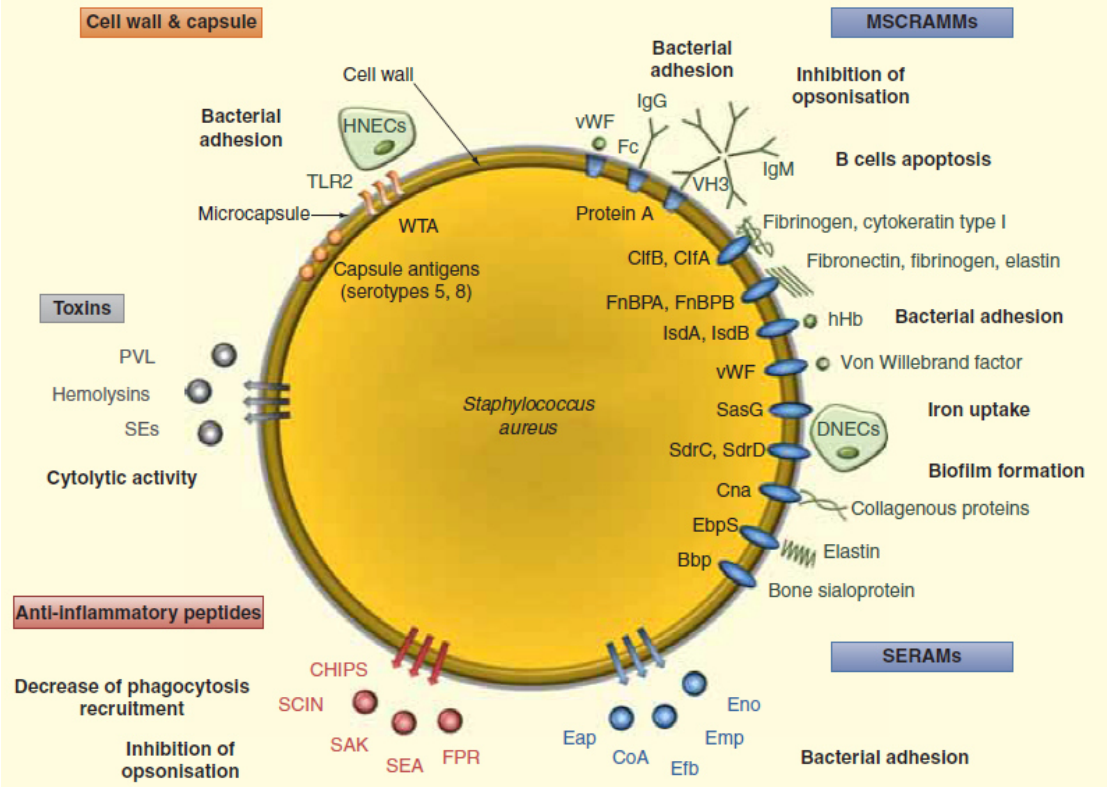

Figure 10 | Virulence factors of *S. aureus* potentially involved in the field of vaccination against *S. aureus* infections. Bbp: Bone-binding protein; CHIPS: Chemotaxis inhibitory protein of *Staphylococcus aureus*; Clf: Clumping factor; Cna: Collagen-binding protein; CoA: Coagulase; DNECs: Desquamated Nasal Epithelial Cells; Eap: Extracellular adherence proteins; EbpS: Elastin-bonding protein; Efb: Extracellular fibrinogen-binding protein; Emp: Extracellular matrix-binding protein; Eno: Enolase (laminin-binding protein); FnBP: Fibronectin-binding protein; FPR: Formyl peptide receptor; hHb: Human hemoglobin; HNECs: Human nasal epithelial cells; Isd: Iron-regulated surface determinant; MSCRAMMs: Microbial surface component recognizing adhesive matrix molecules; PVL: Panton-Valentine leucocidin; SAK: Staphylokinase; SasG: *Staphylococcus aureus* surface protein G; SCIN: Staphylococcal complement inhibitor; Sdr: Serine-aspartic acid repeat protein; SEA: Staphylococcal enterotoxin A; SEs: Staphylococcal enterotoxins; TLR2: Toll-like receptor 2; vWF: Von willebrand factor adhesion; WTA: Wall teichoic acids. From [237].

S. aureus possesses a variety of means to both colonize the host (around 20% of adults are persistent carriers of this microorganism [238]) and evade the immune system by inhibiting phagocytic uptake and killing [239,240] **(Fig. 11)**.

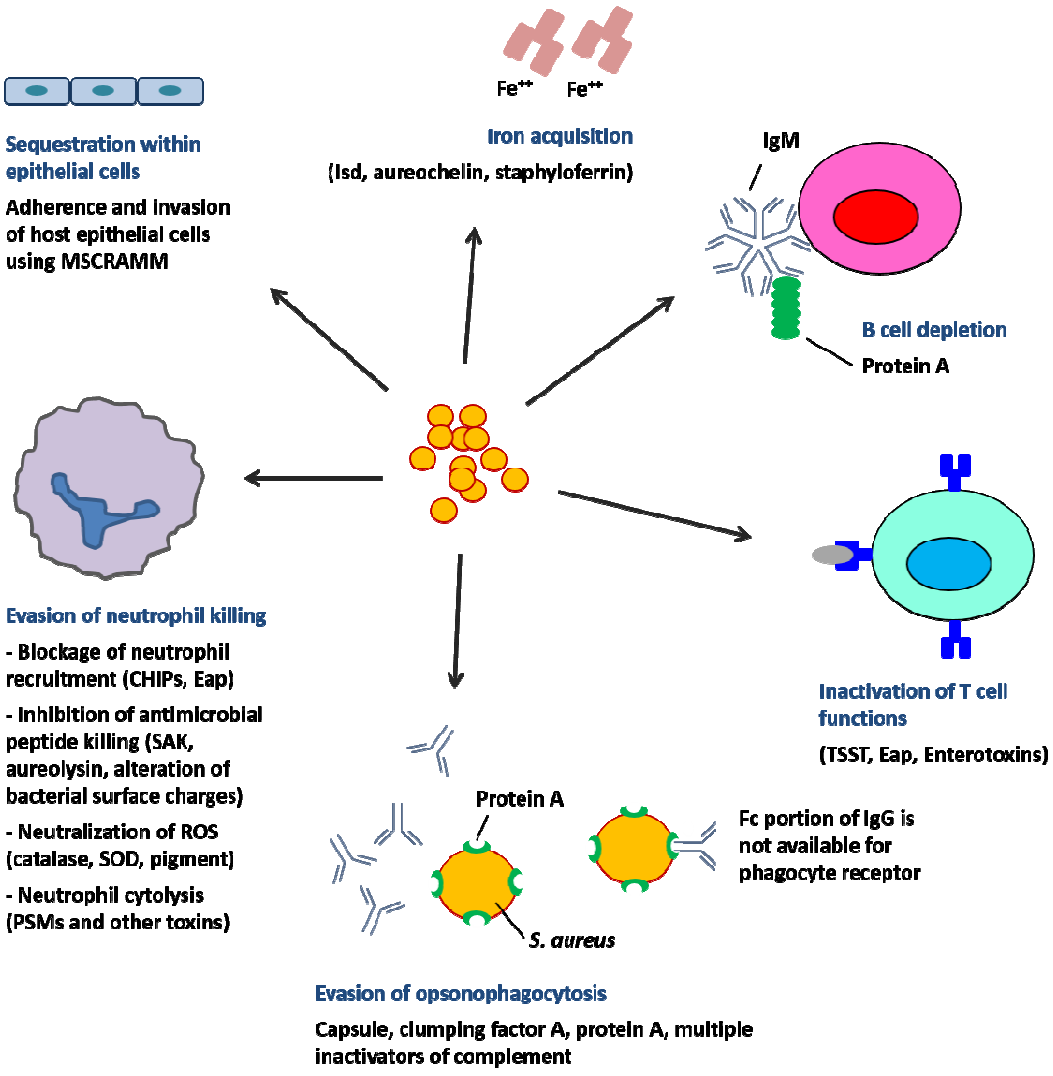

Figure 11 | *S. aureus* survival strategies during infection. CHIPS: Chemotaxis inhibitory protein of *Staphylococcus aureus*; Eap: Extracellular adherence proteins; Isd: Iron-regulated surface determinant; MSCRAMMs: Microbial surface component recognizing adhesive matrix molecules; ROS: Reactive oxygen species; SAK: Staphylokinase; SOD: Superoxide dismutase; PSM: Phenol soluble modulin; TSST: toxic shock syndrome toxin. Adapted from [239].

This bacterium has developed a large armamentarium of virulence factors to enable it to adapt and survive in a variety of host niches and as a result, to cause a multitude of diverse infection pathologies (ranging from relative mild skin infections to life-threatening wound and bloodstream infections). These are some of its most important abilities:

- Entry into the host by breaching the protective physical barriers to infection (skin, mucosa), or by entering a lesion. *S. aureus* adheres to extracellular matrix components and invades host epithelial cells using a variety of molecules that are collectively termed MSCRAMM (Microbial surface component recognizing adhesive

matrix molecules). These include fibronectin-binding proteins (FnBPA, FnBPB) [241-242], fibrinogen-binding proteins also known as “Clumping factors” (ClfA, ClfB) [243-244] and collagen-binding protein (Cna) [245]. Two factors, ClfB and wall-associated teichoic acids, have so far proven roles in nasal colonization of humans and rats [246,247].

- Obtains the essential nutrients for growth that are restricted in the host, such as iron and manganese, by expressing iron acquisition receptors, such as Iron-regulated surface determinant (IsdB) [248], and manganese uptake receptors, such as the ABC transporter MntABC [249].

- *S. aureus* has been generally recognized to survive well both inside and outside of host cells. In the extracellular milieu, *S. aureus* must overcome opsonization by complement and antibodies, which directly or indirectly leads to killing of *S. aureus* or uptake by phagocytes through Fc or complement receptors. *S. aureus* avoids opsonophagocytosis by expressing on its surface an anti-phagocytic polysaccharide capsule (CP5 or CP8) [250], ClfA [251], protein A (Spa) [252,253], Sbi (second immunoglobulin-binding protein of *S. aureus*) [254] and a number of complement inhibitors, like SCIN (Staphylococcal complement inhibitor) [255], all of which inactivate or prevent host opsonins from binding or targeting the bacterium for destruction. Specifically, Spa is known to inhibit opsonophagocytosis by binding IgG by the Fc region, which prevents classical complement fixation and recognition by the neutrophil Fc receptor [253].

- *S. aureus* can shelter within epithelial cells, endothelial cells, and even macrophages [256]. By contrast, neutrophils present a more formidable challenge to *S. aureus*. *S. aureus* deploys a number of strategies to resist neutrophil killing. First, it secretes two molecules, CHIP (Chemotaxis inhibitory protein) and Eap (Extracellular adherence protein), which respectively block neutrophil recognition of chemotactic factors [257] and neutrophil binding to endothelial adhesion molecule ICAM-1 [258]. Inhibition of ICAM-1 binding prevents leukocyte adhesion, diapedesis, and extravasation from the bloodstream to the site of infection. *S. aureus* also mediates defense against ROS (reactive oxygen species), RNS (reactive nitrogen species) and antimicrobial peptides that are unleash by neutrophils at the site of infection. *S. aureus* deploys a large number of antioxidant enzymes (e.g. catalase, pigment, superoxide dismutase) that neutralize ROS and RNS [253] and

antimicrobial peptides are degraded by aureolysin [259] and neutralized by SAK (staphylokinase) [260]. Also, *S. aureus* counters by secreting specific toxins [261], which lyse neutrophils. The phenol soluble modulin (PSM) is a group of bacterial peptides previously described in *S. epidermidis*, which induce inflammation and neutrophil cytolysis. The virulence role of PSM peptides has been confirmed in a CA-MRSA skin infection model [262].

- In addition, *S. aureus* can evade immune killing by producing multiple toxins that are either lethal to immune cells, such as alpha toxin and Panton-Valentine leucocidin (PVL), or act as superantigens, such as toxic shock syndrome toxin (TSST) and staphylococcal enterotoxin B (SEB) [263-265]. The mechanism underlying evasion of adaptive immune response is poorly understood, however studies have shown that staphylococcal enterotoxins, TSST, and Eap (a MHC class II analog) could all alter T cell functions by targeting the T cell receptor activation pathway [266,267].

- Spa has been shown to deplete splenic marginal zone B cells, which are precursor to B cells [268]. The results could be poor generation of specific B cell response. This mechanism, coupled with strategies described above to block effective antibody binding to bacterial surface and inactivation of T cell functions, could had been construed as a tactic devised by *S. aureus* to prevent development of long-term memory and be important underlying reasons why this pathogen has the ability to infect the human host repeatedly throughout life.

While several vaccines have shown efficacy in preclinical models, and despite of ongoing efforts, there is no licensed vaccine against *S. aureus*, because no human clinical trial has yet been well succeeded **(see Table 4)**.

Table 4| Recent phase II and III clinical trials of passive and active immunization for *S. aureus* and coagulase negative staphylococci.

Compound	Product	Phase	Study design	Results
Active Immunization				
StaphVax (NABI Biopharmaceuticals) [269]	Bivalent vaccine of capsular polysaccharide (CP) 5 & 8 conjugated individually to recombinant exoprotein A	Phase III	Randomized, double-blind, placebo-controlled trial of StaphVax in prevention of *S. aureus* bacteremia in hemodialysis dependent adults (*n* = 1804)	Efficacy in reduction of *S. aureus* bacteremia at 54 weeks non-significant (*P*=0.23); post-hoc efficacy estimate at 40 weeks: 57% (*P*=0.02)
V710 (Merck Sharp & Dohme Corp.) [230]	IsdB	Phase III	Randomized, double-blind, placebo-controlled, event trial of efficacy of V710 to prevent major *S. aureus* infection in adults undergoing median sternotomy (*n* = 8031)	Study stopped prematurely by data monitoring committee; no significant efficacy. Vaccine recipients who developed *S. aureus* infection were 5 times more likely to die than control recipients who developed *S. aureus* infection (23.0 *vs* 4.2 per 100 person-years)
Passive Immunization - Treatment				
Aurexis Tefibazumab (Bristol-Myers Squibb) [270]	Humanized monoclonal anti-clumping factor A antibodies	Phase II	Randomized, double-blind, placebo-controlled trial of standard treatment plus either Aurexis or placebo (*n* = 63)	No differences in adverse events or rate of death, relapse, or complications
Altastaph (NABI Biopharmaceuticals) [271]	Pooled human anti-capsular polysaccharide (CP) types 5 & 8 antibodies	Phase II	Randomized, double-blind, placebo-controlled trial of standard treatment plus Altastaph or placebo for *S. aureus* bacteremia in adults (*n* = 40)	No significant mortality difference; shorter length of stay in Altastaph *vs* placebo (9 days *vs* 14 days; *P*=0.03)
Aurograb (NeuTec Pharma) (not published in peer-reviewed journal)	Single-chain antibody variable fragment against ABC transporter component GrfA	Phase III	Unpublished by sponsor	Addition of Aurograb to standard therapy for life-threatening staphylococcal infections failed to show efficacy

Table 4 (cont.) | Recent phase II and III clinical trials of passive and active immunization for *S. aureus* and coagulase negative staphylococci.

Compound	Product	Phase	Study design	Results
Passive Immunization - Prevention				
MEDI4893, SAATELLITE (MedImmune LLC) [272]	A human monoclonal antibody against *S. aureus* alpha toxin	Phase II	Randomized, double-blind, placebo-controlled, single-dose, dose-ranging study of the efficacy and safety of MEDI4893 for prevention of pneumonia caused by *S. aureus* in mechanically ventilated adult subjects.	(Recruiting)
Altastaph (NABI Biopharmaceuticals) [273]	Immune serum from subjects vaccinated with StaphVax	Phase II	Randomized, double-blind, placebo-controlled trial of Altastaph or placebo for prevention of nosocomial *S. aureus* infections in very low birth weight babies (*n* = 206)	High levels of antibodies; no difference in rate of invasive *S. aureus*
Veronate (Bristol-Myers Squibb) [274]	Pooled human IgG to ClfA (*S. aureus*) and SdrG (*S. epidermidis*)	Phase III	Double-blind, placebo-controlled trial of INH-21 *vs* placebo for prevention of staphylococcal late-onset sepsis in infants with birth weights 500 to 1,250 g (*n* = 1983)	No difference in staphylococcal late-onset sepsis (5% INH-21 vs 6% placebo; *P*=0.34)
Pagibaximab (Biosynexus Incorporated) [275]	Humanized mouse chimeric mouse monoclonal antibody against lipoteichoic acid	Phase II	Randomized, double-blind, placebo-controlled dose ranging study for prevention of staphylococcal infection in patients with birth weights 700 to 1,300 g (*n* = 88)	Definite staphylococcal sepsis occurred in 0% (90 mg/kg), 20% (60 mg/kg), and 13% (placebo) (*P*=0.11). Findings not confirmed in Phase III trial

While some studies have identified genes commonly found among a large majority of clinical isolates [276,277] no single essential virulence factor needed for infection in most settings that can be targeted as a vaccine is known, exceptions being diseases mediated

purely by toxins such as toxic-shock syndrome toxin [278,279], exfoliative dermatitis and mediators of staphylococcal food poisoning [280,281]. Extensive genetic [282] and hence antigenic variability in many potential antigens precludes their use as vaccines. Variability in the level of expression leading to a highly variable surface [283,284] provides an easy means for bacterial escape from immune effectors by merely reducing levels of antigens to below that needed for elimination or killing of bacteria. *S. aureus* is also notorious for causing frequent reinfections, indicating natural infection does not readily induce acquired immunity that can be defined and used to guide vaccine development.

In many reviews [285-290], the major point made is that we have insufficient insight into the basis for virulence and immunity of this organism to rationally design vaccines targeting known protective immune effectors. The biological complexity based on redundant and wide variety of virulence factors, the undefined mechanisms of host immunity, the high recurrence rates seen in humans, particularly with MRSA infections [291-293] and evidence for inadequate immune responses following infection [294-297] may be insurmountable challenges to finding a broadly-effective vaccine for *S. aureus*.

Because vaccine results obtained with mice, rats and rabbits do not predict human immunity, animal studies cannot be improved for vaccine development [298]. As all of the failed *S. aureus* vaccines tested to date in humans [230,299-301] have shown reductions in bacterial burdens and even protection from lethality [302,306] in many animal models, it is clear these models have no predictive capacity for effectiveness in humans. Therefore, animal and human susceptibility and the course of *S. aureus* infections are just too damn different from lab animals, and few other animals are routinely available to study vaccines.

Overall, developing a universal vaccine for *S. aureus* is a top priority but to date we have only had failures in human clinical trials. Given the plethora of bacterial virulence factors, broad range of humans at-risk for infections, lack of any information regarding immune effectors mediating protection for any manifestation of *S. aureus* infection and overall competence of this organism as a colonizer, commensal and pathogen, it seems that getting a universal vaccine will be a very difficult task.

This text was adapted from [239,285,286,307].

1.5. Glutamate racemase, D-amino acid transaminase and the mechanism of peptidoglycan formation

The bacterial cell wall is a highly cross-linked polymeric structure consisting of repeating peptidoglycan units of disaccharides (joined in β1-4 linkage) which contain a novel pentapeptide substitution [308]. Cross-linking occurs through transpeptidation of the peptide linkages between adjacent glycan strands resulting a structural mesh that acts as a cellular skeleton that protects the cell from rupture due to the osmotic pressure gradient. Inhibition of cell wall production renders the bacteria susceptible to lysis by osmotic pressure and inhibitors that target this pathway are generally bactericidal.

The conversion of glucosamine-1-phosphate to UDP-N-acetylglucosamine (UDP-GlcNAc) is the first committed step to peptidoglycan synthesis and culminates with the production of UDP-N-acetyl muramic acid-pentapeptide (UDP-MurNAc-pentapeptide) **(Fig. 12)**. A key feature of the peptidoglycan is the incorporation of D-amino acids, D-glutamate (D-Glu) by the ligase MurD and D-alanine (D-Ala) as a dipeptide formed by D-Ala-D-Ala ligase, which is a substrate of the ligase MurF. It is presumed that these unusual residues provide a defense against hydrolysis of the bacterial capsule, as host proteases are unable to recognize sequences containing D-amino acid residues. While there is some variation in the peptide composition of the pentapeptide intermediate, incorporation of D-Glu as the second amino acid is strictly conserved across the bacterial kingdom [308].

Glutamate racemase (MurI), a member of the co-factor-independent, two-thiol-based family of amino acid racemases that converts L-glutamate (L-Glu) to D-Glu, has been implicated in the production and maintenance of sufficient D-Glu pool levels required for the early phases of peptidoglycan biosynthesis. This enzyme was the subject of four decades of research, and it is now evident that it is conserved and essential for growth across the bacterial kingdom.

Using the mutant strain WM355 of *Escherichia coli* [309], which requires D-Glu for growth, MurI activity was unambiguously assigned to an open reading frame encoding a protein of 289 amino acids in the 90 min region of the chromosome, near the *murA* and *murB* genes, but quite distant from the remaining Phase I peptidoglycan biosynthetic genes [310]. Disruption of this gene, denoted *murI*, was found to alter the peptidoglycan precursor pool distribution and ultimately lead to cellular lysis [311]. Subsequent studies

confirmed the essentiality of *murI* for cellular growth through more detailed genetic dissection of the WM335 mutant strain [312].

D-amino acid transaminase (Dat) is the enzyme that catalyzes the conversion of D-Ala to D-Glu. Dat activity is found in various Gram-positive bacteria, including *Bacillus* [313-315], *Staphylococcus* [316] and *Listeria* [317].

The dawn of the genomic era rapidly established the presence of MurI in all species of bacteria encoding a cell wall and its essential role in peptidoglycan biosynthesis has been confirmed in species spanning the bacterial kingdom, including Gram-positive bacteria that encode the Dat pathway for D-Glu production [318-321]. Furthermore, the Dat gene in *S. aureus* has shown to be non-essential based on a high frequency of transposon insertions mapped through the gene encoding this activity [318].

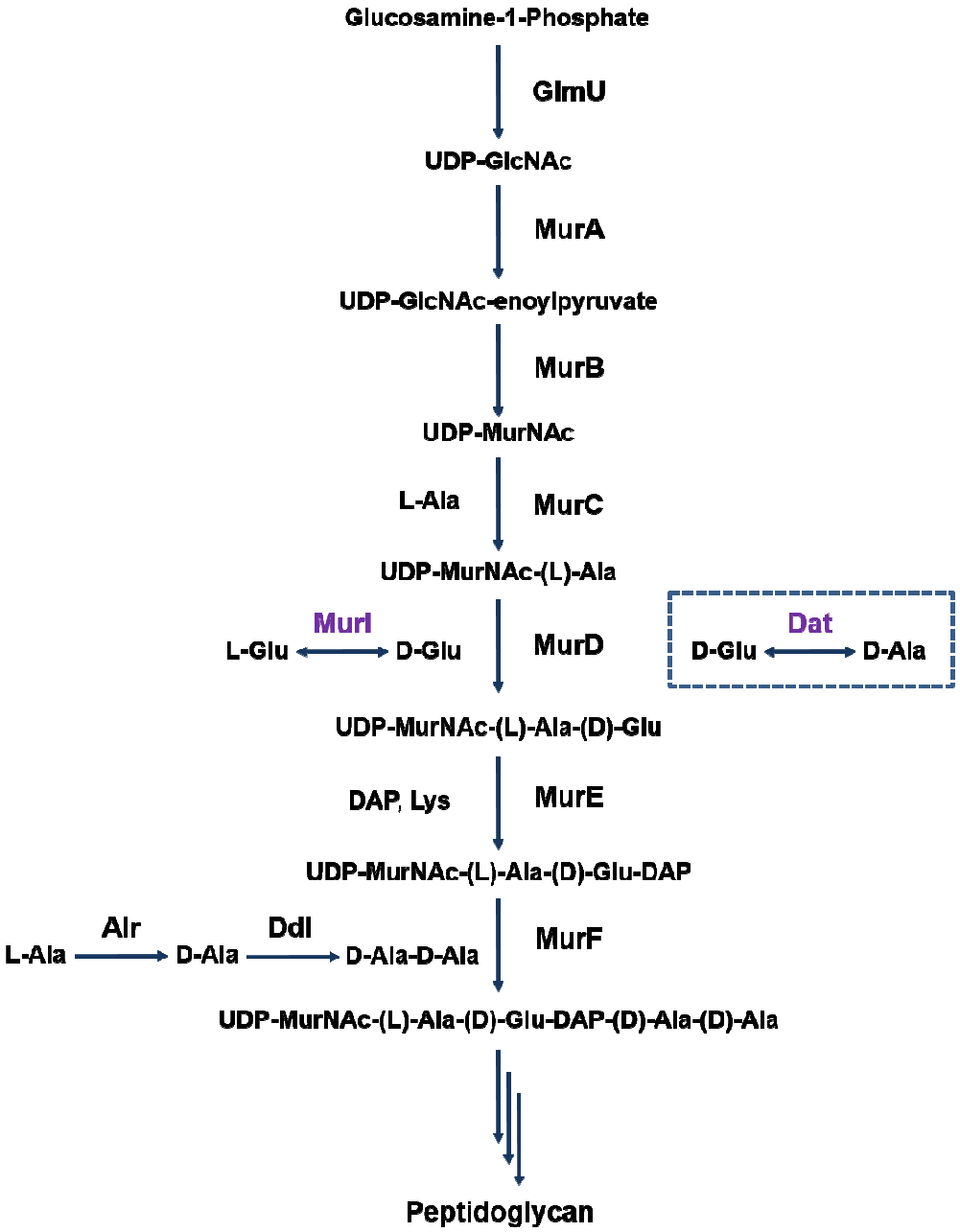

Figure 12 | Schematic of Phase I peptidoglycan biosynthesis. MurI and Dat are depicted in violet. Adapted from [308].

2. HYPOTHESIS AND OBJECTIVES

2. HYPOTHESIS AND OBJECTIVES

D-Glu is an essential component of bacterial peptidoglycan and is found in the cell wall of virtually all bacteria [308]. Earlier work suggests that MurI, enzyme that converts L-Glu to D-Glu for the synthesis of peptidoglycan, can be targeted for antibiotic development [322,323]. However, it is worth noting that none of the previous work proposed the usefulness of MurI mutants as live attenuated bacterial vaccines.

Here it is proposed a novel platform for the generation of effective live attenuated bacterial vaccines composed of D-Glu auxotrophic strains, which can be obtained through the inactivation of the gene (or genes) encoding MurI and also the gene (or genes) coding for Dat capable of catalysing the interconversion of D-Ala to D-Glu **(Fig. 13)**. It was hypothesized that the strict requirement of sufficient D-Glu pool levels impairs the correct replication of D-Glu auxotrophic bacteria in the mammal host, and this could result in a remarkable level of attenuation and high effectiveness of these strains as whole-cell vaccines.

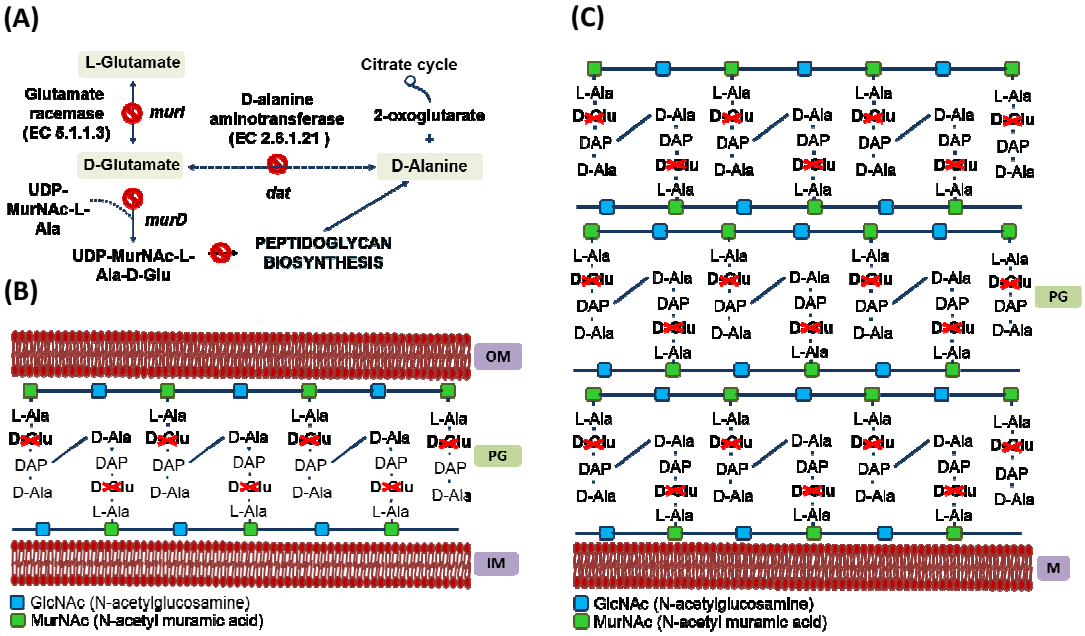

Figure 13 | D-Glu auxotrophy is achieved by inactivation of D-Glu producing enzymes. A, Sequence of metabolic processes culminating in the formation of D-Glu and the incorporation in the bacterial peptidoglycan. **B,** Cell wall structure of a Gram-negative bacterium (non-depicted lipopolysaccharides and proteins). **C,** Cell wall structure of a Gram-positive bacterium (non-depicted teichoic acids and proteins). PG: peptidoglycan. OM: outer membrane. IM: inner membrane. M: cytoplasmic membrane.

Further, the emergence of MDR-*A. baumannii*, MDR-*P. aeruginosa* and MRSA and the lack of licensed vaccines against these pathogens has resulted in significantly increased mortality rates with limited or no options for therapeutic interventions [121,285,286].

Hence, by creating MurI$^-$ (and MurI$^-$Dat$^-$) mutants, we took advantage of this technology to create three prototypes of experimental vaccines against *A. baumannii*, *P. aeruginosa* and *S. aureus* using D-Glu auxotrophic strains. Once obtained, we demonstrated their reliable efficacy as live vaccines in a mouse model of acute lethal infection. More importantly, we demonstrated that this strategy has potential application to any bacterial pathogen.

In this Doctoral Thesis, the following objectives were established:

- Obtain MurI$^-$ mutants of *A. baumannii* and *P. aeruginosa*, auxotrophic for D-Glu;
- Obtain a MurI$^-$Dat$^-$ mutant of *S. aureus,* auxotrophic for D-Glu;
- Characterize MurI$^-$ or MurI$^-$Dat$^-$ mutants of *A. baumannii*, *P. aeruginosa* and *S. aureus* at the phenotypic and ultrastructural level;
- Optimize and implement models of acute lethal infection for testing wild-type *A. baumannii*, *P. aeruginosa* and *S. aureus* strains, in BALB/c and C57BL/6 mice;
- Estimate the level of attenuation of MurI$^-$ or MurI$^-$Dat$^-$ mutants using the previously optimized model of acute lethal infection;
- Determine the immunogenic potential of MurI$^-$ or MurI$^-$Dat$^-$ mutants used as vaccines, by measuring IgM and IgG immunoglobulins and exploring the nature of T cell responses generated in the vaccinated individuals;
- Examine the cross-reactivity of IgG antibodies produced against heterologous strains not included in the vaccine compositions;
- Determine anti-*A. baumannii*, -*P. aeruginosa* and -*S. aureus* vaccine efficacy against acute lethal infection by challenging vaccinated mice with several genetically and epidemiologically unrelated bacterial isolates, including

multidrug-resistant, virulent and high-risk clones such as *S. aureus* USA300LAC;

- Evaluate the protection conferred by the passive transfer of antibodies to naïve mice, obtained from mice administered these vaccines;
- Exploit alternative routes of vaccine administration;
- Assess *in vivo* safety of D-Glu auxotrophic bacterial vaccines through monitoring blood clearance of MurI^{-} or MurI^{-}Dat^{-} mutants once administered to mice;
- Assess environmental safety of D-Glu auxotrophic bacterial vaccines through evaluation of phenotypic stability and persistence of MurI^{-} or MurI^{-}Dat^{-} mutants, when compared to their wild-type homologues.

3. MATERIALS AND METHODS

3. MATERIALS AND METHODS

3.1. Bacterial strains, growth conditions and reagents

All bacterial strains and plasmids used in this study are listed in **Table 5**. We selected *A. baumannii* ATCC 17978, *P. aeruginosa* PAO1 and *S. aureus* 132 for genetic manipulation to generate the indicated mutant strains, creating mutant derivatives with in-frame deletions in MurI or MurI plus Dat coding genes. *A. baumannii* ATCC 17978 and *P. aeruginosa* PAO1 are reference strains. *S. aureus* 132 is an MRSA strain isolated from a patient at the Microbiology Department of the Clínica Universitaria de Navarra (Pamplona, Spain). This strain is able to produce alternative biofilm matrix depending on environmental conditions consisting of proteins or exopolysaccharides [324]. All *E. coli*, *A. baumannii* and *P. aeruginosa* strains were grown in Luria-Bertani broth (LB: 10 g/L tryptone, 5 g/L yeast extract, 10 g/L sodium chloride) or on LB agar at 37 ºC unless otherwise stated. *S. aureus* strains were grown in Tryptic Soy Broth (TSB) or in TSB agar at 37 ºC unless otherwise stated. Ampicillin, kanamycin, gentamycin and erythromycin, when appropriate for plasmid selection, were added at a concentration of 100, 50, 30 and 10 µg/mL, respectively. X-Gal (5-bromo-4-chloro-3-indolyl β-D-galactopyranoside) was used at a concentration of 150 µg/mL. All primers and chemicals were purchased from Sigma-Aldrich, unless mentioned.

Table 5 | Strains and plasmids used in the present work.

Strain or plasmid	Relevant features	Source or reference
***A. baumannii* strains**		
ATCC 17978	Reference strain	ATCC
ATCC 17978 Δ*murI1*	ATCC 17978 derivative, ΔA1S_0380	This study
ATCC 17978 Δ*murI2*	ATCC 17978 derivative, ΔA1S_3398	This study
ATCC 17978 Δ*murI1* Δ*murI2*	ATCC 17978 derivative, ΔA1S_0380 ΔA1S_3398	This study
ATCC 19606	Reference strain	Laboratory collection
AbH12O-A2	Multidrug-resistant clinical isolate from an outbreak, Spain, 2006-2008	[325]
Ab307-0294	Encapsulated clinical isolate from blood, Buffalo, NY, 1994	[326]
***P. aeruginosa* strains**		
PAO1	Reference strain	CECT
PAO1 Δ*murI*	PAO1 derivative, ΔPA4662	This study
PA14	Hypervirulent strain from burn infection	[327]
PA21_ST175	Multidrug-resistant high-risk clone	[328]
PA12142	Liverpool epidemic strain isolate from a CF patient	[329]

Table 5 (cont.) | Strains and plasmids used in the present work.

Strain or plasmid	Relevant features	Source or reference
***P. aeruginosa* strains**		
PA51441321	A Coruña Hospital isolate from bronchiectasis patient; Mem^R, Fep^R	Laboratory collection
PA51442390	A Coruña Hospital isolate from a CF patient; mucoid phenotype; Mem^R	Laboratory collection
LES400	Liverpool epidemic strain from a CF patient with chronic infection	[330]
LES431	Liverpool epidemic strain from a non-CF parent with pneumonia	[330]
PA28562	A Coruña Hospital isolate from bronchiectasis patient; mucoid phenotype;	Laboratory collection
***E. coli* strains**		
S17-1	*recA*$^-$, *thi*$^-$, *pro*$^-$, *hsdR*$^-$ (RP4-2Tc::Mu Km::Tn7)	[331]
TG1	*supE thi-1 Δ(lac-proAB) Δ(mcrB-hsdSM)5, ($r_K^-m_K^-$)[F' traD36 proAB lacI^{q}ZΔM15]*	[332]
DC10β	Δ*dcm* in the DH10B background [F- mcrA Δ(*mrr-hsdRMS-mcr*BC) *Φ80dlacZΔM15 ΔlacX74 endA1 recA1 deoR Δ(ara,leu)7697 araD139 galU galK nupG rpsL λ-]*	[333]
***S. aureus* strains**		
132	MRSA clinical isolate	[324]
132 Δ*murI*	132 derivative, Δ*murI*	This study
132 Δ*dat*	132 derivative, Δ*dat*	This study
132 Δ*murI* Δ*dat*	132 derivative, Δ*murI* Δ*dat*	This study
132 Δ*spa*	132 derivative, Δ*spa* protein A-deficient	[324]
RN4220	restriction-deficient NCTC 8325 derivative, *rsbU*$^-$, *agr*$^-$	[334]
FPR3757 (USA300LAC)	Community-acquired MRSA strain from wrist abscess; USA300 epidemic clone	[335]
RF122	ST151 and CC151 strain from bulk milk (Ireland)	[336]
ED133 (formerly 1174)	ST133 and CC133 strain from ovine mastitis (France)	[337]
ED98	ST5 and CC5 strain from broiler chicken (skeletal infection, United Kingdom)	[338]
Plasmids		
pMo130	Km^R; *oriT*$^+$ *sacB*$^+$ *xylE*$^+$, gene replacement vector for allelic exchange in Burkholderia; ColE1 *ori*	[339]
pEX18Gm	Gm^R; *oriT*$^+$ *sacB*$^+$, gene replacement vector with MCS from pUC18	[340]
pMAD	Amp^R; Ery^R, *bgaB*$^+$, *E. coli/S. aureus* shuttle vector that is temperature – sensitive in *S. aureus*	[341]

3.2. Construction of *A. baumannii* MurI⁻, *P. aeruginosa* PAO1 MurI⁻ and *S. aureus* MurI⁻Dat⁻ mutants

Mutant alleles, designated Δ*murI1* and Δ*murI2* in *A. baumannii* ATCC 17978, Δ*murI* in *P. aeruginosa* PAO1, and Δ*murI* and Δ*dat* in *S. aureus* 132 with in-frame deletions corresponding to *murI1*, *murI2*, *murI*, *murI* and *dat* genes were constructed. These mutant alleles were replaced, either singly or together, by the corresponding wild-type alleles using the previously described allelic exchange systems with the pMo130, pEX18Gm and pMAD plasmids in *A. baumannii*, *P. aeruginosa* and *S. aureus*, respectively. Primers used are listed in **Table 6**. Restrictions enzymes, GoTaq DNA polymerase and T4 DNA Ligase were purchased from Promega (Biotech Ibérica, SL) and used as recommended by the supplier. The Expand High Fidelity PCR System was obtained from Roche (Roche Farma, S.A.). Plasmid DNA isolation from *E. coli* was achieved using the Wizard *Plus SV* Minipreps DNA Purification System, from Promega or the Plasmid Midi Kit, from Qiagen (IZASA, S.A.). Genomic DNA from *A. baumannii* and *P. aeruginosa* was obtained using the High Pure PCR Template Preparation Kit, from Roche. Genomic DNA from *S. aureus* was obtained using the Wizard Genomic DNA Purification Kit, from Promega. Electrotransformation of *A. baumannii*, *E. coli, P. aeruginosa* and *S. aureus* was performed according to the Gene Pulser Xcell Electroporation System instructions, Biorad (Bio-Rad Laboratories, S.A.) or protocols described elsewhere [333]. The GeneRuler 1 kb Plus DNA Ladder (Thermo Fisher Scientific) was used as molecular weight marker.

Table 6 | Oligonucleotides designed for the present work.

Analysis, gene or primer	Orientation	Primer sequence (5'-3')
Unmarked deletion of *A. baumannii murI1* and *murI2* genes		
UP_*murI1*(NotI)	Forward	cccgcggccgcggggtcctgcacctacgatga
UP_*murI1*(BamHI)	Reverse	cccggatccgggacctccaatacctgaatc
DOWN_*murI1*(BamHI)	Forward	cccggatccggggctctgttgtaggcattc
DOWN_*murI1*(SphI)	Reverse	cccgcatgcgggcatccttgtgattgcatt
UP_*murI2*(NotI)II	Forward	cccgcggccgcgggttggtcaggtccttgttg
UP_*murI2*(BamHI)II	Reverse	cccggatccgggtacagccgtcatggtgtt
DOWN_*murI2*(BamHI)	Forward	cccggatccgggacgcgtttacctgtagaa
DOWN_*murI2*(SphI)	Reverse	cccgcatgcgggagcggtacaactaattgg
EXTfw_*murI1*	Forward	gcaattaggcacttgagg
EXTrv_*murI1*	Reverse	atacgctcaggttgcatc
INTfw_*murI1*	Forward	agcctatgttccgtatgg
INTrv_*murI1*	Reverse	tcaaccagtgtgaattgg
EXTfw_*murI2*	Forward	ccgattggaatgattgac

Table 6 (cont.) | Oligonucleotides designed for the present work.

Analysis, gene or primer	Orientation	Primer sequence (5'-3')
Unmarked deletion of *A. baumannii murI1* and *murI2* genes		
EXTrv_*murI2*	Reverse	agagcattctggtcgaag
INTfw_*murI2*	Forward	tagcaatagaaccagcgg
INTrv_*murI2*	Reverse	ttgtgccgttacagcttc
Unmarked deletion of *P. aeruginosa murI* gene		
UP_*murI*(HindIII)II	Forward	cccaagcttgggggcaatccgccgtatatc
UP_*murI*(NotI)	Reverse	cccgcggccgcgggggcgttgcccgcagacgg
DOWN_*murI*(NotI)	Forward	cccgcggccgcgggtcgttcctggcagacgtg
DOWN_*murI*(XbaI)	Reverse	ccctctagagggtccgctctcgcagtccga
EXTfw_*murI*	Forward	gtatcggcaaggtggagt
EXTrv_*murI*	Reverse	gaatggcttgatcgagtc
INTfw_*murI*	Forward	atccgaatcgttgctcta
INTrv_*murI*	Reverse	acaatacgcgctccagct
Unmarked deletion of *S. aureus murI* and *dat* genes		
UP_*murI*(MluI)	Forward	cccacgcgtgggccgaaacaaaaaacagta
UP_*murI*(NotI)	Reverse	cccgcggccgcgggattcggtcatccttactt
DOWN_*murI*(NotI)	Forward	cccgcggccgcggggaggatttttaatgaaag
DOWN_*murI*(BglII)	Reverse	cccagatctgggtttcttccattgaacttc
UP_*dat*(MluI)	Forward	cccacgcgtgaaacgtattcatatgat
UP_*dat*(NotI)	Reverse	cccgcggccgcatattattcctccacgca
DOWN_*dat*(NotI)	Forward	cccgcggccgcaattctttcatcatattt
DOWN_*dat*(BglII)	Reverse	cccagatctgcgaatctaaactcggta
EXTfw_*murI*	Forward	gcttgccctaaaggtattcc
EXTrv_*murI*	Reverse	gggccactcatacttatgac
INTfw_*murI*	Forward	tgtcggaggtttgacagtag
INTrv_*murI*	Reverse	ctaacttcacgagccgtttc
EXTfw-seq-UP_*murI*	Forward	atgactgaacaatcagtgaa
EXTrv-seq-DOWN_*murI*	Reverse	tgatggtgccatgtaaagtt
EXTfw_dat	Forward	gtcatgggtgacgtgacaac
EXTrv_dat	Reverse	gcaccacctgctgaatcaag
INTfw_dat	Forward	tattcaagcaacgcgtggtg
INTrv_dat	Reverse	agttgacgtgtaattgggcc
EXTfw-seq-UP_*dat*	Forward	gccggttgtaacagaagatg
EXTrv-seq-DOWN_*dat*	Reverse	caattgccgggtctgcaatc

3.2.1. *A. baumannii* ATCC 17978 Δ*murI1*, ATCC 17978 Δ*murI2* and ATCC 17978 Δ*murI1* Δ*murI2* mutants

In detail, *A. baumannii* DNA fragments of about 1 kb corresponding to the upstream and downstream regions of *murI1* and *murI2* were amplified by PCR with the combination of primers UP_*murI1*(NotI)/UP_*murI1*(BamHI), DOWN_*murI1*(BamHI)/DOWN_*murI1*(SphI), UP_*murI2*(NotI)II/UP_*murI2*(BamHI)II and DOWN_*murI2*(BamHI)/DOWN_*murI2*(SphI). The upstream fragments obtained were digested with NotI and BamHI restriction enzymes; downstream fragments were digested

with BamHI and SphI. Digested products were ligated into pMo130 **(Fig. 14),** which was previously linearized with NotI and SphI and the recombinant plasmids pMo130_UP/DOWN_*murI1* and pMo130_UP/DOWN_*murI2* obtained were independently transformed in *E. coli* S17-1 by electroporation. S17-1 transformants were selected on LB containing kanamycin, sprayed with pyrocatechol, and only yellow colonies expressing the *xylE* reporter gene were analyzed by PCR to confirm the presence of the recombinant plasmids, that were then individually introduced in *A. baumannii* ATCC 17978 by electroporation. *A. baumannii* bright yellow and kanamycin-resistant colonies, representing the first crossover event, were grown on LB supplemented with 15% sucrose for 6 hours, and then plated on the same agar medium. The resulting white colonies (after spraying with pyrocatechol) were analyzed by PCR (using the combination of primers EXTfw_*murI1*/EXTrv_*murI1*, EXTfw_*murI2*/EXTrv_*murI2*, INTfw_*murI1*/INTrv_*murI1*, INTfw_*murI2*/INTrv_*murI2*) to confirm the second crossover event resulting in Δ*murI1* and Δ*murI2* genotypes, produced by the allelic exchange of plasmids pMo130_UP/DOWN_*murI1* and pMo130_UP/DOWN_*murI2* with the *murI1* and *murI2* alleles, respectively **(Fig. 15).** The pMo130_UP/DOWN_*murI2* plasmid was also introduced in the ATCC 17978 Δ*murI1* mutant previously obtained, by electroporation. Transformant bright yellow and kanamycin-resistant colonies, were then grown on LB containing 15% sucrose and supplemented with 10 mM D-Glu for 6 hours, and plated on the same agar medium. The resulting white colonies (after spraying with pyrocatechol) were picked from agar plates containing 10 mM D-Glu and inoculated in patches at comparable locations on LB agar plates with and without 10 mM D-Glu. Presumptive colonies with the Δ*murI1* Δ*murI2* double mutant genotype that grew only on D-Glu containing plates, were analyzed by PCR using the primers EXTfw_*murI2*/EXTrv_*murI2* and INTfw_*murI2*/INTrv_*murI2* to confirm the second crossover event, produced by the allelic exchange of plasmid pMo130_UP/DOWN_*murI2* with the *murI2* allele.

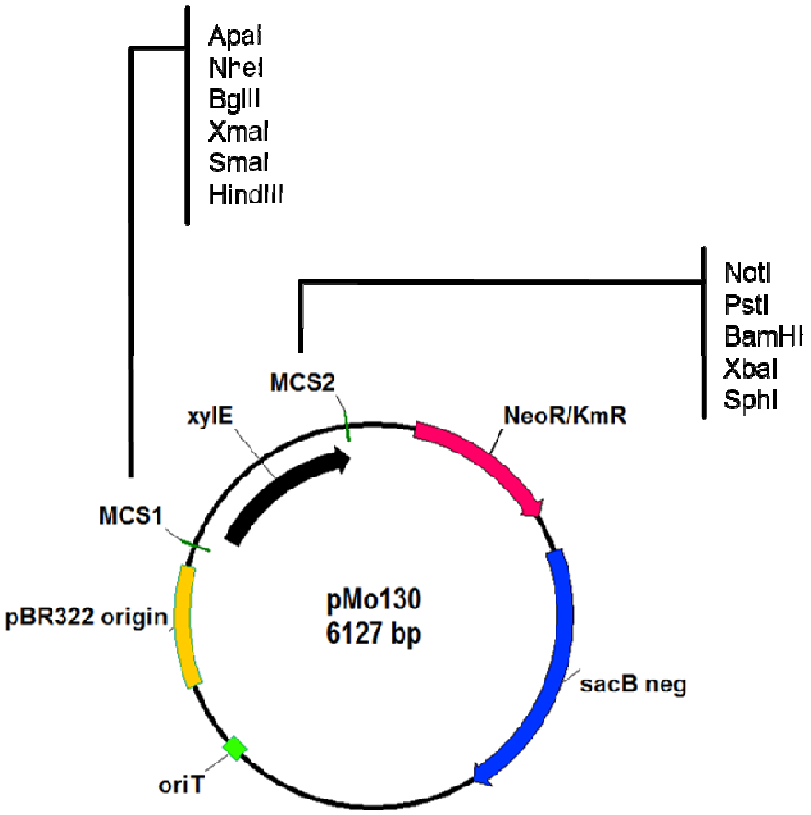

Figure 14 | Map of the pMo130 gene replacement vector. The locations of genes, their transcriptional orientations and the restriction sites of the MCS1 and MCS2, in clockwise order, are shown. pMo130 carries a neomycin-kanamycin resistance cassette (Neo^R/Km^R), a sucrose counter-selectable marker (*sacB*), an origin of transfer (*oriT*) for conjugation-mediated plasmid transfer, a pBR322 origin of replication from ColE1, MCS1, the reporter gene *xylE* and MCS2. MCS, multiple cloning site. Plasmid drawn to scale. Adapted from [339].

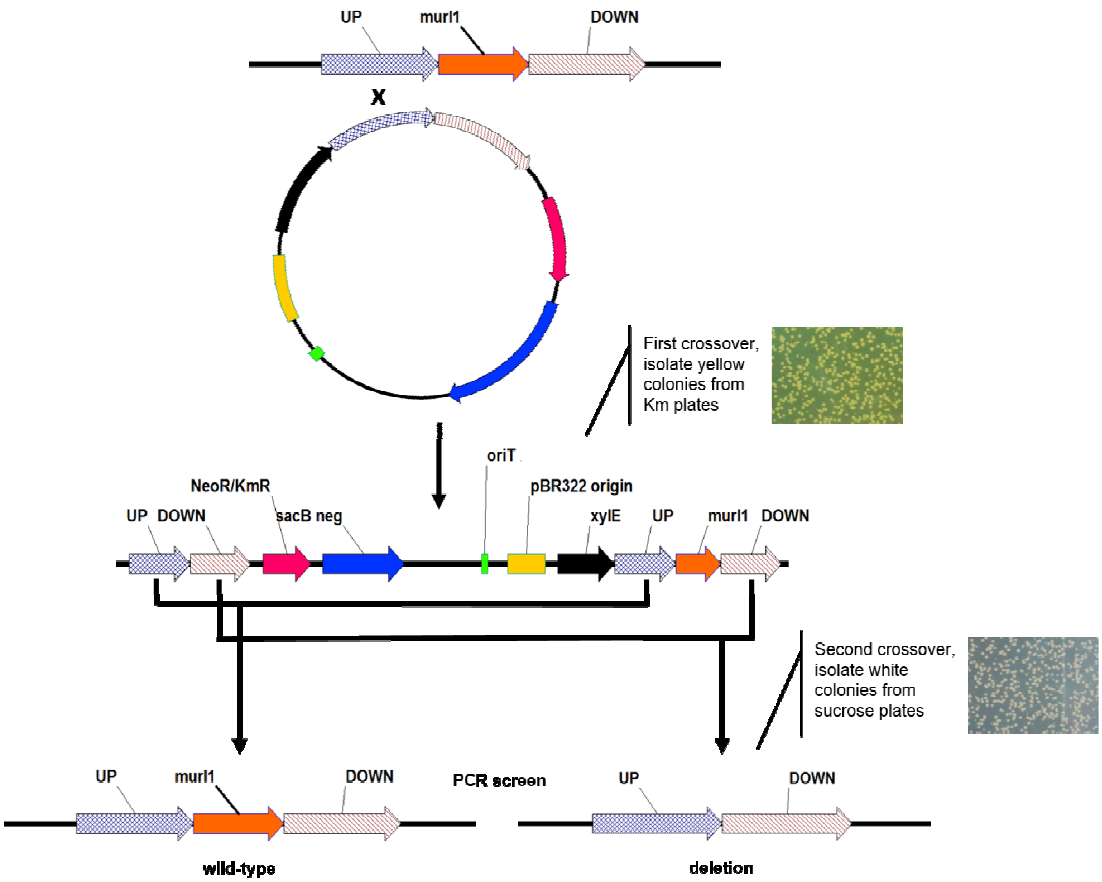

Figure 15 | Allelic exchange of pMo130_UP/DOWN_*murI1* with chromosomic DNA to construct a *murI1* deletion in *A. baumannii* ATCC 17978. DNA fragments upstream and downstream the *murI1* gene are cloned into pMo130 MCS2 to generate pMo13_UP/DOWN_*murI1*. pMo13_UP/DOWN_*murI1* is introduced into *A. baumannii* through transformation and co-integrants are recovered by kanamycin selection and screening for *xylE* positive yellow colonies. Resolved co-integrants are recovered by sucrose counter-selection and screening for *xylE* negative white colonies. Colonies are analyzed by PCR to distinguish deletion mutants from wild-type isolates. Adapted from [339].

3.2.2. *P. aeruginosa* PAO1 Δ*murI* mutant

For *P. aeruginosa*, DNA fragments of about 1 kb in length corresponding to the upstream and downstream regions of the *murI* gene were amplified by PCR with the combination of primers UP_*murI*(HindIII)II/UP_*murI*(NotI) and DOWN_*murI*(NotI)/DOWN_*murI*(XbaI). The upstream fragment obtained was digested with HindIII and NotI restriction enzymes; the downstream fragment was digested with NotI and XbaI. Digested products were ligated into pEX18Gm **(Fig. 16),** which was previously linearized with HindIII and XbaI and the recombinant plasmid pEX18Gm_UP/DOWN_*murI* obtained was transformed in *E. coli* S17-1 by electroporation. S17-1 transformants were

selected on LB containing gentamycin and were analyzed by PCR to confirm the presence of the recombinant plasmid, which was then introduced in *P. aeruginosa* PAO1 by electroporation. *P. aeruginosa* gentamycin-resistant colonies, representing the first crossover event, were grown on LB containing 15% sucrose and 10 mM D-Glu for 6 hours, and plated on the same agar medium. The resulting colonies were picked from agar plates containing 10 mM D-Glu and inoculated in patches at comparable locations on LB agar plates with and without 10 mM D-Glu. Presumptive colonies with the Δ*murI* mutant genotype that grew only on D-Glu containing plates, were analyzed by PCR using the primers EXTfw_*murI*/EXTrv_*murI* and INTfw_*murI*/INTrv_*murI* to confirm the second crossover event, produced by the allelic exchange of plasmid pEX18Gm_UP/DOWN_*murI* with the *murI* allele **(Fig. 17).**

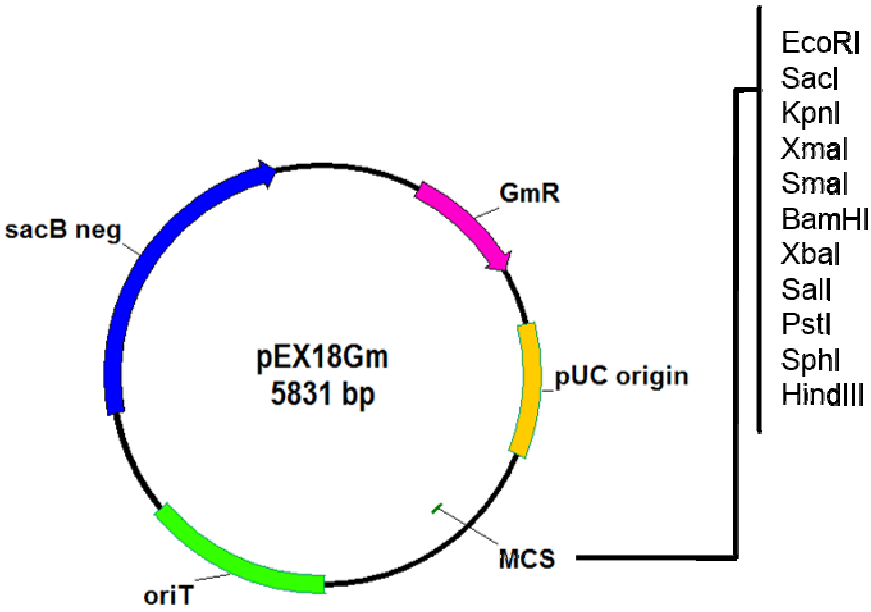

Figure 16 | Map of the pEX18Gm gene replacement vector. The locations of genes, their transcriptional orientations and the restriction sites of the MCS, in clockwise order, are shown. pEX18Gm carries a gentamycin resistance cassette (Gm^R), a pUC origin of replication from ColE1, a MCS from pUC18, an origin of transfer (*oriT*) for conjugation-mediated plasmid transfer and a sucrose counter-selectable marker (*sacB*). MCS, multiple cloning site. Plasmid drawn to scale. Adapted from [340].

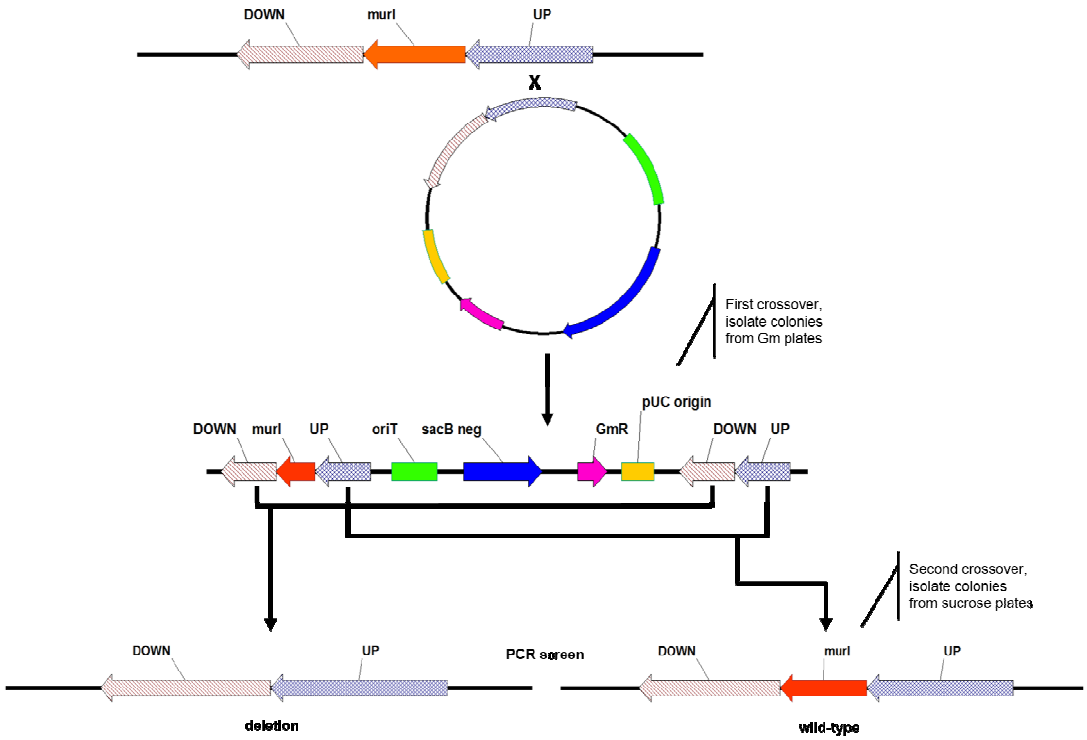

Figure 17 | Allelic exchange of pEX18Gm_UP/DOWN_*murI* with chromosomic DNA to construct a *murI* deletion in *P. aeruginosa* PAO1. DNA fragments upstream and downstream the *murI* gene are cloned into pEX18Gm MCS to generate pEX18Gm_UP/DOWN_*murI*. pEX18Gm_UP/DOWN_*murI* is introduced into *P. aeruginosa* through transformation and co-integrants are recovered by gentamycin selection. Resolved co-integrants are recovered by sucrose counter-selection. Colonies are analyzed by PCR to distinguish deletion mutants from wild-type isolates.

3.2.3. *S. aureus* 132 Δ*murI*, 132 Δ*dat* and 132 Δ*murI* Δ*dat* mutants

For *S. aureus*, DNA fragments of 1 kb corresponding to the upstream and downstream flanking regions of *murI* and *dat* genes were amplified by PCR using primers UP_*murI*(MluI)/UP_*murI*(NotI), DOWN_*murI*(NotI)/DOWN_*murI*(BglII), UP_*dat*(MluI)/UP_*dat*(NotI) and DOWN_*dat*(NotI)/DOWN_*dat*(BglII), and next digested by the restriction enzymes indicated within brackets. Digested products were ligated into pMAD **(Fig. 18),** previously linearized with MluI and BglII. The resulting pMAD_UP/DOWN_*murI* and pMAD_UP/DOWN_*dat* plasmids were confirmed by sequencing and independently transformed by electroporation into *E. coli* TG1 and DC10β, respectively. For the allelic exchange of pMAD_UP/DOWN_*murI* with the *murI* allele, the recombinant plasmid was transformed in *S. aureus* RN4220 and then in *S. aureus* 132 by electroporation. For the allelic exchange of pMAD_UP/DOWN_*dat* with the *dat* allele, the

recombinant plasmid was directly introduced into *S. aureus* 132 from *E. coli* DC10β. Homologous recombination experiments were performed as follows: one blue erythromycin-resistant colony of *S. aureus* containing pMAD_UP/DOWN_*murI* or pMAD_UP/DOWN_*dat* was grown in TSB with erythromycin at 30 ºC for 2 hours and then, at 43.5 ºC, a non-permissive temperature for pMAD replication. Resulting cultures were serially diluted and light blue erythromycin-resistant colonies, representing the first crossover event, were selected at 43.5 ºC in TSB plates with erythromycin and X-Gal. Several of these colonies were grown in TSB without antibiotic at 30 ºC for 18 hours, and then plated on the same agar medium. The resulting white colonies were analyzed by PCR and sequencing (using the combination of primers EXTfw_*murI*/EXTrv_*murI*, INTfw_*murI*/INTrv_*murI*, EXTfw-seq-UP_*murI*/EXTrv-seq-DOWN_*murI*, EXTfw_*dat*/EXTrv_*dat*, INTfw_*dat*/INTrv_*dat* and EXTfw-seq-UP_*dat*/EXTrv-seq-DOWN_*dat*, designed for *S. aureus*) to confirm the Δ*murI* and Δ*dat* genotypes produced by the allelic exchange of plasmids pMAD_UP/DOWN_*murI* **(Fig. 19)** and pMAD_UP/DOWN_*dat* with the *murI* and *dat* alleles, respectively. pMAD_UP/DOWN_*dat* plasmid was also introduced by electroporation in the 132 Δ*murI* mutant. Transformant blue erythromycin-resistant colonies were firstly grown in TSB at 30 ºC and then, at 43.5 ºC to obtain colonies resulting from the first crossover. Several of these colonies were transferred to TSB with 10 mM D-Glu, incubated at 30 ºC for 18 hours, and then plated on the same agar medium. The resulting white colonies were picked and inoculated in patches at comparable locations on TSB agar plates with and without 10 mM D-Glu. Presumptive colonies with the Δ*murI* Δ*dat* double mutant genotype that grew only with D-Glu were confirmed for the second crossover event, produced by the allelic exchange of the plasmid pMAD_UP/DOWN_*dat* with the *dat* allele, by PCR and sequencing using the primers EXTfw_*dat*/EXTrv_*dat*, INTfw_*dat*/INTrv_*dat* and EXTfw-seq-UP_*dat*/EXTrv-seq-DOWN_*dat*.

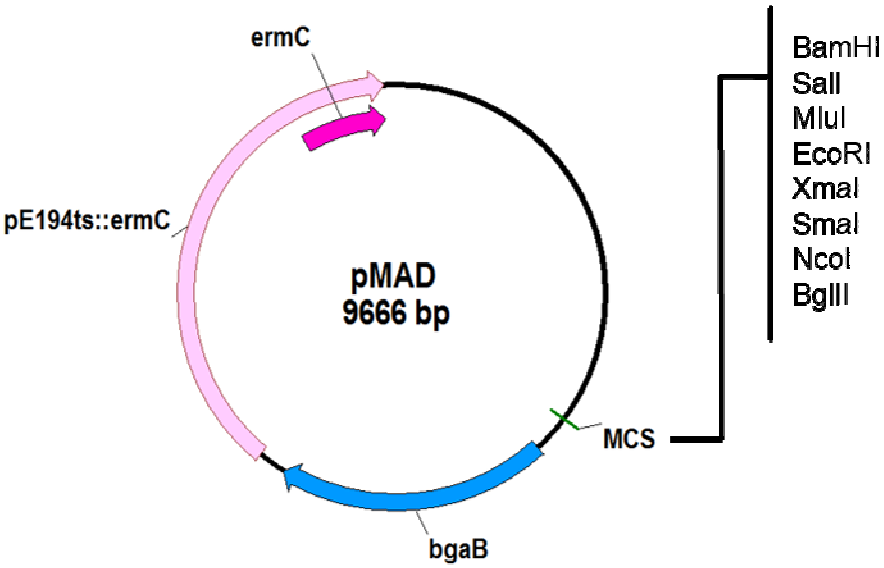

Figure 18 | Map of the pMAD gene replacement vector. The locations of genes, their transcriptional orientations and the restriction sites of the MCS, in clockwise order, are shown. pMAD carries a pE194ts::ermC thermosensitive pE194 replication origin with an erythromycin resistance gene (*ermC*), a MCS and a *bgaB* gene encoding a thermostable β-galactosidase, allowing the easy screening of transformants on X-Gal. MCS, multiple cloning site. Plasmid drawn to scale. Adapted from [341].

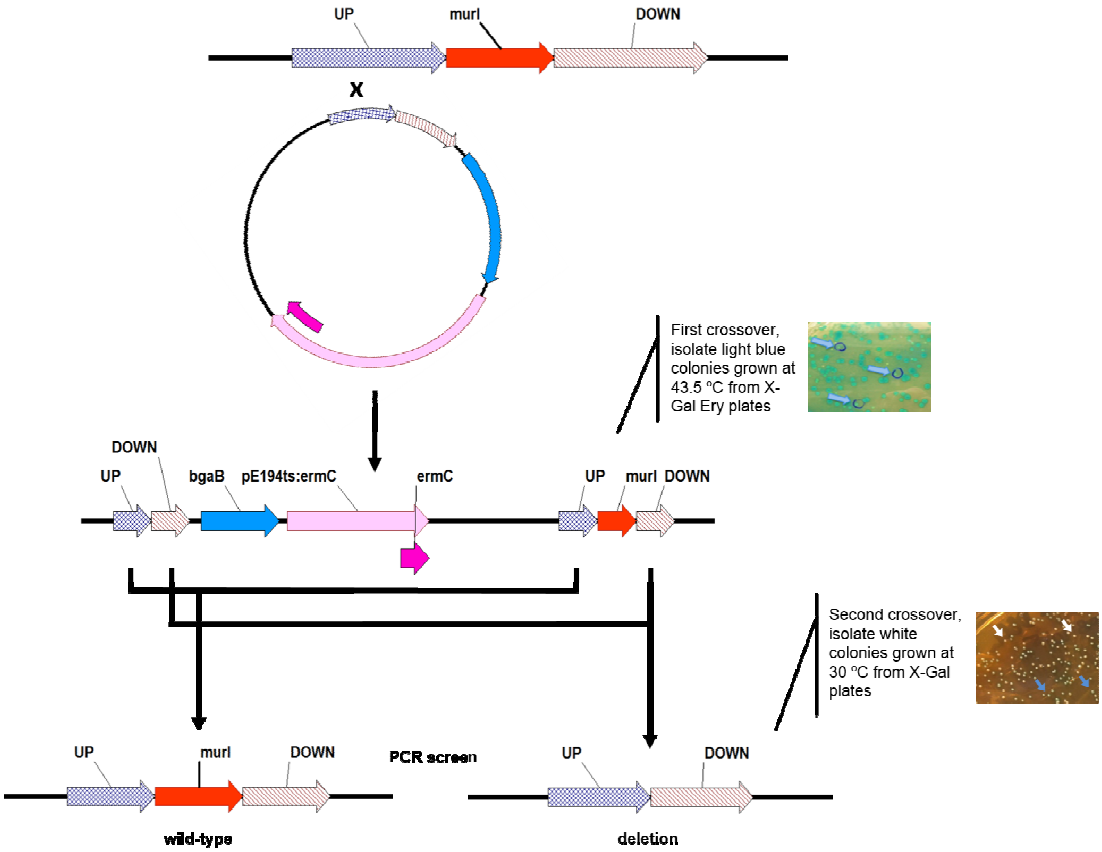

Figure 19 | Allelic exchange of pMAD_UP/DOWN_*murI* with chromosomic DNA to construct a *murI* deletion in *S. aureus* 132. DNA fragments upstream and downstream the *murI* gene are cloned into pMAD MCS to generate pMAD_UP/DOWN_*murI*. pMAD_UP/DOWN_*murI* is introduced into *S. aureus* through transformation and co-integrants grown at 43.5 ºC, a non-permissive temperature for plasmid replication, are recovered by screening for light blue colonies, derived from *bgaB* expression on X-Gal agar plates, and erythromycin resistance, conferred by *ermC*. Resolved co-integrants are recovered by screening for white colonies grown on X-Gal agar plates at 30 ºC, a permissive temperature for plasmid replication which leads to plasmid excision. Colonies are analyzed by PCR to distinguish deletion mutants from wild-type isolates. Adapted from [341].

3.3. Growth and viability curves

To determine the growth and viability of *A. baumannii* ATCC 17978, *P. aeruginosa* PAO1, and derived mutant strains, these bacterial strains were cultured overnight at 37 ºC and 180 rpm in 5 mL LB supplemented with 10 mM D-Glu. Bacterial cultures were centrifuged (4,000 g, 15 min) and the pellets were washed twice with LB. After pellet

suspension in 5 mL LB, 100 µL were used to inoculate 100 mL of LB with or without 10 mM D-Glu and left incubating at 37 ºC under agitation (180 rpm). For *A. baumannii* ATCC 17978 and derived mutants, samples were taken every 60 min for 7 hours to determine the culture turbidity (OD_{600nm}). In parallel, samples were taken every 2 hours up to 6 hours to determine CFU (colony-forming units) in LB agar with 10 mM D-Glu. For *P. aeruginosa* PAO1 and PAO1 Δ*murI*, samples were taken at 0, 60, 180, 300, 480 and 1,320 min to determine the culture turbidity (OD_{600nm}). In parallel, samples were taken at 0, 180, 480 and 1,320 min to determine CFU in LB agar with 10 mM D-Glu. In the case of *S. aureus,* overnight cultures of *S. aureus* 132, 132 Δ*murI*, 132 Δ*dat* and 132 Δ*murI* Δ*dat* were centrifuged (3,900 g, 20 min) and the pellets washed once with TSB. After pellet suspension, cultures adjusted to OD_{600nm} = 2 were used to inoculate 100 mL of TSB with or without 20 mM D-Glu ($\times 10^{-2}$ dilution) and left incubating at 37 ºC under agitation (180 rpm). Samples were taken at 0 and every 60 min up to 8 hours to determine the culture turbidity (OD_{600nm}). In parallel, samples were taken at 0, 120, 240, 360 and 480 min to determine CFU in TSB agar with 10 mM D-Glu for 132 Δ*murI* Δ*dat* or without D-Glu for the remaining strains. All cultures were made in triplicate.

3.4. Real-time RT-PCR

We used quantitative real-time reverse transcription PCR (qRT-PCR) to examine *A. baumannii* ATCC 17978, ATCC 17978 Δ*murI1*, ATCC 17978 Δ*murI2* and ATCC 17978 Δ*murI1* Δ*murI2* strains for the expression of *murI1* and *murI2* genes; *P. aeruginosa* PAO1, PAO1 Δ*murI* strains for the expression of *murI* gene; in turn, *S. aureus* 132, 132 Δ*murI*, 132 Δ*dat* and 132 Δ*murI* Δ*dat* strains for the expression of *murI* and *dat* genes, using the Universal Probe Library (UPL) TaqMan probes (Roche) or TaqMan probes specifically designed (TIB MOLBIOL, Germany) together with the primers listed in **Table 7.** Total DNase-treated RNA (500 ng for *A. baumannii* and 100 ng for *P. aeruginosa* and *S. aureus*) was obtained from log-phase cultures (OD_{600nm} = 0.5 to 0.7) using the High Pure RNA Isolation Kit (Roche). For qRT-PCR, a LightCycler 480 RNA instrument and Master hydrolysis probes kit (both from Roche) were used together with the following protocol: initial incubation at 65 ºC, 3 min, followed by a denaturation step at 95 ºC for 30 s, 45 cycles at 95 ºC, 15 s and 60 ºC, 45 s, and a final elongation step at 40 ºC, 30 s. In all cases, the expression levels were normalized relative to the transcription levels of *gyrB* (*A. baumannii* and *S. aureus*) and *proC* (*P.*

aeruginosa) housekeeping genes, which were assigned a value of 1.0. All assays were performed using samples from three different RNA extractions.

Table 7 | Oligonucleotides and probes used for qRT-PCR.

Analysis, gene and primer	Orientation	Primer sequence (5'-3')	UPL probe
***A. baumannii* qRT-PCR**			
***gyrB* (A1S_0004)**	Forward	tctctagtcaggaagtgggtacatt	76
	Reverse	ggttatattcttcacggccaat	
***murI1* (A1S_0380)**	Forward	ggcactaaaacctgccgtat	145
	Reverse	catctttaatgagttgtccacga	
***murI2* (A1S_3398)**	Forward	gcaatgactttgagcaagca	87
	Reverse	aacttttttaagtttttgcccttc	
***P. aeruginosa* qRT-PCR**			
***proC* (PA0393)**	Forward	cttcgaagcactggtggag	20
	Reverse	ttattggccaagctgttcg	
***murI* (PA4662)**	Forward	gagcggatcggtgatttc	50
	Reverse	attgcaggccagtaccagag	
***S. aureus* qRT-PCR**			
gyrB	Forward	cggtggcggatacaaagt	131
	Reverse	gcgtttacaactgatgaacca	
murI	Forward	cagcaactgctgtagctttagaat	118
	Reverse	gcacctggttcaattacgc	
dat	Forward	tggtgtagctgaaaggaatcatagc	- (*)
	Reverse	accatcggatatcttcaacgga	- (*)

(*) These primers were used with D-Ala P-Taqman probe 6FAM-tcccgacacctgaagtagaaccagca-BBQ (6FAM, 6-carboxyfluorescein; BBQ, BlackBerry Quencher).

3.5. Scanning electron microscopy (SEM)

In order to take microphotographs by SEM, *A. baumannii* ATCC 17978, ATCC 17978 Δ*murI1* Δ*murI2*, *P. aeruginosa* PAO1 and PAO1 Δ*murI* strains were cultured overnight at 37 ºC in 5 mL LB supplemented with 10 mM D-Glu. Bacterial cultures were centrifuged (4,000 g, 15 min) and the pellets were washed twice with 0.9% NaCl. After pellet suspension in 5 mL LB, 1 mL was used to inoculate 100 mL of LB. The cultures were incubated at 37 ºC for 2 hours under agitation (180 rpm) and then centrifuged and washed twice with 0.9% NaCl. After pellet suspension in 100 mL LB, 50 µL were used to inoculate 5 mL of LB with D-Glu at 0, 0.1, 1.25 and 10 mM. The cultures were incubated at 37 ºC under agitation (180 rpm) for 2 hours and were subsequently centrifuged and washed twice with PBS. *S. aureus* 132 and 132 Δ*murI* Δ*dat* strains were cultured overnight at 37 ºC in 5 mL of TSB supplemented with 20 mM D-Glu. Bacterial cultures were centrifuged (3,900 g, 20 min) and the pellets were washed twice with 0.9% NaCl. After pellet suspension in 1 mL TSB, 50 µL of each suspension

were used to inoculate 5 mL of TSB with D-Glu at 0, 0.1, 1.5 and 20 mM. Then cultures were incubated at 37 ºC with shaking (180 rpm) for 3 hours and were subsequently centrifuged and washed twice with PBS. The pellets were then fixed with 4% paraformaldehyde in 0.1 M PBS pH 7.4 for 30 min and washed again twice with PBS. Each sample was dehydrated in increasing series of ethanol (50%, 70%, 90% and 100%) for 10-15 min and then dried to the critical point with CO_2 (Bal-Tec CPD 030). One drop of each sample was placed onto a slide cover and fixed in aluminium supports for gold coating (Bal-Tec SCD 004 sputter coater). Observation was conducted and photographs were taken using a Jeol JSM-6400 electron microscope.

3.6. Transmission electron microscopy (TEM)

In order to take microphotographs using TEM, *A. baumannii* ATCC 17978, ATCC 17978 Δ*murI1* Δ*murI2*, *P. aeruginosa* PAO1, PAO1 Δ*murI*, *S. aureus* 132 and 132 Δ*murI* Δ*dat* strains were cultured overnight at 37 ºC in LB or TSB agar supplemented with 10 mM D-Glu. After incubation, 2-3 colonies of each strain were plated onto MH (Mueller Hinton), LB, LB supplemented with $MgCl_2$ (30 mg/L) and $CaCl_2$ (75 mg/L) and LB supplemented with 10 mM D-Glu agar and incubated overnight at 37 ºC. After incubation, 2-3 colonies obtained in the first streak of each plate were dissolved in PBS buffer, the suspension was centrifuged and the resulting pellet was washed first with cacodylate buffer, and immediately after that the cells were fixed in ice cold 2.5% glutaraldehyde prepared in 0.2 M sodium cacodylate buffer, pH 7.4 for 4 hours at room temperature. The pellets were then washed with cacodylate buffer, dehydrated in acetone and embedded in SPURR (Spurr's Epoxy Embedding Medium). Ultrathin sections (70 nm) of these samples were obtained and they were stained with uranyl acetate and lead citrate for observation under a JEOL JEM 1010 (80 kV) transmission electron microscope.

3.7. Animal experiments

All mice and rats were maintained in the specific pathogen-free (SPF) facility at the Centro Tecnológico de Formación de la Xerencia de Xestión Integrada A Coruña (CTF-XXIAC), Servicio Galego de Saúde. All experiments were done with the approval of and in accordance with regulatory guidelines and standards set by the Comité Ético de

Experimentación Animal of CHUAC (Complejo Hospitalario Universitario A Coruña). Male and female mice were used for first time procedures between the ages of 6 and 8 weeks. BALB/c mice were bred in our colony and used for all experiments, unless noted. C57BL/6 mice were purchased from Harlan Sprague Dawley Inc. Female Winstar rat were bred in our colony and used for first time procedures at 6 months of age. Studies were not blinded.

3.7.1. Blood samples

Blood samples were collected from the submandibular vein of anesthetized mice, and sera were separated from the blood cells by centrifugation (1,500 g, 15 min) and stored at –80 ºC until subsequent analysis. Blood samples from rats were collected by heart puncture and sera were obtained as before.

3.7.2. Bacterial burden in tissues

To assess bacterial burden in tissues, vaccinated and control mice were euthanized at indicated time points for each experiment, tissues were extracted aseptically, homogenized in sterile NaCl 0.9% and CFU enumerated by plating $\times 10^{-2}$-fold serial dilutions in agar plates.

3.7.3. Inocula preparation for immunizations and infections

To prepare inocula for active immunizations and infections, bacteria were cultured at 37 ºC under agitation (180-210 rpm) until reaching OD_{600nm} = 0.7 (this inoculum was designated 1X, unless otherwise stated). The cultures were harvested by centrifugation, pellets washed twice, suspended and adjusted in sterile NaCl 0.9% according to the previous OD_{600nm} to different doses (0.1X meaning as bacterial inocula diluted 1:10, 2X the bacterial inocula 2:1 concentrated, and so on…). Prior to mice inoculation, bacterial inocula were quantified by CFU enumeration in agar plates **(Table 8)**.

Table 8 | Equivalents of bacteria dosage and CFU used for *in vivo* experiments.

Bacteria	Purpose	Dose	Inoculum (CFU/mouse)	Related item
***A. baumannii* strains**				
ATCC 17978	LD	1X	8×10^6	**Fig. 30**
	LD	2X	3×10^7	
	LD	2.5X	4×10^7	
	LD	3X	4×10^7	
	Challenge	4X	7×10^7	**Fig. 46**
	Blood clearance	1X	1×10^7	**Figs. 55, 56**
ATCC 17978 Δ*murI1* Δ*murI2*	LD	3X	1×10^8	**Fig. 30**
		4X	2×10^8	
		6X	2×10^8	
		8X	3×10^8	
	Vaccination	1X	4×10^7	**Figs. 31, 34**
		0.000 1X	4×10^3	**Fig. 33**
	Vaccination	0.01X	7×10^5	**Fig. 32**
		0.05X	2×10^6	
		0.1X	3×10^6	
		0.5X	2×10^7	
		1X	9×10^7	
	Blood clearance	1X	1×10^8	**Figs. 55, 56**
AbH12O-A2	Challenge	4X	4×10^7	**Fig. 46**
Ab307-0294	Challenge	0.75X	6×10^6	**Fig. 46**
***P. aeruginosa* strains**				
PAO1	LD	0.1X	$\sim6\times10^6$	**Fig. 30**
		0.4X	$\sim2\times10^7$	
		1X	$\sim6\times10^7$	
		4X	2×10^8	
	Challenge	0.4X	3×10^7	**Fig. 47**
	Blood clearance	0.4X	2×10^7	**Fig. 55**
PAO1 Δ*murI1*	LD	1X	$\sim1\times10^8$	**Fig. 30**
		4X	$\sim4\times10^8$	
		10X	$\sim1\times10^9$	
		40X	$\sim4\times10^9$	
	Vaccination	0.4X	2×10^7	**Fig. 31**
	Vaccination	0.1X	$\sim1\times10^7$	**Fig. 32**
		0.4X	4×10^7	
		1X	$\sim1\times10^8$	
		4X	$\sim4\times10^8$	
		10X	$\sim1\times10^9$	
		40X	$\sim4\times10^9$	
	Blood clearance	0.4X	2×10^7	**Fig. 55**
PA28562	Challenge	0.5X	4×10^7	**Fig. 47**
PA14	Challenge	0.2X	4×10^6	**Fig. 48**

~, estimated values.

Table 8 (cont.) | Equivalents of bacteria dosage and CFU used for *in vivo* experiments.

Bacteria	Purpose	Dose	Inoculum (CFU/mouse)	Related item
***S. aureus* strains**				
132	LD	0.05X	3-4×10^6	**Fig. 30**
		0.5X	3-4×10^7	
		1X	7×10^7	
		2.5X	1-2×10^8	
	Challenge	0.5-1X	2-7×10^7	**Figs. 45, 49, 50, 54**
	Blood clearance	0.5X	5-6×10^7	**Fig. 55**
132 Δ*murI* Δ*dat*	LD	1X	2×10^7	**Fig. 30**
		5X	8-9×10^7	
		10X	1-2×10^8	
	Vaccination	1X	2-3×10^7	**Figs. 31, 32, 34, 45, 49, 50**
	Vaccination	0.2X	5-7×10^6	**Fig. 32**
		5X	~7.5×10^7	**Fig. 32**
		10X	1-2×10^8	**Figs. 32, 54**
	Blood clearance	2.5X	~6×10^7	**Fig. 55**
USA300LAC	Challenge	0.4X	~6×10^7	**Fig. 50**
RF122	Challenge	0.25X	2-3×10^7	**Fig. 50**
ED98	Challenge	0.5X	~1×10^7	**Fig. 50**

~, estimated values.

In detail, *A. baumannii* ATCC 17978, ATCC 17978 Δ*murI1*, ATCC 17978 Δ*murI2*, ATCC 17978 Δ*murI1* Δ*murI2*, *P. aeruginosa* PAO1 and PAO1 Δ*murI* were cultured in LB with 10 mM D-Glu (D-Glu auxotrophic strains) and LB (remaining strains) at 37 ºC and 180 rpm, harvested (4,000 g, 15 min), washed twice with LB and finally adjusted with saline as above. For intraperitoneal (IP) and intramuscular (IM) injections of *A. baumannii* and *P. aeruginosa* strains, we used a total volume of 100 and 50 µL, respectively, and insulin syringes (29G × 1/2 in., Becton Dickinson). The manual restrain of mice and syringe insertion are shown in **Fig. 20.** For PA28562 infection, bacterial pellet was suspended in NaCl 0.9% containing 3% of mucin from porcine stomach, type II. Mucin stock solution was solubilized in PBS at 6% w/v, sterilized by autoclaving for 10 min and rapidly cooled in ice. Exceptionally for *P. aeruginosa* PA28562, we used a 250 µL volume for infection. Independently of the bacterial strain administrated, mice were monitored for 7 days after injections. All challenges were made using the IP route of administration. To prepare inocula of *S. aureus* 132 and 132 Δ*murI* Δ*dat*, these strains were grown in TSB or TSB with 20 mM D-Glu at 37 ºC and 210 rpm until OD_{600nm} = 0.7. For 132 Δ*murI* Δ*dat*, cultures were concentrated from OD_{600nm} = 0.7 to 0.8 in saline prior to washing steps. Then, bacterial cultures were then centrifuged (3,900 g, 20 min), washed twice with sterile NaCl 0.9% and suspended in the same solution. For *S.*

aureus infections, we prepared inocula with 3% mucin (as described above). Both for immunizations and infections, mice were administered using the IP route with a total volume of 250 µL and, unless otherwise stated, monitored for morbidity and mortality for 14 days after injections. When pertinent, mice challenged with *S. aureus* were weighed daily. For active immunization assays, mice were injected with D-Glu auxotrophic strains ATCC 17978 Δ*murI1* Δ*murI2*, PAO1 Δ*murI1* or 132 Δ*murI* Δ*dat* at a 14-day interval with a total of two or three injections depending on the schedule. Control mice were administrated saline on parallel. Mice were challenged with bacterial strains 7 days after the last vaccine dose, unless otherwise stated.

(A) **(B)**

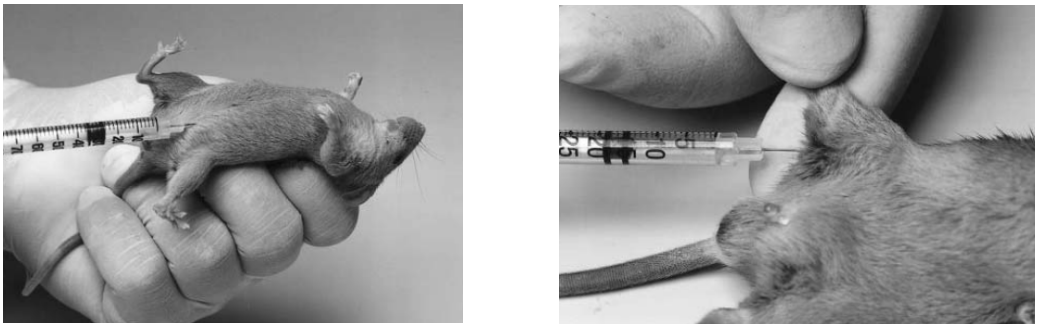

Figure 20 | Routes of administration used for injecting mice with bacterial inocula or saline. A, Administration of intraperitoneal (IP) injection to lower left quadrant. **B,** Intramuscular (IM) injection into the leg muscle. From [342].

3.7.4. Sera and passive immunizations

To generate naïve and anti-*A. baumannii* serum (anti-Ab) to be used in passive immunizations before challenging mice with *A. baumannii* ATCC 17978, BALB/c mice (*n* = 6/group) were administered three IP injections of ATCC 17978 Δ*murI1* Δ*murI2* (1X), or saline, at a 14-day interval. Blood was collected on days 36, 40 and 42; serum was pooled and titers of total IgG were determined by indirect ELISA. IP adoptive transfer of either 250 µL anti-Ab (1:163,840) or naïve serum (1:40) was made in naïve mice (*n* = 8/group) 3.5 hours prior to the challenge. To generate naïve and anti-*P. aeruginosa* serum (anti-Pa) to be used in passive immunizations before challenging mice with *P. aeruginosa* PAO1, BALB/c mice (*n* = 5/group) were administered two IP injections of PAO1 Δ*murI1* (0.4X), or saline, at a 12-day interval. Blood was collected on day 19; serum was pooled and IP adoptive transfer of either 200 µL anti-Pa or naïve serum was made in naïve mice (*n* = 8/group) 3.5

hours prior to the challenge. To generate naïve and anti-*S. aureus* (anti-Sa) serum to be used in passive immunization before challenging mice with *S. aureus* 132, Winstar rats (*n* = 1/group) were administered five IP injections (250 µL) of *S. aureus* 132 Δ*murI* Δ*dat* (10X), or saline, at a 14-day interval. Blood was collected on day 70; serum was pooled as before and titers of total IgG were determined by indirect ELISA using a 1:5,000 dilution of peroxidase conjugated goat anti-rat IgG (Life Technologies S.A.) as a detection antibody. IP adoptive transfer of either 200 µL anti-Sa (>1:81,920) or naïve serum (1:320) was made in naïve mice (*n* = 6/group) 3.5 hours prior to challenge.

3.8. Indirect ELISA

Quantification of IgM, total IgG, IgG1, IgG2a, IgG2b and IgG3 in mouse sera was performed using an indirect Enzyme-linked Immunosorbent Assay (ELISA). 96-well ELISA plates were "coated" with *A. baumannii*, *P. aeruginosa* and *S. aureus* strains, which were fixed to the bottom of the wells after overnight incubation at 4 ºC in 100 mM carbonate-bicarbonate buffer, pH 9.6. For the detection of specific antibodies against *S. aureus* 132, a derived mutant strain deficient for the protein A (132 Δ*spa* [324]) was used to avoid nonspecific binding between protein A and IgG or IgM antibodies. After coating, plates were washed five times with phosphate buffered saline (PBS) to remove any unfixed bacteria. The residual sites were blocked with 200 µL per well of blocking solution (5% skim milk in PBS) for 2 hours at room temperature. An additional blocking step was used with 200 µL of rabbit serum diluted 1:1000 in PBS for 1 hour at 37 ºC to block protein A cell surface receptors, for those *S. aureus* strains whose derived Δ*spa* mutants were not available. Plates were aspirated and washed 5 times with washing buffer (0.005% Tween 20 in PBS) and incubated overnight at 4 ºC with mouse sera serially diluted in DMEM culture medium supplemented with 10% fetal bovine serum (FBS) (Gibco, Life Technologies).After incubation, plates were washed five times with washing buffer to remove unbound antibodies, and 100 µL of secondary antibody (peroxidase-labelled anti-mouse IgM, IgG, IgG1, IgG2a, IgG2b or IgG3) diluted 1:5000 in DMEM culture medium supplemented with 10% FBS was added to each well and left incubating for 2 hours in the dark. Plates were washed five times with washing buffer to remove any unbound secondary antibodies. Then, 100 µL of 3,3'5,5'-Tetramethylbenzidine (TMB) was added to each well. The reaction was stopped after 2-3 min with 50 µL of 1M H_2SO_4 per well, and the peroxidase reaction product was read at 450 nm. For endpoint assays, the endpoint titer was defined as the

maximum dilution having a value that exceeded the blank absorbance reading by 0.1 values.

3.9. ELISpot assay

IFN-γ, IL-4 and IL-17-producing splenocytes were quantified by ELISpot analysis (R&D Systems) with splenocytes obtained from immunized (*n* = 6) and control (*n* = 6-7) mice, and exposed *ex vivo* to ATCC 17978 Δ*murI1* Δ*murI2* ($4x10^5$ CFU), PAO1 Δ*murI* ($8x10^4$ CFU) and 132 Δ*murI* Δ*dat* ($3x10^6$ CFU) during 43 hours at 37 ºC, 5% CO_2. Mice spleens were aseptically removed after the second vaccine or saline administration, mechanically disrupted and washed in saline by centrifugation at 400 g for 10 min at room temperature. The suspension of spleen cells was enriched in lymphocytes using the Histopaque solution, counted in a Neubauer haemacytometer and adjusted to $4x10^6$ or $8x10^6$ cells/mL in RPMI 1640 medium containing 10% FBS. Next, 100 µL were transferred to 96-well EliSpot plates, and restimulated with 100 µL of vaccine strain, 100 µL of 1X cell stimulation cocktail (positive control) or 100 µL RPMI + 10% FBS (negative control). The number of the spot-forming units were visually determined using images obtained with a dissecting microscope (Nikon SMZ-745, Nikon Corporation). Spot frequency in simulated wells was corrected by subtracting background signal from wells with cells plus media alone.

3.10. Control of phenotypic stability

A. baumannii ATCC 17978 Δ*murI1* Δ*murI2* and *P. aeruginosa* PAO1 Δ*murI* were cultured overnight at 37 ºC in 5 mL LB supplemented with 10 mM D-Glu. *S. aureus* 132 Δ*murI* Δ*dat* was grown overnight at 37 ºC in 5 mL TSB supplemented with 20 mM D-Glu. After incubation, 1 mL of each was used to inoculate 100 mL of LB or TSB with 10 or 20 mM D-Glu, respectively. All the cultures were incubated at 37 ºC under agitation (180-210 rpm) for up to 8 days. Samples from these cultures were taken at the beginning of the incubation period and on days 1, 2, 3, 4 and 8, washed twice, plated in LB or TSB agar with 0 and 10 mM D-Glu and incubated at 37 ºC for 3 days. Cultures were made in triplicate.

3.11. Water osmolisis assay

To determine the viability of *A. baumannii* ATCC 17978, ATCC 17978 Δ*murI1* Δ*murI2*, *P. aeruginosa* PAO1, PAO1 Δ*murI*, *S. aureus* 132 and 132 Δ*murI* Δ*dat* in water, these bacterial strains were cultured overnight at 37 ºC in LB or TSB agar with (mutant strains) and without (wild-type strains) 10 mM D-Glu, adjusted to 0.5 McFarland in water, and left incubating at 37 ºC under agitation (180 rpm) for the time necessary to observe the loss of viability of cells. For *A. baumannii* strains, daily samples of culture were taken initially for 2 days, next, samples were taken twice a week until day 26 and thereafter, once a week until day 40 for the determination of CFU counts in LB agar (wild-type strain) and LB agar with 10 mM D-Glu (mutant strain). For *P. aeruginosa* strains, daily samples of culture were taken initially for 3 days, next samples were taken twice a week until day 48. Finally, samples were taken at least once every two weeks until day 157 for the determination of CFU counts in LB agar (wild-type strain) and LB agar supplemented with 10 mM D-Glu (mutant strain). For *S. aureus*, daily samples of culture were taken until day 5 for the determination of CFU counts in TSB agar (wild-type strain) and TSB agar supplemented with 10 mM D-Glu (mutant strain). Cultures were made in triplicate.

3.12. Desiccation assay

To determine the viability of *S. aureus* 132 and 132 Δ*murI* Δ*dat* after being kept in stressful conditions (drought tolerance), these bacterial strains were cultured at 37 ºC under agitation (210 rpm) in TSB and TSB with 20 mM D-Glu, respectively. Log-phase cultures (OD_{600} = 0.5-0.6) were centrifuged (3,900 g, 20 min), washed once and serially diluted in TSB. Drops of 5 µL from undiluted, 10^{-1}- and 10^{-2}-diluted cultures were then spotted on sterile cellulose filters (0.45 µm pore size) and sequentially placed on TSB agar with D-Glu 10 mM at day 0 (control) and after keeping for 4, 5, 6, 11, 18, 25 and 31 days at room temperature (desiccation stress). Agar plates were incubated at 37 ºC for 16 hours. All cultures were made in triplicate.

3.13. Statistics

Means were compared by using Student's t test for hypothesis testing to compare individual conditions and corresponding control groups. Mann-Whitney U test was applied if data set failed the Kolmogorov-Smirnov normality test. The one-way analysis of variance (ANOVA) was used for multiple comparisons, followed by Bonferroni's post hoc test. Survival data were compared using the log-rank test. Differences were considered significant when $P<0.05$. *$P<0.05$ compared with control group. #$P<0.05$ compared with the preceding group represented. All statistical analyses were performed using Prism 6.0 (GraphPad Prism, GraphPad Software, Inc.).

4. RESULTS

4. RESULTS

4.1. Characterization of D-Glu auxotrophic strains

Analysis of the genome sequence of *A. baumannii* strain ATCC 17978 [343] revealed two MurI (EC 5.1.1.3) genes: A1S_0380 (*murI1*) which encodes a 288 amino acid protein, and A1S_3398 (*murI2*) which encodes a 266 amino acid protein. Analysis of the genome sequence of *P. aeruginosa* strain PAO1 [344] revealed a single MurI gene: PA4662 (*murI*) which encodes a 265 amino acid protein. Analysis of the genome sequence of *S. aureus* strain 132 [324] revealed a single MurI gene (*murI*) which encodes a 266 amino acid protein, and a single Dat gene (*dat*) which encodes a 282 amino acid protein. All these genes were targeted for unmarked in-frame deletion. **Figure 21** shows the phenotypic screening of *A. baumannii*, *P. aeruginosa* and *S. aureus* mutants in the final step of the allelic replacement method for obtaining D-Glu auxotrophic strains, whereas **Figure 22** shows the PCR screening using primers EXTfw and EXTrv for the above mentioned genes.

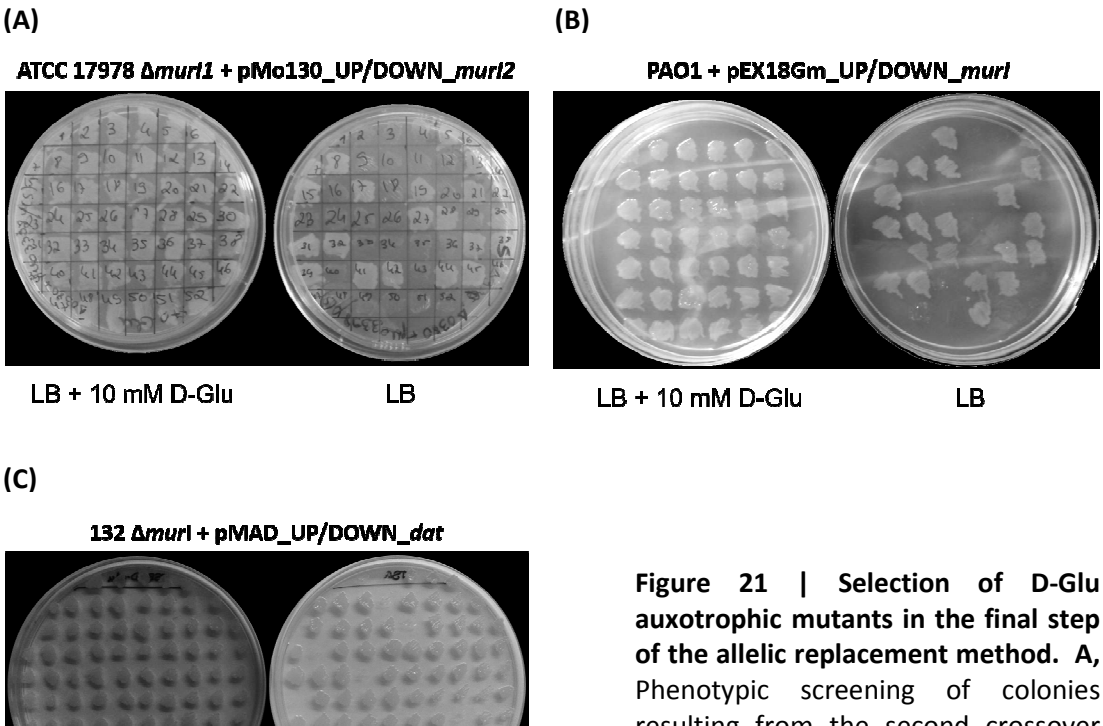

Figure 21 | Selection of D-Glu auxotrophic mutants in the final step of the allelic replacement method. A, Phenotypic screening of colonies resulting from the second crossover event of pMo130_UP/DOWN_*murI2* with ATCC 17978 Δ*murI1* chromosome during construction of *A. baumannii* ATCC 17978 Δ*murI1* Δ*murI2*. Individual colonies were picked from LB agar plates with 15% sucrose and 10 mM D-Glu and inoculated in patches at comparable locations in LB agar plates with and without 10 mM D-Glu. Colonies with the Δ*murI1* Δ*murI2* genotype grew exclusively in supplemented plates; colonies with the Δ*murI1* genotype grew with and without D-Glu. **B,** Phenotypic screening of colonies resulting from the second crossover event of pEX18Gm_UP/DOWN_*murI* with PAO1 chromosome during construction of *P. aeruginosa* PAO1 Δ*murI*. Individual colonies were picked from LB agar plates with 15% sucrose and 10 mM D-Glu and inoculated in patches at comparable locations in LB agar plates with and without 10 mM D-Glu. Colonies with the Δ*murI* genotype grew exclusively in supplemented plates; colonies with the wild-type genotype grew with and without D-Glu. **C,** Phenotypic screening of colonies resulting from the second crossover event of pMAD_UP/DOWN_*dat* with 132 Δ*murI* chromosome during construction of *S. aureus* 132 Δ*murI* Δ*dat*. Individual colonies were picked from TSB agar plates with 10 mM D-Glu and inoculated in patches at comparable locations in TSB agar plates with and without 10 mM D-Glu. Colonies with the Δ*murI* Δ*dat* genotype grew exclusively in supplemented plates; colonies with the Δ*murI* genotype grew with and without D-Glu.

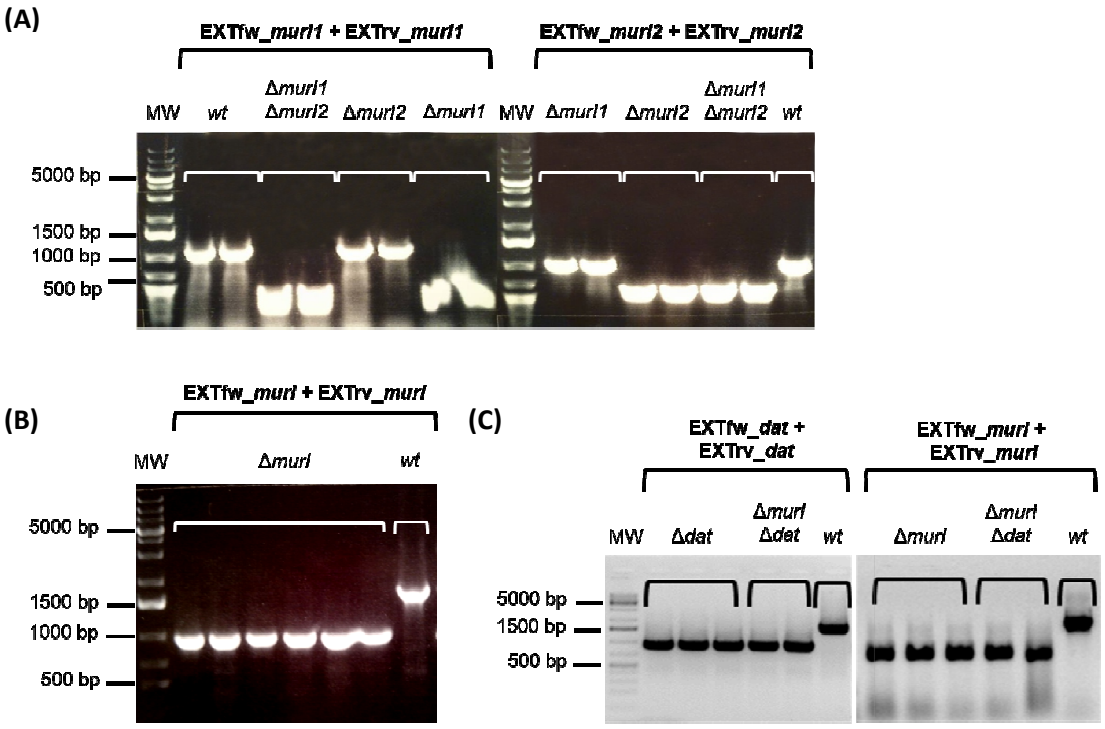

Figure 22 | PCR screening of *A. baumannii* MurI^{-}, *P. aeruginosa* PAO1 MurI^{-} and *S. aureus* 132 MurI^{-}Dat^{-} mutants. A, Oligonucleotides EXTfw_*murI1* and EXTrv_*murI1* generated fragments with 1116 bp from *A. baumannii* ATCC 17978 colonies carrying the wild-type *murI1* allele or fragments with 345 bp from colonies carrying the mutant Δ*murI1* allele. Oligonucleotides EXTfw_*murI2* and EXTrv_*murI2* generated fragments with 1056 bp from *A. baumannii* ATCC 17978 colonies carrying the wild-type *murI2* allele or fragments with 516 bp from colonies carrying the mutant Δ*murI2* allele. **B,** Oligonucleotides EXTfw_*murI* and EXTrv_*murI* generated fragments with 1741 bp from *P. aeruginosa* PAO1 colonies carrying the wild-type *murI* allele or fragments with 943 bp from colonies carrying the mutant Δ*murI* allele. **C,** Oligonucleotides EXTfw_*dat* and EXTrv_*dat* generated fragments with 1892 bp from *S. aureus* 132 colonies carrying the wild-type *dat* allele or fragments with 1049 bp from colonies carrying the mutant Δ*dat* allele. Oligonucleotides EXTfw_*murI* and EXTrv_*murI* generated fragments with 1481 bp from *S. aureus* 132 colonies carrying the wild-type *murI* allele or fragments with 739 bp from colonies carrying the mutant Δ*murI* allele. **A-C,** MW, molecular weight marker.

In *A. baumannii* ATCC 17978, the resulting single mutants ATCC 17978 Δ*murI1* and ATCC 17978 Δ*murI2* grew normally, while the ATCC 17978 Δ*murI1* Δ*murI2* double mutant required exogenous D-Glu for growth. In *P. aeruginosa* PAO1, the resulting mutant PAO1 Δ*murI* also required exogenous D-Glu. In *S. aureus* 132, the single mutants 132 Δ*murI* and 132 Δ*dat* grew normally, while the 132 Δ*murI* Δ*dat* double mutant required exogenous D-Glu **(Fig. 23).**

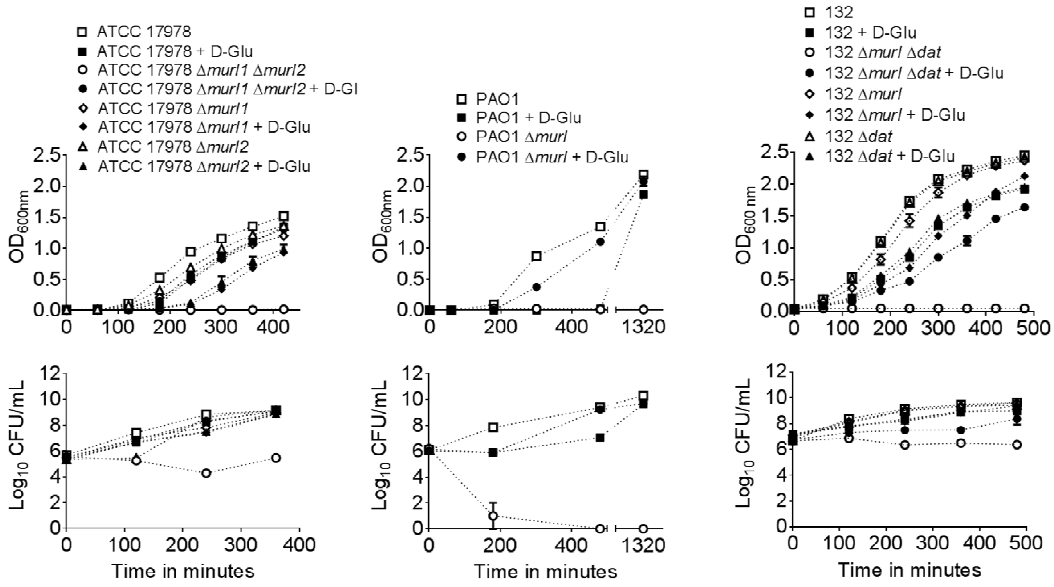

Figure 23 | Characterization of *A. baumannii* MurI⁻, *P. aeruginosa* MurI⁻ and *S. aureus* MurI⁻Dat⁻ D-Glu auxotrophic strains. Growth and viability of *A. baumannii* ATCC 17978, *P. aeruginosa* PAO1, *S. aureus* 132 and derived mutant strains (mean ± s.e.m.). ATCC 17978 Δ*murI1* Δ*murI2*, PAO1 Δ*murI* and 132 Δ*murI* Δ*dat* show normal grow in culture medium supplemented with D-Glu but are unable to grow without the exogenous supply of this compound. In contrast, the wild-type strains grow as per normal in medium with and without the addition of D-Glu.

Using real time qRT-PCR **(Fig. 24),** the absence of MurI and Dat genes mRNA in these mutant strains was confirmed. This shows the involvement of the *murI* genes in the production of D-Glu in *A. baumannii* ATCC 17978 and *P. aeruginosa* PAO1 and both *murI* and *dat* genes in the case of *S. aureus* 132. This means that for those bacteria not possessing the Dat enzyme, the inactivation of a single or multiple MurI genes is requisite to produce an auxotrophic strain for D-Glu, as in the respective cases of *P. aeruginosa* PAO1 and *A. baumannii* ATCC 17978 (MurI⁻ mutants). In other cases, the inactivation of genes

coding for MurI protein as well as those coding for Dat is required (MurI⁻Dat⁻ mutants), as in the case of some Gram-positive bacteria like *S. aureus*.

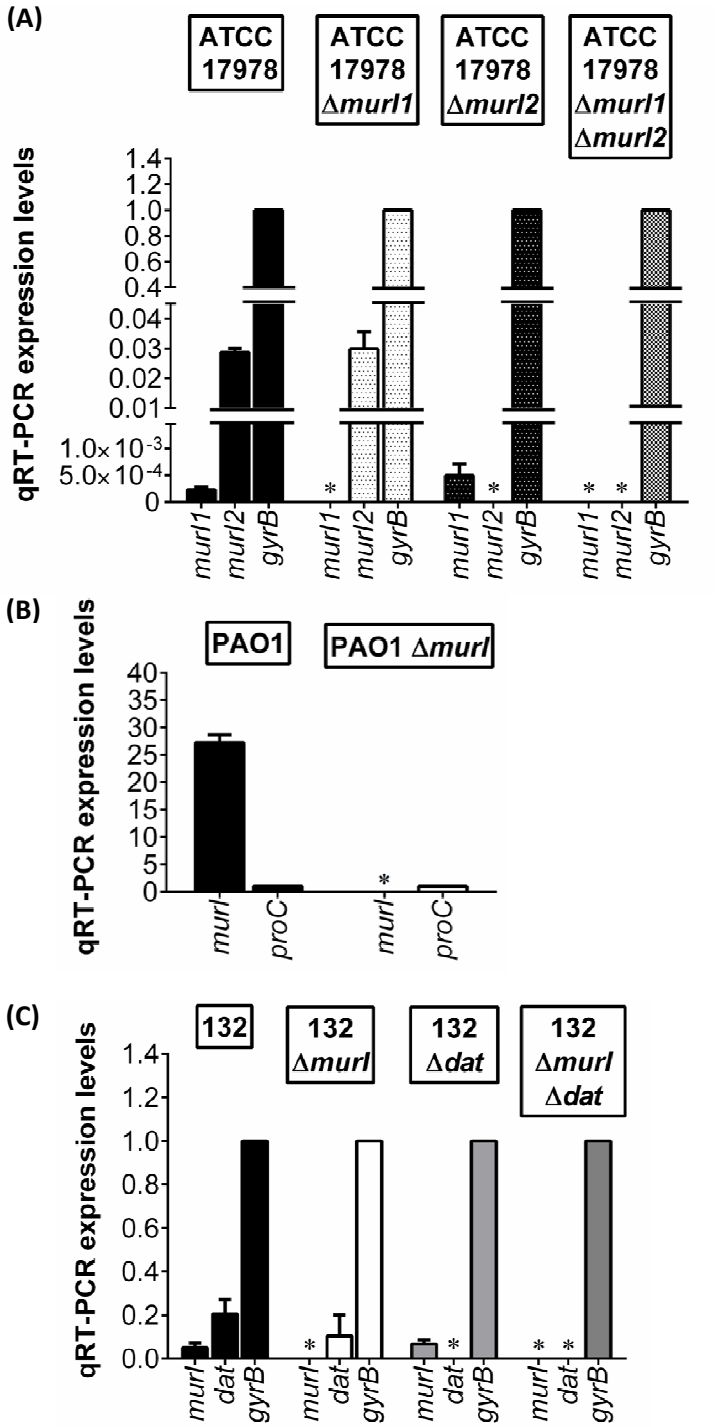

Figure 24 | qRT-PCR of MurI⁻, Dat⁻, and MurI⁻Dat⁻ mutants. A, Comparative expression levels by qRT-PCR of *murI* in ATCC 17978 (normalized relative to *gyrB*) and derived mutant strains. **B,** Comparative expression levels by qRT-PCR of *murI* in PAO1 (normalized relative to *proC*) and derived mutant strain. **C,** Comparative expression levels by qRT-PCR of *murI* and *dat* in 132 (normalized relative to *gyrB*) and derived mutant strains (mean ± s.d.). **P*<0.05.

To assess the effects of D-Glu deprivation on cellular growth of the wild-type and D-Glu auxotrophic strains, bacteria grown in media supplemented with different concentrations of D-Glu were collected and analysed by scanning electron microscopy (SEM) for morphology alterations **(Fig. 25).** The ATCC 17978 Δ*murI1* Δ*murI2*, PAO1 Δ*murI* and 132 Δ*murI* Δ*dat* strains showed significant growth impairment when the exogenous supply of D-Glu decreased, until complete loss of replication. Some bacteria detected on the culture medium without D-Glu were reminiscent of the inoculum previously grown with this compound. Moreover, both ATCC 17978 Δ*murI1* Δ*murI2* and 132 Δ*murI* Δ*dat* strains exhibited an altered pattern of cell division when D-Glu was supplied at 0.1 mM. With 1.25 mM D-Glu for *A. baumannii* and 1.5 mM D-Glu for *S. aureus* a greater cell density was seen with respect to the preceding condition (reflection of a higher growth rate) but with many visible protoplast-like structures. Also, though lower in number, some cells had an appearance similar to their wild-type morphology. Finally, when D-Glu was supplemented at 10 or 20 mM, both morphology and cell density of the mutant strains were indistinguishable from the corresponding wild-type homologues.

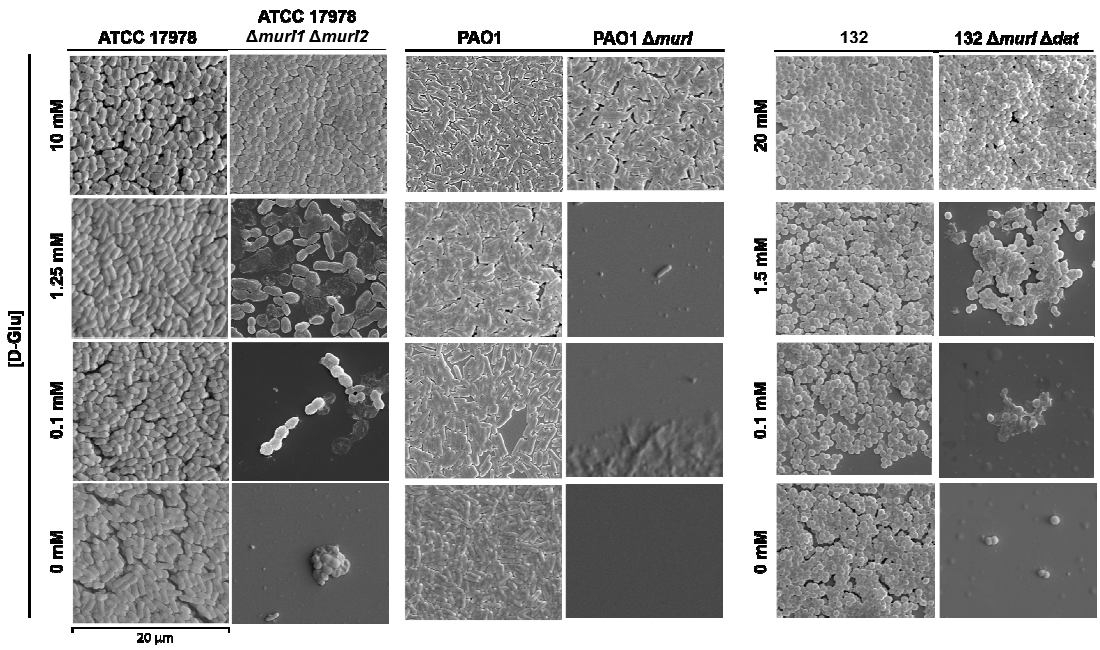

Figure 25 | *A. baumannii* MurI⁻ and *S. aureus* MurI⁻Dat⁻ impaired growth in D-Glu deprivation conditions. SEM of *A. baumannii* ATCC 17978, *P. aeruginosa* PAO1, *S. aureus* 132 and derived D-Glu auxotrophic strains in the presence of different D-Glu concentrations.

In addition to growth impairment, both ATCC 17978 Δ*murI1* Δ*murI2* and 132 Δ*murI* Δ*dat* strains exhibited an altered pattern of cell division when D-Glu was supplied at 0.1 mM **(Fig. 26).** The ATCC 17978 Δ*murI1* Δ*murI2* mutant strain showed filamentous aggregates consisting of three or more units of cells with atypical binary fission while 132 Δ*murI* Δ*dat* displayed large clusters of irregular cells due to impaired cell separation. A mass of presumptive protoplasts was observed in the vicinity of the intact cell forms of the mutant strains.

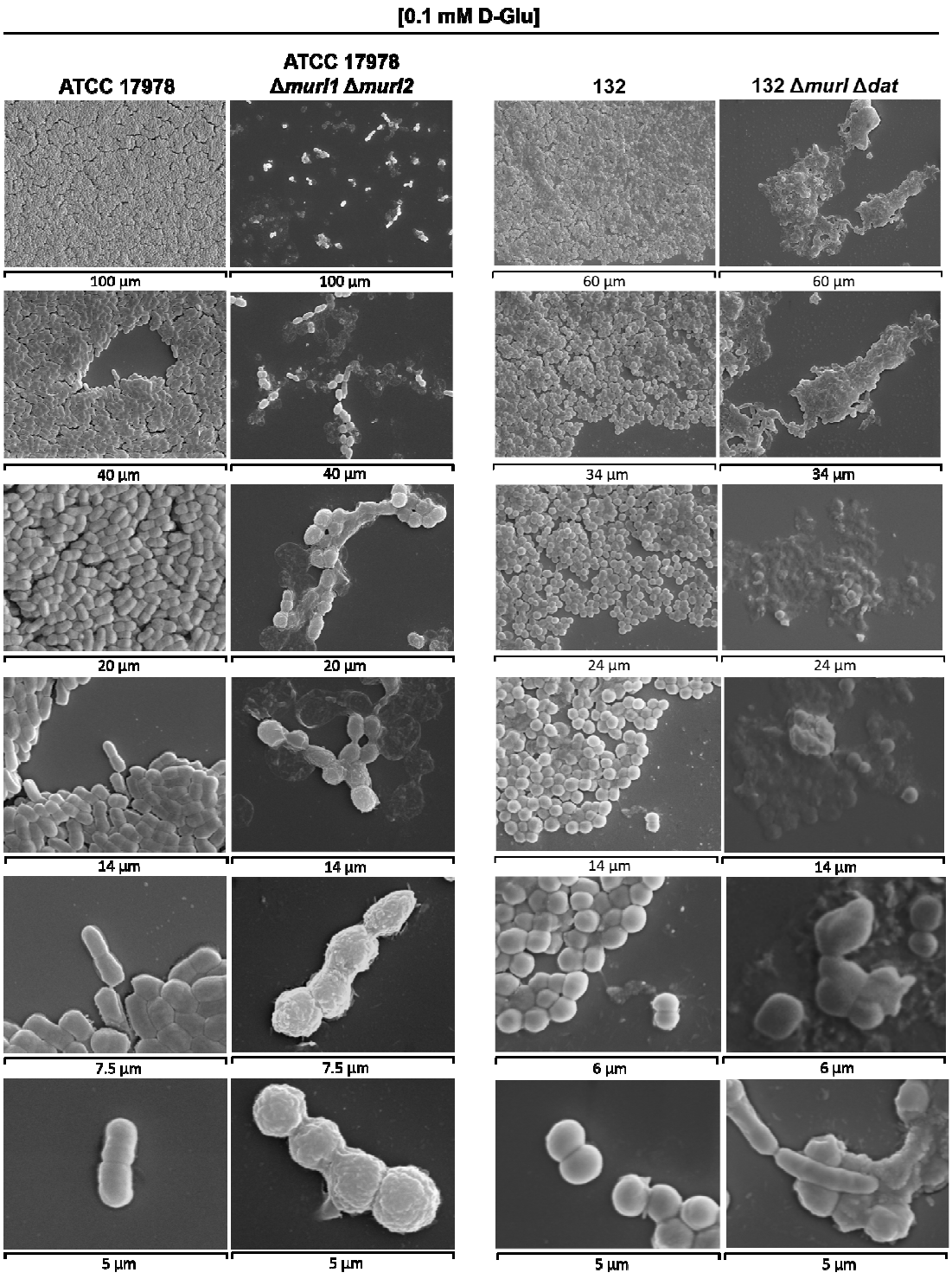

Figure 26 | *A. baumannii* MurI^{-} and *S. aureus* MurI^{-}Dat^{-} altered pattern of cell division. SEM of *A. baumannii* ATCC 17978, ATCC 17978 Δ*murI1* Δ*murI2*, *S. aureus* 132 and 132 Δ*murI* Δ*dat* in the presence of 0.1 mM D-Glu showing differences at the bacterial cell morphology and altered pattern of cell division.

Similarly, transmission electron microscopy (TEM) was performed showing that the cell walls of ATCC 17978 Δ*murI1* Δ*murI2* **(Fig. 27A)**, PAO1 Δ*murI* **(Fig. 27B)** and 132 Δ*murI* Δ*dat* **(Fig. 27C)**, experience progressive destruction when kept in the absence of D-Glu as a result of the blockage of peptidoglycan biosynthesis. Micrographs presented show cells with altered conformation that lose their semi-rigid structure, cells with several ruptures and displacement of membranes, lysis and extrusion of the intracellular content. Thus, the mechanism of lysis of D-Glu auxotrophic bacteria can be represented as follows **(Fig. 28).** First, inhibition of cell wall production leaves the protoplasm surrounded only by the inner (gram-negative) or cell membrane (Gram-positive bacteria), which renders this cell body susceptible to the variations in the osmolarity of the medium. Ultimately, lysis occurs through osmotic pressure, leaving traces of the cytoplasmic membranes that can form aggregates, and internal cellular content. These phenomena may occur either simultaneously or sequentially.

(A)

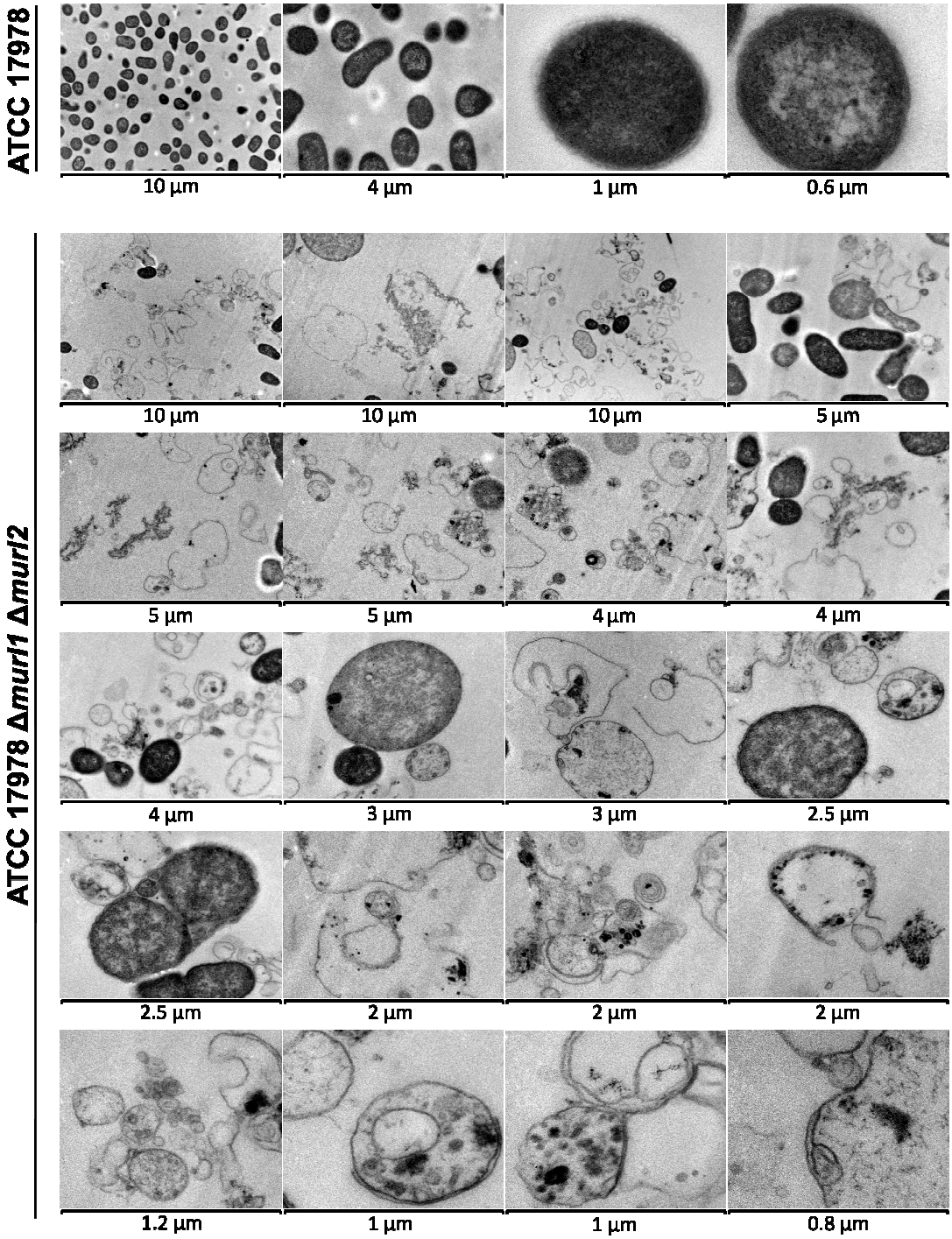

Figure 27 | D-Glu auxotrophy produces cell wall degeneration and bacterial lysis. Different atypical morphologies, progressive degeneration of the cell wall and lysis of D-Glu auxotrophic strains when kept in the absence of D-Glu. Micrographs were taken with a transmission electron microscope at different scales. **A,** *A. baumannii* ATCC 17978 and ATCC 17978 Δ*murI1* Δ*murI2*. **B,** *P. aeruginosa* PAO1 and PAO1 Δ*murI*. **C,** *S. aureus* 132 and 132 Δ*murI* Δ*dat*.

(B)

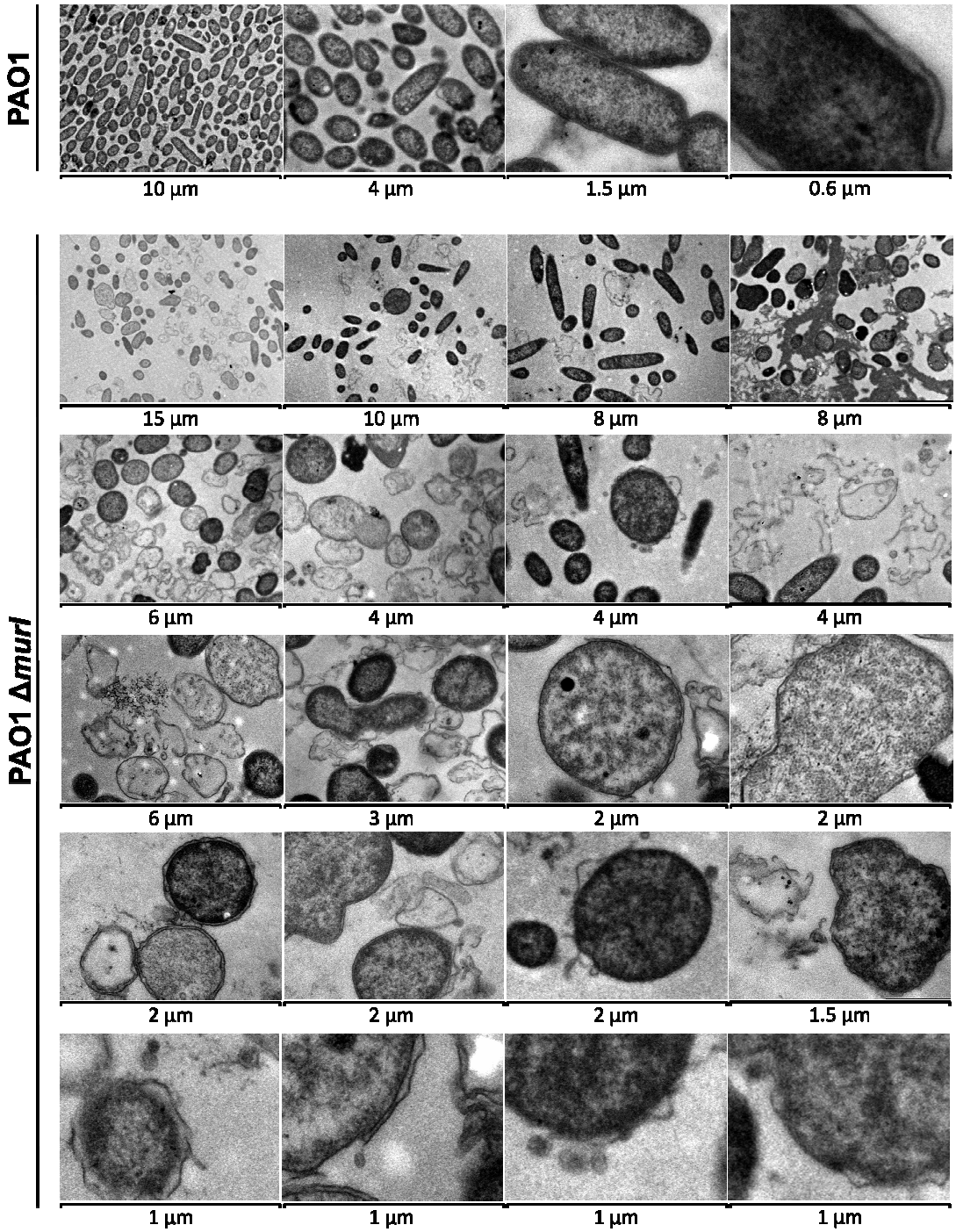

Figure 27 | D-Glu auxotrophy produces cell wall degeneration and bacterial lysis. Different atypical morphologies, progressive degeneration of the cell wall and lysis of D-Glu auxotrophic strains when kept in the absence of D-Glu. Micrographs were taken with a transmission electron microscope at different scales. **A,** *A. baumannii* ATCC 17978 and ATCC 17978 Δ*murI1* Δ*murI2*. **B,** *P. aeruginosa* PAO1 and PAO1 Δ*murI*. **C,** *S. aureus* 132 and 132 Δ*murI* Δ*dat*.

(C)

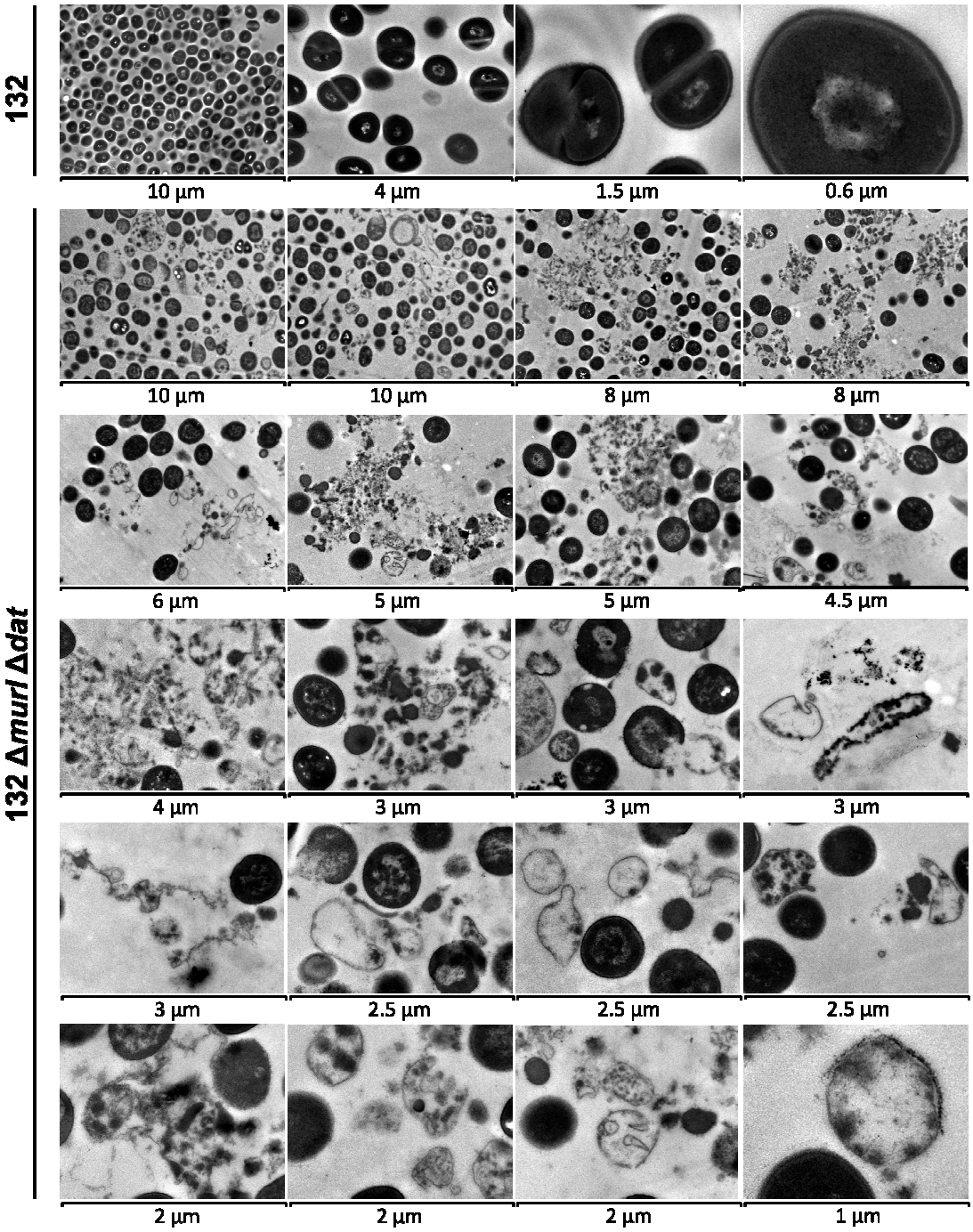

Figure 27 | D-Glu auxotrophy produces cell wall degeneration and bacterial lysis. Different atypical morphologies, progressive degeneration of the cell wall and lysis of D-Glu auxotrophic strains when kept in the absence of D-Glu. Micrographs were taken with a transmission electron microscope at different scales. **A,** *A. baumannii* ATCC 17978 and ATCC 17978 Δ*murI1* Δ*murI2*. **B,** *P. aeruginosa* PAO1 and PAO1 Δ*murI*. **C,** *S. aureus* 132 and 132 Δ*murI* Δ*dat*.

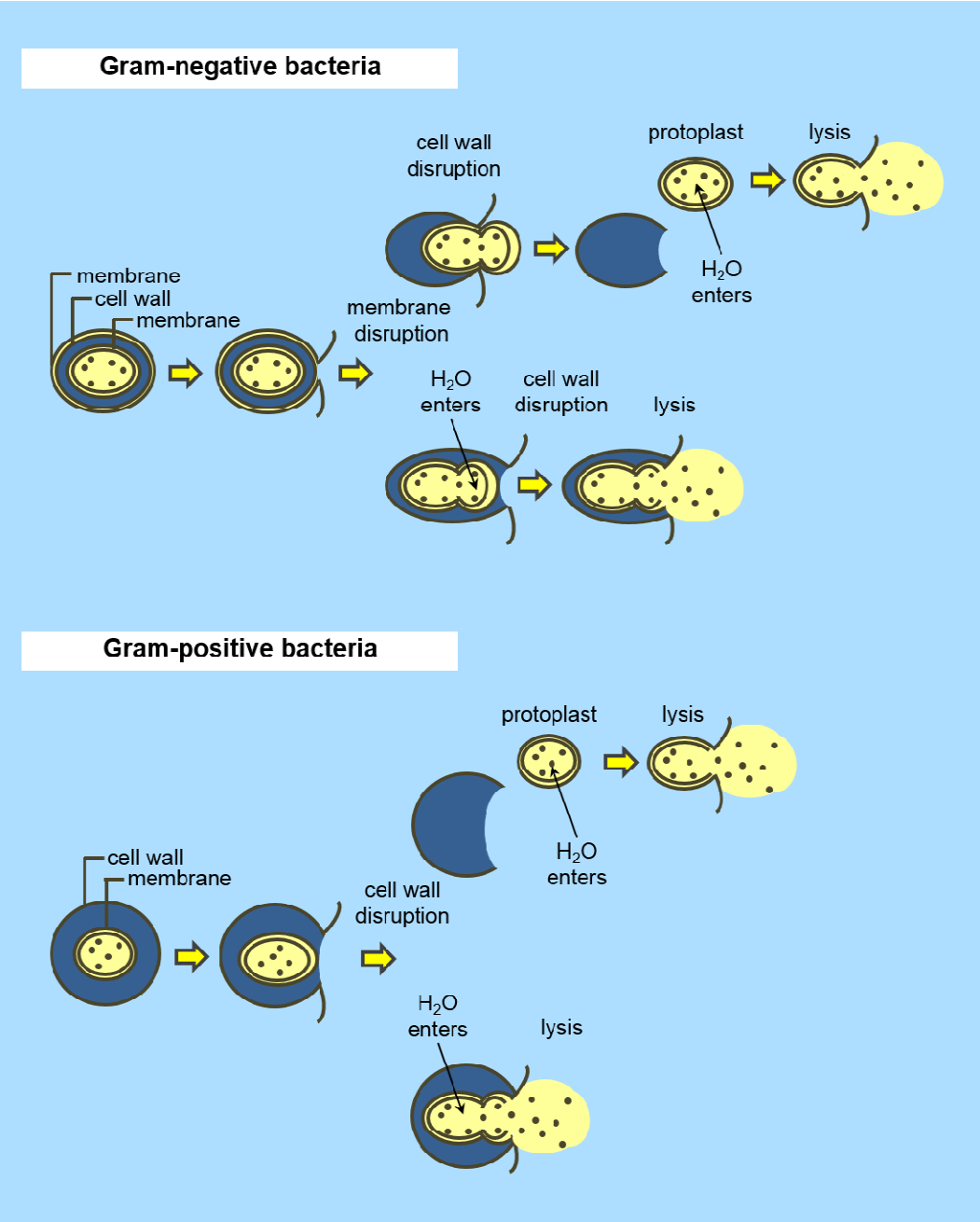

Figure 28 | Proposed schematic mechanism of cell wall degeneration and bacterial lysis of Gram-negative and Gram-positive bacteria auxotrophic for D-Glu.

4.2. Virulence attenuation of MurI⁻ and MurI⁻Dat⁻ mutants

One of the main characteristics that makes GMOs especially suitable for use as vaccines is the higher level of virulence attenuation respective to parental strains [58]. To test the hypothesis that bacteria auxotrophic for D-Glu are attenuated, the invasive capacity of the different *A. baumannii* ATCC 17978 mutants was first evaluated in comparison with the parental strain. BALB/c mice were injected intraperitoneally (IP) (2X)

with ATCC 17978, ATCC 17978 Δ*murI1*, ATCC 17978 Δ*murI2* and ATCC 17978 Δ*murI1* Δ*murI2.* After 12 hours, the following bacterial loads (Log10 CFU/g average values) in livers were obtained: 8.29 (mice administered ATCC 17978), 6.88 (mice administered ATCC 17978 Δ*murI1*), 8.06 (mice administered ATCC 17978 Δ*murI2*) and 1.59 (mice administered ATCC 17978 Δ*murI1* Δ*murI2*) **(Fig. 29)**. Moreover, in 4 of the 9 mice injected ATCC 17978 Δ*murI1* Δ*murI2*, bacteria were not recovered. Although significant differences were observed also for ATCC 17978 Δ*murI1,* the most accentuated reduction in bacterial burden resulted from the ATCC 17978 Δ*murI1* Δ*murI2* administration. These results suggested that combined Δ*murI1* and Δ*murI2* mutations prevent the invasive and replicative capacities of *A. baumannii*.

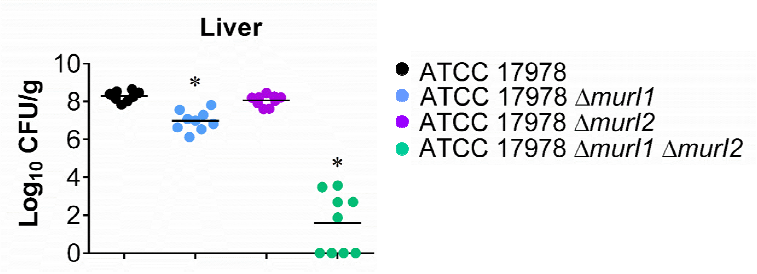

Figure 29 | Bacterial burden after infection. Bacterial loads in livers of BALB/c mice 12 hours after IP injection with *A. baumannii* ATCC 17978 (*n* = 8), ATCC 17978 Δ*murI1* (*n* = 9), ATCC 17978 Δ*murI2* (*n* = 9) and ATCC 17978 Δ*murI1* Δ*murI2* (*n* = 9). Each dot represents one mouse and each horizontal line represents the mean for each group. **P*<0.05 compared to ATCC 17978.

Next, mice survival was measured after IP injection with ATCC 17978 Δ*murI1* Δ*murI2*, PAO1 Δ*murI* and 132 Δ*murI* Δ*dat*. Using this acute lethal infection model, the LD_{100} (the minimal lethal dose for 100% of mice) of wild-type homologues were 2.5X for *A. baumannii* ATCC 17978, 0.4X for *P. aeruginosa* PAO1 and 1X for *S. aureus* 132. In contrast, the observed LD_{100} for ATCC 17978 Δ*murI1* Δ*murI2*, PAO1 Δ*murI* and 132 Δ*murI* Δ*dat* were 6X, >40X and >10X, respectively **(Fig. 30)**. These results evidenced that D-Glu auxotrophic strains are attenuated in comparison with the parental strains.

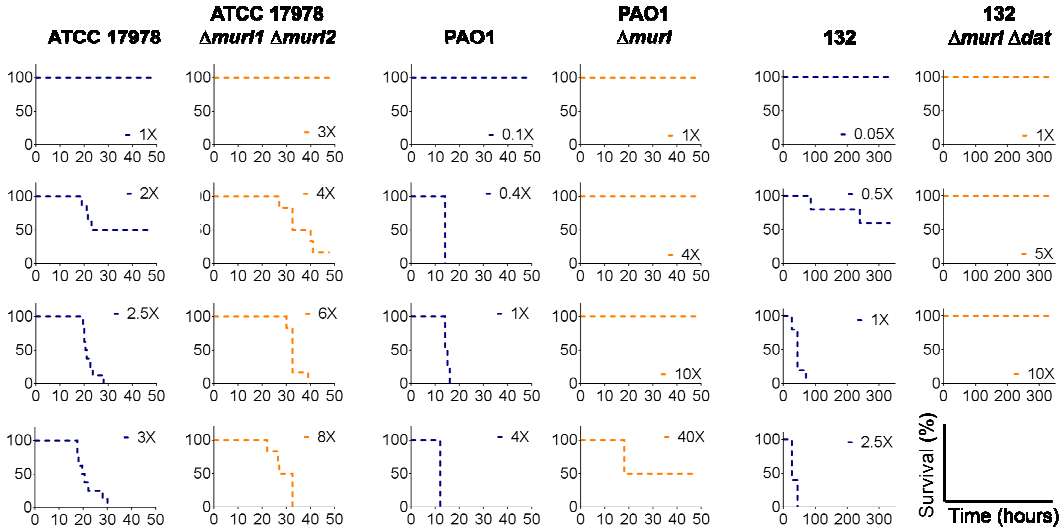

Figure 30 | D-Glu auxotrophic strains are attenuated respective to parental strains. Survival of BALB/c mice inoculated IP with *A. baumannii* ATCC 17978 (*n* = 8), ATCC 17978 Δ*murI1* Δ*murI2* (*n* = 6), *P. aeruginosa* PAO1 (*n* = 4), PAO1 Δ*murI* (*n* = 4), *S. aureus* 132 (*n* = 5) and 132 Δ*murI* Δ*dat* (*n* = 4) with different bacterial doses.

4.3. Generation of antibody-mediated immune responses

To measure the antibody-mediated immune responses at different vaccination regimens, BALB/c mice were immunized with D-Glu auxotrophic strains or administered saline according to **Figure 31**, and antibody titers were determined by ELISA. As shown, significant levels of IgM, IgG, IgG1, IgG2a, IgG2b and IgG3 against *A. baumannii* ATCC 17978, *P. aeruginosa* PAO1 and protein A-deficient *S. aureus* 132 (132 Δ*spa* [324]) were present in all immunized mice at the end of the immunization schedules. Antibody production after two immunizations was significantly higher than with one immunization, except for IgM with PAO1 Δ*murI*. Analysis of the IgG isotype revealed that vaccination with any of the D-Glu auxotrophic strains triggered a dominant IgG1 response, consistent with a predominant activation of Th2 lymphocytes [345]. Despite IgG2a, IgG2b and IgG3 levels being substantially lower in response to 132 Δ*murI* Δ*dat,* titers were still significant in all vaccinated groups. These results indicate that a Th1 differentiation was also stimulated upon vaccination [345].

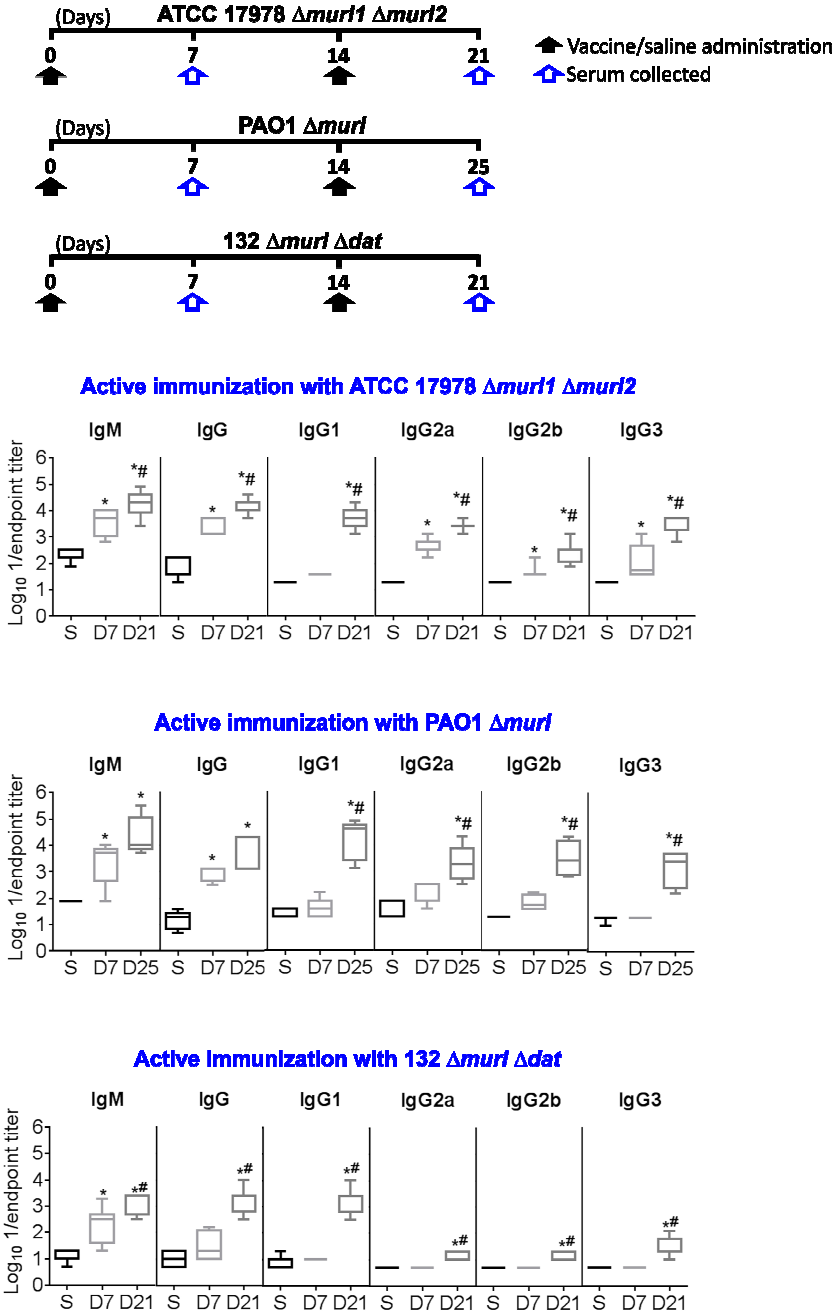

Figure 31 | Vaccination with D-Glu auxotrophic strains elicit high level of specific antibodies. Antibody titers against *A. baumannii* ATCC 17978 (*n* = 5-13), *P. aeruginosa* PAO1 (*n* = 4-7) and *S. aureus* 132 Δ*spa* (*n* = 5-7) in vaccinated and control mice after one or two injections with ATCC 17978 Δ*murI1* Δ*murI2* (1X, ±10^7 CFU/mouse), PAO1 Δ*murI* (0.4X, ±10^7 CFU/mouse) and 132 Δ*murI* Δ*dat* (1X, ±10^7 CFU/mouse), respectively, or saline. S, saline; D, day. **P*<0.05, compared with saline group. #*P*<0.05, compared with the preceding condition.

Immune responses after administering different doses of ATCC 17978 Δ*murI1* Δ*murI2*, PAO1 Δ*murI* and 132 Δ*murI* Δ*dat* were also evaluated. To that end, groups of mice

were immunized on days 0 and 14 with ATCC 17978 Δ*murI1* Δ*murI2*: 0.01X, 0.05X, 0.1X, 0.5X and 1X. On day 21, serum was obtained. For *P. aeruginosa*, groups of mice were immunized once with the following PAO1 Δ*murI* doses: 0.1X, 0.4X, 1X, 4X, 10X and 40X. Serum was obtained on day 40. For *S. aureus*, groups of mice were immunized on days 0 and 14 with the following 132 Δ*murI* Δ*dat* doses: 0.2X, 1X, 5X and 10X; sera were obtained on day 21. Control mice were administered saline (0X). As shown in **Figure 32**, significant levels of IgM and total IgG were present in all immunized mice at the end of the immunization schedules. All tested ATCC 17978 Δ*murI1* Δ*murI2* vaccine doses above 0.05X elicited significant levels of IgG1, IgG2a, IgG2b and IgG3 subtypes. Although PAO1 Δ*murI* 0.1X was sufficient to induce IgM and IgG titers significantly, total IgG titers were higher when using a dose of 0.4X. For 132 Δ*murI* Δ*dat*, only 5X and 10X doses raised significantly all IgG subtypes; using 132 Δ*murI* Δ*dat* 1X elicited IgG1 and IgG3 subtypes only. Altogether, these results suggest that these D-Glu auxotrophic vaccines drive the production of antibodies in a dose-dependent manner.

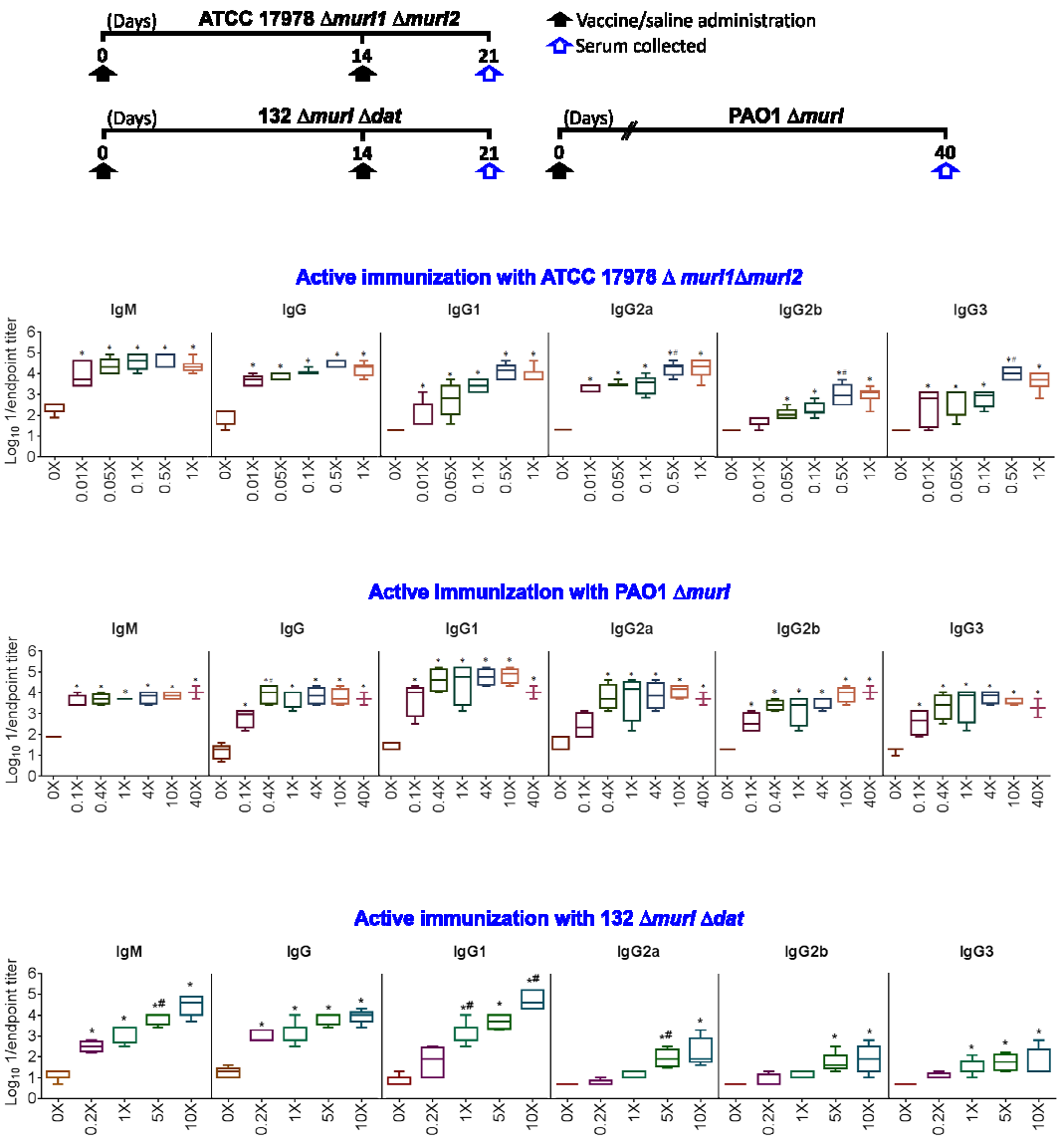

Figure 32 | Antibody-mediated immune response activation by D-Glu auxotrophic strains is dose-dependent. Antibody titers elicited in mice by administration of different doses of ATCC 17978 Δ*murI1* Δ*murI2* (*n* = 5-10), PAO1 Δ*murI* (*n* = 2-7) and 132 Δ*murI* Δ*dat* (*n* = 4-7) on days 21 (after two immunizations), 40 (one immunization) and 21 (two immunizations), respectively. **P*<0.05, compared with saline group (0X). #*P*<0.05 compared with antibody production of an immediate lower dose.

The exposure to foreign antigen yields a biphasic response: the first phase is associated with production of IgM followed by production of IgG, the second phase is characterized by a reduction in IgM followed by an increase of IgG. Higher proportion of IgG and other isotypes of antibodies compared with the level of IgM also characterizes memory antibody responses. Indeed, using a single immunization low dose (0.0001X) of ATCC 17978 Δ*murI1* Δ*murI2*, it was possible to detect antigen-specific IgM, IgG, IgG1, IgG2a, IgG2b and

IgG3 in the sera of mice, 123 days and 1 year after immunization **(Fig. 33)**. Also, IgM titers were higher at day 7 but markedly reduced on day 123. In contrast, IgG1, IgG2b and IgG3 titers increased significantly between days 7 and 123; total IgG levels were maintained until 1 year after immunization, indicating a biphasic response and a long-term antibody memory.

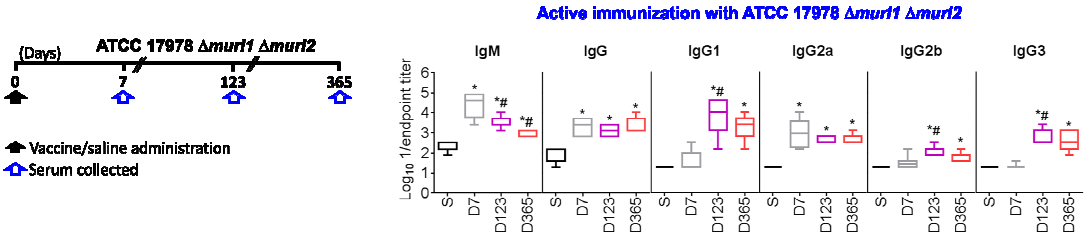

Figure 33 | ATCC 17978 Δ*murI1* Δ*murI2* vaccination elicits long-term antibody memory. Antibody titers (*n* = 5-8) against ATCC 17978 on days 7, 123 and 365 after ATCC 17978 Δ*murI1* Δ*murI2* (0.0001X) administration, or saline. S, saline; D, day. **P*<0.05, compared with saline group. #*P*<0.05, compared with the preceding condition.

A key feature of any vaccine is its ability to generate a broad immune response; it is crucial that vaccination with a single strain preparation induces antibodies reactive against heterologous strains. As shown in **Figure 34**, IgG antibodies elicited with ATCC 17978 Δ*murI1* Δ*murI2* were cross-reactive with ATCC 19606, MDR-AbH12O-A2 and encapsulated-Ab307-0294 **(see Table 5)**. IgG titers obtained after two PAO1 Δ*murI* immunizations were cross-reactive with PA21_ST175, PA14, PA51441321, LES431, PA28562 and PA51442390 **(see Table 5)**. IgG titers obtained with three PAO1 Δ*murI* immunizations were cross-reactive with the previous strains plus PA12142 and LES400 **(see Table 5)**. Of note, PA28562 and PA51442390 present the mucoid phenotype associated with chronic infections from CF patients [346]. IgG antibodies elicited with 132 Δ*murI* Δ*dat* were cross-reactive with FPR3757 strain of the high-risk clone CA-MRSA USA300, and with *S. aureus* strains of animal origin, RF122 (bovine), ED133 (ovine) and ED98 (poultry) **(see Table 5)**. IgG titers and cross-reactivity were significantly raised when a higher dose of 132 Δ*murI* Δ*dat* was used (10X). Taken together our data indicate that IgG induced by ATCC 17978 Δ*murI1* Δ*murI2*, PAO1 Δ*murI1* and 132 Δ*murI* Δ*dat* is cross-reactive to a wide variety of *A. baumannii*, *P. aeruginosa* and *S. aureus* strains, respectively.

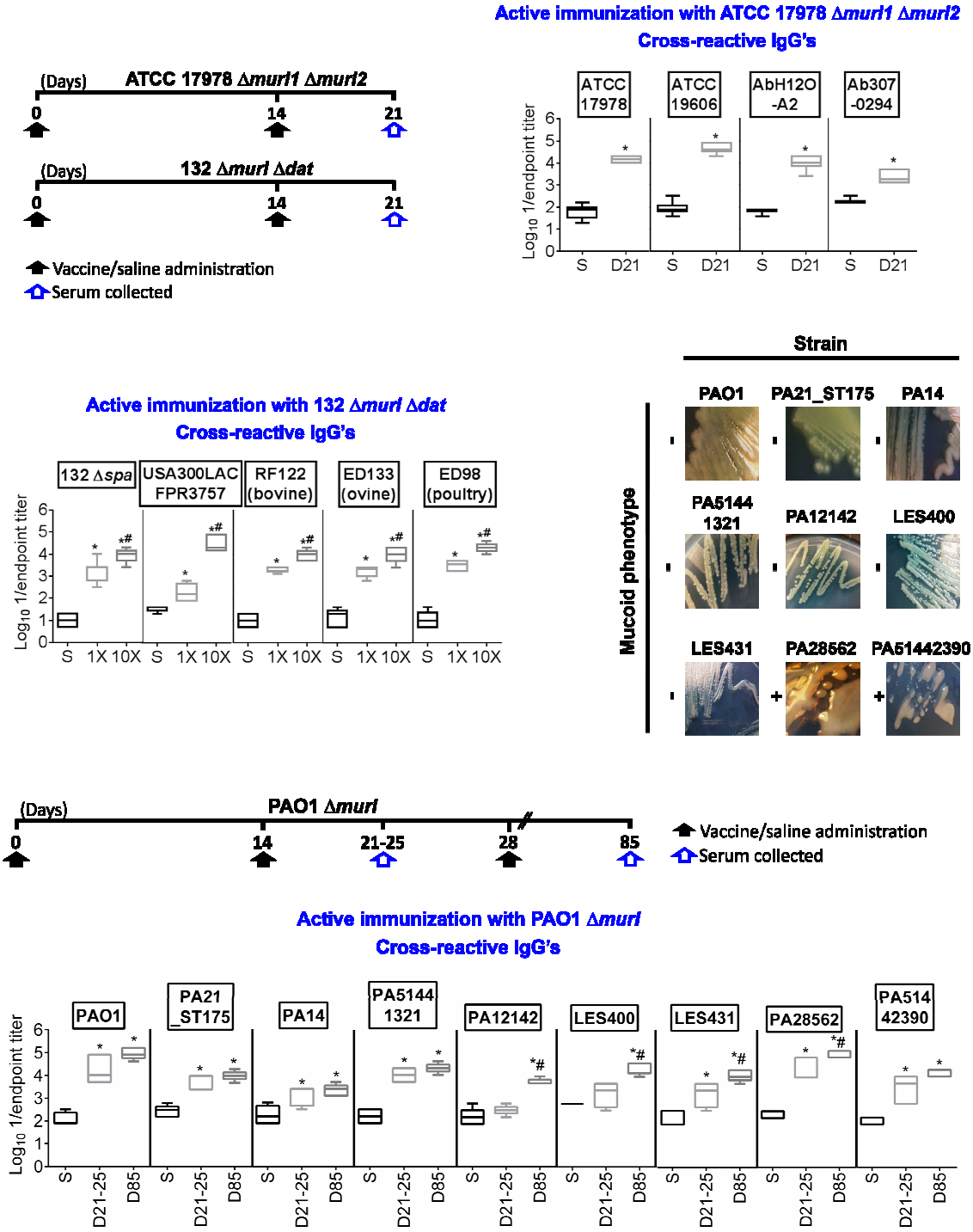

Figure 34 | Vaccination with D-Glu auxotrophic strains elicit high levels of cross-reactive antibodies. IgG titers against different *A. baumannii* (*n* = 6), *P. aeruginosa* (*n* = 5) and *S. aureus* (*n* = 5-9) strains in vaccinated and control mice after two or three injections with ATCC 17978 Δ*murI1* Δ*murI2* (1X), PAO1 Δ*murI* (0.4X) and 132 Δ*murI* Δ*dat* (1X and 10X), respectively, or saline. Mucoid (+) and non-mucoid (–) phenotype appearance of tested *P. aeruginosa* strains. S, saline; D, day. **P*<0.05, compared with saline group. #*P*<0.05, compared with the preceding condition.

4.4. Activation of cell-mediated immunity

A successful vaccine should potentially trigger an appropriate cellular immune response. To explore the nature of T cell responses generated by the vaccine strains, we measured antigen specific IFN-γ-, IL-4-, and IL-17-secreting splenocytes after *ex vivo* restimulation with *A. baumannii* ATCC 17978 Δ*murI1* Δ*murI2*, *P. aeruginosa* PAO1 Δ*murI* and *S. aureus* Δ*murI* Δ*dat*, using ELISpot **(Figs. 35-43)**. These cytokines were selected as markers of Th1, Th2 and Th17 T cell subsets, respectively. ATCC 17978 Δ*murI1* Δ*murI2*, PAO1 Δ*murI* and 132 Δ*murI* Δ*dat* mediated a significant increase in the number of IL-17-secreting splenocytes and it was the predominant T cell subset triggered by 132 Δ*murI* Δ*dat* **(Fig. 44).** A significant number of IFN-γ-secreting splenocytes was triggered by 132 Δ*murI* Δ*dat*, while a substantial increment – although not significant – was observed with ATCC 17978 Δ*murI1* Δ*murI2* and PAO1 Δ*murI* **(Fig. 44)**. IL-4-producing splenocytes were stimulated in response to ATCC 17978 Δ*murI1* Δ*murI2* and PAO1 Δ*murI*, but not in response to 132 Δ*murI* Δ*dat* **(Fig. 44).** These data indicate that active immunization with ATCC 17978 Δ*murI1* Δ*murI2* and PAO1 Δ*murI* triggers a consistent Th2 immune response while 132 Δ*murI* Δ*dat* elicits a Th1 response.

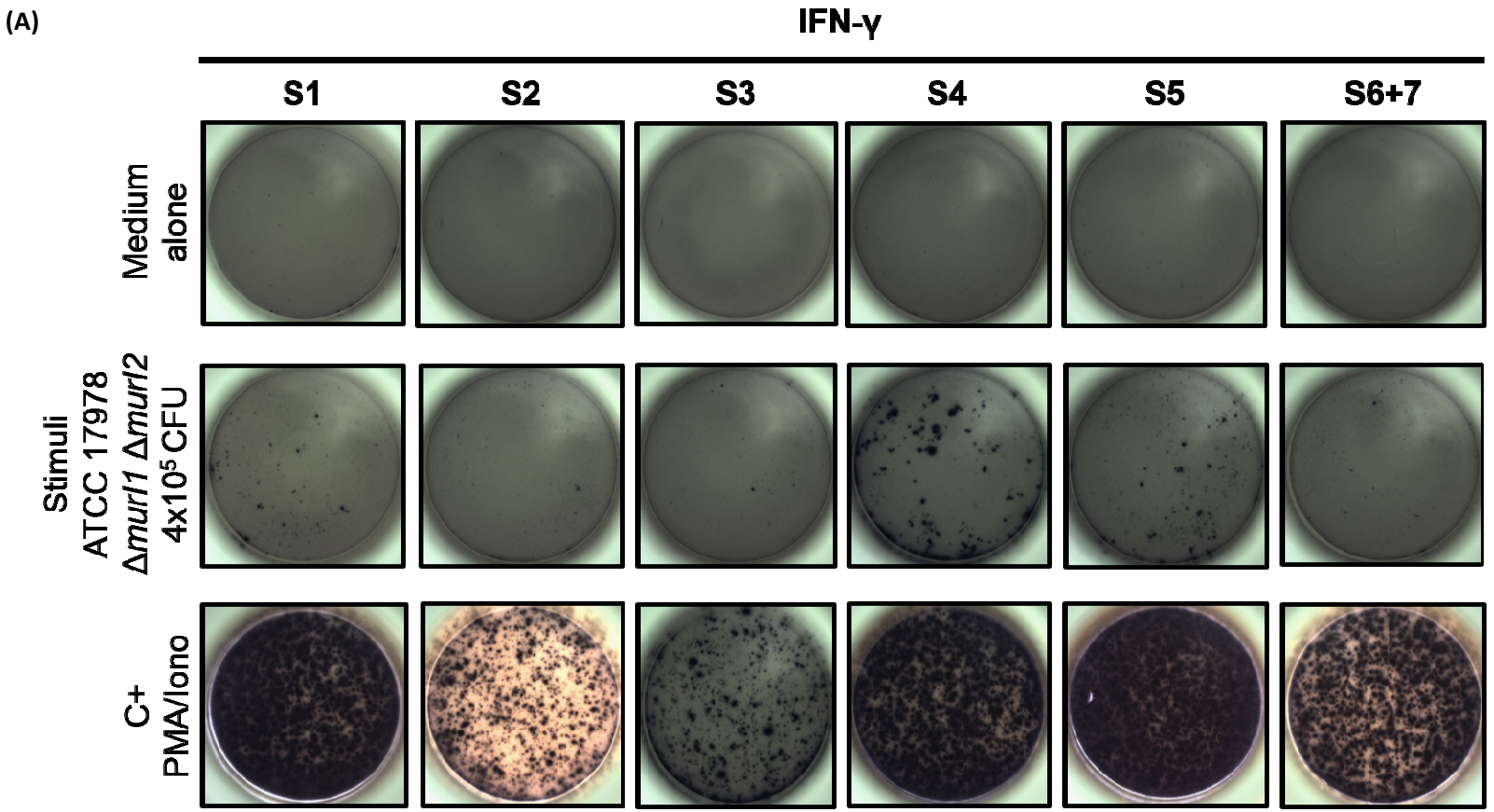

Figure 35 | Vaccination with ATCC 17978 Δ*murI1* Δ*murI2* triggers IFN-γ cytokine-secreting T cells. Detection of antigen-specific IFN-γ-secreting T cells collected at day 82 from the spleens of **A,** saline mice (*n* = 7) and **B,** vaccinated mice (*n* = 6), after being restimulated *ex vivo* for 43 hours with ATCC 17978 Δ*murI1 murI2*, PMA (phorbol 12-myristate 13-acetate)/Ionomycin, or medium alone. **A-B,** Each well contains 4×10^5 splenocytes. S, saline; V, vaccinated.

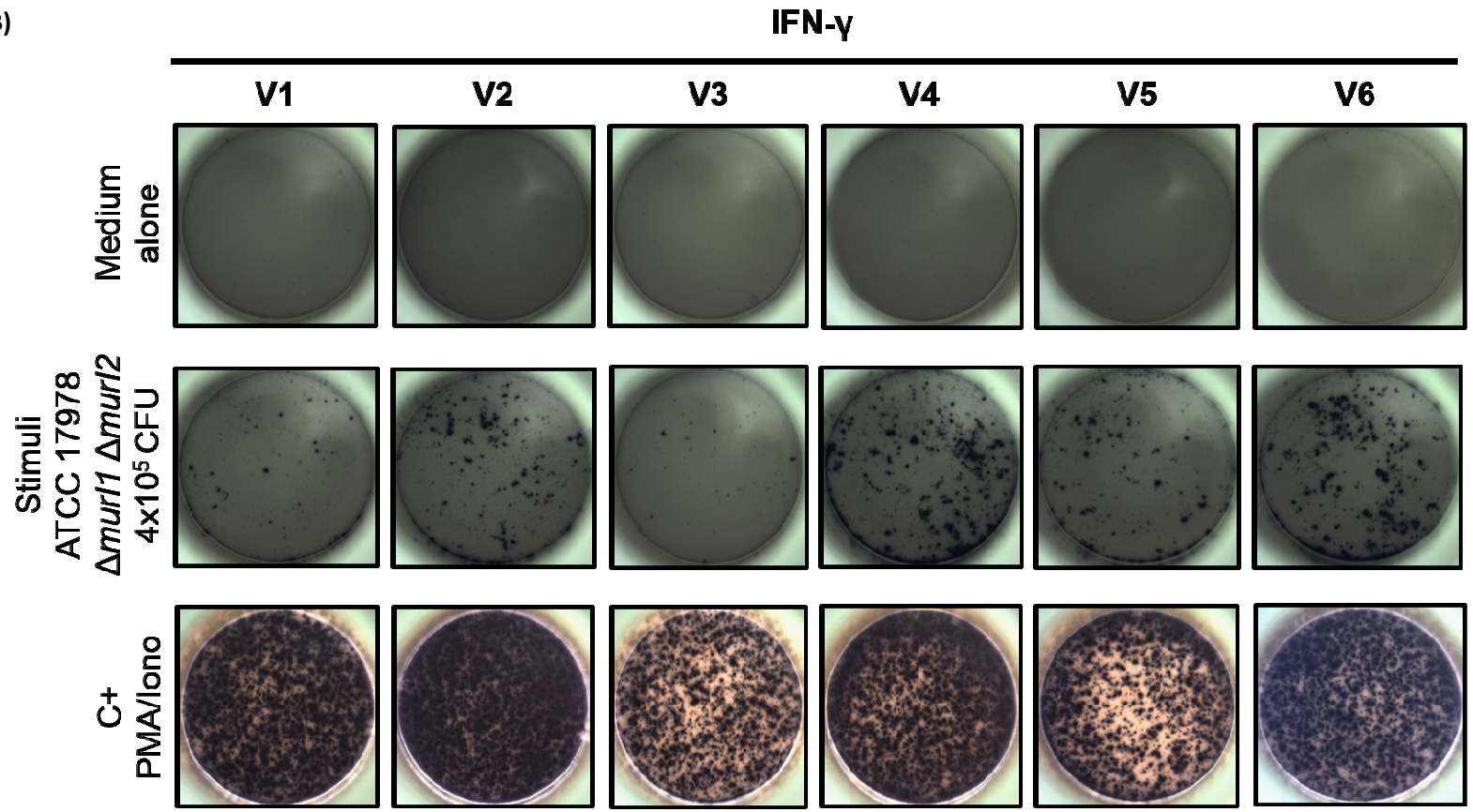

Figure 35 | Vaccination with ATCC 17978 Δ*murI1* Δ*murI2* triggers IFN-γ cytokine-secreting T cells. Detection of antigen-specific IFN-γ-secreting T cells collected at day 82 from the spleens of **A,** saline mice (*n* = 7) and **B,** vaccinated mice (*n* = 6), after being restimulated *ex vivo* for 43 hours with ATCC 17978 Δ*murI1*Δ *murI2*, PMA (phorbol 12-myristate 13-acetate)/Ionomycin, or medium alone. **A-B,** Each well contains 4×10^5 splenocytes. S, saline; V, vaccinated.

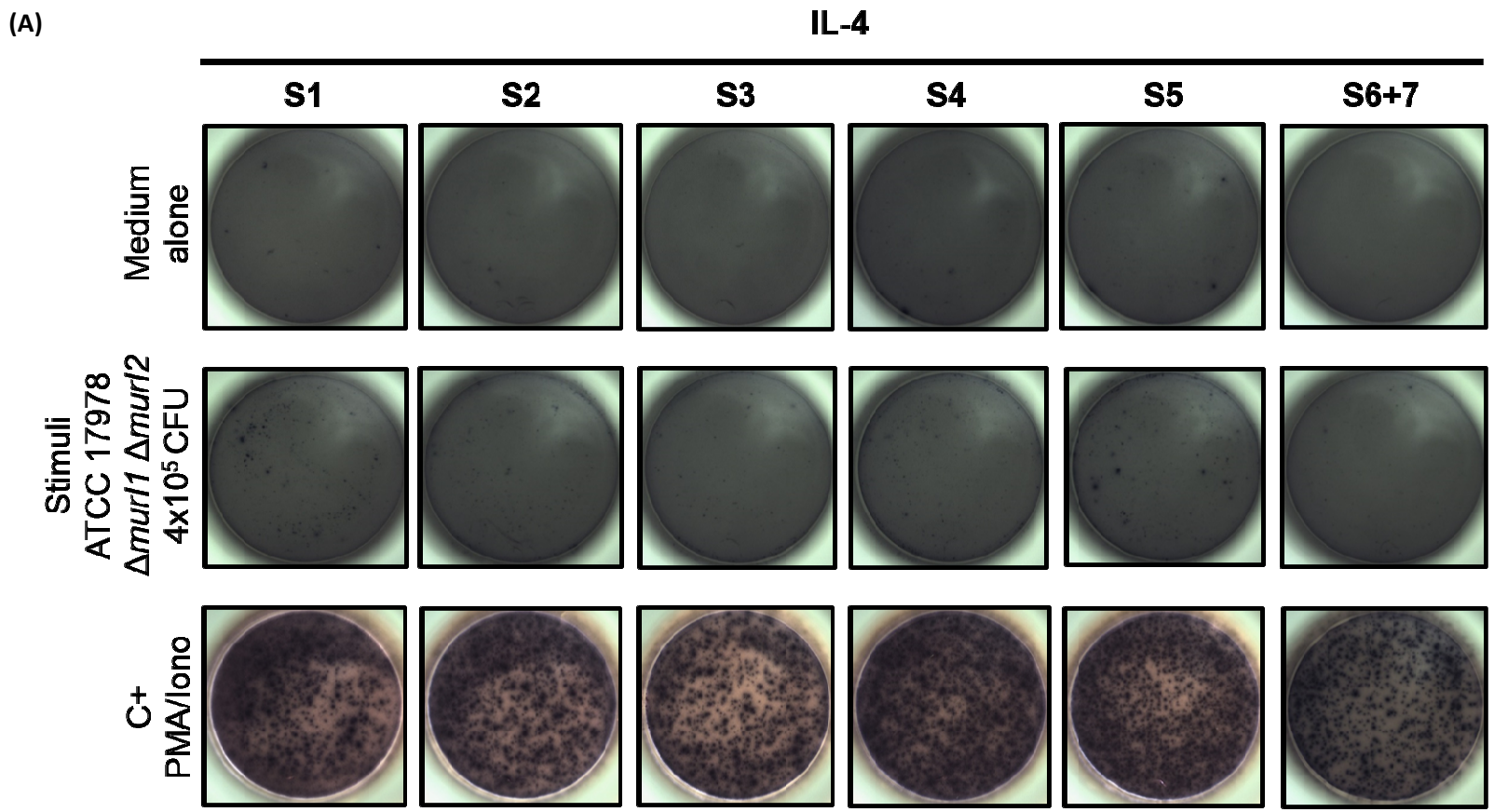

Figure 36 | Vaccination with ATCC 17978 Δ*murI1* Δ*murI2* triggers IL-4 cytokine-secreting T cells. Detection of antigen-specific IL-4-secreting T cells collected at day 82 from the spleens of **A,** saline mice (*n* = 7) and **B,** vaccinated mice (*n* = 6), after being restimulated *ex vivo* for 43 hours with ATCC 17978 Δ*murI1* Δ*murI2*, PMA (phorbol 12-myristate 13-acetate)/Ionomycin, or medium alone. **A-B,** Each well contains 4×10^5 splenocytes. S, saline; V, vaccinated.

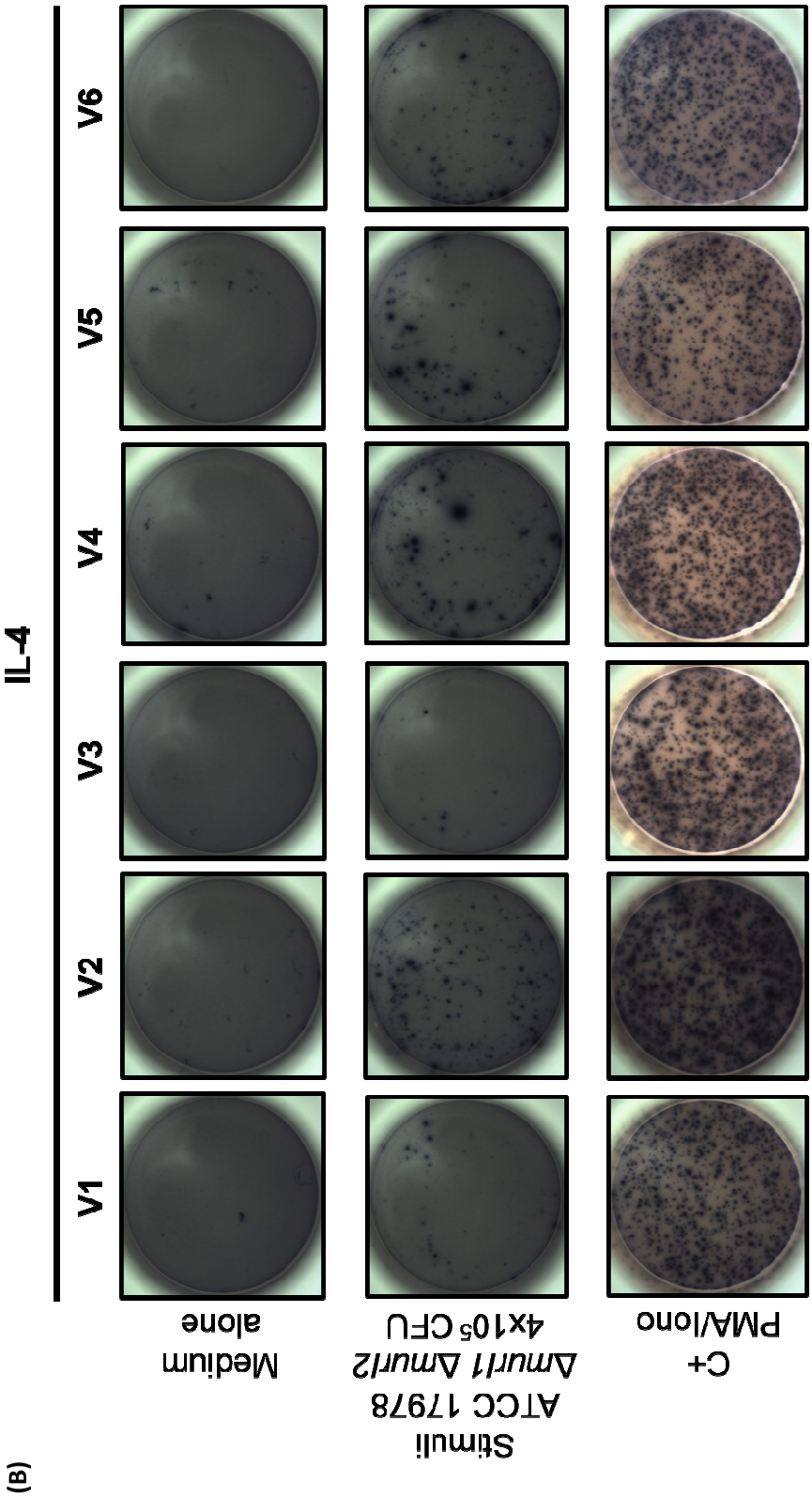

Figure 36 | Vaccination with ATCC 17978 *Δmurl1 Δmurl2* triggers IL-4 cytokine-secreting T cells. Detection of antigen-specific IL-4-secreting T cells collected at day 82 from the spleens of **A,** saline mice (n = 7) and **B,** vaccinated mice (n = 6), after being restimulated *ex vivo* for 43 hours with ATCC 17978 *Δmurl1 Δmurl2*, PMA (phorbol 12-myristate 13-acetate)/Ionomycin, or medium alone. **A-B,** Each well contains 4×10^5 splenocytes. S, saline; V, vaccinated.

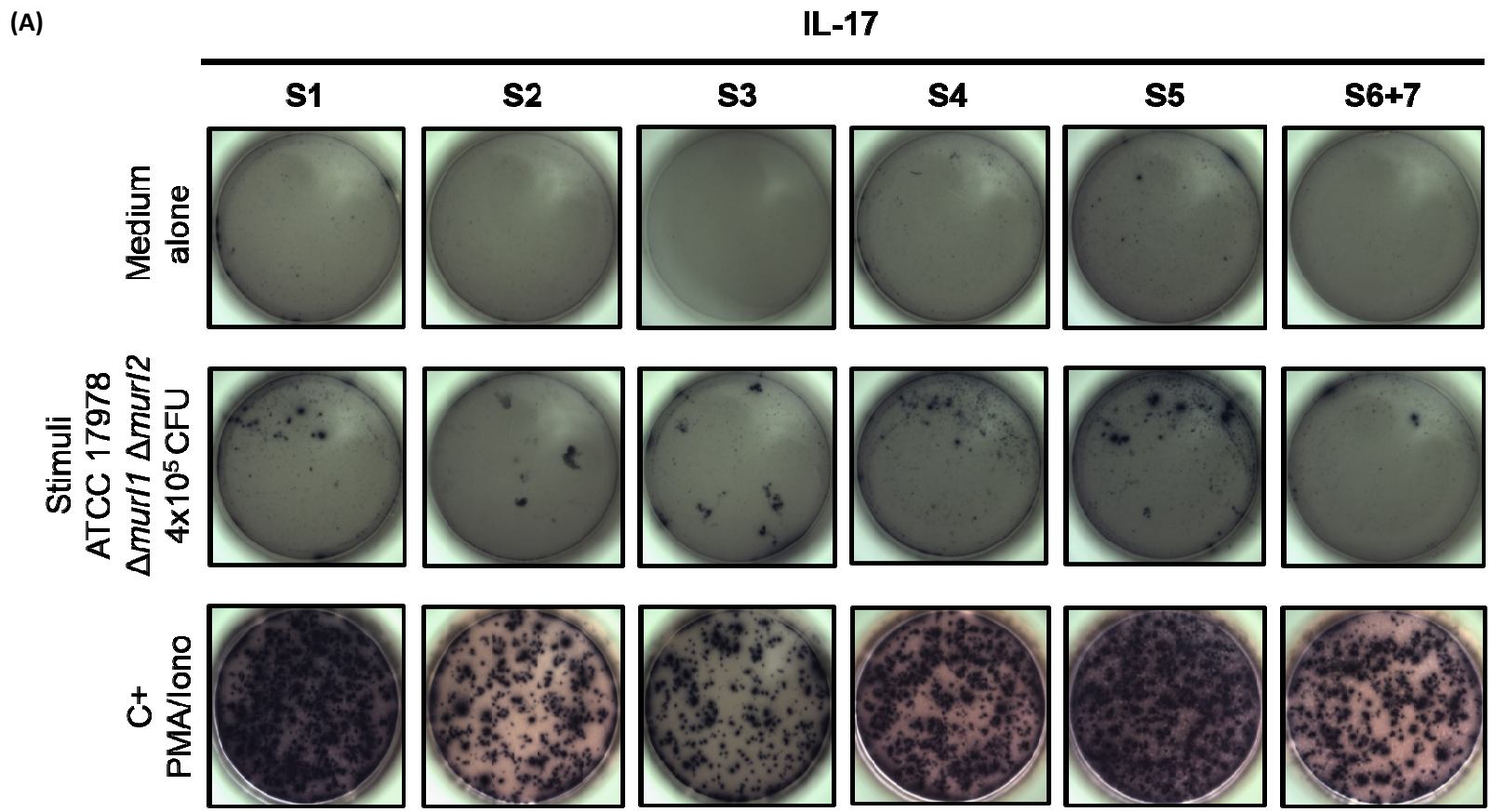

Figure 37 | Vaccination with ATCC 17978 Δ*murI1* Δ*murI2* triggers IL-17 cytokine-secreting T cells. Detection of antigen-specific IL-17-secreting T cells collected at day 82 from the spleens of **A,** saline mice (*n* = 7) and **B,** vaccinated mice (*n* = 6), after being restimulated *ex vivo* for 43 hours with ATCC 17978 Δ*murI1* Δ*murI2*, PMA (phorbol 12-myristate 13-acetate)/Ionomycin, or medium alone. **A-B,** Each well contains 4×10^5 splenocytes. S, saline; V, vaccinated.

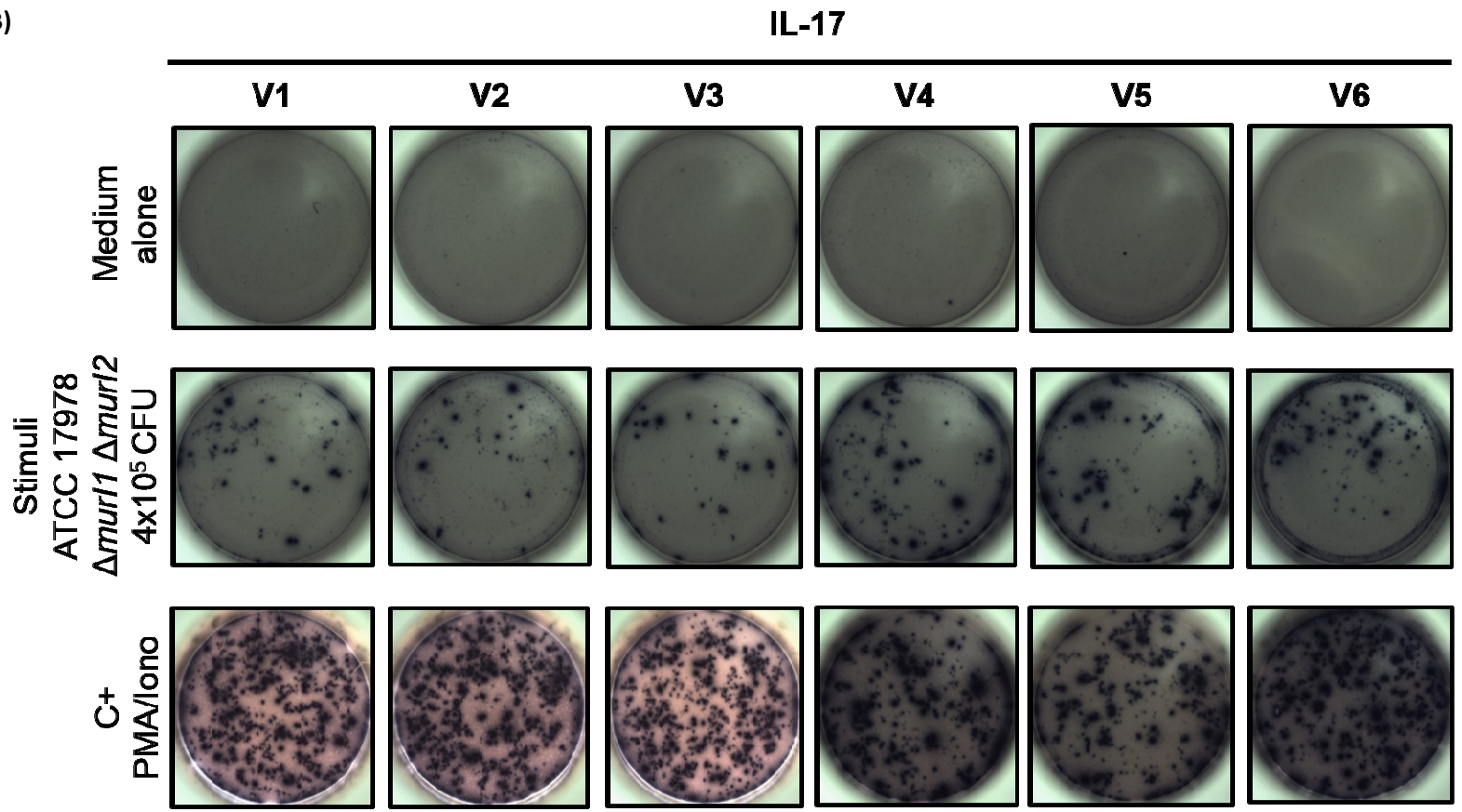

Figure 37 | Vaccination with ATCC 17978 Δ*murI1* Δ*murI2* triggers IL-17 cytokine-secreting T cells. Detection of antigen-specific IL-17-secreting T cells collected at day 82 from the spleens of **A,** saline mice (*n* = 7) and **B,** vaccinated mice (*n* = 6), after being restimulated *ex vivo* for 43 hours with ATCC 17978 Δ*murI1* Δ*murI2*, PMA (phorbol 12-myristate 13-acetate)/Ionomycin, or medium alone. **A-B,** Each well contains 4×10^5 splenocytes. S, saline; V, vaccinated.

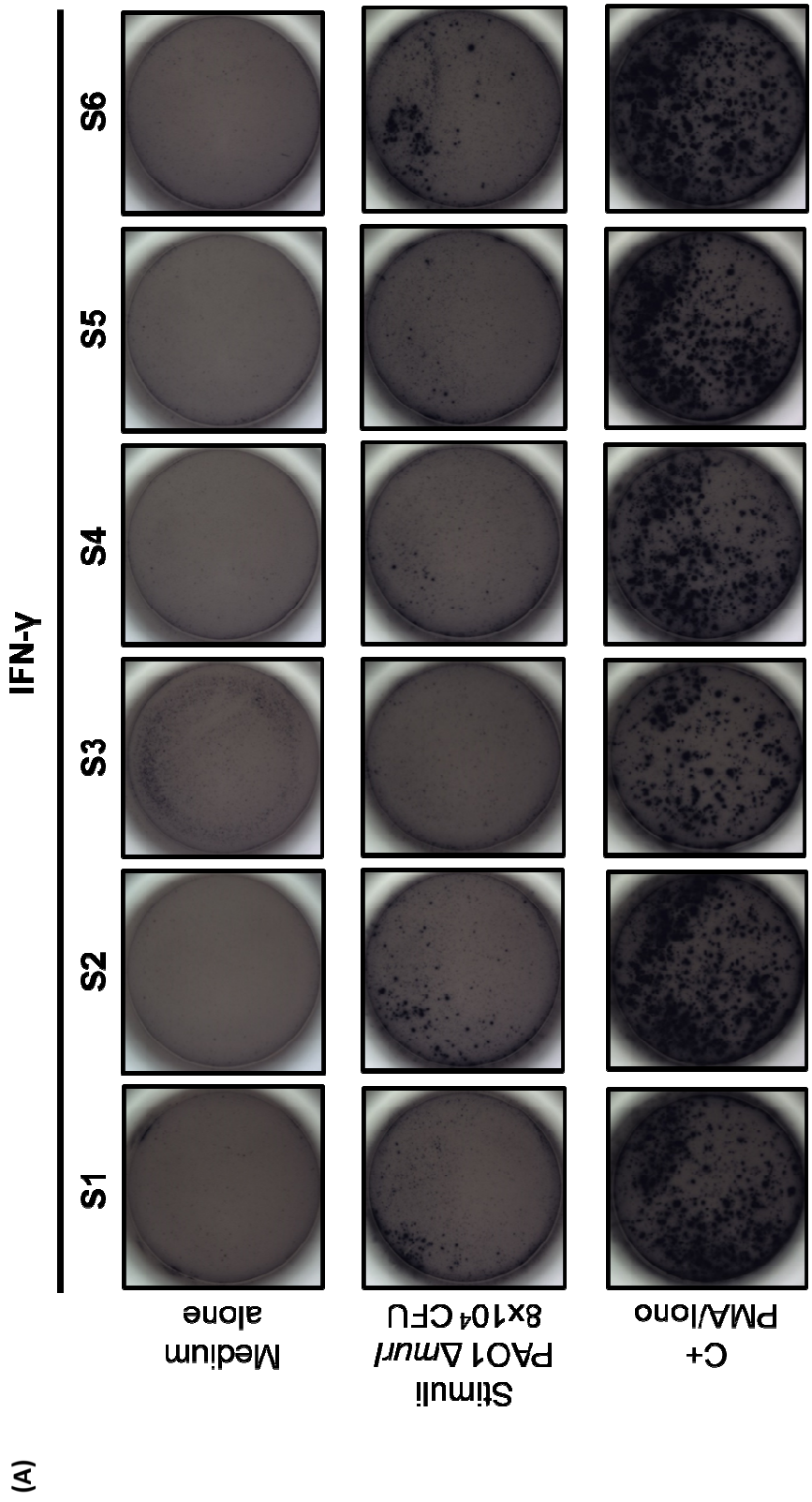

Figure 38 | Vaccination with PAO1 Δ*murI* triggers IFN-γ cytokine-secreting T cells. Detection of antigen-specific IFN-γ-secreting T cells collected at day 68 from the spleens of **A,** saline mice (n = 6) and **B,** vaccinated mice (n = 6), after being restimulated *ex vivo* for 43 hours with PAO1 Δ*murI*, PMA (phorbol 12-myristate 13-acetate)/Ionomycin, or medium alone. **A-B,** Each well contains 8×10^5 splenocytes. S, saline; V, vaccinated.

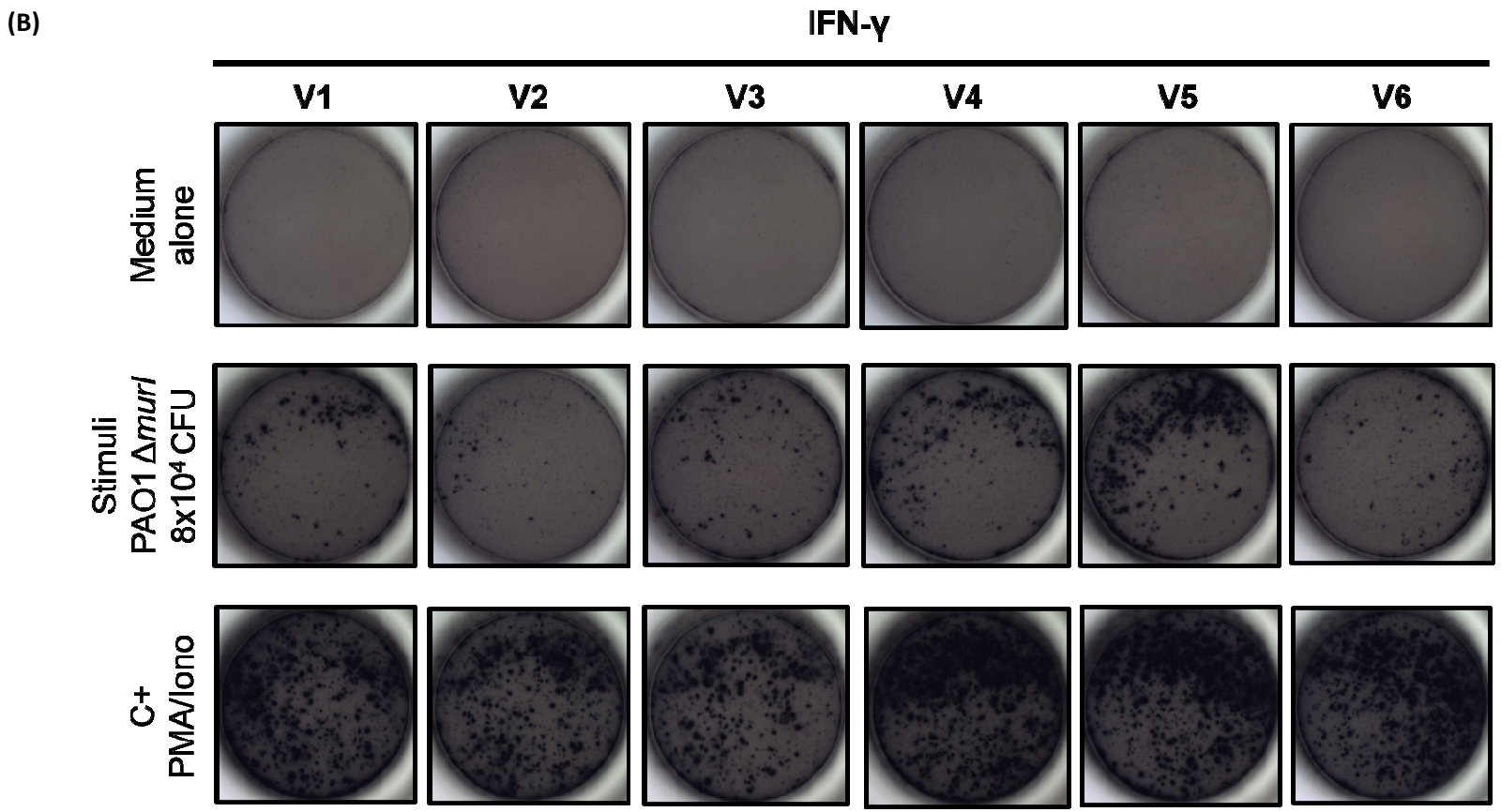

Figure 38 | Vaccination with PAO1 Δ*murI* triggers IFN-γ cytokine-secreting T cells. Detection of antigen-specific IFN-γ-secreting T cells collected at day 68 from the spleens of **A,** saline mice (*n* = 6) and **B,** vaccinated mice (*n* = 6), after being restimulated *ex vivo* for 43 hours with PAO1 Δ*murI*, PMA (phorbol 12-myristate 13-acetate)/Ionomycin, or medium alone. **A-B,** Each well contains 8×10^5 splenocytes. S, saline; V, vaccinated.

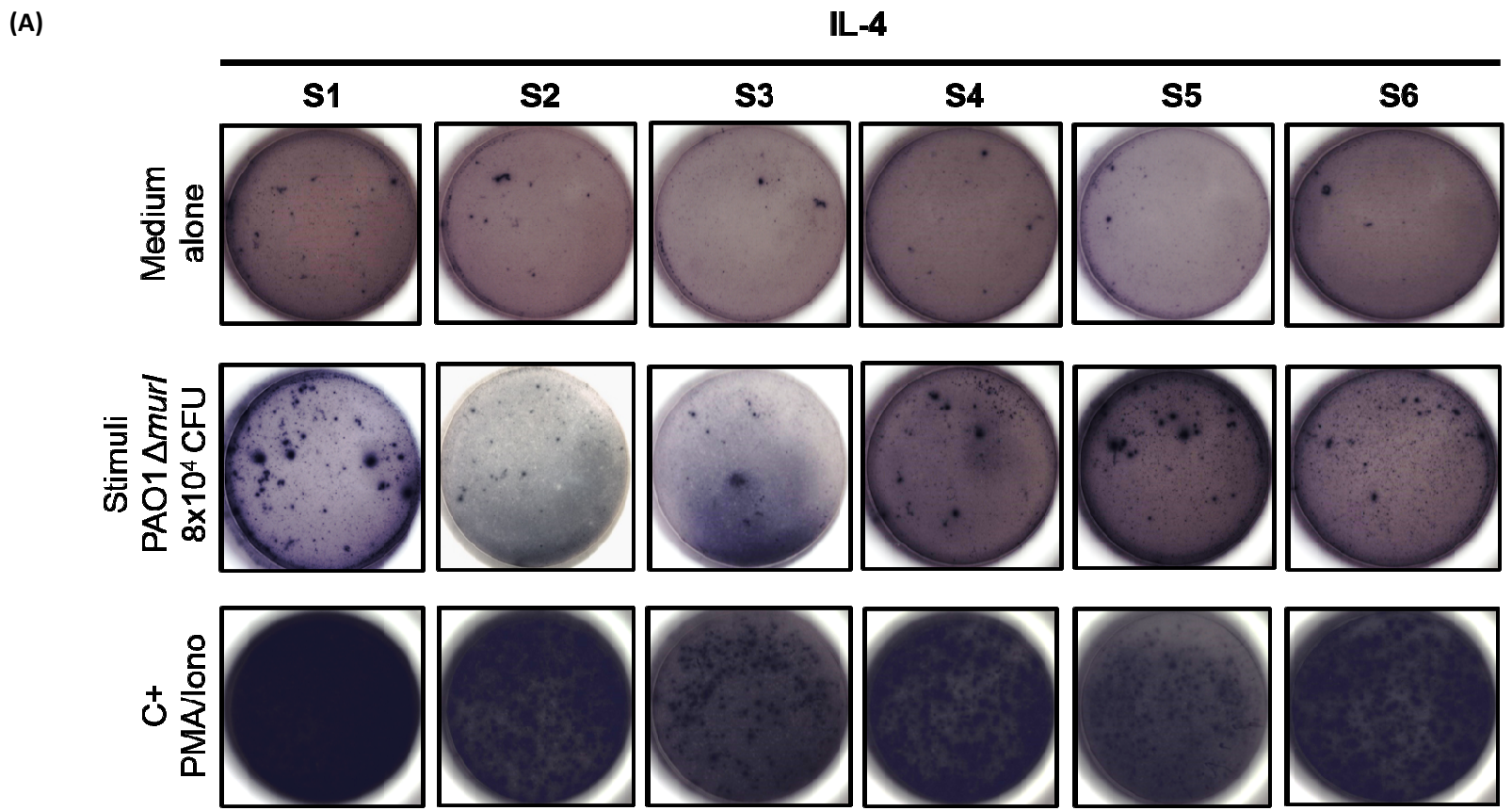

Figure 39 | Vaccination with PAO1 Δ*murI* triggers IL-4 cytokine-secreting T cells. Detection of antigen-specific IL-4-secreting T cells collected at day 68 from the spleens of **A,** saline mice (*n* = 6) and **B,** vaccinated mice (*n* = 6), after being restimulated *ex vivo* for 43 hours with PAO1 Δ*murI*, PMA (phorbol 12-myristate 13-acetate)/Ionomycin, or medium alone. **A-B,** Each well contains 8×10^5 splenocytes. S, saline; V, vaccinated.

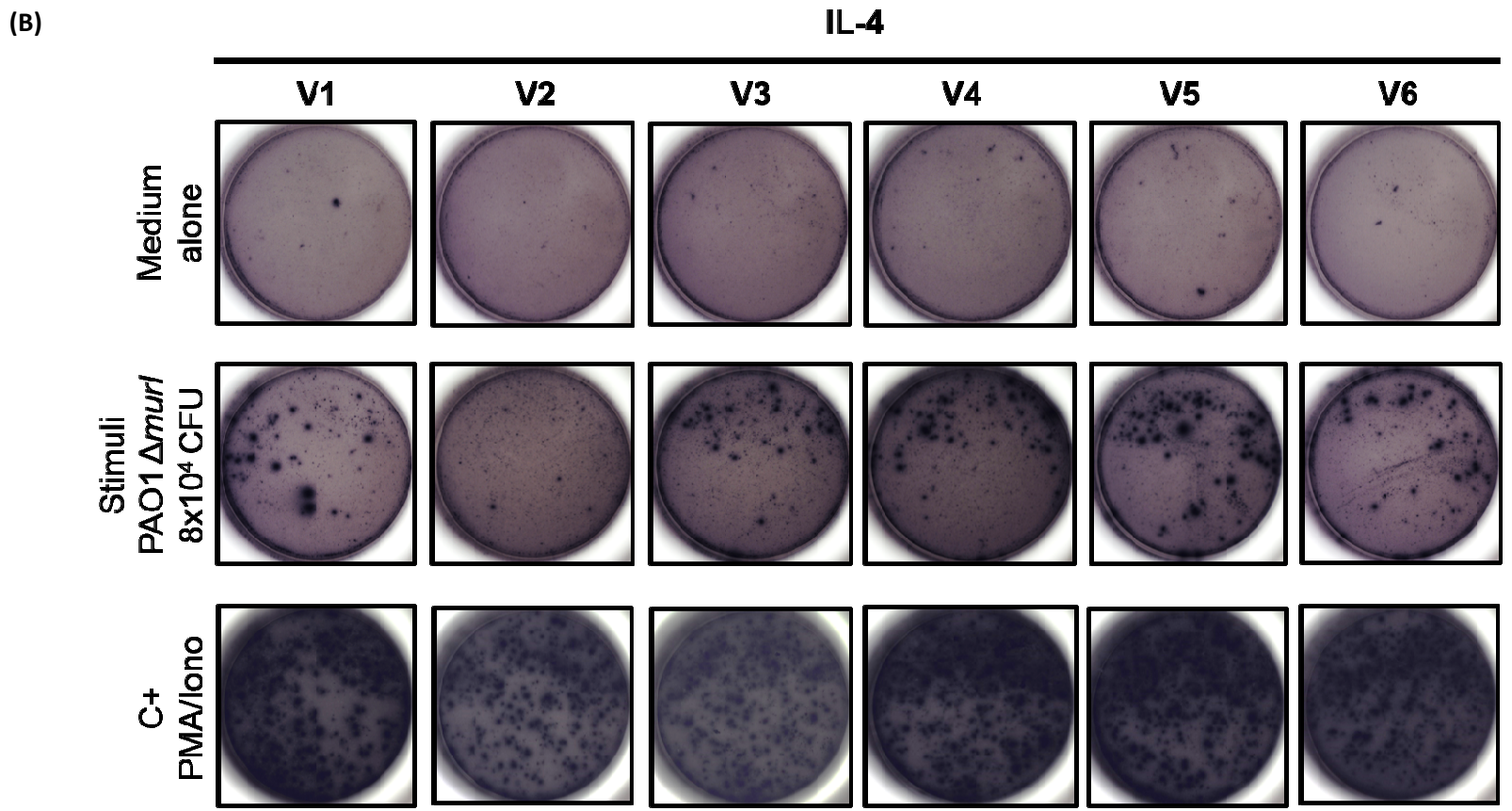

Figure 39 | Vaccination with PAO1 Δ*murI* triggers IL-4 cytokine-secreting T cells. Detection of antigen-specific IL-4-secreting T cells collected at day 68 from the spleens of **A,** saline mice (*n* = 6) and **B,** vaccinated mice (*n* = 6), after being restimulated *ex vivo* for 43 hours with PAO1 Δ*murI*, PMA (phorbol 12-myristate 13-acetate)/Ionomycin, or medium alone. **A-B,** Each well contains 8×10^5 splenocytes. S, saline; V, vaccinated.

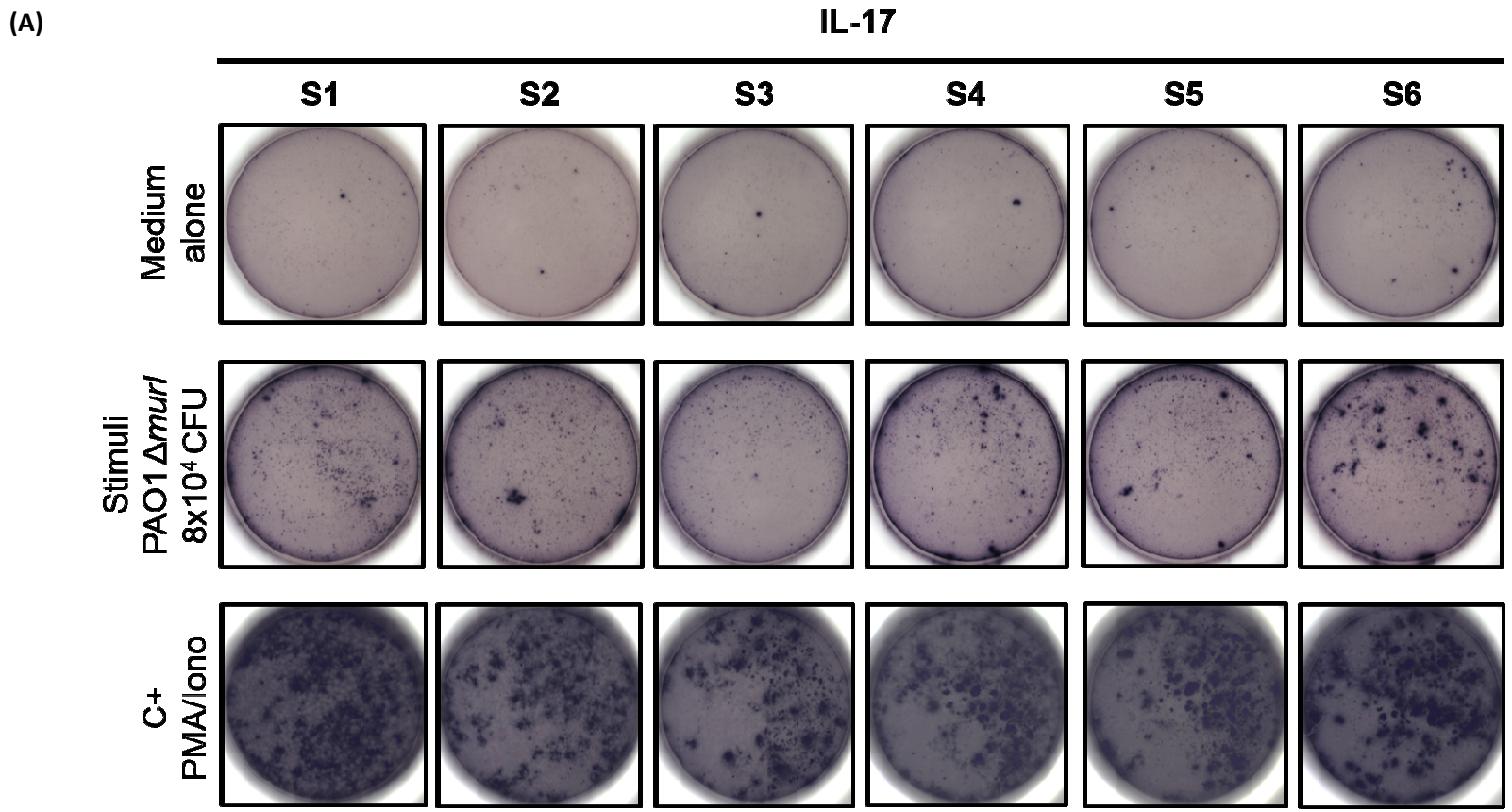

Figure 40 | Vaccination with PAO1 Δ*murI* triggers IL-17 cytokine-secreting T cells. Detection of antigen-specific IL-17-secreting T cells collected at day 68 from the spleens of **A,** saline mice (*n* = 6) and **B,** vaccinated mice (*n* = 6), after being restimulated *ex vivo* for 43 hours with PAO1 Δ*murI*, PMA (phorbol 12-myristate 13-acetate)/Ionomycin, or medium alone. **A-B,** Each well contains 8×10^5 splenocytes. S, saline; V, vaccinated.

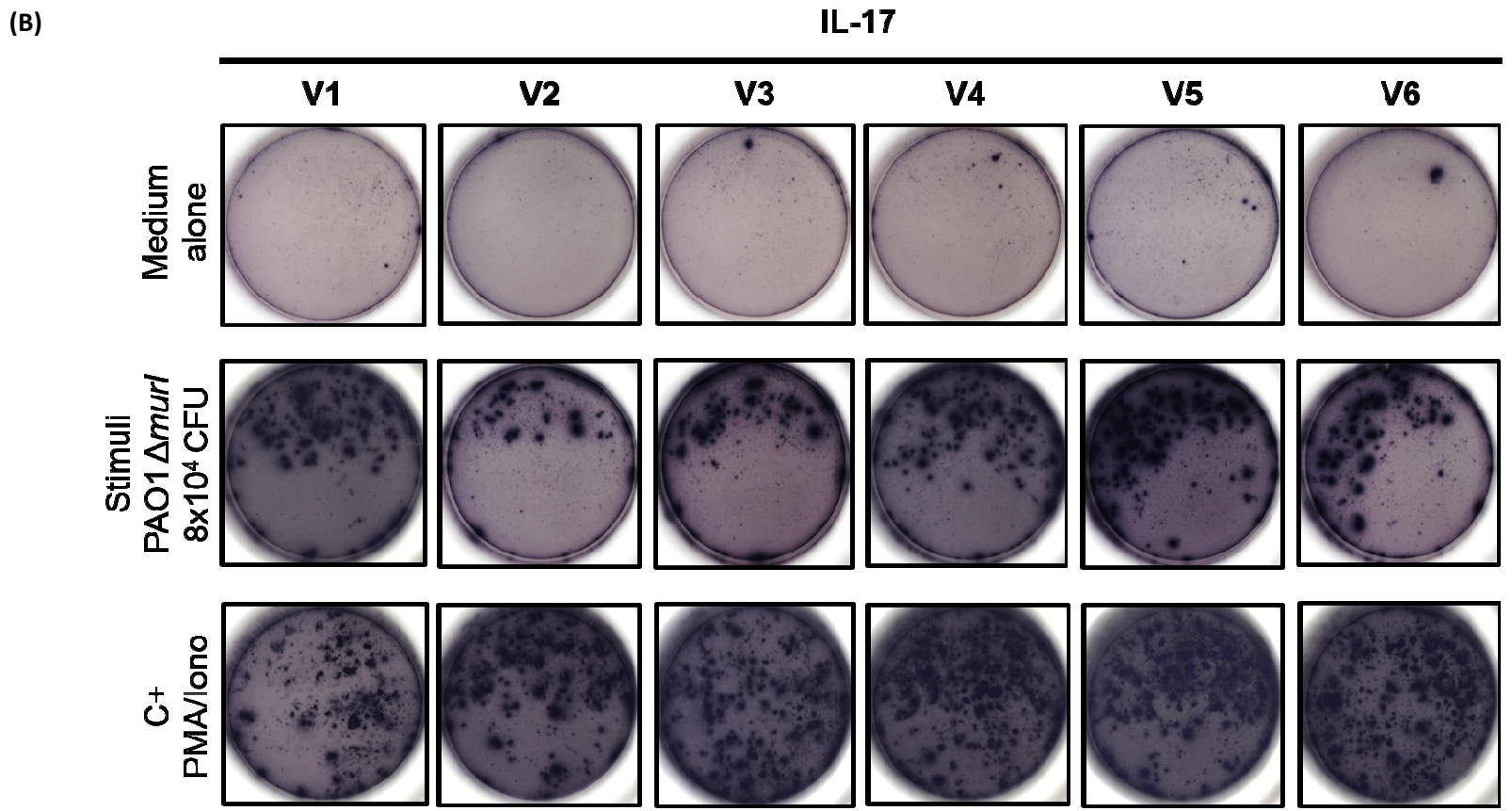

Figure 40 | Vaccination with PAO1 Δ*murI* triggers IL-17 cytokine-secreting T cells. Detection of antigen-specific IL-17-secreting T cells collected at day 68 from the spleens of **A,** saline mice (*n* = 6) and **B,** vaccinated mice (*n* = 6), after being restimulated *ex vivo* for 43 hours with PAO1 Δ*murI*, PMA (phorbol 12-myristate 13-acetate)/Ionomycin, or medium alone. **A-B,** Each well contains 8×10^5 splenocytes. S, saline; V, vaccinated.

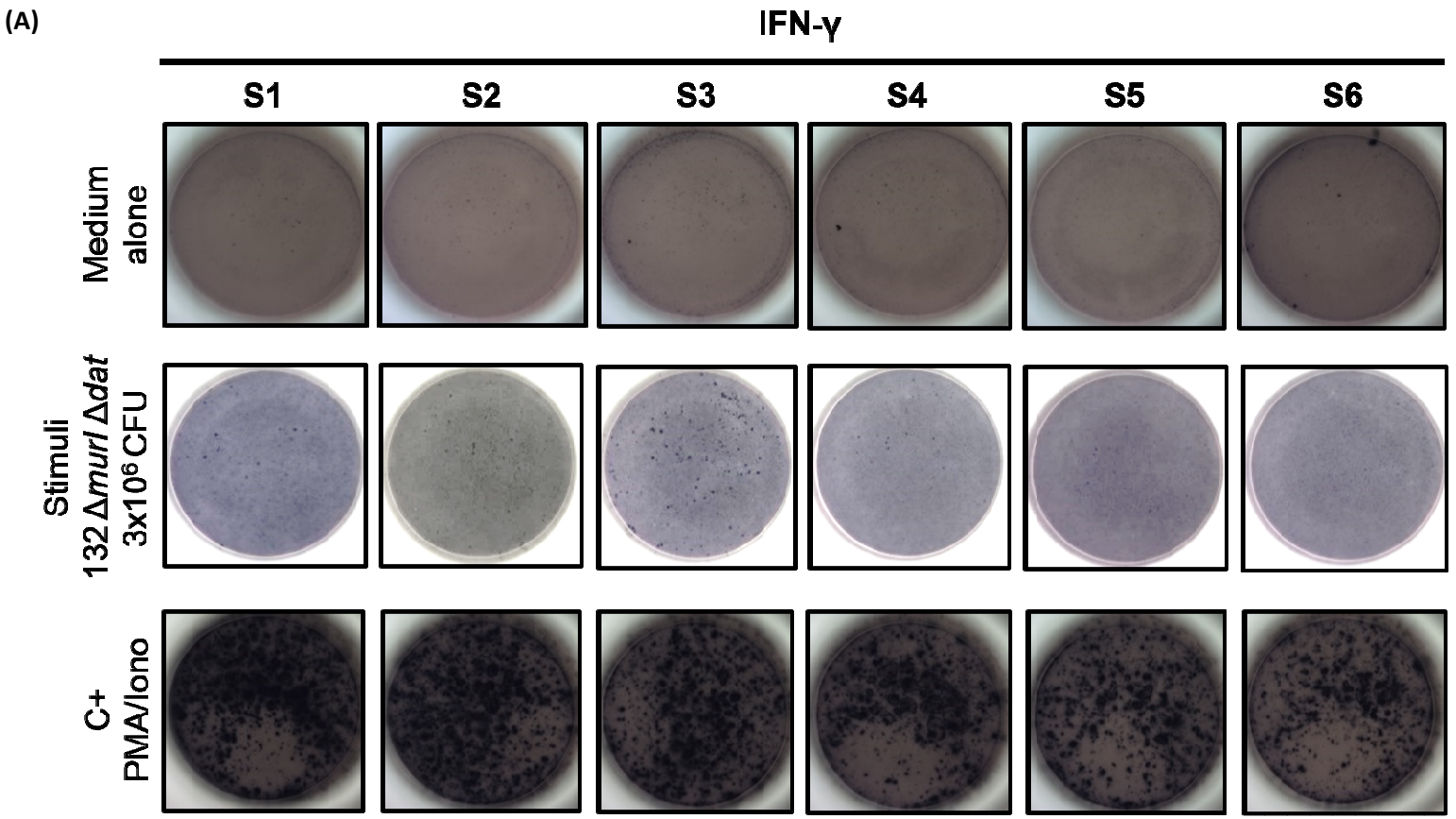

Figure 41 | Vaccination with 132 Δ*murI* Δ*dat* triggers IFN-γ cytokine-secreting T cells. Detection of antigen-specific IFN-γ-secreting T cells collected at day 50 from the spleens of **A,** saline mice (*n* = 6) and **B,** vaccinated mice (*n* = 6), after being restimulated *ex vivo* for 43 hours with 132 Δ*murI* Δ*dat*, PMA (phorbol 12-myristate 13-acetate)/Ionomycin, or medium alone. **A-B,** Each well contains 8×10^5 splenocytes. S, saline; V, vaccinated.

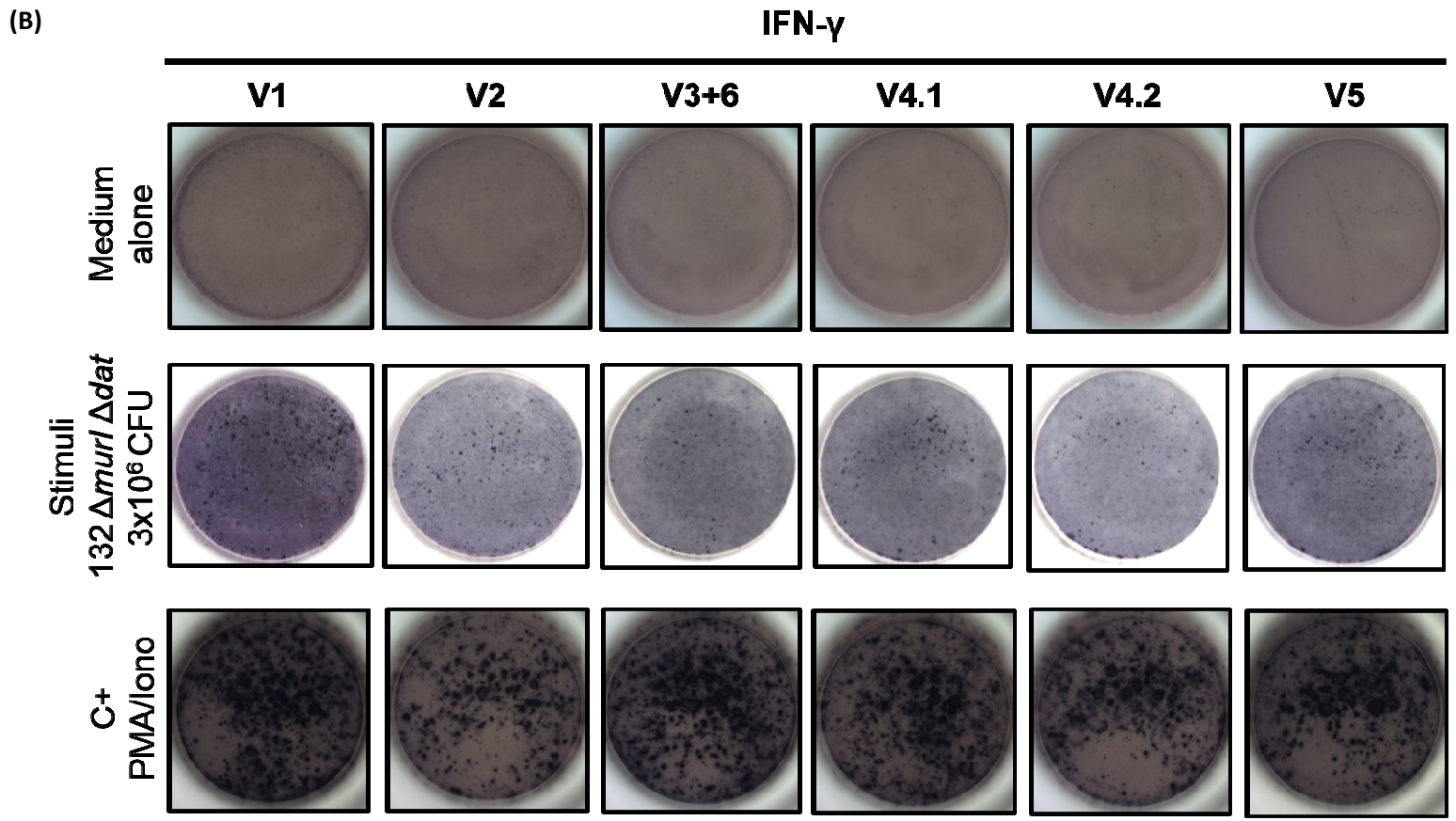

Figure 41 | Vaccination with 132 Δ*murI* Δ*dat* triggers IFN-γ cytokine-secreting T cells. Detection of antigen-specific IFN-γ-secreting T cells collected at day 50 from the spleens of **A,** saline mice (*n* = 6) and **B,** vaccinated mice (*n* = 6), after being restimulated *ex vivo* for 43 hours with 132 Δ*murI* Δ*dat*, PMA (phorbol 12-myristate 13-acetate)/Ionomycin, or medium alone. **A-B,** Each well contains 8×10^5 splenocytes. S, saline; V, vaccinated.

Figure 42 | Vaccination with 132 Δ*murI* Δ*dat* does not trigger IL-4 cytokine-secreting T cells. Detection of antigen-specific IL-4-secreting T cells collected at day 50 from the spleens of **A,** saline mice (*n* = 6) and **B,** vaccinated mice (*n* = 6), after being restimulated *ex vivo* for 43 hours with 132 Δ*murI* Δ*dat*, PMA (phorbol 12-myristate 13-acetate)/Ionomycin, or medium alone. **A-B,** Each well contains 8×10^5 splenocytes. S, saline; V, vaccinated.

Figure 42 | Vaccination with 132 Δ*murI* Δ*dat* does not trigger IL-4 cytokine-secreting T cells. Detection of antigen-specific IL-4-secreting T cells collected at day 50 from the spleens of **A,** saline mice (*n* = 6) and **B,** vaccinated mice (*n* = 6), after being restimulated *ex vivo* for 43 hours with 132 Δ*murI* Δ*dat*, PMA (phorbol 12-myristate 13-acetate)/Ionomycin, or medium alone. **A-B,** Each well contains 8×10^5 splenocytes. S, saline; V, vaccinated.

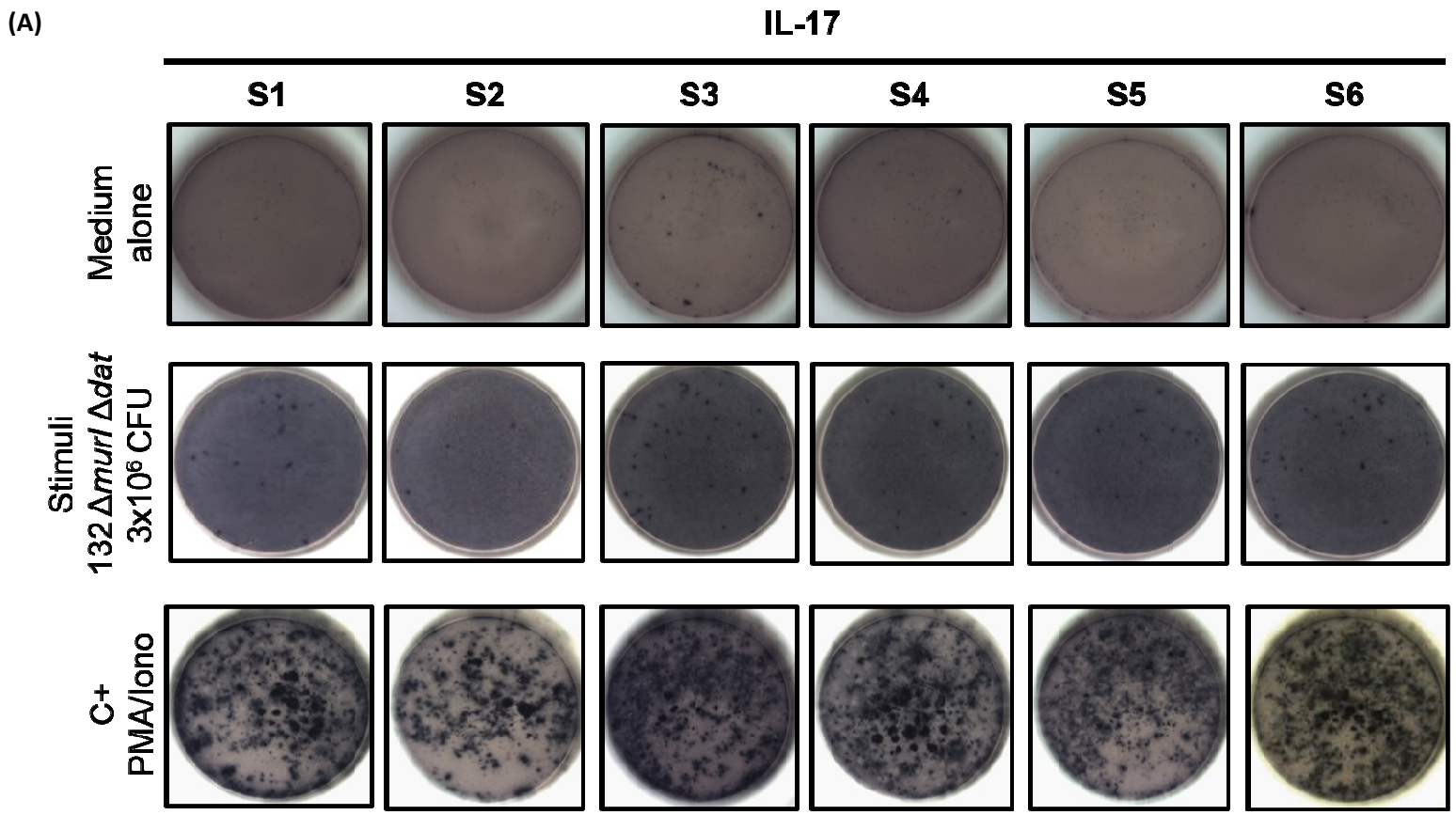

Figure 43 | Vaccination with 132 Δ*murI* Δ*dat* triggers IL-17 cytokine-secreting T cells. Detection of antigen-specific IL-17-secreting T cells collected at day 50 from the spleens of **A,** saline mice (*n* = 6) and **B,** vaccinated mice (*n* = 6), after being restimulated *ex vivo* for 43 hours with 132 Δ*murI* Δ*dat*, PMA (phorbol 12-myristate 13-acetate)/Ionomycin, or medium alone. **A-B,** Each well contains 8×10^5 splenocytes. S, saline; V, vaccinated.

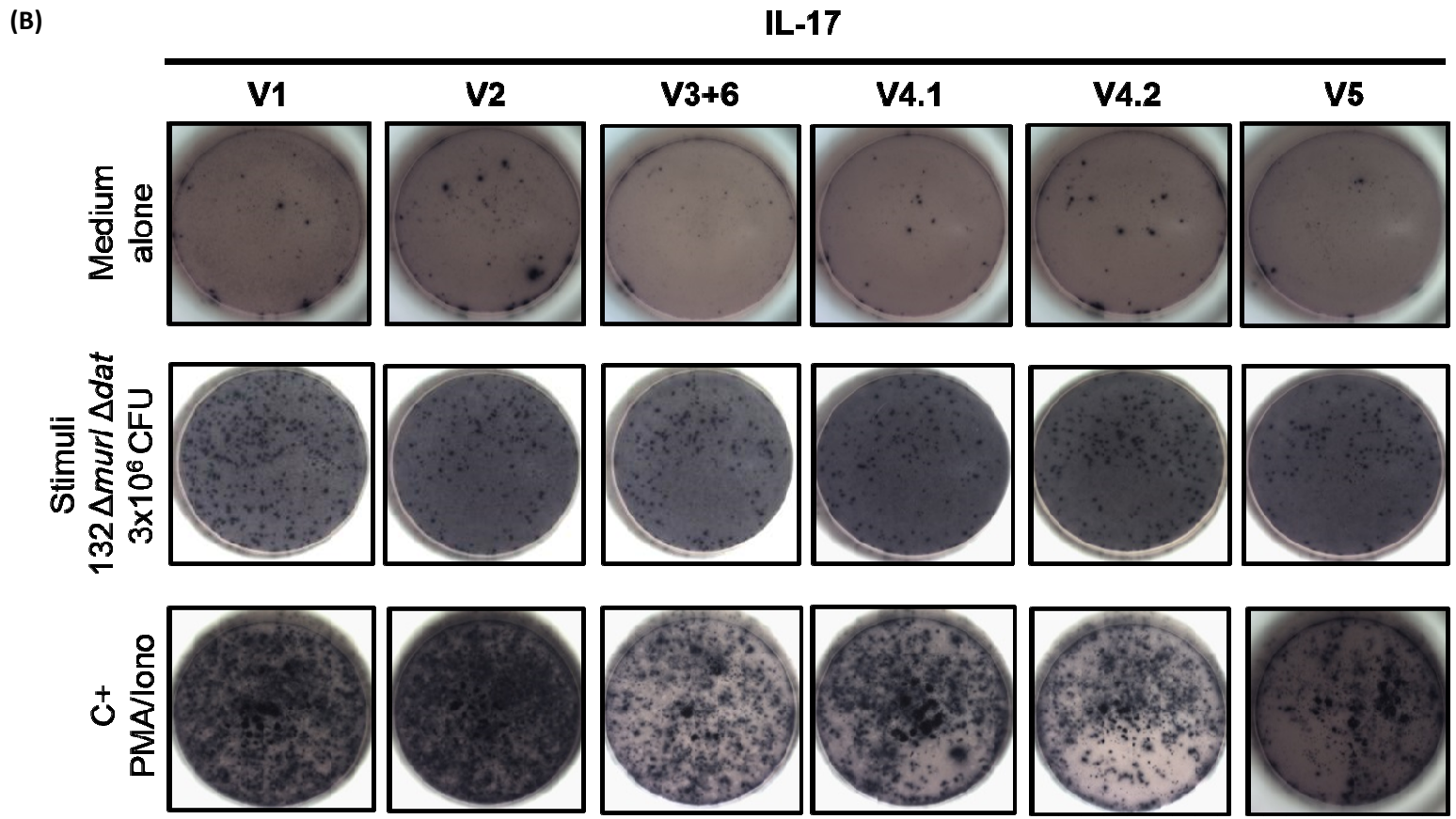

Figure 43 | Vaccination with 132 Δ*murI* Δ*dat* triggers IL-17 cytokine-secreting T cells. Detection of antigen-specific IL-17-secreting T cells collected at day 50 from the spleens of **A,** saline mice (*n* = 6) and **B,** vaccinated mice (*n* = 6), after being restimulated *ex vivo* for 43 hours with 132 Δ*murI* Δ*dat*, PMA (phorbol 12-myristate 13-acetate)/Ionomycin, or medium alone. **A-B,** Each well contains 8×10^5 splenocytes. S, saline; V, vaccinated.

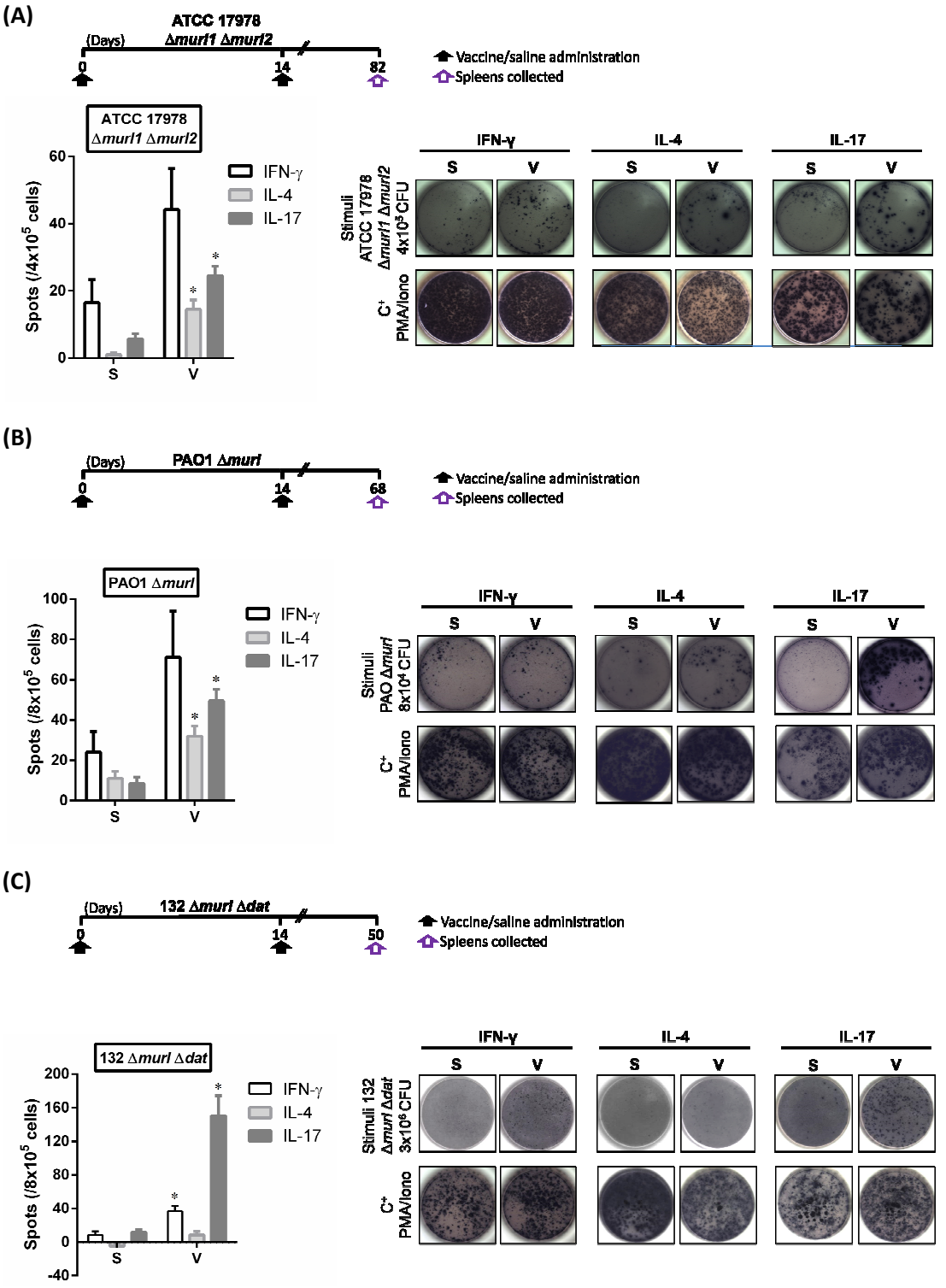

Figure 44 | Vaccination with D-Glu auxotrophic strains triggers cytokine-secreting T cells. **A,** Number of spot forming cells per 4×10^5 splenocytes collected at day 82 from mice vaccinated twice with ATCC 17978 Δ*murI1* Δ*murI2* (1X) (*n* = 6) and control mice (*n* = 7) after being restimulated *ex vivo* with ATCC 17978 Δ*murI1* Δ*murI2* for 43 hours. **B,** Number of spot forming cells per 8×10^5 splenocytes collected at day 68 from mice vaccinated twice with PAO1 Δ*murI* (0.4X) (*n* = 6) and control mice (*n* = 6) after being restimulated *ex vivo* with PAO1 Δ*murI* for 43 hours. **C,** Number of spot forming cells per 8×10^5 splenocytes collected at day 50 from mice vaccinated twice with 132 Δ*murI* Δ*dat* (1X) (*n* = 6) and control mice (*n* =

6) after being restimulated *ex vivo* with 132 Δ*murI* Δ*dat* for 43 hours. **A-C,** S, saline; V, vaccinated. **P*<0.05, compared with saline control mice (mean ± s.e.m.). Representative wells for each cytokine, obtained from saline and vaccinated mice after incubation with stimuli or PMA (phorbol 12-myristate 13-acetate)/Ionomycin used as positive control.

4.5. Protective immunity against acute lethal infection

While antibody and cell-mediated immunity are useful markers for protective immune responses, these can only be predictors. To verify whether D-Glu auxotrophic strains confer protection, we assessed their effectiveness using an acute lethal infection model in mice. Firstly, the effect of vaccination was determined by measuring bacterial loads in multiple tissues from vaccinated and control mice after injection with the vaccine wild-type homologues. As illustrated in **Figure 45**, vaccination with D-Glu auxotrophic strains resulted in all cases in a significant reduction in tissue bacterial loads of *A. baumannii* ATCC 17978, *P. aeruginosa* PAO1 and *S. aureus* 132 (10^4-10^6-fold reductions) compared to those observed in control mice. Moreover, 132 Δ*murI* Δ*dat* vaccinatiom prevented mice from severe body weight loss.

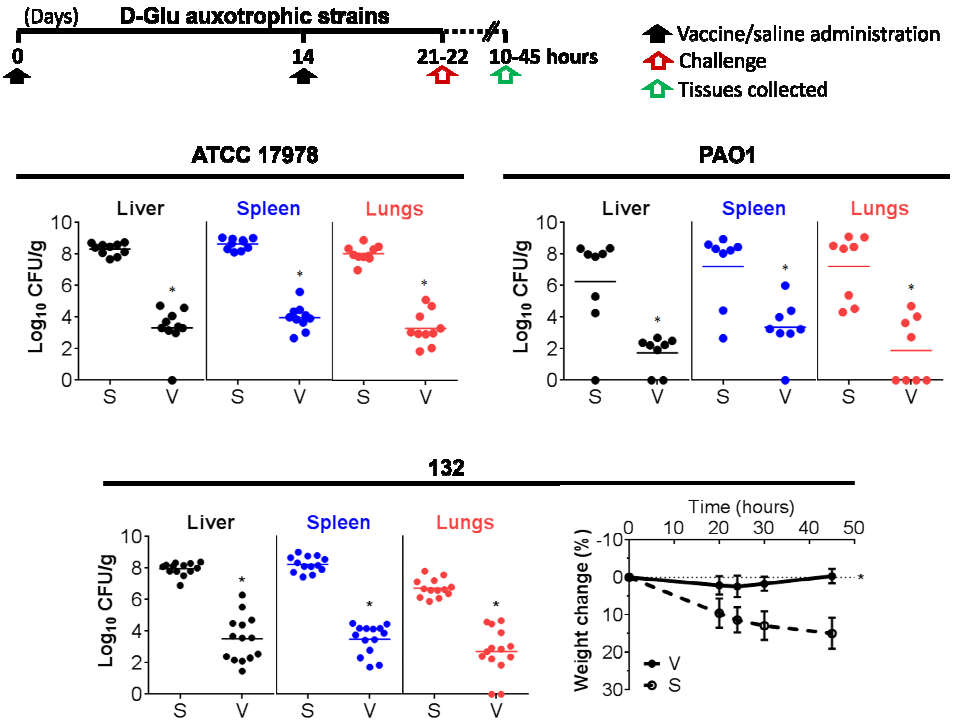

Figure 45 | Immunization with D-Glu auxotrophs protects against bacterial dissemination and prevents weight loss. Bacterial loads in tissues and percentage of body weight loss (mean ± s.e.m.) from vaccinated (ATCC 17978 Δ*murI1* Δ*murI2* 1X, PAO1 Δ*murI* 0.4X and 132 Δ*murI* Δ*dat* 1X) and control mice after challenge with *A. baumannii* ATCC 17978 (4X) (*n* = 10; after 12 hours), *P. aeruginosa* PAO1 (0.4X) (*n* = 8; after 10 hours) and *S. aureus* 132 (0.5X) (*n* = 14, pooled data set form two independent experiments; after 45 hours). S, saline; V, vaccinated. **P*<0.05, compared with control group.

Further, vaccine efficacy was evaluated by determining mice survival after challenge with parental and heterologous strains. As illustrated in **Figure 46**, a two-dose vaccination schedule with ATCC 17978 Δ*murI1* Δ*murI2* protected mice from challenge with ATCC 17978, whereas all control mice died within 24 hours. Likewise, survival rates of vaccinated mice were 100% and 86% after challenge with *A. baumannii* AbH12O-A2 and Ab307-0294, respectively. These observations evidenced that immunization with the ATCC 17978 Δ*murI1* Δ*murI2* provides protective immunity against epidemiologically and genetically unrelated *A. baumannii* strains.

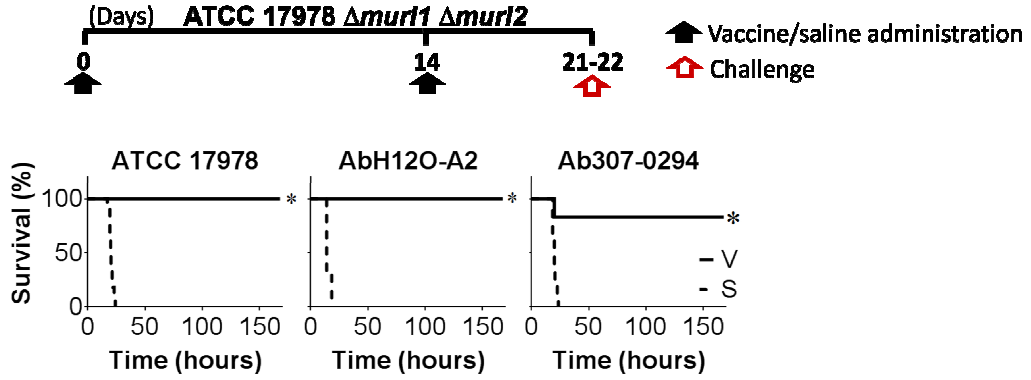

Figure 46 | Immunization with *A. baumannii* ATCC 17978 Δ*murI1* Δ*murI2* protects against ATCC 17978, MDR and highly virulent strains. Mice survival after vaccination with ATCC 17978 Δ*murI1* Δ*murI2* (1X) or saline administration, and challenge with ATCC 17978 (4X) on day 21 (*n* = 11-13), AbH120-A2 (4X) on day 21 (*n* = 9) and Ab307-0294 (0.75X) on day 22 (*n* = 7-8). S, saline; V, vaccinated. **P*<0.05, compared with control group.

Also, mice challenged with *P. aeruginosa* PAO1 presented a 87.5% and a 100% survival after vaccination with 0.04X and 0.4X doses of PAO1 Δ*murI*, respectively. In this case, all control mice died within 15 hours. Similar results were obtained when challenging mice with the mucoid strain PA28562: vaccinated mice registered 100% survival, whereas all control mice died **(Fig. 47)**.

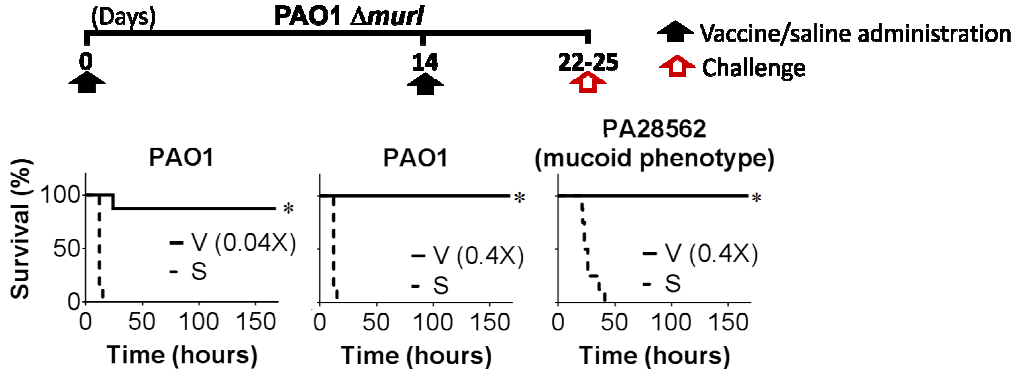

Figure 47 | Immunization with *P. aeruginosa* PAO1 Δ*murI* protects against PAO1 and the mucoid strain PA28562. Mice survival after vaccination with PAO1 Δ*murI* (0.04X and 0.4X) or saline administration, and challenge with PAO1 (0.4X) on day 22 (*n* = 8) and PA28562 (0.5X) on day 25 (*n* = 8). S, saline; V, vaccinated. **P*<0.05, compared with control group.

When immunized through the intramuscular (IM) route, PAO1 Δ*murI* conferred mice protection after challenge with PAO1. Similar results were obtained for the highly virulent strain PA14: all vaccinated mice survived whereas 71% of control mice died **(Fig. 48).** These results suggest that immunization with the PAO1 Δ*murI* provides protective immunity against diverse *P. aeruginosa* strains.

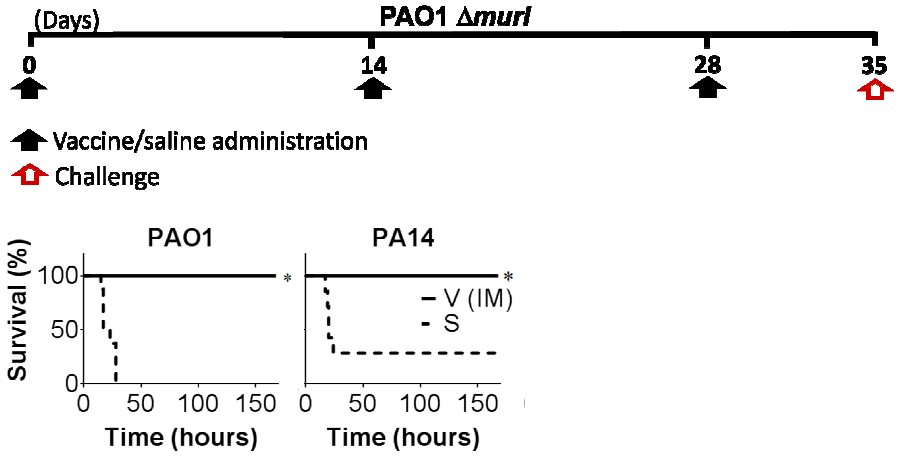

Figure 48 | Intramuscular immunization with *P. aeruginosa* PAO1 Δ*murI* protects against PAO1 and the highly virulent strain PA14. Mice survival after IM vaccination with PAO1 Δ*murI* (0.4X) or saline administration, and challenge with PAO1 (1X) (*n* = 8) and PA14 (0.2X) (*n* = 7-8), on day 35. S, saline; V, vaccinated. **P*<0.05, compared with control group.

As illustrated in **Figure 49,** mice vaccinated with *S. aureus* 132 Δ*murI* Δ*dat* were completely protected from challenge with strain 132, whereas 81.3% of control mice succumbed to infection within 11 days. All vaccinated mice recovered their initial body weight within 85 hours post infection; control mice still alive at this time point (37.5%) presented 19.2% of body weight loss. At day 53, we observed significant differences in bacterial loads (Log_{10} CFU/g) among three individuals randomly selected from saline and vaccinated mice (4.33, 6.66 and 6.96 on livers; 6.71 and 7.41 on kidneys for control mice *vs* 0 for vaccinated mice). Apparently, these mice presented no clinical signs of disease. Multiple abscesses were also evident on the tissues of control mice; but not detected on vaccinated mice.

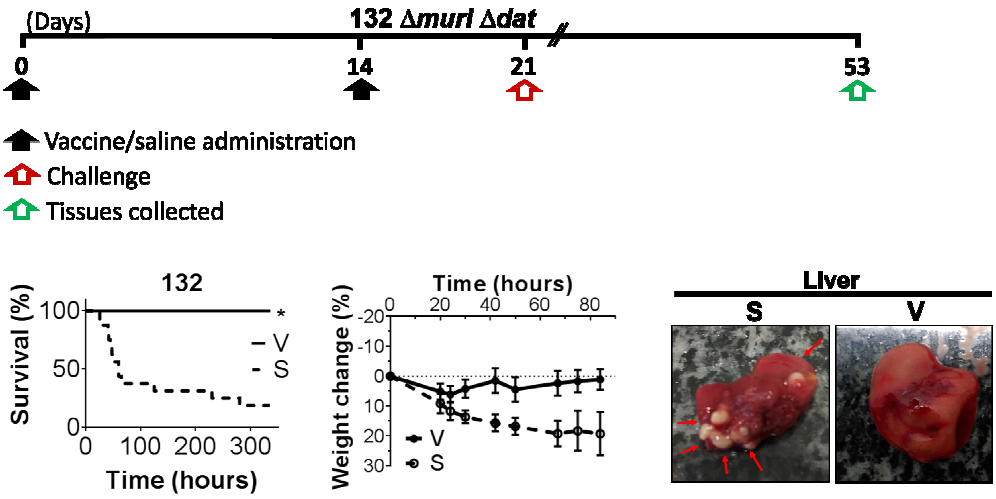

Figure 49 | Immunization with *S. aureus* 132 Δ*murI* Δ*dat* protects against *S. aureus* 132, infection-derived weight loss and abscess formation. Mice survival and percentage of body weight loss (mean ± s.e.m.) after vaccination with 132 Δ*murI* Δ*dat* (1X) or saline administration, and challenge with 132 (0.5X) on day 21 (*n* = 16-17, pooled data set from two independent experiments). Arrows indicate visible liver abscesses after mice necropsy on day 53. S, saline; V, vaccinated. **P*<0.05, compared with control group.

When challenging mice with FRP3757 (CA-MRSA USA300, a highly virulent and epidemic *S. aureus* clone), RF122 (bovine) and ED98 (poultry) strains, we observed 100% survival, whereas all control mice died within 15 hours. All these vaccinated mice completely recovered their initial body weight 85 hours after infection **(Fig. 50)**. These results evidence that immunization with *S. aureus* 132 Δ*murI* Δ*dat* provides protective immunity against epidemic MRSA and diverse *S. aureus* animal *S. aureus* strains.

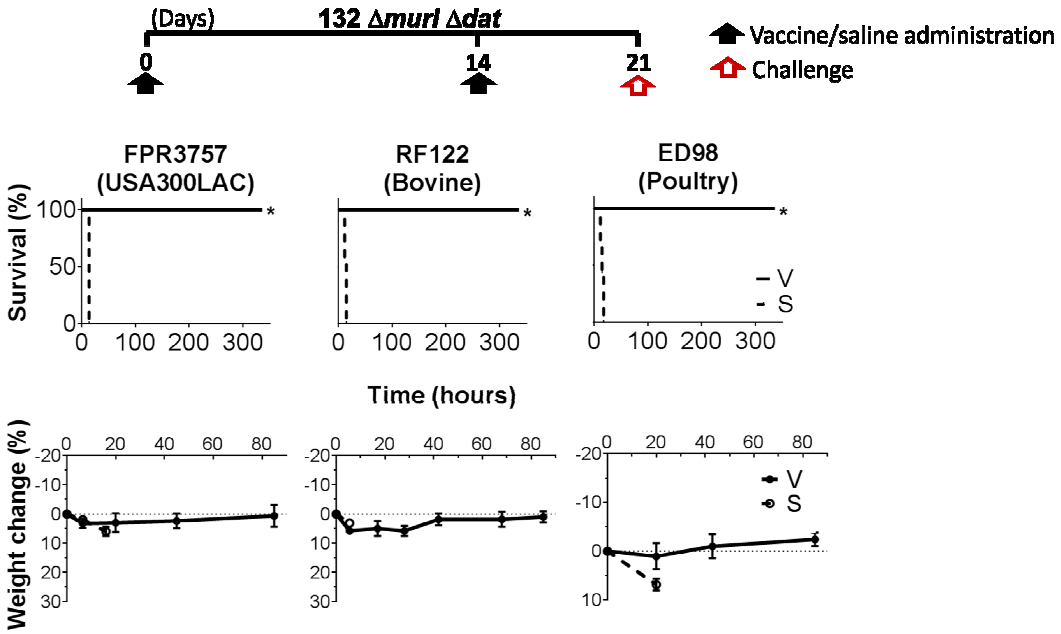

Figure 50 | Immunization with *S. aureus* 132 Δ*murI* Δ*dat* protects against diverse *S. aureus* strains. Mice survival and percentage of body weight loss (mean ± s.e.m.) after vaccination with 132 Δ*murI* Δ*dat* (1X) or saline administration, and challenge with FPR3757-USA300LAC (0.4X) (*n* = 7), RF122 (0.25X) (*n* = 7) and ED98 (0.5X) (*n* = 7) on day 21. S, saline; V, vaccinated. **P*<0.05, compared with control group.

While BALB/c have a Th2-dominant immune response, C57BL/6 mice are prone to response bias Th1 [347]. To rule out any confounding effect of the immune system inherent to the inbred mouse strain, we vaccinated C57BL/6 mice with D-Glu auxotrophic strains. When challenged with ATCC 17978, PAO1 and 132, survival rates were 100% for vaccinated *vs* 0% for control mice. Also, 132 Δ*murI* Δ*dat* vaccinated mice recovered their initial body weight, as BALB/C mice **(Fig 51)**. When PAO1 Δ*murI* was administered IM, survival was 100% for vaccinated *vs* 25% for control mice, after PAO1 infection **(Fig 52)**. Thus, the protective immunity conferred by these D-Glu auxotrophs is independent of different mice genetic backgrounds.

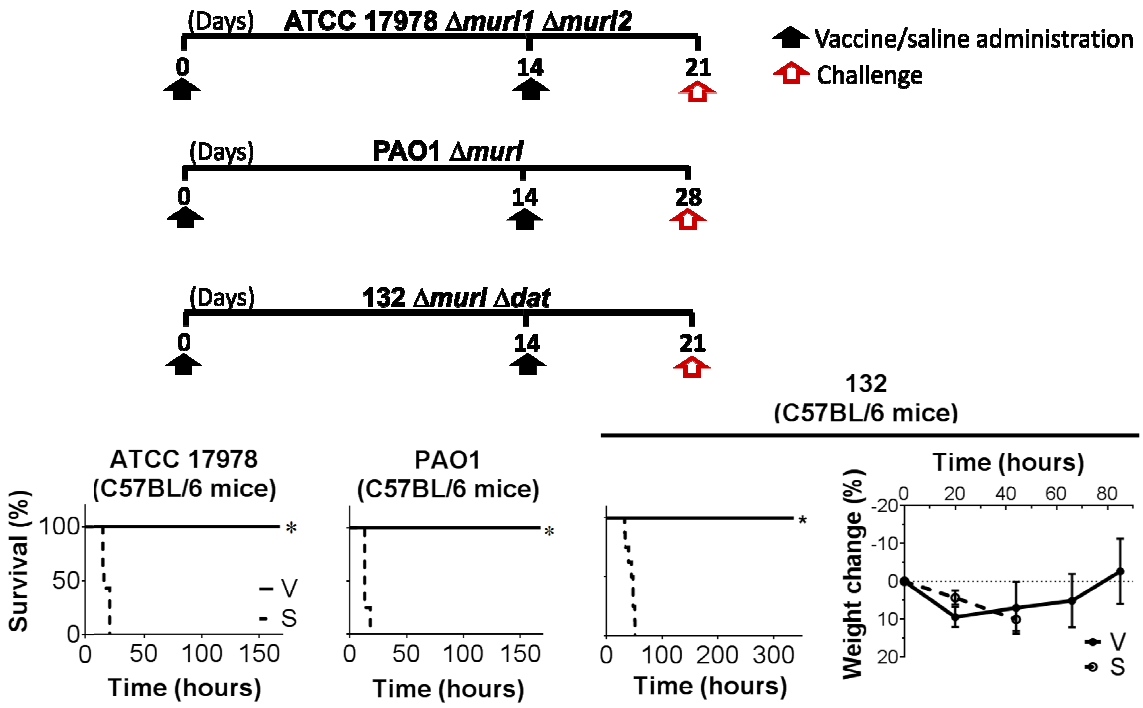

Figure 51 | Immunization with D-Glu auxotrophs protects C57BL/6 mice against acute lethal infection. C57BL/6 mice survival after vaccination with ATCC 17978 Δ*murI1* Δ*murI2* (1X) or saline administration, and challenge with ATCC 17978 (8X) on day 21 (*n* = 8). C57BL/6 mice survival after vaccination with PAO1 Δ*murI* (0.4X) or saline administration, and challenge with PAO1 (0.8X) on day 28 (*n* = 4). C57BL/6 mice survival and percentage of body weight loss (mean ± s.e.m.) after vaccination with 132 Δ*murI* Δ*dat* (1X) or saline administration, and challenge with 132 (1X) on day 21 (*n* = 8). S, saline; V, vaccinated. **P*<0.05, compared with control group.

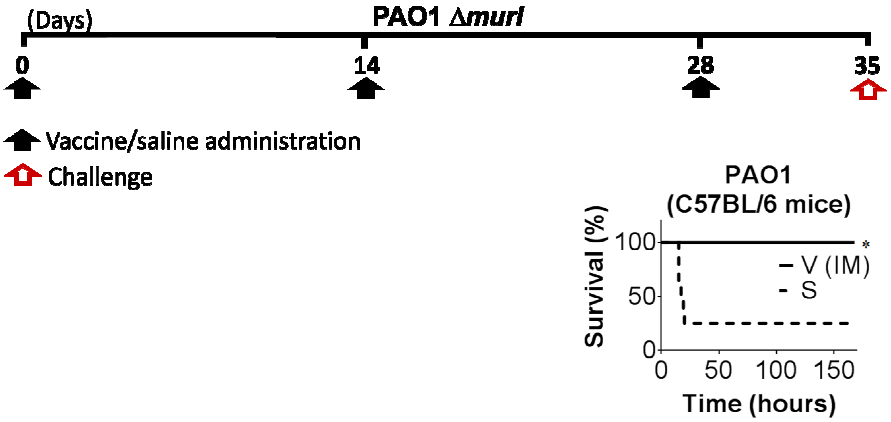

Figure 52 | Intramuscular immunization with *P. aeruginosa* PAO1 Δ*murI* protects C57BL/6 mice against acute lethal infection. C57BL/6 mice survival after IM vaccination with PAO1 Δ*murI* (0.4X) or saline administration, and challenge with PAO1 (0.4X) on day 35 (*n* = 8). S, saline; V, vaccinated. **P*<0.05, compared with control group.

In situations in which the completion of a vaccination schedule is not possible, high-risk situations after pathogen exposure, or when individuals cannot synthesize antibody, the use of passive immunization may be beneficial. Those antibodies formed with ATCC 17978 Δ*murI1* Δ*murI2*, PAO1 Δ*murI1* and 132 Δ*murI* Δ*dat* vaccinations (anti-Ab, anti-Pa and anti-Sa sera, respectively) can be obtained from the host and transferred into another recipient where they can provide immediate passive immunity or help fight the infectious disease **(Fig. 53).**

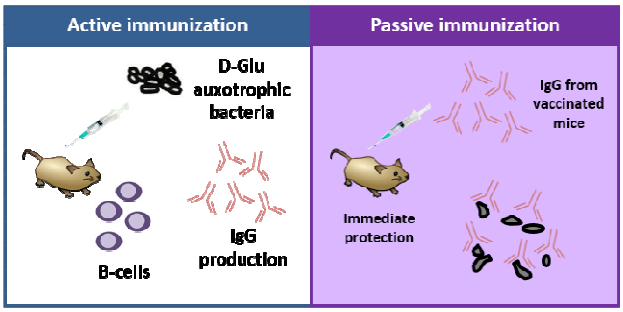

Figure 53 | Active and passive immunization. Antibodies elicited by D-Glu auxotrophic strains can be obtained after active immunization and transferred to naïve mice where they can confer immediate passive protection against infection.

In this sense, we determined if vaccine antisera could be used to therapeutically rescue mice from lethal infection. As shown in **Figure 54**, all mice treated with anti-Ab serum and subsequently challenged with ATCC 17978 survived, whereas all control mice receiving naïve serum succumbed to infection. Similarly, 100% of survival was observed for mice treated with anti-Pa and -Sa sera, and challenged with PAO1 and 132, respectively; survival for controls receiving naïve serum was 50% ($P<0.05$ and $P=0.05$, respectively). These results indicate that at least anti-Ab and -Pa sera can effectively prevent *A. baumannii* and *P. aeruginosa* acute lethal infection, respectively, whereas antibodies alone are sufficient to provide protective immunity.

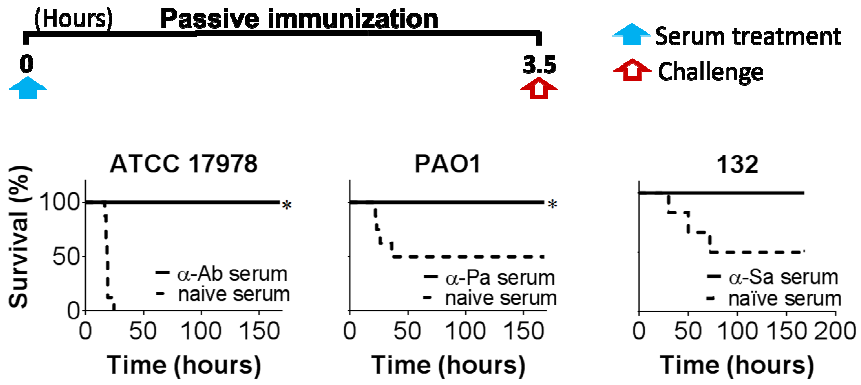

Figure 54 | Immunization with D-Glu auxotrophs induces therapeutically active antisera. Survival of mice treated with anti-Ab, anti-Pa, anti-Sa or naïve serum and challenged with ATCC 17978 (5X) (*n* = 8), PAO1 (0.4X) (*n* = 8) or 132 (1X) (*n* = 6), 3.5 hours after treatment. S, saline; V, vaccinated. **P*<0.05, compared with control group.

4.6. *In vivo* and environmental safety of D-Glu auxotrophic bacteria as GMO vaccines

The attenuation should be carried out in such a way that it permits the vaccine strain to be sufficiently invasive and to induce both a strong primary and long lasting memory immune response, but not a persistent carrier state of the vaccinee [348]**.** This can be achieved by the auxotrophic strain's ability to colonize and multiply in the host over a limited period, before it lyses, being eliminated without causing the disease. This was observed for *A. baumannii* ATCC 17978, *P. aeruginosa* PAO1 and *S. aureus* 132 D-Glu auxotrophic strains when injected to mice, as they were eliminated from blood faster than the wild-type homologues **(Fig 55)**. Unlike ATCC 17978 (1X), we could not recover ATCC 17978 Δ*murI1* Δ*murI2* (1X) 6 hours after injection, as all blood cultures became negative after this time **(Fig. 56)**. In the case of PAO1 Δ*murI* (0.4X), this strain was also rapidly eliminated from the blood, with negative blood cultures obtained 4 hours after administration. Unlike *S. aureus* 132 (0.5X), 132 Δ*murI* Δ*dat* (2.5X) could not be recovered beyond 17 hours. Hence, these observations suggest that these strains present no potential risk for causing disease and spreading to non-target recipients.

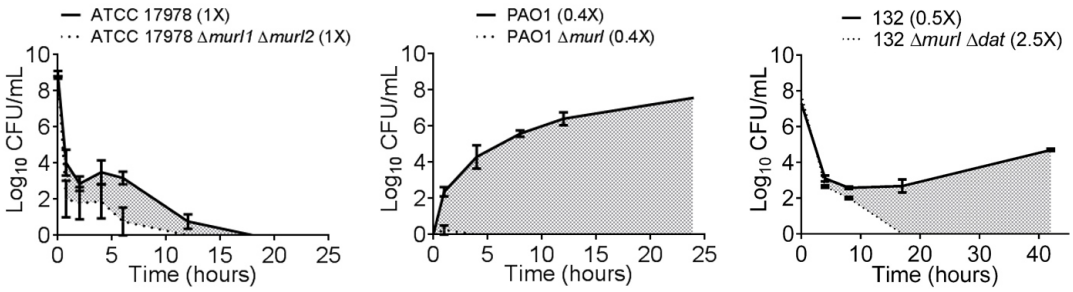

Figure 55 | D-Glu auxotrophic bacteria are eliminated from the blood within hours. *A. baumannii* ATCC 17978 (*n* = 3), ATCC 17978 Δ*murI1* Δ*murI2* (*n* = 3), *P. aeruginosa* PAO1 (*n* = 4), PAO1 Δ*murI* (*n* = 4), *S. aureus* 132 (*n* = 4) and 132 Δ*murI* Δ*dat* (*n* = 4) colonies recovered over time from the blood of BALB/c mice upon injection (mean ± s.e.m.).

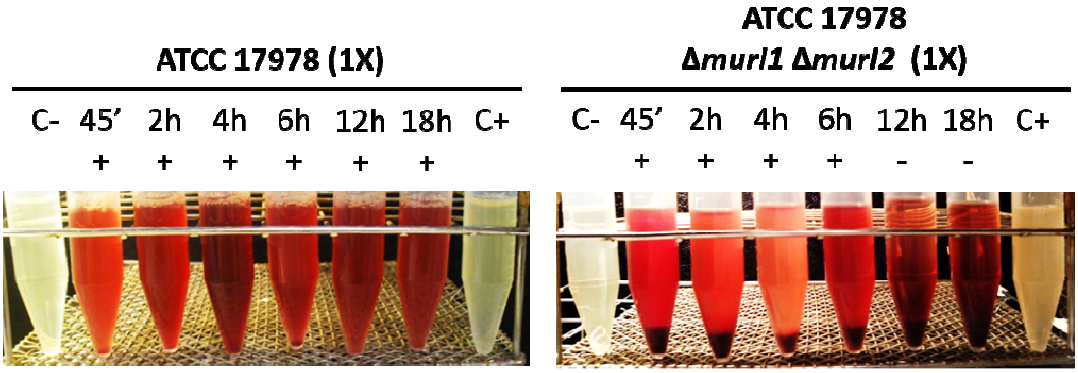

Figure 56 | Blood cultures of mice injected *A. baumannii* ATCC 17978 (1X) or ATCC 17978 Δ*murI1* Δ*murI2* (1X). Blood samples were collected at the indicated time points after bacterial injection and incubated at 37 ºC, for 3 days, in medium supplemented with 10 mM D-Glu. C-, negative controls: medium alone. C+, positive controls: medium inoculated with ATCC 17978. +, positive blood culture. -, negative blood culture.

Also, to be safe and suitable as a genetically modified organism (GMO) vaccine, an inherent property of these organisms must be that the attenuation mutations are not reversible [58]. To check the irreversibility of the nutritional auxotrophy of ATCC 17978 Δ*murI1* Δ*murI2*, PAO1 Δ*murI* and 132 Δ*murI* Δ*dat*, these strains were grown with D-Glu for 8 days and their viability evaluated over time on agar plates with and without D-Glu. In the hypothetical case of a phenotype reversion, similar bacterial counts would be expected in supplemented and non-supplemented agar plates. Even considering that agar plates were incubated for 3 days to encourage phenotype reversion, higher bacterial counts were observed in supplemented plates at the initial stage of incubation and on subsequent days **(Fig. 57)**, indicating that these strains remain auxotrophic for D-Glu over time.

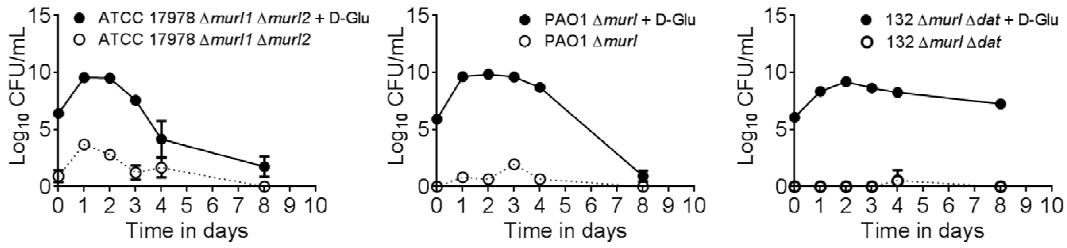

Figure 57 | D-Glu auxotrophic strains cannot revert to the wild-type phenotype. Viable counts of ATCC 17978 Δ*murI1* Δ*murI2*, PAO1 Δ*murI*, and 132 Δ*murI* Δ*dat* obtained on agar plates (○) and agar supplemented with 10 mM D-Glu (●) after cultivation on media supplemented with 10 mM D-Glu (ATCC 17978 Δ*murI1* Δ*murI2* and PAO1 Δ*murI* strains) or 20 mM D-Glu (132 Δ*murI* Δ*dat* strain) during 8 days.

Finally, any live attenuated bacterial strain constituting the active ingredient of a vaccine should be unable of replicating and persisting in the general environment if it hypothetically leaves the vaccinated individual. Spreading of live vaccines, including GMOs, must be compared with the wild-type pathogens from diseased individuals and the risk of creating epidemics [58]. Thus, persistence of D-Glu auxotrophic strains was compared with that of their wild-type homologues. When analysing survival in water **(Fig. 58A)**, marked differences in the viability of ATCC 17978 Δ*murI1* Δ*murI2* and PAO1 Δ*murI* with respect to wild-type strains were observed. Using the same model, no significant differences for *S. aureus* were seen, as no viable bacteria were recovered after 72 and 96 hours from 132 Δ*murI* Δ*dat* and 132 water cultures, respectively. This may be related with the physiology of this bacterium. Alternatively, we compared tolerance to drought stress of both *S. aureus* strains, using a desiccation model **(Fig. 58B).** Indeed, a progressive reduction in the viability of 132 Δ*murI* Δ*dat* was observed along the time when this strains was kept under drought stress as no viable 132 Δ*murI* Δ*dat* were recovered from 10^{-1} and 10^{-2}-spotted cultures after the 18th day. In contrast, the 132 strain showed resistance to desiccation and remained viable until day 31, even when $\times 10^{-2}$-diluted.

(A)

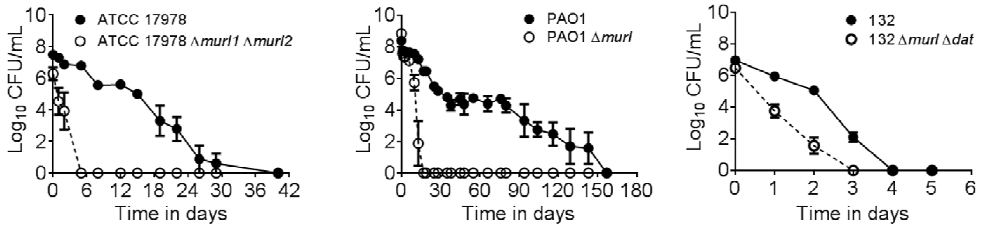

(B)

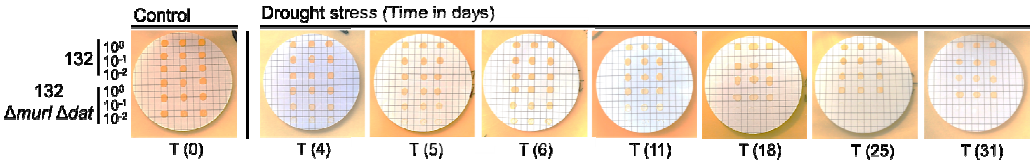

Figure 58 | D-Glu auxotrophic strains show lower persistence than wild-type homologues. **A,** Viable counts of ATCC 17978, ATCC 17978 Δ*murI1* Δ*murI2*, PAO1, PAO1 Δ*murI*, 132 and 132 Δ*murI* Δ*dat* recovered from water during 40, 157 and 5 days (mean ± s.e.m.). **B,** Viability of spotted cultures of *S. aureus* 132 and 132 Δ*murI* Δ*dat* obtained on agar plates supplemented with 10 mM D-Glu at day 0 (control) and after being kept under desiccation conditions during 31 days.

5. DISCUSSION

5. DISCUSSION

Having a whole-cell vaccine that contains all the antigenic determinants to induce protective immunity in the vaccinee, including those that are synthesized only during infection, without the risk of clinical disease, and with minimal possibilities of adverse reactions, is the paradigm for effective and safe immunizations. Live vaccines composed of bacteria attenuated by natural selection or genetic engineering can afford some of these aspects. However, these strains require particular attention regarding their safety as they may propagate in the host and be released into the environment by the vaccinees [58]. Safety issues of these strains involve changes in cell tissue and host tropism, reversion of virulence by acquisition of complementation genes, exchange of genetic information with other vaccine or wild-type strains of the carrier organism and spread of undesired genes such as antibiotic resistance genes, and must be considered carefully. Furthermore, obtaining virulence attenuation is usually impeded by the laborious identification of rational targets in each particular bacterium.

D-Glu is an essential component of the bacterial cell wall. MurI, enzyme that converts L-glutamate (L-Glu) to D-Glu, is present in all species of bacteria and its essential role in peptidoglycan biosynthesis has been confirmed in species spanning the bacterial kingdom, including Gram-positive bacteria that encode the Dat for D-Glu production. In a previous study performed by our group in which different proteomic approaches were used to study biofilm-associated proteins of *A.* baumannii [349], we observed a clear up-regulation of proteins that were directly or indirectly related to L-histidine metabolism. Together with L-aspartate, L-arginine and L-histidine, L-Glu was found to triggers biofilm formation *in vitro*. Moreover, the metabolic routes of these amino acids converged unequivocally into L-Glu. This observation prompted us to investigate the influence of *A. baumannii* Δ*murI* mutants in biofilm formation, considering that L-Glu is the substrate of MurI. Indeed, *A. baumannii* ATCC 17978 Δ*murI1* and ATCC 17978 Δ*murI1* Δ*murI2* were found to produce less biofilm than wild-type strain (data not shown). Further, *A. baumannii* ATCC 17978 Δ*murI1* Δ*murI2* was investigated as a vaccine candidate against *A. baumannii* infections, considering its marked virulence attenuation *in vivo*. This observation was the starting point for a more broad approach to generate and validate experimental live vaccines based on MurI deletion mutants and D-Glu auxotrophy also in *P. aeruginosa* and *S. aureus* bacteria.

Although D-amino acids are increasingly recognized as physiologically functional molecules in mammals, the amounts of free D-Glu are trace substances in most cases [350]. Detailed distributions of D-Glu in the brain and peripheral tissues of the rat have been clarified and were extremely low, ranging between 1.9 to 9.0 nmol/g [351].

Hence, by creating MurI^{-} (and MurI^{-}Dat^{-}) mutants, we took advantage of the highly conserved function of MurI in bacteria and the strict requirement of sufficient D-Glu pool levels to impair bacterial replication in the host, considering that amounts of free D-amino acids are trace substances in mammals. Indeed, *A. baumannii*, *P. aeruginosa* and *S. aureus* D-Glu auxotrophic strains presented here were incapable of proliferating in mice due to the blockage of the cell wall synthesis, overcoming the problem of *in vivo* bacterial growth. These GMOs were attenuated in comparison with the parental strains and triggered the appropriate cellular immune responses and the production of specific and cross-reactive antibodies to a wide variety of clonally unrelated epidemic, MDR and highly virulent strains of *A. baumannii*, *P. aeruginosa* and *S. aureus*. These results correlated with protection against acute lethal infection mainly through using a two-dose immunization schedule. In addition, these strains did not appear to represent a risk for causing disease and spreading to non-target recipients, considering their rapid elimination from the blood and their limited persistence in non-optimal conditions, more likely to occur in the hypothetical case of an accidental environmental release. These attributes constitute advantages in relation to attenuated and inactivated vaccines, and are summarized in **Table 9**.

Table 9 | Characteristics of attenuated, inactivated and auxotrophic vaccines compared.

	Attenuated	Inactivated	Auxotrophic
No. of doses	One or few	Several	**One or few**
Need for booster doses	Lesser	Higher	**Lesser**
Cross protection from unrelated strains	Present	Rare	**Present**
Growth of bacteria *in vivo*	Yes	No	**No (self-limited)**
Risk of disease	Yes	No	**No**
Risk of transmission	Yes	No	**No**
Possibility of reversion	Yes	No	**No**
Humoral immune response	Yes	Yes	**Yes**
Cellular immune response	Yes	Scarce	**Yes**

A. baumannii is an opportunistic pathogen with notorious ability to withstand desiccation and disinfection processes and to persist in the hospital environment. The escalating number of infections involving multidrug or pandrug resistant strains of this bacterium necessitates the development of new options for preventing against this

emerging threat. Although anti-*A. baumannii* vaccines based on a single, highly purified bacterial antigens of *A. baumannii* (Ata, K1 polysaccharide, OmpA, PNAG, Bap, OmpW) are attractive on the basis that these vaccine preparations are well defined and may produce a more predictable immune response, this approach has some limitations. Importantly, a vaccine targeting a single bacterial antigen would not have activity against strains that lack or down regulate the expression of the target gene. Such a decrease in target antigen expression could occur due to adaptation to immune pressure or during the acquisition of antibiotic resistance, since it has been shown that the expression of certain *A. baumannii* outer membrane proteins is decreased upon the acquisition of resistance [352]. Secondly, the process required for antigen purification may alter the conformation of the antigen. Multicomponent vaccines composed of outer membrane vesicles and formalin-inactivated whole-cells can overcome these problems as these vaccines can elicit antibodies against multiple bacterial antigens and better coverage against circulating strains since the decreased expression of a single bacterial antigen would likely have less effect on the efficacy of such a vaccine. However, the high endotoxin levels present in these vaccines due to the presence of LPS complicates their use in human vaccination. Immunization with an LPS-deficient whole-cell of *A. baumannii* provided protective immunity in mice and could present a good anti-*A. baumannii* vaccine. But, like many Gram-negative bacteria, the LPS of *A. baumannii* is highly immunostimulatory [353] and removing this immune-activating molecule could impair a broader immune response. Considering the rapid elimination of *A. baumannii* ATCC 17978 MurI^{-} from the blood of mice and in view of the absence of adverse effects, it seems that there is no risk for endotoxin accumulation when administering this vaccine. However, further studies will be needed to address this aspect.

Although considerable progress has been made towards understanding the epidemiology, mechanisms of antibiotic resistance and persistence, much less is known regarding the pathogenesis of *A. baumannii* and the influence of immune responses to control *A. baumannii* disease. Considering the cellular immune responses elicited in response to *A. baumannii* ATCC 17978 MurI^{-}, a significant increment in IL-4-producing splenocytes was observed, consistent with a Th2 response. However, the role of IL-4 cytokines in host defense against this pathogen is poorly defined. Also, ATCC 17978 MurI^{-} mediated a significant increase in the number of IL-17-secreting splenocytes, however IL-17 seems not to play a major role against systemic *A. baumannii* infection [354].

The alternative complement pathway, a major bactericidal component in serum that limits microbial dissemination, is responsible for *A. baumannii* killing in human serum;

however, clinically relevant strains can be resistant to complement activity. This pathway is activated leading to deposition of complement factor on the surface of bacteria and consequent bacterial lysis or opsonin-mediated phagocytosis. There is considerable debate over the mechanism behind the serum resistance of *A. baumannii*. Proposed models include bacterial-mediated inactivation of the alternative complement pathway inhibitor Factor H [355], *A. baumannii* release of LPS [356], and the modification of peptidoglycan by the penicillin-binding protein PBP-7/8 [357]. Furthermore, the presence of surface polysaccharides or capsule protects Gram-negative bacteria from host antimicrobials in serum, and several strains of *A. baumannii*, like Ab307-0294, produce a polysaccharide capsule [326]. Considering that *A. baumannii* ATCC 17978 does not produces a capsule, the ability of the ATCC 17978 MurI$^-$ mutant to elicit protective immunity against Ab307-0294 was noteworthy. Cross protection observed against this strain could be derived from the broadly reactive antibodies elicited against whole cell antigens presented by ATCC 17978 MurI$^-$.

Therefore, anti-*A. baumannii* vaccine composed of MurI$^-$ mutants, auxotrophic for D-Glu might be a viable approach to effectively control *A. baumannii* infections.

It is well established that *P. aeruginosa* is a frequent and virulent pulmonary pathogen in patients with CF and other forms of bronchiectasis [358]. After a period of intermittent colonization, the organism becomes permanently established and is difficult to eradicate. Most patients with CF become chronically infected with wild-type *P. aeruginosa* strains in early childhood and during the years following initial colonization, the wild-type strains uniformly mutate into mucoid variants [359]. High resistance to antibiotics, hypermutability, biofilm growth and alginate hyperproduction, or a customized pathogenicity which may include the loss of classical virulence factors and metabolic changes, are the traits that contribute to *P. aeruginosa* ability to colonize and persist in the lungs as chronic respiratory infections in patients suffering from CF or other chronic respiratory diseases [360].

Despite considerable advances in antimicrobial therapy, effective treatment and control of *P. aeruginosa* infections remains a persistent problem, primarily because of the natural resistance of the organism and its remarkable ability to acquire resistance to multiple antimicrobial agents by various mechanisms [361]. As an alternative strategy to prevent *P. aeruginosa* infections in susceptible populations, effective immunotherapies or vaccines against *P. aeruginosa* have long been sought. A vaccine to delay or prevent initial

pulmonary infection in individuals with CF would have significant impact and may be accomplished in the future.

As *P. aeruginosa* is an extracellular pathogen, humoral, mucosal or systemic opsonizing immunity is most effective to prevent bacterial colonization and infection. However, T cell responses can also mediate protective immunity in individuals with *P. aeruginosa* infections [362-364].

P. aeruginosa PAO1 MurI$^-$ triggered a substantial increment – although not significant – in IFN-γ-secreting splenocytes, as marker of Th1, as well a significant increment in IL-4-producing splenocytes, consistent with a Th2 immune response. IL-4 is known to enhance pulmonary clearance of *P. aeruginosa* in mice [365]. However, comparing the CF patients with and without chronic lung infection suggested that a Th2 type response correlated with infection, implying that a Th1 response may be more protective [366,367]. More importantly, *P. aeruginosa* MurI$^-$ mediated a significant increase in the number of IL-17-secreting splenocytes, essential in acute pulmonary *P. aeruginosa* infection [181,368].

The most similar to MurI$^-$ experimental vaccines obtained so far against *P. aeruginosa* are those derived from *P. aeruginosa* Δ*aroA* deletion mutants. These mutants are unable to synthesize aromatic amino acids and cannot efficiently acquire them from the host and hence can survive at detectable levels only up to 3–4 days following administration [179]. Recently, a multivalent vaccine composed of different *P. aeruginosa* Δ*aroA* strains induced multifactorial immune responses against diverse bacterial antigens and protected against acute fatal lung infection [183]. Despite these results, residual virulence in these strains was observed [179,180,182,183]. In the case of *P. aeruginosa* MurI$^-$, this strain was rapidly eliminated from the blood of BALB/c mice, with negative blood cultures and no viable bacterial counts 4 hours after administration. Although we did not evaluate the clearance of *P. aeruginosa* from lungs, it seems that *P. aeruginosa* MurI$^-$ can overcome the limitations presented by Δ*aroA* mutants.

Considering all these aspects, an anti-*P. aeruginosa* vaccine composed of MurI$^-$ mutants, auxotrophic for D-Glu, might be a viable approach to effectively control *P. aeruginosa* infections in CF and non-CF patients.

With the increasing propensity of *S. aureus* to develop resistance to essentially all classes of antibiotics, alternative strategies, such as prophylactic vaccination to prevent *S. aureus* infections, are actively being pursued in healthcare settings. Within the last decade,

the *S. aureus* vaccine field as witnessed two major vaccine failures in phase III clinical trials designed to prevent *S. aureus* infections in either patients undergoing cardiothoracic surgery or patients with end-stage renal disease undergoing haemodialysis, evidencing the need for an effective vaccine.

Preclinical and clinical data indicate that immunization with intact whole *S. aureus* bacteria induces high immune titers, but does not confer protection from *S. aureus* disease [369,370]. Additionally, the *S. aureus* stimulated humoral immune response may not play a meaningful role in bacterial clearance in some models. While antibodies undoubtedly play some role in protection, they may not be determinative for vaccine protective efficacy because animals and humans already have sufficient baseline opsonins to allow for phagocytic uptake by neutrophils. T cells were observed to play a pivotal role in the prevention of *S. aureus* infection, as demonstrated in models of disseminated as well as local infection. In this study, *S. aureus* MurI^{-}Dat^{-} vaccine triggered an appropriate cellular immune response, with IL-17-secreting splenocytes being the predominant T cell subset triggered. Th17/IL-17 pathway was demonstrated to be essential in defence against *S. aureus* acute lethal infection in mice [304,371]. Also, a significant number of IFN-γ-secreting splenocytes was elicited. Th1 effector cytokines such as IFN-γ may play a crucial role in the eradication of *S. aureus* [372]. These data indicate that active immunization with *S. aureus* MurI^{-}Dat^{-} elicits a Th1 and Th17 response.

The precise immunopathological mechanisms that predispose a given individual to to *S. aureus* disease are still unclear. Preclinical animal models have thus been developed to study *S. aureus* pathogenesis but these models are limited by the fact that *S. aureus* is exquisitely adapted to the human host. Therefore, no preclinical animal model of infection fully recapitulates the natural infections process in humans, due to differences in host cell proteins, such as haemoglobin [373], and the requirement for high bacterial challenge doses [374] in the non-human host. The experimental *S. aureus* MurI^{-}Dat^{-} vaccine presented here demonstrated to be highly effective using a preclinical model of mouse acute lethal infection, and perhaps, these results would apply to humans. Further studies need to be accomplished.

Therefore, our D-Glu auxotrophs are promising whole-cell vaccines against the high-priority pathogens *A. baumannii*, *P. aeruginosa* and *S. aureus*. Moreover, this pioneering approach of bacterial attenuation can be more broadly applied to other Gram-negative and Gram-positive pathogens of global concern, and individual vaccine

compositions obtained this way can be reinforced with the combination of multiple bacterial strains for their use as prophylactics for human or animal health in the future.

6. CONCLUSIONS

6. CONCLUSIONS

6.1. Characterization of MurI⁻ and MurI⁻Dat⁻ mutants

6.1.1. MurI⁻ mutants of *Acinetobacter baumannii* ATCC 17978 and *Pseudomonas aeruginosa* PAO1 are auxotrophic for D-Glu

6.1.2. The MurI⁻Dat⁻ mutant of *Staphylococcus aureus* 132 is auxotrophic for D-Glu

6.1.3. *A. baumannii* MurI⁻ and *S. aureus* MurI⁻Dat⁻ present an altered pattern of cell division in the presence of low D-Glu concentrations

6.1.4. D-Glu auxotrophy produces cell wall degeneration and bacterial lysis of MurI⁻ or MurI⁻Dat⁻ mutants

6.2. Virulence attenuation of MurI⁻ and MurI⁻Dat⁻ mutants

6.2.1. D-Glu auxotrophic strains are attenuated respective to parental strains in a mouse model of acute lethal infection

6.3. Generation of antibody-mediated immune responses

6.3.1. Vaccination with D-Glu auxotrophic strains elicits high level of specific antibodies in BALB/c mice

6.3.2. Antibody-mediated immune response activation by D-Glu auxotrophic strains is dose-dependent

6.3.3. The MurI⁻ mutant of *A. baumannii* elicits long-term antibody memory

6.3.4. Immunization with D-Glu auxotrophic strains elicits high levels of cross-reactive IgG antibodies against clonally unrelated bacterial strains

6.4. Activation of cell-mediated immunity

6.4.1. Immunization with *A. baumannii* MurI⁻ and *P. aeruginosa* MurI⁻ elicits consistent Th2 and Th17 immune responses

6.4.2. Immunization with *S. aureus* MurI⁻Dat⁻ elicits consistent Th1 and Th17 immune responses

6.5. Protective immunity against acute lethal infection

6.5.1. Vaccination with *A. baumannii* MurI⁻ and *P. aeruginosa* MurI⁻ protects against bacterial dissemination after challenge

6.5.2. Vaccination with *S. aureus* MurI⁻Dat⁻ protects against bacterial dissemination and prevents weight loss after challenge

6.5.3. Vaccination with *A. baumannii* MurI⁻ protects against *A. baumannii* parental, MDR and highly virulent strains

6.5.4. Vaccination with *P. aeruginosa* MurI⁻ protects against *P. aeruginosa* parental, mucoid and highly virulent strains

6.5.5. Vaccination with *S. aureus* MurI⁻Dat⁻ protects against *S. aureus* parental, MRSA, highly disseminated, bovine and poultry strains

6.5.6. The protective efficacy of vaccination with MurI⁻ and MurI⁻Dat⁻ mutants against parental strains is independent of different mice genetic backgrounds

6.5.7. Intramuscular vaccination with *P. aeruginosa* MurI⁻ confers protection against parental and highly virulent *P. aeruginosa* strains

6.5.8. Vaccination with D-Glu auxotrophic strains induces therapeutically active antisera

6.6. *In vivo* and environmental safety of D-Glu auxotrophic bacteria as GMO vaccines

6.6.1. *A. baumannii* MurI⁻, *P. aeruginosa* MurI⁻ and *S. aureus* MurI⁻Dat⁻ are eliminated from the blood of mice within hours, and appear safe for parenteral administrations

6.6.2. MurI⁻ or MurI⁻Dat⁻ mutants of *A. baumannii*, *P. aeruginosa* and *S. aureus* do not revert to the wild-type phenotype *in vitro*

6.1.5. MurI⁻ mutants of *A. baumannii* and *P. aeruginosa* are more susceptible to osmolisis than its wild-type homologues

6.1.6. MurI⁻Dat⁻ mutant of *S. aureus* is more susceptible to desiccation than its wild-type homologue

7. REFERENCES

7. REFERENCES

1. Vidarsson, G., Dekkers, G. & Rispens, T. IgG subclasses and allotypes: from structure to effector functions. *Front. Immunol.* **5,** 520 (2014).

2. Wheelock, E. F. Interferon-like virus-inhibitor induced in human leukocytes by phytohemagglutinin. *Science* **149,** 310–1 (1965).

3. Billiau, A. Interferon-gamma: biology and role in pathogenesis. *Adv. Immunol.* **62,** 61–130 (1996).

4. Boehm, U., Klamp, T., Groot, M. & Howard, J. C. Cellular responses to interferon-gamma. *Annu. Rev. Immunol.* **15,** 749–95 (1997).

5. Farrar, M. A. & Schreiber, R. D. The molecular cell biology of interferon-gamma and its receptor. *Annu. Rev. Immunol.* **11,** 571–611 (1993).

6. Puddu, P. *et al.* IL-12 induces IFN-gamma expression and secretion in mouse peritoneal macrophages. *J. Immunol.* **159,** 3490–7 (1997).

7. Sugaya, M., Nakamura, K. & Tamaki, K. Interleukins 18 and 12 synergistically upregulate interferon-gamma production by murine dendritic epidermal T cells. *J. Invest. Dermatol.* **113,** 350–4 (1999).

8. Ohteki, T. *et al.* Interleukin 12-dependent interferon gamma production by CD8alpha+ lymphoid dendritic cells. *J. Exp. Med.* **189,** 1981–6 (1999).

9. Gupta, A. A., Leal-Berumen, I., Croitoru, K. & Marshall, J. S. Rat peritoneal mast cells produce IFN-gamma following IL-12 treatment but not in response to IgE-mediated activation. *J. Immunol.* **157,** 2123–8 (1996).

10. Howard, M. *et al.* Identification of a T cell-derived b cell growth factor distinct from interleukin 2. *J. Exp. Med.* **155,** 914–23 (1982).

11. Brown, M. A. & Hural, J. Functions of IL-4 and control of its expression. *Crit. Rev. Immunol.* **17,** 1–32 (1997).

12. Noma, Y. *et al.* Cloning of cDNA encoding the murine IgG1 induction factor by a novel strategy using SP6 promoter. *Nature* **319,** 640–6

13. Yokota, T. *et al.* Isolation and characterization of a human interleukin cDNA clone, homologous to mouse B-cell stimulatory factor 1, that expresses B-cell- and T-cell-

stimulating activities. *Proc. Natl. Acad. Sci. U. S. A.* **83,** 5894–8 (1986).

14. Arai, N. *et al.* Complete nucleotide sequence of the chromosomal gene for human IL-4 and its expression. *J. Immunol.* **142,** 274–82 (1989).

15. McKnight, A. J., Barclay, A. N. & Mason, D. W. Molecular cloning of rat interleukin 4 cDNA and analysis of the cytokine repertoire of subsets of CD4+ T cells. *Eur. J. Immunol.* **21,** 1187–94 (1991).

16. Mosmann, T. R. *et al.* Species-specificity of T cell stimulating activities of IL 2 and BSF-1 (IL 4): comparison of normal and recombinant, mouse and human IL 2 and BSF-1 (IL 4). *J. Immunol.* **138,** 1813–6 (1987).

17. Ramírez, F., Stumbles, P., Puklavec, M. & Mason, D. Rat interleukin-4 assays. *J. Immunol. Methods* **221,** 141–50 (1998).

18. Ho, I. C., Hodge, M. R., Rooney, J. W. & Glimcher, L. H. The proto-oncogene c-maf is responsible for tissue-specific expression of interleukin-4. *Cell* **85,** 973–83 (1996).

19. Nakamura, E. *et al.* Involvement of NK1+ CD4- CD8- alphabeta T cells and endogenous IL-4 in non-MHC-restricted rejection of embryonal carcinoma in genetically resistant mice. *J. Immunol.* **158,** 5338–48 (1997).

20. Launois, P., Ohteki, T., Swihart, K., MacDonald, H. R. & Louis, J. A. In susceptible mice, Leishmania major induce very rapid interleukin-4 production by CD4+ T cells which are NK1.1-. *Eur. J. Immunol.* **25,** 3298–307 (1995).

21. Kelleher, P., Maroof, A. & Knight, S. C. Retrovirally induced switch from production of IL-12 to IL-4 in dendritic cells. *Eur. J. Immunol.* **29,** 2309–18 (1999).

22. Adachi, Y., Kindzelskii, A. L., Ohno, N., Yadomae, T. & Petty, H. R. Amplitude and frequency modulation of metabolic signals in leukocytes: synergistic role of IFN-gamma in IL-6- and IL-2-mediated cell activation. *J. Immunol.* **163,** 4367–74 (1999).

23. Rumbley, C. A. *et al.* Activated eosinophils are the major source of Th2-associated cytokines in the schistosome granuloma. *J. Immunol.* **162,** 1003–9 (1999).

24. Seder, R. A. *et al.* Mouse splenic and bone marrow cell populations that express high-affinity Fc epsilon receptors and produce interleukin 4 are highly enriched in basophils. *Proc. Natl. Acad. Sci. U. S. A.* **88,** 2835–9 (1991).

25. Pan, P. Y. & Rothman, P. IL-4 receptor mutations. *Curr. Opin. Immunol.* **11,** 615–20 (1999).

26. Faquim-Mauro, E. L., Coffman, R. L., Abrahamsohn, I. A. & Macedo, M. S. Cutting edge: mouse IgG1 antibodies comprise two functionally distinct types that are differentially regulated by IL-4 and IL-12. *J. Immunol.* **163,** 3572–6 (1999).

27. Hart, P. H. *et al.* Differential responses of human monocytes and macrophages to IL-4 and IL-13. *J. Leukoc. Biol.* **66,** 575–8 (1999).

28. O'Garra, A. Cytokines induce the development of functionally heterogeneous T helper cell subsets. *Immunity* **8,** 275–83 (1998).

29. Korn, T., Bettelli, E., Oukka, M. & Kuchroo, V. K. IL-17 and Th17 Cells. *Annu. Rev. Immunol.* **27,** 485–517 (2009).

30. Kolls, J. K. & Lindén, A. Interleukin-17 family members and inflammation. *Immunity* **21,** 467–76 (2004).

31. Witowski, J., Ksiazek, K. & Jörres, A. Interleukin-17: a mediator of inflammatory responses. *Cell. Mol. Life Sci.* **61,** 567–79 (2004).

32. Schwarzenberger, P. *et al.* Requirement of endogenous stem cell factor and granulocyte-colony-stimulating factor for IL-17-mediated granulopoiesis. *J. Immunol.* **164,** 4783–9 (2000).

33. Jovanovic, D. V *et al.* IL-17 stimulates the production and expression of proinflammatory cytokines, IL-beta and TNF-alpha, by human macrophages. *J. Immunol.* **160,** 3513–21 (1998).

34. Numasaki, M., Takahashi, H., Tomioka, Y. & Sasaki, H. Regulatory roles of IL-17 and IL-17F in G-CSF production by lung microvascular endothelial cells stimulated with IL-1β and/or TNF-α. *Immunol. Lett.* **95,** 97–104 (2004).

35. Miljkovic, D. *et al.* The role of interleukin-17 in inducible nitric oxide synthase-mediated nitric oxide production in endothelial cells. *Cell. Mol. Life Sci.* **60,** 518–25 (2003).

36. Chen, K. *et al.* Th17 Cells Mediate Clade-Specific, Serotype-Independent Mucosal Immunity. *Immunity* **35,** 997–1009 (2011).

37. Khader, S. A. *et al.* IL-23 and IL-17 in the establishment of protective pulmonary CD4+ T cell responses after vaccination and during *Mycobacterium tuberculosis* challenge. *Nat. Immunol.* **8,** 369–77 (2007).

38. Lindenstrøm, T. *et al.* Vaccine-induced th17 cells are maintained long-term postvaccination as a distinct and phenotypically stable memory subset. *Infect. Immun.* **80,** 3533–44 (2012).

39. Aggarwal, S. & Gurney, A. L. IL-17: prototype member of an emerging cytokine family. *J. Leukoc. Biol.* **71,** 1–8 (2002).

40. Moseley, T. A., Haudenschild, D. R., Rose, L. & Reddi, A. H. Interleukin-17 family and IL-17 receptors. *Cytokine Growth Factor Rev.* **14,** 155–74 (2003).

41. Yao, Z. *et al.* Human IL-17: a novel cytokine derived from T cells. *J. Immunol.* **155,** 5483–6 (1995).

42. Rouvier, E., Luciani, M. F., Mattéi, M. G., Denizot, F. & Golstein, P. CTLA-8, cloned from an activated T cell, bearing AU-rich messenger RNA instability sequences, and homologous to a herpesvirus saimiri gene. *J. Immunol.* **150,** 5445–56 (1993).

43. Kennedy, J. *et al.* Mouse IL-17: a cytokine preferentially expressed by alpha beta TCR + CD4-CD8-T cells. *J. Interferon Cytokine Res.* **16,** 611–7 (1996).

44. Liang, S. C. *et al.* Interleukin (IL)-22 and IL-17 are coexpressed by Th17 cells and cooperatively enhance expression of antimicrobial peptides. *J. Exp. Med.* **203,** 2271–9 (2006).

45. Mitsdoerffer, M. *et al.* Proinflammatory T helper type 17 cells are effective B-cell helpers. *Proc. Natl. Acad. Sci. U. S. A.* **107,** 14292–7 (2010).

46. Leo, O., Cunningham, A. & Stern, P. L. *Understanding modern vaccines: perspectives in vaccinology.* 25–59 (Elsevier B.V., 2011).

47. Levine, M. M. *et al.* Safety, immunogenicity, and efficacy of recombinant live oral cholera vaccines, CVD 103 and CVD 103-HgR. *Lancet (London, England)* **2,** 467–70 (1988).

48. Simanjuntak, C. H. *et al.* Oral immunisation against typhoid fever in Indonesia with Ty21a vaccine. *Lancet* **338,** 1055–9 (1991).

49. Liu, J., Tran, V., Leung, A. S., Alexander, D. C. & Zhu, B. BCG vaccines: their mechanisms of attenuation and impact on safety and protective efficacy. *Hum. Vaccin.* **5,** 70–8 (2009).

50. Michael, A., Geier, E., Konshtok, R., Hertman, I. & Markenson, J. Attenutated live fowl cholera vaccine. III. Laboratory and field vaccination trials in turkeys and

chickens. *Avian Dis.* **23,** 878–85 (1979).

51. Panciera, R. J., Corstvet, R. E., Confer, A. W. & Gresham, C. N. Bovine pneumonic pasteurellosis: effect of vaccination with live Pasteurella species. *Am. J. Vet. Res.* **45,** 2538–42 (1984).

52. Sakano, T., Sakurai, K., Furutani, T. & Shimizu, T. Immunogenicity and safety of an attenuated *Bordetella bronchiseptica* vaccine in pigs. *Am. J. Vet. Res.* **45,** 1814–7 (1984).

53. Turnbull, P. C. B. Review Anthrax vaccines : past , present and future. **9,** 533–9 (1991).

54. Thiaucourt, F. *et al.* Contagious bovine pleuropneumonia. A reassessment of the efficacy of vaccines used in Africa. *Ann. N. Y. Acad. Sci.* **916,** 71–80 (2000).

55. Schurig, G. G., Sriranganathan, N. & Corbel, M. J. Brucellosis vaccines : past , present and future. **90,** 479–96 (2002).

56. Begg, D. J. & Griffin, J. F. T. Vaccination of sheep against *M. paratuberculosis*: Immune parameters and protective efficacy. *Vaccine* **23,** 4999–5008 (2005).

57. Lee, Y. J., Mo, I. P. & Kang, M. S. Safety and efficacy of *Salmonella gallinarum* 9R vaccine in young laying chickens. *Avian Pathol.* **34,** 362–6 (2005).

58. Frey, J. Biological safety concepts of genetically modified live bacterial vaccines. *Vaccine* **25,** 5598–605 (2007).

59. Crump, J. A. & Mintz, E. D. Global trends in typhoid and paratyphoid Fever. *Clin. Infect. Dis.* **50,** 241–6 (2010).

60. Engels, E. A., Falagas, M. E., Lau, J. & Bennish, M. L. Typhoid fever vaccines: a meta-analysis of studies on efficacy and toxicity. *BMJ* **316,** 110–6 (1998).

61. Fraser, A., Paul, M., Goldberg, E., Acosta, C. J. & Leibovici, L. Typhoid fever vaccines: systematic review and meta-analysis of randomised controlled trials. *Vaccine* **25,** 7848–57 (2007).

62. Guzman, C. A. *et al.* Vaccines against typhoid fever. *Vaccine* **24,** 3804–11 (2006).

63. Germanier, R. & Füer, E. Isolation and characterization of Gal E mutant Ty 21a of *Salmonella typhi*: a candidate strain for a live, oral typhoid vaccine. *J. Infect. Dis.* **131,**

553–8 (1975).

64. Kopecko, D. J. *et al.* Genetic stability of vaccine strain Salmonella Typhi Ty21a over 25 years. *Int. J. Med. Microbiol.* **299,** 233–46 (2009).

65. Germanier, R. & Fürer, E. Characteristics of the attenuated oral vaccine strain '*S. typhi*' Ty 21a. *Dev. Biol. Stand.* **53,** 3–7 (1983).

66. Gentschev, I. *et al.* Vivotif--a 'magic shield' for protection against typhoid fever and delivery of heterologous antigens. *Chemotherapy* **53,** 177–80 (2007).

67. Anwar, E. *et al.* Vaccines for preventing typhoid fever. *Cochrane database Syst. Rev.* **1,** CD001261 (2014).

68. Raffatellu, M., Wilson, R. P., Winter, S. E. & Bäumler, A. J. Clinical pathogenesis of typhoid fever. *J. Infect. Dev. Ctries.* **2,** 260–6 (2008).

69. Breen, J. F. & Apicella, M. A. Immunogenicity of gonococcal Gc2 polysaccharide: comparative studies with pneumococcal type III polysaccharide and *Salmonella typhosa* Vi antigen. *Infect. Immun.* **22,** 195–9 (1978).

70. Lake, J. P., Reed, N. D., Ulrich, J. T. & Varitek, V. A. Development of a localized hemolysis-in-gel assay for Vi antigen: characterization of the Vi-specific PFC response of nude and normal mice. *Immunol. Commun.* **6,** 149–65 (1977).

71. Ryan, E. T. & Calderwood, S. B. Cholera vaccines. *Clin. Infect. Dis.* **31,** 561–5 (2000).

72. Ketley, J. M., Michalski, J., Galen, J., Levine, M. M. & Kaper, J. B. Construction of genetically marked *Vibrio cholerae* O1 vaccine strains. *FEMS Microbiol. Lett.* **111,** 15–21 (1993).

73. Kotloff, K. L. *et al.* Safety and immunogenicity in North Americans of a single dose of live oral cholera vaccine CVD 103-HgR: results of a randomized, placebo-controlled, double-blind crossover trial. *Infect. Immun.* **60,** 4430–2 (1992).

74. Tacket, C. O. *et al.* Onset and duration of protective immunity in challenged volunteers after vaccination with live oral cholera vaccine CVD 103-HgR. *J. Infect. Dis.* **166,** 837–41 (1992).

75. Tacket, C. O. *et al.* Randomized, double-blind, placebo-controlled, multicentered trial of the efficacy of a single dose of live oral cholera vaccine CVD 103-HgR in preventing cholera following challenge with *Vibrio cholerae* O1 El tor inaba three months after vaccination. *Infect. Immun.* **67,** 6341–5 (1999).

76. Kenner, J. R. *et al.* Peru-15, an improved live attenuated oral vaccine candidate for *Vibrio cholerae* O1. *J. Infect. Dis.* **172,** 1126–9 (1995).

77. Sack, D. A. *et al.* Evaluation of Peru-15, a new live oral vaccine for cholera, in volunteers. *J. Infect. Dis.* **176,** 201–5 (1997).

78. Qadri, F. *et al.* Randomized, controlled study of the safety and immunogenicity of Peru-15, a live attenuated oral vaccine candidate for cholera, in adult volunteers in Bangladesh. *J. Infect. Dis.* **192,** 573–9 (2005).

79. Qadri, F. *et al.* Peru-15, a live attenuated oral cholera vaccine, is safe and immunogenic in Bangladeshi toddlers and infants. *Vaccine* **25,** 231–8 (2007).

80. Benítez, J. A. *et al.* Preliminary assessment of the safety and immunogenicity of a new CTXPhi-negative, hemagglutinin/protease-defective El Tor strain as a cholera vaccine candidate. *Infect. Immun.* **67,** 539–45 (1999).

81. García, L. *et al.* The vaccine candidate *Vibrio cholerae* 638 is protective against cholera in healthy volunteers. *Infect. Immun.* **73,** 3018–24 (2005).

82. Thungapathra, M. *et al.* Construction of a recombinant live oral vaccine from a non-toxigenic strain of *Vibrio cholerae* O1 serotype inaba biotype E1 Tor and assessment of its reactogenicity and immunogenicity in the rabbit model. *Immunol. Lett.* **68,** 219–27 (1999).

83. Liang, W. *et al.* Construction and evaluation of a safe, live, oral *Vibrio cholerae* vaccine candidate, IEM108. *Infect. Immun.* **71,** 5498–504 (2003).

84. Ryan, E. T., Calderwood, S. B. & Qadri, F. Live attenuated oral cholera vaccines. *Expert Rev. Vaccines* **5,** 483–94 (2006).

85. Weekly epidemiological record Relevé épidémiologique hebdomadaire. World Health Organization. **79,** 25–40 (2004).

86. Leung, A. S. *et al.* Novel genome polymorphisms in BCG vaccine strains and impact on efficacy. *BMC Genomics* **9,** 413 (2008).

87. Chen, J. M., Islam, S. T., Ren, H. & Liu, J. Differential productions of lipid virulence factors among BCG vaccine strains and implications on BCG safety. *Vaccine* **25,** 8114–22 (2007).

88. Bonah, C. The 'experimental stable' of the BCG vaccine: safety, efficacy, proof, and standards, 1921-1933. *Stud. Hist. Philos. Biol. Biomed. Sci.* **36,** 696–721 (2005).

89. Mahairas, G. G., Sabo, P. J., Hickey, M. J., Singh, D. C. & Stover, C. K. Molecular analysis of genetic differences between *Mycobacterium bovis* BCG and virulent *M. bovis*. *J. Bacteriol.* **178,** 1274–82 (1996).

90. Behr, M. A. *et al.* Comparative genomics of BCG vaccines by whole-genome DNA microarray. *Science* **284,** 1520–3 (1999).

91. Abdallah, A. M. *et al.* Type VII secretion--mycobacteria show the way. *Nat. Rev. Microbiol.* **5,** 883–91 (2007).

92. Pym, A. S. *et al.* Recombinant BCG exporting ESAT-6 confers enhanced protection against tuberculosis. *Nat. Med.* **9,** 533–9 (2003).

93. Sherman, D. R. *et al. Mycobacterium tuberculosis* H37Rv: Delta RD1 is more virulent than *M. bovis* bacille Calmette-Guérin in long-term murine infection. *J. Infect. Dis.* **190,** 123–6 (2004).

94. Brosch, R. *et al.* Genome plasticity of BCG and impact on vaccine efficacy. *Proc. Natl. Acad. Sci. U. S. A.* **104,** 5596–601 (2007).

95. Onwueme, K. C., Vos, C. J., Zurita, J., Ferreras, J. A. & Quadri, L. E. N. The dimycocerosate ester polyketide virulence factors of mycobacteria. *Prog. Lipid Res.* **44,** 259–302 (2005).

96. Frigui, W. *et al.* Control of *M. tuberculosis* ESAT-6 secretion and specific T cell recognition by PhoP. *PLoS Pathog.* **4,** (2008).

97. Lee, J. S. *et al.* Mutation in the transcriptional regulator PhoP contributes to avirulence of *Mycobacterium tuberculosis* H37Ra strain. *Cell Host Microbe* **3,** 97–103 (2008).

98. Martin, C. *et al.* The live *Mycobacterium tuberculosis* phoP mutant strain is more attenuated than BCG and confers protective immunity against tuberculosis in mice and guinea pigs. *Vaccine* **24,** 3408–19 (2006).

99. Chesne-Seck, M.-L. *et al.* A point mutation in the two-component regulator PhoP-PhoR accounts for the absence of polyketide-derived acyltrehaloses but not that of phthiocerol dimycocerosates in *Mycobacterium tuberculosis* H37Ra. *J. Bacteriol.* **190,** 1329–34 (2008).

100. Cole, S. T. *et al.* Deciphering the biology of *Mycobacterium tuberculosis* from the complete genome sequence. *Nature* **393,** 537–44 (1998).

101. Burian, J. *et al.* The mycobacterial antibiotic resistance determinant WhiB7 acts as a transcriptional activator by binding the primary sigma factor SigA (RpoV). *Nucleic Acids Res.* **41,** 10062–76 (2013).

102. Ramón-García, S. *et al.* WhiB7, an Fe-S-dependent transcription factor that activates species-specific repertoires of drug resistance determinants in actinobacteria. *J. Biol. Chem.* **288,** 34514–28 (2013).

103. Larsson, C. *et al.* Gene expression of *Mycobacterium tuberculosis* putative transcription factors whiB1-7 in redox environments. *PLoS One* **7,** e37516 (2012).

104. Steyn, A. J. C. *et al. Mycobacterium tuberculosis* WhiB3 interacts with RpoV to affect host survival but is dispensable for *in vivo* growth. *Proc. Natl. Acad. Sci. U. S. A.* **99,** 3147–52 (2002).

105. Singh, A. *et al. Mycobacterium tuberculosis* WhiB3 maintains redox homeostasis by regulating virulence lipid anabolism to modulate macrophage response. *PLoS Pathog.* **5,** e1000545 (2009).

106. Parish, T. *et al.* Deletion of two-component regulatory systems increases the virulence of *Mycobacterium tuberculosis*. *Infect. Immun.* **71,** 1134–40 (2003).

107. Casali, N. & Riley, L. W. A phylogenomic analysis of the Actinomycetales mce operons. *BMC Genomics* **8,** 60 (2007).

108. Mostowy, S., Tsolaki, A. G., Small, P. M. & Behr, M. A. The *in vitro* evolution of BCG vaccines. *Vaccine* **21,** 4270–4 (2003).

109. Pandey, A. K. & Sassetti, C. M. Mycobacterial persistence requires the utilization of host cholesterol. *Proc. Natl. Acad. Sci. U. S. A.* **105,** 4376–80 (2008).

110. Rathor, N. *et al.* An insight into the regulation of mce4 operon of *Mycobacterium tuberculosis*. *Tuberculosis (Edinb).* **93,** 389–97 (2013).

111. WHO Information sheet: observed rate of vaccine reactions bacilli Calmette-Guérin (BCG) vaccine. Global Vaccine Safety, Immunizations and Biologicals (2012).

112. Malaga, W., Perez, E. & Guilhot, C. Production of unmarked mutations in mycobacteria using site-specific recombination. *FEMS Microbiol. Lett.* **219,** 261–8 (2003).

113. Arbues, A. *et al.* Construction, characterization and preclinical evaluation of MTBVAC, the first live-attenuated *M. tuberculosis*-based vaccine to enter clinical trials. *Vaccine* **31,** 4867–73 (2013).

114. Roberts, M., Maskell, D., Novotny, P. & Dougan, G. Construction and characterization in vivo of *Bordetella pertussis* aroA mutants. *Infect. Immun.* **58,** 732–9 (1990).

115. Mielcarek, N. *et al.* Live attenuated *B. pertussis* as a single-dose nasal vaccine against whooping cough. *PLoS Pathog.* **2,** 0662–70 (2006).

116. Mielcarek, N., Debrie, A.-S., Mahieux, S. & Locht, C. Dose response of attenuated *Bordetella pertussis* BPZE1-induced protection in mice. *Clin. Vaccine Immunol.* **17,** 317–24 (2010).

117. Feunou, P., Kammoun, H. & Debrie, A. Long-term immunity against pertussis induced by a single nasal administration of live attenuated *B . pertussis* BPZE1. *Vaccine* **28,** 7047–53 (2010).

118. Kammoun, H. *et al.* Dual mechanism of protection by live attenuated *Bordetella pertussis* BPZE1 against *Bordetella bronchiseptica* in mice. *Vaccine* **30,** 5864–70 (2012).

119. Thorstensson, R. *et al.* A phase I clinical study of a live attenuated *Bordetella pertussis* vaccine--BPZE1; a single centre, double-blind, placebo-controlled, dose-escalating study of BPZE1 given intranasally to healthy adult male volunteers. *PLoS One* **9,** e83449 (2014).

120. Locht, C. A common vaccination strategy to solve unsolved problems of tuberculosis and pertussis? *Microbes Infect.* **10,** 1051–6 (2008).

121. Boucher, H. W. *et al.* Bad bugs, no drugs: no ESKAPE! An update from the Infectious Diseases Society of America. *Clin. Infect. Dis.* **48,** 1–12 (2009).

122. Spellberg, B. *et al.* The epidemic of antibiotic-resistant infections: a call to action for the medical community from the Infectious Diseases Society of America. *Clin. Infect. Dis.* **46,** 155–64 (2008).

123. Peleg, A. Y., Seifert, H. & Paterson, D. L. *Acinetobacter baumannii*: Emergence of a successful pathogen. *Clin. Microbiol. Rev.* **21,** 538–82 (2008).

124. Kempf, M. & Rolain, J.-M. Emergence of resistance to carbapenems in *Acinetobacter*

baumannii in Europe: clinical impact and therapeutic options. *Int. J. Antimicrob. Agents* **39,** 105–14 (2012).

125. Lin, M.-F. & Lan, C.-Y. Antimicrobial resistance in *Acinetobacter baumannii*: From bench to bedside. *World J. Clin. cases* **2,** 787–814 (2014).

126. Wright, M. S. *et al.* New insights into dissemination and variation of the health care-associated pathogen *Acinetobacter baumannii* from genomic analysis. *MBio* **5,** e00963–13 (2014).

127. Peleg, A. Y. *et al.* The success of acinetobacter species; genetic, metabolic and virulence attributes. *PLoS One* **7,** e46984 (2012).

128. Pachón, J. & McConnell, M. J. Considerations for the development of a prophylactic vaccine for *Acinetobacter baumannii*. *Vaccine* **32,** 2534–6 (2014).

129. Xiao, W. *et al.* A genomic storm in critically injured humans. *J. Exp. Med.* **208,** 2581–90 (2011).

130. Marik, P. E. & Flemmer, M. The immune response to surgery and trauma: Implications for treatment. *J. Trauma Acute Care Surg.* **73,** 801–8 (2012).

131. van Faassen, H. *et al.* Neutrophils play an important role in host resistance to respiratory infection with *Acinetobacter baumannii* in mice. *Infect. Immun.* **75,** 5597–608 (2007).

132. Qiu, H. *et al.* Role of macrophages in early host resistance to respiratory *Acinetobacter baumannii* infection. *PLoS One* **7,** e40019 (2012).

133. Weinberger, B., Herndler-Brandstetter, D., Schwanninger, A., Weiskopf, D. & Grubeck-Loebenstein, B. Biology of immune responses to vaccines in elderly persons. *Clin. Infect. Dis.* **46,** 1078–84 (2008).

134. Bentancor, L. V., O'malley, J. M., Bozkurt-Guzel, C., Pier, G. B. & Maira-Litrán, T. Poly-n-acetyl-β-(1-6)-glucosamine is a target for protective immunity against *Acinetobacter baumannii* infections. *Infect. Immun.* **80,** 651–6 (2012).

135. Bentancor, L. V. *et al.* Evaluation of the trimeric autotransporter ata as a vaccine candidate against *Acinetobacter baumannii* infections. *Infect. Immun.* **80,** 3381–8 (2012).

136. McConnell, M. J. & Pachón, J. Active and passive immunization against *Acinetobacter baumannii* using an inactivated whole cell vaccine. *Vaccine* **29,** 1–5 (2010).

137. Huang, W. *et al.* Immunization against multidrug-resistant *Acinetobacter baumannii* effectively protects mice in both pneumonia and sepsis models. *PLoS One* **9,** 16–9 (2014).

138. Russo, T. a. *et al.* The K1 capsular polysaccharide from *Acinetobacter baumannii* is a potential therapeutic target via passive immunization. *Infect. Immun.* **81,** 915–22 (2013).

139. McConnell, M. J. *et al.* Vaccination with outer membrane complexes elicits rapid protective immunity to multidrug-resistant *Acinetobacter baumannii*. *Infect. Immun.* **79,** 518–26 (2011).

140. Luo, G. *et al.* Active and passive immunization protects against lethal, extreme drug resistant-*Acinetobacter baumannii* infection. *PLoS One* **7,** (2012).

141. Fattahian, Y. *et al.* Protection against *Acinetobacter baumannii* infection via its functional deprivation of biofilm associated protein (Bap). *Microb. Pathog.* **51,** 402–6 (2011).

142. Huang, W. *et al.* OmpW is a potential target for eliciting protective immunity against *Acinetobacter baumannii* infections. *Vaccine* **33,** 4479–85 (2015).

143. McConnell, M. J., Rumbo, C., Bou, G. & Pachón, J. Outer membrane vesicles as an acellular vaccine against *Acinetobacter baumannii*. *Vaccine* **29,** 5705–10 (2011).

144. Harris, G. *et al.* A mouse model of *Acinetobacter baumannii*-associated pneumonia using a clinically isolated hypervirulent strain. *Antimicrob. Agents Chemother.* **57,** 3601–13 (2013).

145. KuoLee, R. *et al.* Intranasal immunization protects against *Acinetobacter baumannii*-associated pneumonia in mice. *Vaccine* **33,** 260–7 (2015).

146. García-Quintanilla, M., Pulido, M. R., Pachón, J. & McConnell, M. J. Immunization with lipopolysaccharide-deficient whole cells provides protective immunity in an experimental mouse model of *Acinetobacter baumannii* infection. *PLoS One* **9,** e114410 (2014).

147. Adams, M. D. *et al.* Comparative genome sequence analysis of multidrug-resistant *Acinetobacter baumannii*. *J. Bacteriol.* **190,** 8053–64 (2008).

148. Perez, F. & Bonomo, R. a. Vaccines for *Acinetobacter baumannii*: Thinking 'out of the box'. *Vaccine* **32,** 2537–9 (2014).

149. Zhang, S., McCormack, F. X., Levesque, R. C., O'Toole, G. A. & Lau, G. W. The flagellum of *Pseudomonas aeruginosa* is required for resistance to clearance by surfactant protein A. *PLoS One* **2,** e564 (2007).

150. Gaynes, R. & Edwards, J. R. Overview of nosocomial infections caused by gram-negative bacilli. *Clin. Infect. Dis.* **41,** 848–54 (2005).

151. Thirumala, R., Ramaswamy, M. & Chawla, S. Diagnosis and management of infectious complications in critically ill patients with cancer. *Crit. Care Clin.* **26,** 59–91 (2010).

152. Carratalà, J., Rosón, B., Fernández-Sevilla, A., Alcaide, F. & Gudiol, F. Bacteremic pneumonia in neutropenic patients with cancer: causes, empirical antibiotic therapy, and outcome. *Arch. Intern. Med.* **158,** 868–72 (1998).

153. Murray, C. K. *et al.* Infections complicating the care of combat casualties during operations Iraqi Freedom and Enduring Freedom. *J. Trauma* **71,** S62–73 (2011).

154. Petersen, K. *et al.* Trauma-related infections in battlefield casualties from Iraq. *Ann. Surg.* **245,** 803–11 (2007).

155. Folkesson, A. *et al.* Adaptation of *Pseudomonas aeruginosa* to the cystic fibrosis airway: an evolutionary perspective. *Nat. Rev. Microbiol.* **10,** 841–51 (2012).

156. Driebe, W. T. Present status of contact lens-induced corneal infections. *Ophthalmol. Clin. North Am.* **16,** 485–94, viii (2003).

157. Parkins, M. D., Gregson, D. B., Pitout, J. D. D., Ross, T. & Laupland, K. B. Population-based study of the epidemiology and the risk factors for *Pseudomonas aeruginosa* bloodstream infection. *Infection* **38,** 25–32 (2010).

158. Dantes, R. *et al.* National burden of invasive methicillin-resistant *Staphylococcus aureus* infections, United States, 2011. *JAMA Intern. Med.* **173,** 1970–8 (2013).

159. Sievert, D. M. *et al.* Antimicrobial-resistant pathogens associated with healthcare-associated infections: summary of data reported to the National Healthcare Safety Network at the Centers for Disease Control and Prevention, 2009-2010. *Infect. Control Hosp. Epidemiol.* **34,** 1–14 (2013).

160. Rello, J. *et al.* Survival in patients with nosocomial pneumonia: impact of the severity of illness and the etiologic agent. *Crit. Care Med.* **25,** 1862–7 (1997).

161. Gibson, R. L., Burns, J. L. & Ramsey, B. W. Pathophysiology and management of pulmonary infections in cystic fibrosis. *Am. J. Respir. Crit. Care Med.* **168,** 918–51 (2003).

162. Lam, J. S., Taylor, V. L., Islam, S. T., Hao, Y. & Kocíncová, D. Genetic and functional diversity of *Pseudomonas aeruginosa* lipopolysaccharide. *Front. Microbiol.* **2,** 118 (2011).

163. Fisher, M. W., Devlin, H. B. & Gnabasik, F. J. New immunotype schema for *Pseudomonas aeruginosa* based on protective antigens. *J. Bacteriol.* **98,** 835–6 (1969).

164. Pier, G. B. Promises and pitfalls of *Pseudomonas aeruginosa* lipopolysaccharide as a vaccine antigen. *Carbohydr. Res.* **338,** 2549–56 (2003).

165. Alexander, J. W., Fisher, M. W. & MacMillan, B. G. Immunological control of Pseudomonas infection in burn patients: a clinical evaluation. *Arch. Surg.* **102,** 31–5 (1971).

166. Young, L. S., Meyer, R. D. & Armstrong, D. *Pseudomonas aeruginosa* vaccine in cancer patients. *Ann. Intern. Med.* **79,** 518–27 (1973).

167. Haghbin, M., Armstrong, D. & Murphy, M. L. Controlled prospective trial of *Pseudomonas aeruginosa* vaccine in children with acute leukemia. *Cancer* **32,** 761–6 (1973).

168. Pennington, J. E., Reynolds, H. Y., Wood, R. E., Robinson, R. A. & Levine, A. S. Use of a *Pseudomonas aeruginosa* vaccine in pateints with acute leukemia and cystic fibrosis. *Am. J. Med.* **58,** 629–36 (1975).

169. MacIntyre, S., McVeigh, T. & Owen, P. Immunochemical and biochemical analysis of the polyvalent *Pseudomonas aeruginosa* vaccine PEV. *Infect. Immun.* **51,** 675–86 (1986).

170. Langford, D. T. & Hiller, J. Prospective, controlled study of a polyvalent pseudomonas vaccine in cystic fibrosis--three year results. *Arch. Dis. Child.* **59,** 1131–4 (1984).

171. Hatano, K. *et al.* Immunogenic and antigenic properties of a heptavalent high-molecular-weight O-polysaccharide vaccine derived from *Pseudomonas aeruginosa*. *Infect. Immun.* **62,** 3608–16 (1994).

172. Hatano, K. & Pier, G. B. Complex serology and immune response of mice to variant high-molecular-weight O polysaccharides isolated from *Pseudomonas aeruginosa*

serogroup O2 strains. *Infect. Immun.* **66,** 3719–26 (1998).

173. Hancock, R. E. *et al. Pseudomonas aeruginosa* isolates from patients with cystic fibrosis: a class of serum-sensitive, nontypable strains deficient in lipopolysaccharide O side chains. *Infect. Immun.* **42,** 170–7 (1983).

174. Pier, G. B. *et al.* Opsonophagocytic killing antibody to *Pseudomonas aeruginosa* mucoid exopolysaccharide in older noncolonized patients with cystic fibrosis. *N. Engl. J. Med.* **317,** 793–8 (1987).

175. Cryz, S. J., Fürer, E. & Que, J. U. Synthesis and characterization of a *Pseudomonas aeruginosa* alginate-toxin A conjugate vaccine. *Infect. Immun.* **59,** 45–50 (1991).

176. Kashef, N. *et al.* Synthesis and characterization of *Pseudomonas aeruginosa* alginate-tetanus toxoid conjugate. *J. Med. Microbiol.* **55,** 1441–6 (2006).

177. Theilacker, C. *et al.* Construction and characterization of a *Pseudomonas aeruginosa* mucoid exopolysaccharide-alginate conjugate vaccine. *Infect. Immun.* **71,** 3875–84 (2003).

178. Pier, G. B. *et al.* Human monoclonal antibodies to *Pseudomonas aeruginosa* alginate that protect against infection by both mucoid and nonmucoid strains. *J. Immunol.* **173,** 5671–8 (2004).

179. Priebe, G. P. *et al.* Construction and characterization of a live, attenuated aroA deletion mutant of *Pseudomonas aeruginosa* as a candidate intranasal vaccine. *Infect. Immun.* **70,** 1507–17 (2002).

180. Priebe, G. P., Meluleni, G. J., Coleman, F. T., Goldberg, J. B. & Pier, G. B. Protection against fatal *Pseudomonas aeruginosa* pneumonia in mice after nasal immunization with a live, attenuated aroA deletion mutant. *Infect. Immun.* **71,** 1453–61 (2003).

181. Priebe, G. P. *et al.* IL-17 is a critical component of vaccine-induced protection against lung infection by lipopolysaccharide-heterologous strains of *Pseudomonas aeruginosa*. *J. Immunol.* **181,** 4965–75 (2008).

182. Zaidi, T. S., Priebe, G. P. & Pier, G. B. A live-attenuated *Pseudomonas aeruginosa* vaccine elicits outer membrane protein-specific active and passive protection against corneal infection. *Infect. Immun.* **74,** 975–83 (2006).

183. Kamei, A., Coutinho-Sledge, Y. S., Goldberg, J. B., Priebe, G. P. & Pier, G. B. Mucosal vaccination with a multivalent, live-attenuated vaccine induces multifactorial immunity against *Pseudomonas aeruginosa* acute lung infection. *Infect. Immun.* **79,** 1289–99 (2011).

184. DiGiandomenico, A., Rao, J. & Goldberg, J. B. Oral vaccination of BALB/c mice with *Salmonella enterica* serovar Typhimurium expressing *Pseudomonas aeruginosa* O antigen promotes increased survival in an acute fatal pneumonia model. *Infect. Immun.* **72,** 7012–21 (2004).

185. DiGiandomenico, A. *et al.* Intranasal immunization with heterologously expressed polysaccharide protects against multiple *Pseudomonas aeruginosa* infections. *Proc. Natl. Acad. Sci. U. S. A.* **104,** 4624–9 (2007).

186. Scarff, J. M. & Goldberg, J. B. Vaccination against *Pseudomonas aeruginosa* pneumonia in immunocompromised mice. *Clin. Vaccine Immunol.* **15,** 367–75 (2008).

187. Faure, K. *et al.* O-antigen serotypes and type III secretory toxins in clinical isolates of *Pseudomonas aeruginosa*. *J. Clin. Microbiol.* **41,** 2158–60 (2003).

188. Arnold, H. *et al.* Enhanced immunogenicity in the murine airway mucosa with an attenuated Salmonella live vaccine expressing OprF-OprI from *Pseudomonas aeruginosa*. *Infect. Immun.* **72,** 6546–53 (2004).

189. Bumann, D. *et al.* Systemic, nasal and oral live vaccines against *Pseudomonas aeruginosa*: a clinical trial of immunogenicity in lower airways of human volunteers. *Vaccine* **28,** 707–13 (2010).

190. Finke, M., Duchêne, M., Eckhardt, A., Domdey, H. & von Specht, B. U. Protection against experimental *Pseudomonas aeruginosa* infection by recombinant *P. aeruginosa* lipoprotein I expressed in Escherichia coli. *Infect. Immun.* **58,** 2241–4 (1990).

191. von Specht, B. U. *et al.* Safety and immunogenicity of a *Pseudomonas aeruginosa* outer membrane protein I vaccine in human volunteers. *Vaccine* **14,** 1111–7 (1996).

192. Mansouri, E. *et al.* Safety and immunogenicity of a *Pseudomonas aeruginosa* hybrid outer membrane protein F-I vaccine in human volunteers. *Infect. Immun.* **67,** 1461–70 (1999).

193. Westritschnig, K. *et al.* A randomized, placebo-controlled phase I study assessing the safety and immunogenicity of a *Pseudomonas aeruginosa* hybrid outer membrane protein OprF/I vaccine (IC43) in healthy volunteers. *Hum. Vaccin. Immunother.* **10,** 170–83 (2014).

194. Ding, B., von Specht, B.-U. & Li, Y. OprF/I-vaccinated sera inhibit binding of human interferon-gamma to *Pseudomonas aeruginosa*. *Vaccine* **28,** 4119–22 (2010).

195. Döring, G., Meisner, C. & Stern, M. A double-blind randomized placebo-controlled phase III study of a *Pseudomonas aeruginosa* flagella vaccine in cystic fibrosis patients. *Proc. Natl. Acad. Sci. U. S. A.* **104,** 11020–5 (2007).

196. Arora, S. K., Ritchings, B. W., Almira, E. C., Lory, S. & Ramphal, R. The *Pseudomonas aeruginosa* flagellar cap protein, FliD, is responsible for mucin adhesion. *Infect. Immun.* **66,** 1000–7 (1998).

197. Cobb, L. M., Mychaleckyj, J. C., Wozniak, D. J. & López-Boado, Y. S. *Pseudomonas aeruginosa* flagellin and alginate elicit very distinct gene expression patterns in airway epithelial cells: implications for cystic fibrosis disease. *J. Immunol.* **173,** 5659–70 (2004).

198. Ramphal, R., Guay, C. & Pier, G. B. *Pseudomonas aeruginosa* adhesins for tracheobronchial mucin. *Infect. Immun.* **55,** 600–3 (1987).

199. Döring, G. & Pier, G. B. Vaccines and immunotherapy against *Pseudomonas aeruginosa*. *Vaccine* **26,** 1011–24 (2008).

200. Campodónico, V. L., Llosa, N. J., Bentancor, L. V, Maira-Litran, T. & Pier, G. B. Efficacy of a conjugate vaccine containing polymannuronic acid and flagellin against experimental *Pseudomonas aeruginosa* lung infection in mice. *Infect. Immun.* **79,** 3455–64 (2011).

201. Castric, P. A. & Deal, C. D. Differentiation of *Pseudomonas aeruginosa* pili based on sequence and B-cell epitope analyses. *Infect. Immun.* **62,** 371–6 (1994).

202. Kus, J. V, Tullis, E., Cvitkovitch, D. G. & Burrows, L. L. Significant differences in type IV pilin allele distribution among *Pseudomonas aeruginosa* isolates from cystic fibrosis (CF) versus non-CF patients. *Microbiology* **150,** 1315–26 (2004).

203. Sawa, T. *et al.* Active and passive immunization with the Pseudomonas V antigen protects against type III intoxication and lung injury. *Nat. Med.* **5,** 392–8 (1999).

204. Holder, I. A., Neely, A. N. & Frank, D. W. PcrV immunization enhances survival of burned *Pseudomonas aeruginosa*-infected mice. *Infect. Immun.* **69,** 5908–10 (2001).

205. Markham, A. P. *et al.* Formulation and immunogenicity of a potential multivalent type III secretion system-based protein vaccine. *J. Pharm. Sci.* **99,** 4497–509 (2010).

206. Chen, T. Y. *et al.* A nontoxic Pseudomonas exotoxin A induces active immunity and passive protective antibody against Pseudomonas exotoxin A intoxication. *J. Biomed.*

Sci. **6,** 357–63

207. Denis-Mize, K. S., Price, B. M., Baker, N. R. & Galloway, D. R. Analysis of immunization with DNA encoding *Pseudomonas aeruginosa* exotoxin A. *FEMS Immunol. Med. Microbiol.* **27,** 147–54 (2000).

208. Shiau, J. W. *et al.* Mice immunized with DNA encoding a modified *Pseudomonas aeruginosa* exotoxin A develop protective immunity against exotoxin intoxication. *Vaccine* **19,** 1106–12 (2000).

209. Döring, G. *et al. In vivo* activity of proteases of *Pseudomonas aeruginosa* in a rat model. *J. Infect. Dis.* **149,** 532–7 (1984).

210. Fick, R. B., Baltimore, R. S., Squier, S. U. & Reynolds, H. Y. IgG proteolytic activity of *Pseudomonas aeruginosa* in cystic fibrosis. *J. Infect. Dis.* **151,** 589–98 (1985).

211. Parmely, M., Gale, A., Clabaugh, M., Horvat, R. & Zhou, W. W. Proteolytic inactivation of cytokines by *Pseudomonas aeruginosa*. *Infect. Immun.* **58,** 3009–14 (1990).

212. Horvat, R. T. & Parmely, M. J. *Pseudomonas aeruginosa* alkaline protease degrades human gamma interferon and inhibits its bioactivity. *Infect. Immun.* **56,** 2925–32 (1988).

213. Kharazmi, A., Eriksen, H. O., Döring, G., Goldstein, W. & Høiby, N. Effect of *Pseudomonas aeruginosa* proteases on human leukocyte phagocytosis and bactericidal activity. *Acta Pathol. Microbiol. Immunol. Scand. C.* **94,** 175–9 (1986).

214. Theander, T. G. *et al.* Inhibition of human lymphocyte proliferation and cleavage of interleukin-2 by *Pseudomonas aeruginosa* proteases. *Infect. Immun.* **56,** 1673–7 (1988).

215. Pedersen, B. K. & Kharazmi, A. Inhibition of human natural killer cell activity by *Pseudomonas aeruginosa* alkaline protease and elastase. *Infect. Immun.* **55,** 986–9 (1987).

216. Homma, J. Y. *et al.* Effectiveness of immunization with single and multi-component vaccines prepared from a common antigen (OEP), protease and elastase toxoids of *Pseudomonas aeruginosa* on protection against hemorrhagic pneumonia in mink due to *P. aeruginosa*. *Jpn. J. Exp. Med.* **48,** 111–33 (1978).

217. Hirao, Y. & Homma, J. Y. Therapeutic effect of immunization with OEP, protease toxoid and elastase toxoid on corneal ulcers in mice due to *Pseudomonas aeruginosa* infection. *Jpn. J. Exp. Med.* **48,** 41–51 (1978).

218. Kawaharajo, K. & Homma, J. Y. Effects of elastase, protease and common antigen (OEP) from *Pseudomonas aeruginosa* on protection against burns in mice. *Jpn. J. Exp. Med.* **47,** 495–500 (1977).

219. Matsumoto, T. *et al.* Efficacies of alkaline protease, elastase and exotoxin A toxoid vaccines against gut-derived *Pseudomonas aeruginosa* sepsis in mice. *J. Med. Microbiol.* **47,** 303–8 (1998).

220. Priebe, G. P. & Goldberg, J. B. Vaccines for *Pseudomonas aeruginosa*: a long and winding road. *Expert Rev. Vaccines* **13,** 507–19 (2014).

221. Sharma, A., Krause, A. & Worgall, S. Recent developments for Pseudomonas vaccines. *Hum. Vaccin.* **7,** 999–1011 (2011).

222. DiGiandomenico, A. *et al.* A multifunctional bispecific antibody protects against *Pseudomonas aeruginosa*. *Sci. Transl. Med.* **6,** 262ra155 (2014).

223. Cohen, M. L. *Staphylococcus aureus*: biology, mechanisms of virulence, epidemiology. *J. Pediatr.* **108,** 796–9 (1986).

224. Klevens, R. M., Edwards, J. R. & Gaynes, R. P. The impact of antimicrobial-resistant, health care-associated infections on mortality in the United States. *Clin. Infect. Dis.* **47,** 927–30 (2008).

225. Klevens, R. M. *et al.* Invasive methicillin-resistant *Staphylococcus aureus* infections in the United States. *JAMA* **298,** 1763–71 (2007).

226. Forstner, C. *et al.* Predictors of clinical and microbiological treatment failure in patients with methicillin-resistant *Staphylococcus aureus* (MRSA) bacteraemia: a retrospective cohort study in a region with low MRSA prevalence. *Clin. Microbiol. Infect.* **19,** E291–7 (2013).

227. Peyrani, P. *et al.* Severity of disease and clinical outcomes in patients with hospital-acquired pneumonia due to methicillin-resistant *Staphylococcus aureus* strains not influenced by the presence of the Panton-Valentine leukocidin gene. *Clin. Infect. Dis.* **53,** 766–71 (2011).

228. de Kraker, M. E. A., Davey, P. G. & Grundmann, H. Mortality and hospital stay associated with resistant *Staphylococcus aureus* and *Escherichia coli* bacteremia: estimating the burden of antibiotic resistance in Europe. *PLoS Med.* **8,** e1001104 (2011).

229. Lambert, M.-L. *et al.* Clinical outcomes of health-care-associated infections and antimicrobial resistance in patients admitted to European intensive-care units: a cohort study. *Lancet. Infect. Dis.* **11,** 30–8 (2011).

230. Fowler, V. G. *et al.* Effect of an investigational vaccine for preventing *Staphylococcus aureus* infections after cardiothoracic surgery: a randomized trial. *JAMA* **309,** 1368–78 (2013).

231. Koch, K., Nørgaard, M., Schønheyder, H. C., Thomsen, R. W. & Søgaard, M. Effect of socioeconomic status on mortality after bacteremia in working-age patients. A Danish population-based cohort study. *PLoS One* **8,** e70082 (2013).

232. Jung, W. J. *et al.* Prediction of methicillin-resistant *Staphylococcus* aureus in patients with non-nosocomial pneumonia. *BMC Infect. Dis.* **13,** 370 (2013).

233. Su, C.-H. *et al.* Excess mortality and long-term disability from healthcare-associated *staphylococcus aureus* infections: a population-based matched cohort study. *PLoS One* **8,** e71055 (2013).

234. Cosgrove, S. E. *et al.* Comparison of mortality associated with methicillin-resistant and methicillin-susceptible *Staphylococcus aureus* bacteremia: a meta-analysis. *Clin. Infect. Dis.* **36,** 53–9 (2003).

235. David, M. Z. & Daum, R. S. Community-associated methicillin-resistant *Staphylococcus aureus*: epidemiology and clinical consequences of an emerging epidemic. *Clin. Microbiol. Rev.* **23,** 616–87 (2010).

236. Klevens, R. M. *et al.* Invasive methicillin-resistant *Staphylococcus aureus* infections in the United States. *JAMA* **298,** 1763–71 (2007).

237. Botelho-Nevers, E. *et al.* Staphylococcal vaccine development: review of past failures and plea for a future evaluation of vaccine efficacy not only on staphylococcal infections but also on mucosal carriage. *Expert Rev. Vaccines* **12,** 1249–59 (2013).

238. Wertheim, H. F. L. *et al.* The role of nasal carriage in *Staphylococcus aureus* infections. *Lancet. Infect. Dis.* **5,** 751–62 (2005).

239. Liu, G. Y. Molecular pathogenesis of *Staphylococcus aureus* infection. *Pediatr. Res.* **65,** 71R–77R (2009).

240. Kim, H. K., Thammavongsa, V., Schneewind, O. & Missiakas, D. Recurrent infections and immune evasion strategies of *Staphylococcus aureus*. *Curr. Opin. Microbiol.* **15,** 92–9 (2012).

241. Jönsson, K., Signäs, C., Müller, H. P. & Lindberg, M. Two different genes encode fibronectin binding proteins in *Staphylococcus aureus*. The complete nucleotide sequence and characterization of the second gene. *Eur. J. Biochem.* **202,** 1041–8 (1991).

242. Massey, R. C. *et al.* Fibronectin-binding protein A of *Staphylococcus aureus* has multiple, substituting, binding regions that mediate adherence to fibronectin and invasion of endothelial cells. *Cell. Microbiol.* **3,** 839–51 (2001).

243. McDevitt, D. *et al.* Characterization of the interaction between the *Staphylococcus aureus* clumping factor (ClfA) and fibrinogen. *Eur. J. Biochem.* **247,** 416–24 (1997).

244. Ní Eidhin, D. *et al.* Clumping factor B (ClfB), a new surface-located fibrinogen-binding adhesin of *Staphylococcus aureus*. *Mol. Microbiol.* **30,** 245–57 (1998).

245. Patti, J. M. *et al.* Molecular characterization and expression of a gene encoding a *Staphylococcus aureus* collagen adhesin. *J. Biol. Chem.* **267,** 4766–72 (1992).

246. Wertheim, H. F. L. *et al.* Key role for clumping factor B in *Staphylococcus aureus* nasal colonization of humans. *PLoS Med.* **5,** e17 (2008).

247. Weidenmaier, C. *et al.* Role of teichoic acids in *Staphylococcus aureus* nasal colonization, a major risk factor in nosocomial infections. *Nat. Med.* **10,** 243–5 (2004).

248. Torres, V. J., Pishchany, G., Humayun, M., Schneewind, O. & Skaar, E. P. *Staphylococcus aureus* IsdB is a hemoglobin receptor required for heme iron utilization. *J. Bacteriol.* **188,** 8421–9 (2006).

249. Horsburgh, M. J. *et al.* MntR modulates expression of the PerR regulon and superoxide resistance in *Staphylococcus aureus* through control of manganese uptake. *Mol. Microbiol.* **44,** 1269–86 (2002).

250. Nanra, J. S. *et al.* Capsular polysaccharides are an important immune evasion mechanism for *Staphylococcus aureus*. *Hum. Vaccin. Immunother.* **9,** 480–7 (2013).

251. Hair, P. S., Ward, M. D., Semmes, O. J., Foster, T. J. & Cunnion, K. M. *Staphylococcus aureus* clumping factor A binds to complement regulator factor I and increases factor I cleavage of C3b. *J. Infect. Dis.* **198,** 125–33 (2008).

252. Forsgren, A. & Sjöquist, J. 'Protein A' from *S. aureus*. I. Pseudo-immune reaction with human gamma-globulin. *J. Immunol.* **97,** 822–7 (1966).

253. Foster, T. J. Immune evasion by staphylococci. *Nat. Rev. Microbiol.* **3,** 948–58 (2005).

254. Smith, E. J., Visai, L., Kerrigan, S. W., Speziale, P. & Foster, T. J. The Sbi protein is a multifunctional immune evasion factor of *Staphylococcus aureus*. *Infect. Immun.* **79,** 3801–9 (2011).

255. Rooijakkers, S. H. M. *et al.* Immune evasion by a staphylococcal complement inhibitor that acts on C3 convertases. *Nat. Immunol.* **6,** 920–7 (2005).

256. Kubica, M. *et al.* A potential new pathway for *Staphylococcus aureus* dissemination: the silent survival of *S. aureus* phagocytosed by human monocyte-derived macrophages. *PLoS One* **3,** e1409 (2008).

257. de Haas, C. J. C. *et al.* Chemotaxis inhibitory protein of *Staphylococcus aureus*, a bacterial antiinflammatory agent. *J. Exp. Med.* **199,** 687–95 (2004).

258. Chavakis, T. *et al. Staphylococcus aureus* extracellular adherence protein serves as anti-inflammatory factor by inhibiting the recruitment of host leukocytes. *Nat. Med.* **8,** 687–93 (2002).

259. Sieprawska-Lupa, M. *et al.* Degradation of human antimicrobial peptide LL-37 by *Staphylococcus aureus*-derived proteinases. *Antimicrob. Agents Chemother.* **48,** 4673–9 (2004).

260. Jin, T. *et al. Staphylococcus aureus* resists human defensins by production of staphylokinase, a novel bacterial evasion mechanism. *J. Immunol.* **172,** 1169–76 (2004).

261. Tomita, T. & Kamio, Y. Molecular biology of the pore-forming cytolysins from *Staphylococcus aureus*, alpha- and gamma-hemolysins and leukocidin. *Biosci. Biotechnol. Biochem.* **61,** 565–72 (1997).

262. Wang, R. *et al.* Identification of novel cytolytic peptides as key virulence determinants for community-associated MRSA. *Nat. Med.* **13,** 1510–4 (2007).

263. Bhakdi, S. & Tranum-Jensen, J. Alpha-toxin of *Staphylococcus aureus*. *Microbiol. Rev.* **55,** 733–51 (1991).

264. Choi, Y. W. *et al.* Interaction of *Staphylococcus aureus* toxin 'superantigens' with human T cells. *Proc. Natl. Acad. Sci. U. S. A.* **86,** 8941–5 (1989).

265. Genestier, A.-L. *et al. Staphylococcus aureus* Panton-Valentine leukocidin directly targets mitochondria and induces Bax-independent apoptosis of human neutrophils.

J. Clin. Invest. **115,** 3117–27 (2005).

266. Lee, L. Y. *et al.* The *Staphylococcus aureus* Map protein is an immunomodulator that interferes with T cell-mediated responses. *J. Clin. Invest.* **110,** 1461–71 (2002).

267. Llewelyn, M. & Cohen, J. Superantigens: microbial agents that corrupt immunity. *Lancet. Infect. Dis.* **2,** 156–62 (2002).

268. Goodyear, C. S. & Silverman, G. J. Staphylococcal toxin induced preferential and prolonged *in vivo* deletion of innate-like B lymphocytes. *Proc. Natl. Acad. Sci. U. S. A.* **101,** 11392–7 (2004).

269. Shinefield, H. *et al.* Use of a *Staphylococcus aureus* conjugate vaccine in patients receiving hemodialysis. *N. Engl. J. Med.* **346,** 491–6 (2002).

270. Weems, J. J. *et al.* Phase II, randomized, double-blind, multicenter study comparing the safety and pharmacokinetics of tefibazumab to placebo for treatment of *Staphylococcus aureus* bacteremia. *Antimicrob. Agents Chemother.* **50,** 2751–5 (2006).

271. Rupp, M. E. *et al.* Phase II, randomized, multicenter, double-blind, placebo-controlled trial of a polyclonal anti-*Staphylococcus aureus* capsular polysaccharide immune globulin in treatment of *Staphylococcus aureus* bacteremia. *Antimicrob. Agents Chemother.* **51,** 4249–54 (2007).

272. Hua, L. *et al.* MEDI4893* Promotes survival and extends the antibiotic treatment window in a *Staphylococcus aureus* immunocompromised pneumonia model. *Antimicrob. Agents Chemother.* **59,** 4526–32 (2015).

273. Benjamin, D. K. *et al.* A blinded, randomized, multicenter study of an intravenous *Staphylococcus aureus* immune globulin. *J. Perinatol.* **26,** 290–5 (2006).

274. DeJonge, M. *et al.* Clinical trial of safety and efficacy of INH-A21 for the prevention of nosocomial staphylococcal bloodstream infection in premature infants. *J. Pediatr.* **151,** 260–5, 265.e1 (2007).

275. Weisman, L. E. *et al.* A randomized study of a monoclonal antibody (pagibaximab) to prevent staphylococcal sepsis. *Pediatrics* **128,** 271–9 (2011).

276. Nethercott, C. *et al.* Molecular characterization of endocarditis-associated *Staphylococcus aureus*. *J. Clin. Microbiol.* **51,** 2131–8 (2013).

277. Peacock, S. J. *et al.* Virulent combinations of adhesin and toxin genes in natural

populations of *Staphylococcus aureus*. *Infect. Immun.* **70,** 4987–96 (2002).

278. Bonventre, P. F. *et al.* Antibody responses to toxic-shock-syndrome (TSS) toxin by patients with TSS and by healthy staphylococcal carriers. *J. Infect. Dis.* **150,** 662–6 (1984).

279. Christensson, B. & Hedström, S. A. Serological response to toxic shock syndrome toxin in *Staphylococcus aureus* infected patients and healthy controls. *Acta Pathol. Microbiol. Immunol. Scand. B.* **93,** 87–90 (1985).

280. Johnson, H. M., Russell, J. K. & Pontzer, C. H. Staphylococcal enterotoxin microbial superantigens. *FASEB J.* **5,** 2706–12 (1991).

281. Novick, R. P. Mobile genetic elements and bacterial toxinoses: the superantigen-encoding pathogenicity islands of *Staphylococcus aureus*. *Plasmid* **49,** 93–105 (2003).

282. Golubchik, T. *et al.* Within-host evolution of *Staphylococcus aureus* during asymptomatic carriage. *PLoS One* **8,** e61319 (2013).

283. Dreisbach, A. *et al.* Profiling the surfacome of *Staphylococcus aureus*. *Proteomics* **10,** 3082–96 (2010).

284. Dreisbach, A. *et al.* Surface shaving as a versatile tool to profile global interactions between human serum proteins and the *Staphylococcus aureus* cell surface. *Proteomics* **11,** 2921–30 (2011).

285. Scully, I. L., Liberator, P. A., Jansen, K. U. & Anderson, A. S. Covering all the bases: preclinical development of an effective *Staphylococcus aureus* vaccine. *Front. Immunol.* **5,** 109 (2014).

286. Fowler, V. G. & Proctor, R. A. Where does a *Staphylococcus aureus* vaccine stand? *Clin. Microbiol. Infect.* **20 Suppl 5,** 66–75 (2014).

287. Brown, A. F., Leech, J. M., Rogers, T. R. & McLoughlin, R. M. *Staphylococcus aureus* colonization: modulation of host immune response and impact on human vaccine design. *Front. Immunol.* **4,** 507 (2014).

288. Proctor, R. A. Challenges for a universal *Staphylococcus aureus* vaccine. *Clin. Infect. Dis.* **54,** 1179–86 (2012).

289. Bagnoli, F., Bertholet, S. & Grandi, G. Inferring reasons for the failure of *Staphylococcus aureus* vaccines in clinical trials. *Front. Cell. Infect. Microbiol.* **2,** 16

(2012).

290. Daum, R. S. & Spellberg, B. Progress toward a *Staphylococcus aureus* vaccine. *Clin. Infect. Dis.* **54,** 560–7 (2012).

291. Avery, T. R., Kleinman, K. P., Klompas, M., Aschengrau, A. & Huang, S. S. Inclusion of 30-day postdischarge detection triples the incidence of hospital-onset methicillin-resistant *Staphylococcus aureus*. *Infect. Control Hosp. Epidemiol.* **33,** 114–21 (2012).

292. Huang, S. S. & Platt, R. Risk of methicillin-resistant *Staphylococcus aureus* infection after previous infection or colonization. *Clin. Infect. Dis.* **36,** 281–5 (2003).

293. Duffy, J. *et al.* Community-onset invasive methicillin-resistant *Staphylococcus aureus* infections following hospital discharge. *Am. J. Infect. Control* **41,** 782–6 (2013).

294. Skurnik, D. *et al.* Natural antibodies in normal human serum inhibit *Staphylococcus aureus* capsular polysaccharide vaccine efficacy. *Clin. Infect. Dis.* **55,** 1188–97 (2012).

295. Skurnik, D. *et al.* Animal and human antibodies to distinct *Staphylococcus aureus* antigens mutually neutralize opsonic killing and protection in mice. *J. Clin. Invest.* **120,** 3220–33 (2010).

296. Kim, H. K., Cheng, A. G., Kim, H.-Y., Missiakas, D. M. & Schneewind, O. Nontoxigenic protein A vaccine for methicillin-resistant *Staphylococcus aureus* infections in mice. *J. Exp. Med.* **207,** 1863–70 (2010).

297. Kim, H. K., Thammavongsa, V., Schneewind, O. & Missiakas, D. Recurrent infections and immune evasion strategies of *Staphylococcus aureus*. *Curr. Opin. Microbiol.* **15,** 92–9 (2012).

298. Salgado-Pabón, W. & Schlievert, P. M. Models matter: the search for an effective *Staphylococcus aureus* vaccine. *Nat. Rev. Microbiol.* **12,** 585–91 (2014).

299. Weisman, L. E. *et al.* Phase 1/2 double-blind, placebo-controlled, dose escalation, safety, and pharmacokinetic study of pagibaximab (BSYX-A110), an antistaphylococcal monoclonal antibody for the prevention of staphylococcal bloodstream infections, in very-low-birth-weight neon. *Antimicrob. Agents Chemother.* **53,** 2879–86 (2009).

300. Shinefield, H. R. Use of a conjugate polysaccharide vaccine in the prevention of invasive staphylococcal disease: is an additional vaccine needed or possible? *Vaccine* **24 Suppl 2,** S2–65–9 (2006).

301. Vernachio, J. *et al.* Anti-clumping factor A immunoglobulin reduces the duration of methicillin-resistant *Staphylococcus aureus* bacteremia in an experimental model of infective endocarditis. *Antimicrob. Agents Chemother.* **47,** 3400–6 (2003).

302. Josefsson, E., Hartford, O., O'Brien, L., Patti, J. M. & Foster, T. Protection against experimental *Staphylococcus aureus* arthritis by vaccination with clumping factor A, a novel virulence determinant. *J. Infect. Dis.* **184,** 1572–80 (2001).

303. Fattom, A. I., Sarwar, J., Ortiz, A. & Naso, R. A *Staphylococcus aureus* capsular polysaccharide (CP) vaccine and CP-specific antibodies protect mice against bacterial challenge. *Infect. Immun.* **64,** 1659–65 (1996).

304. Joshi, A. *et al.* Immunization with *Staphylococcus aureus* iron regulated surface determinant B (IsdB) confers protection via Th17/IL17 pathway in a murine sepsis model. *Hum. Vaccin. Immunother.* **8,** 336–46 (2012).

305. Kim, H. K. *et al.* IsdA and IsdB antibodies protect mice against *Staphylococcus aureus* abscess formation and lethal challenge. *Vaccine* **28,** 6382–92 (2010).

306. Hall, A. E. *et al.* Characterization of a protective monoclonal antibody recognizing *Staphylococcus aureus* MSCRAMM protein clumping factor A. *Infect. Immun.* **71,** 6864–70 (2003).

307. Pier, G. B. Will there ever be a universal *Staphylococcus aureus* vaccine? *Hum. Vaccin. Immunother*. **9,** 1865–76 (2013).

308. van Heijenoort, J. Formation of the glycan chains in the synthesis of bacterial peptidoglycan. *Glycobiology* **11,** 25R–36R (2001).

309. Hoffmann, B., Messer, W. & Schwarz, U. Regulation of polar cap formation in the life cycle of *Escherichia coli*. *J. Supramol. Struct.* **1,** 29–37 (1972).

310. Doublet, P., van Heijenoort, J. & Mengin-Lecreulx, D. Identification of the *Escherichia coli* murI gene, which is required for the biosynthesis of D-glutamic acid, a specific component of bacterial peptidoglycan. *J. Bacteriol.* **174,** 5772–9 (1992).

311. Doublet, P., van Heijenoort, J., Bohin, J. P. & Mengin-Lecreulx, D. The murI gene of *Escherichia coli* is an essential gene that encodes a glutamate racemase activity. *J. Bacteriol.* **175,** 2970–9 (1993).

312. Dougherty, T. J., Thanassi, J. A. & Pucci, M. J. The *Escherichia coli* mutant requiring D-glutamic acid is the result of mutations in two distinct genetic loci. *J. Bacteriol.* **175,** 111–6 (1993).

313. Fotheringham, I. G., Bledig, S. A. & Taylor, P. P. Characterization of the genes encoding D-amino acid transaminase and glutamate racemase, two D-glutamate biosynthetic enzymes of *Bacillus sphaericus* ATCC 10208. *J. Bacteriol.* **180,** 4319–23 (1998).

314. Tanizawa, K., Masu, Y., Asano, S., Tanaka, H. & Soda, K. Thermostable D-amino acid aminotransferase from a thermophilic Bacillus species. Purification, characterization, and active site sequence determination. *J. Biol. Chem.* **264,** 2445–9 (1989).

315. Taylor, P. P. & Fotheringham, I. G. Nucleotide sequence of the *Bacillus licheniformis* ATCC 10716 dat gene and comparison of the predicted amino acid sequence with those of other bacterial species. *Biochim. Biophys. Acta* **1350,** 38–40 (1997).

316. Pucci, M. J., Thanassi, J. A., Ho, H. T., Falk, P. J. & Dougherty, T. J. *Staphylococcus haemolyticus* contains two D-glutamic acid biosynthetic activities, a glutamate racemase and a D-amino acid transaminase. *J. Bacteriol.* **177,** 336–42 (1995).

317. Thompson, R. J., Bouwer, H. G., Portnoy, D. A. & Frankel, F. R. Pathogenicity and immunogenicity of a *Listeria monocytogenes* strain that requires D-alanine for growth. *Infect. Immun.* **66,** 3552–61 (1998).

318. Bae, T. *et al. Staphylococcus aureus* virulence genes identified by bursa aurealis mutagenesis and nematode killing. *Proc. Natl. Acad. Sci. U. S. A.* **101,** 12312–7 (2004).

319. Kada, S., Nanamiya, H., Kawamura, F. & Horinouchi, S. Glr, a glutamate racemase, supplies D-glutamate to both peptidoglycan synthesis and poly-gamma-glutamate production in gamma-PGA-producing *Bacillus subtilis*. *FEMS Microbiol. Lett.* **236,** 13–20 (2004).

320. Kimura, K., Tran, L.-S. P. & Itoh, Y. Roles and regulation of the glutamate racemase isogenes, racE and yrpC, in *Bacillus subtilis*. *Microbiology* **150,** 2911–20 (2004).

321. Song, J.-H. *et al.* Identification of essential genes in *Streptococcus pneumoniae* by allelic replacement mutagenesis. *Mol. Cells* **19,** 365–74 (2005).

322. Fisher, S. L. Glutamate racemase as a target for drug discovery. *Microb. Biotechnol.* **1,** 345–60 (2008).

323. Oh, S.-Y., Richter, S. G., Missiakas, D. M. & Schneewind, O. Glutamate racemase mutants of *Bacillus anthracis*. *J. Bacteriol.* **197,** 1854–61 (2015).

324. Vergara-Irigaray, M. *et al.* Relevant role of fibronectin-binding proteins in *Staphylococcus aureus* biofilm-associated foreign-body infections. *Infect. Immun.* **77,**

3978–91 (2009).

325. Acosta, J. *et al.* Multidrug-resistant *Acinetobacter baumannii* harboring OXA-24 carbapenemase, Spain. *Emerg. Infect. Dis.* **17,** 1064–67 (2011).

326. Russo, T. a. *et al.* The K1 capsular polysaccharide of *Acinetobacter baumannii* strain 307-0294 is a major virulence factor. *Infect. Immun.* **78,** 3993–4000 (2010).

327. Lee, D. G. *et al.* Genomic analysis reveals that *Pseudomonas aeruginosa* virulence is combinatorial. *Genome Biol.* **7,** R90 (2006).

328. Viedma, E., Juan, C., Otero, J. R., Oliver, A. & Chaves, F. Draft genome sequence of VIM-2-producing multidrug-resistant *Pseudomonas aeruginosa* ST175, an epidemic high-risk clone. *Genome Announc.* **1,** e0011213

329. Tomás, M. *et al.* Efflux pumps, OprD porin, AmpC β-lactamase, and multiresistance in *Pseudomonas aeruginosa* isolates from cystic fibrosis patients. *Antimicrob. Agents Chemother.* **54,** 2219–24 (2010).

330. Salunkhe, P. *et al.* A Cystic Fibrosis Epidemic Strain of. *J. Bacteriol.* **187,** 4908–20 (2005).

331. Simon, R., Priefer, U. & Pühler, A. A broad host range mobilization system for *in vivo* genetic engineering: transposon mutagenesis in Gram negative bacteria. *Bio/Technology* **1,** 784–91 (1983).

332. Sambrook, J., Fritsch, E. F. & Maniatis, T. *Molecular cloning: a laboratory manual, 2nd ed.* (Cold Spring Harbor Laboratory Press, Cold Spring Harbor, N.Y., 1989).

333. Monk, I. R., Shah, I. M., Xu, M., Tan, M.-W. & Foster, T. J. Transforming the untransformable: application of direct transformation to manipulate genetically *Staphylococcus aureus* and *Staphylococcus epidermidis*. *MBio* **3,** (2012).

334. Kreiswirth, B. N. *et al.* The toxic shock syndrome exotoxin structural gene is not detectably transmitted by a prophage. *Nature* **305,** 709–12

335. Diep, B. A. *et al.* Complete genome sequence of USA300, an epidemic clone of community-acquired meticillin-resistant *Staphylococcus aureus*. *Lancet (London, England)* **367,** 731–9 (2006).

336. Fitzgerald, J. R. *et al.* Characterization of a putative pathogenicity island from bovine *Staphylococcus aureus* encoding multiple superantigens. *J. Bacteriol.* **183,** 63–70 (2001).

337. Ben Zakour, N. L. *et al.* Genome-wide analysis of ruminant *Staphylococcus aureus* reveals diversification of the core genome. *J. Bacteriol.* **190,** 6302–17 (2008).

338. Lowder, B. V *et al.* Recent human-to-poultry host jump, adaptation, and pandemic spread of *Staphylococcus aureus*. *Proc. Natl. Acad. Sci. U. S. A.* **106,** 19545–50 (2009).

339. Hamad, M. A., Zajdowicz, S. L., Holmes, R. K. & Voskuil, M. I. An allelic exchange system for compliant genetic manipulation of the select agents *Burkholderia pseudomallei* and *Burkholderia mallei*. *Gene* **430,** 123–31 (2009).

340. Hoang, T. T., Karkhoff-Schweizer, R. R., Kutchma, A. J. & Schweizer, H. P. A broad-host-range F1p-FRT recombination system for site-specific excision of chromosomally-located DNA sequences: Application for isolation of unmarked *Pseudomonas aeruginosa* mutants. *Gene* **212,** 77–86 (1998).

341. Arnaud, M., Chastanet, A. & De, M. New vector for efficient allelic replacement in naturally Gram-positive bacteria. *Appl. Enviromental Microbiol.* **70,** 6887–91 (2004).

342. Shimizu, S. *The Laboratory Mouse* (Elsevier Ltd, 2004).

343. Smith, M. G. *et al.* New insights into *Acinetobacter baumannii* pathogenesis revealed by high-density pyrosequencing and transposon mutagenesis. *Genes Dev.* **21,** 601–14 (2007).

344. Stover, C. K. *et al.* Complete genome sequence of *Pseudomonas aeruginosa* PAO1, an opportunistic pathogen. *Nature* **406,** 959–64 (2000).

345. Lefeber, D. J. *et al.* Th1-directing adjuvants increase the immunogenicity of oligosaccharide-protein conjugate vaccines related to *Streptococcus pneumoniae* type 3. *Infect. Immun.* **71,** 6915–20 (2003).

346. Pritt, B., O'Brien, L. & Winn, W. Mucoid Pseudomonas in cystic fibrosis. *Am. J. Clin. Pathol.* **128,** 32–34 (2007).

347. Mills, C. D., Kincaid, K., Alt, J. M., Heilman, M. J. & Hill, a M. M-1/M-2 macrophages and the Th1/Th2 paradigm. *J. Immunol.* **164,** 6166–73 (2000).

348. Curtiss, R. Bacterial infectious disease control by vaccine development. *J. Clin. Invest.* **110,** 1061–66 (2002).

349. Cabral, M. P. *et al.* Proteomic and functional analyses reveal a unique lifestyle for *Acinetobacter baumannii* biofilms and a key role for histidine metabolism. *J. Proteome Res.* **10,** 3399–417 (2011).

350. Miyoshi, Y., Oyama, T., Itoh, Y. & Hamase, K. Enantioselective two-dimensional high-performance liquid chromatographic determination of amino acids ; analysis and physiological significance of D-amino acids in mammals. *Chromatography* **35,** 49–57 (2014).

351. Han, H. *et al.* Simultaneous determination of D-aspartic acid and D-glutamic acid in rat tissues and physiological fluids using a multi-loop two-dimensional HPLC procedure. *J. Chromatogr. B Analyt. Technol. Biomed. Life Sci.* **879,** 3196-202 (2011).

352. Vila, J., Martí, S. & Sánchez-Céspedes, J. Porins, efflux pumps and multidrug resistance in *Acinetobacter baumannii*. *J. Antimicrob. Chemother.* **59,** 1210–5 (2007).

353. García, A. *et al.* Some immunological properties of lipopolysaccharide from *Acinetobacter baumannii*. *J. Med. Microbiol.* **48,** 479–83 (1999).

354. Breslow, J. M. *et al.* Innate immune responses to systemic *Acinetobacter baumannii* infection in mice: neutrophils, but not interleukin-17, mediate host resistance. *Infect. Immun.* **79,** 3317–27 (2011).

355. Kim, S. W. *et al.* Serum resistance of *Acinetobacter baumannii* through the binding of factor H to outer membrane proteins. *FEMS Microbiol. Lett.* **301,** 224–31 (2009).

356. García, A., Solar, H., González, C. & Zemelman, R. Effect of EDTA on the resistance of clinical isolates of *Acinetobacter baumannii* to the bactericidal activity of normal human serum. *J. Med. Microbiol.* **49,** 1047–50 (2000).

357. Russo, T. A. *et al.* Penicillin-binding protein 7/8 contributes to the survival of *Acinetobacter baumannii in vitro* and *in vivo*. *J. Infect. Dis.* **199,** 513–21 (2009).

358. Govan, J. R. & Deretic, V. Microbial pathogenesis in cystic fibrosis: mucoid *Pseudomonas aeruginosa* and *Burkholderia cepacia*. *Microbiol. Rev.* **60,** 539–74 (1996).

359. Li, Z. *et al.* Longitudinal development of mucoid *Pseudomonas aeruginosa* infection and lung disease progression in children with cystic fibrosis. *JAMA* **293,** 581–8 (2005).

360. Rodríguez-Rojas, A., Oliver, A. & Blázquez, J. Intrinsic and environmental mutagenesis drive diversification and persistence of *Pseudomonas aeruginosa* in chronic lung infections. *J. Infect. Dis.* **205,** 121–7 (2012).

361. Tenover, F. C. Mechanisms of antimicrobial resistance in bacteria. *Am. J. Infect. Control* **34,** S3–10; discussion S64–73 (2006).

362. Dunkley, M. L., Clancy, R. L. & Cripps, A. W. A role for CD4+ T cells from orally immunized rats in enhanced clearance of *Pseudomonas aeruginosa* from the lung. *Immunology* **83,** 362–9 (1994).

363. Dunkley, M. L., Cripps, A. W., Reinbott, P. W. & Clancy, R. L. Immunity to respiratory *Pseudomonas aeruginosa* infection: the role of gut-derived T helper cells and immune serum. *Adv. Exp. Med. Biol.* **371B,** 771–5 (1995).

364. Stevenson, M. M., Kondratieva, T. K., Apt, A. S., Tam, M. F. & Skamene, E. *In vitro* and *in vivo* T cell responses in mice during bronchopulmonary infection with mucoid *Pseudomonas aeruginosa*. *Clin. Exp. Immunol.* **99,** 98–105 (1995).

365. Jain-Vora, S. *et al.* Interleukin-4 enhances pulmonary clearance of *Pseudomonas aeruginosa*. *Infect. Immun.* **66,** 4229–36 (1998).

366. Jensen, P. Ø., Givskov, M., Bjarnsholt, T. & Moser, C. The immune system vs. *Pseudomonas aeruginosa* biofilms. *FEMS Immunol. Med. Microbiol.* **59,** 292–305 (2010).

367. Moser, C. *et al.* The immune response to chronic *Pseudomonas aeruginosa* lung infection in cystic fibrosis patients is predominantly of the Th2 type. *APMIS* **108,** 329–35 (2000).

368. Liu, J. *et al.* Early production of IL-17 protects against acute pulmonary *Pseudomonas aeruginosa* infection in mice. *FEMS Immunol. Med. Microbiol.* **61,** 179–88 (2011).

369. Lee, J. C. The prospects for developing a vaccine against *Staphylococcus aureus*. *Trends Microbiol.* **4,** 162–6 (1996).

370. Schaffer, A. C. & Lee, J. C. Vaccination and passive immunisation against *Staphylococcus aureus*. *Int. J. Antimicrob. Agents* **32 Suppl 1,** S71–8 (2008).

371. Lin, L. *et al.* Th1-Th17 cells mediate protective adaptive immunity against *Staphylococcus aureus* and *Candida albicans* infection in mice. *PLoS Pathog.* **5,** (2009).

372. Zhao, Y. X., Nilsson, I. M. & Tarkowski, A. The dual role of interferon-gamma in experimental *Staphylococcus aureus* septicaemia versus arthritis. *Immunology* **93,** 80–5 (1998).

373. Pishchany, G. *et al.* Specificity for human hemoglobin enhances *Staphylococcus aureus* infection. *Cell Host Microbe* **8,** 544–50 (2010).

374. Veloso, T. R. *et al.* Use of a human-like low-grade bacteremia model of experimental endocarditis to study the role of *Staphylococcus aureus* adhesins and platelet aggregation in early endocarditis. *Infect. Immun.* **81,** 697–703 (2013).

ATTACHMENTS

A. Resumo

Las vacunas bacterianas vivas son muy eficaces debido a que se tratan de versiones atenuadas de bacterias patógenas que “mimetizan” la infección real pero sin causar la enfermedad. Estas vacunas inducen respuestas inmunitarias de tipo humoral y celular y su empleo suele resultar en una profilaxis muy eficiente, sin necesidad de refuerzos. Vienen siendo utilizadas desde hace muchas décadas para prevenir enfermedades respiratorias, entéricas y con carácter epidémico, tanto en humanos como en animales. Además, suelen ser vacunas de bajo coste de producción y distribución. Para lograr la atenuación de la virulencia bacteriana se realizan pases sucesivos en cultivo hasta obtener una selección natural de microorganismos atenuados, se realiza una mutagenesis aleatoria o, más recientemente, se recurre directamente a la manipulación genética de genes asociados a mecanismos de virulencia. Sin embargo, la utilización de organismos vivos atenuados en vacunas no es libre de riesgos, ya que estos microrganismos mantienen su capacidad de multiplicación en el individuo vacunado y pueden ser liberados en el ambiente accidentalmente. Con lo cual, una vacuna ideal debería contener preferentemente todos los determinantes antigénicos para mantener su capacidad inmunológica intacta, pero sin conllevar a un riesgo de enfermedad. La alternativa que proponemos es la utilización de organismos genéticamente modificados incapaces de sintetizar peptidoglicano, cuya función es esencial para la supervivencia bacteriana ya que es el principal componente de la pared celular. Estos microorganismos genéticamente modificados se ven afectados en la correcta formación de pared bacteriana en el individuo vacunado, de tal forma que no pueden replicarse, minimizando cualquier riesgo de reacción adversa y permitiendo la presentación de todos sus determinantes antigénicos.

El compuesto D-glutamato (D-Glu) es un componente esencial del peptidoglicano de la pared bacteriana. La enzima glutamato racemasa (MurI) es la responsable de transformar L-glutamato en D-Glu, que es enseguida introducido en el peptidoglicano. Aunque varios estudios señalan esta enzima como una diana para nuevos antibióticos, ninguno de los trabajos publicados hasta la fecha demuestra la posibilidad de utilizar mutantes defectivos $MurI^{-}$ como vacunas bacterianas vivas atenuadas, y la evaluación de su eficacia en modelos animales. Estos microorganismos genéticamente modificados, auxótrofos para el compuesto D-Glu, pueden obtenerse mediante la inactivación de los genes codificantes de la enzima MurI y de la enzima D-aminoacido trasaminasa (Dat),

cuando corresponda, responsable por la transformación de la D-alanina en D-Glu, exclusivamente en algunas bacterias Gram-positivas.

Aunque los D-aminoacidos vienen siendo últimamente reconocidos como moléculas funcionales en los mamíferos, estos compuestos suelen presentarse en concentraciones extremadamente bajas, entre los 1.9 y 9.0 nmol/g.

Por otra parte, la emergencia de bacterias multirresistentes tales como *Acinetobacter baumannii*, *Pseudomonas aeruginosa, Staphylococcus aureus* resistente a meticilina (SARM) y la inexistencia de vacunas licenciadas para prevenir las infecciones causadas por estos patógenos resultan en elevados índices de mortalidad y opciones de tratamiento muy limitadas, especialmente en el caso de infecciones causadas por organismos Gram-negativos. Como respuesta a este desafío, recurrimos a la manipulación genética de estas bacterias para obtener cepas auxótrofas para D-Glu, a través de la creación de mutantes con los genes codificantes de MurI o MurI y Dat deleccionados, en las cepas *A. baumannii* ATCC 17978, *P. aeruginosa* PAO1 y *S. aureus* 132. Una vez obtenidas, se evaluó la utilización de estas cepas como vacunas en un modelo de infección aguda letal aguda en ratón.

En el genoma de *A. baumannii* ATCC 17978 se identificaron dos genes MurI: A1S_0380 (*murI1*) y A1S_3398 (*murI2*). En el genoma de *P. aeruginosa* PAO1 encontramos un único gen MurI: PA4662 (*murI*). En el genoma de *S. aureus* se identificó un gen MurI (*murI*) y un gen Dat (*dat*). Una vez identificados, recurrimos a la mutación de estos genes por delección total. Se observó un crecimiento normal en medio de cultivo LB de los mutantes *A. baumannii* ATCC 17978 Δ*murI1* y *A. baumannii* ATCC 17978 Δ*murI2*; sin embargo se observó que el mutante doble *A. baumannii* ATCC 17978 Δ*murI1* Δ*murI2* requiere la adicción exógena de D-Glu para crecer. Igualmente, el mutante *P. aeruginosa* PAO1 Δ*murI* requiere también la adicción de este compuesto para su crecimiento. Respecto a *S. aureus*, se observó un crecimiento normal de los mutantes 132 Δ*murI* y 132 Δ*dat*; sin embargo el mutante doble *S. aureus* 132 Δ*murI* Δ*dat* requiere la adicción exógena de este compuesto. Mediante qRT-PCR se confirmó la ausencia del mRNA codificante para MurI y Dat en estas cepas mutantes. Estos resultados demuestran la implicación de los genes *murI* en la producción de D-Glu en *A. baumannii* ATCC 17978 y *P. aeruginosa* PAO1, pero también la implicación conjunta de los genes *murI* y *dat* en el caso de la cepa *S. aureus* 132. Esto significa que se pueden obtener microorganismos auxótrofos para D-Glu en el caso de bacterias que no poseen la enzima Dat, mediante la inactivación de uno o de múltiples

genes *murI* (mutantes MurI$^-$), como es el caso de *P. aeruginosa* PAO1 y *A. baumannii* ATCC 17978, respectivamente. En el caso de bacterias que poseen la enzima Dat, como *S. aureus* 132, es necesaria la inactivación conjunta de genes *murI* y *dat* (mutantes MurI$^-$ Dat$^-$).

Para evaluar los efectos de la ausencia de D-Glu en el crecimiento bacteriano de las cepas de *A. baumannii* ATCC 17978, *P. aeruginosa* PAO1 y *S. aureus* 132 salvajes, y sus mutantes derivados, se cultivaron las bacterias en medio suplementado con diferentes concentraciones de D-Glu y se evaluaron las morfologías correspondientes por microscopia electrónica de barrido (SEM). Se observó una crecimiento sucesivamente menos evidente de las tres cepas mutantes ATCC 17978 Δ*murI1* Δ*murI2*, PAO1 Δ*murI* y 132 Δ*murI* Δ*dat* con concentraciones decrecientes de D-Glu, hasta su cese total. Algunas de las bacterias que se observaron en el medio de cultivo sin D-Glu parecen ser remanentes del inoculo bacteriano previamente crecido con el compuesto. En el medio de cultivo con una concentración de 0.1 mM D-Glu, se observó un crecimiento anormal de las cepas ATCC 17978 Δ*murI1* Δ*murI2* y 132 Δ*murI* Δ*dat.* La cepa ATCC 17978 Δ*murI1* Δ*murI2* presentó agregados filamentosos con tres o más unidades celulares, con una división celular atípica, mientras que la cepa 132 Δ*murI* Δ*dat* presentó largos “clusters” de células irregulares debido a una división celular aberrante. Se detectaron masas de presuntos protoplastos, en las proximidades de células intactas correspondientes a las cepas mutantes. A la concentración de 1.25 mM D-Glu para *A. baumannii* y 1.5 mM D-Glu para *S. aureus* se observó una más elevada densidad celular, respecto a la condición anterior, reflejo de un crecimiento microbiano más abundante, pero con mas estructuras similares a protoplastos. También se observaron más células con un aspecto similar a las células salvajes. Finalmente, a la concentración de 10 ó 20 mM, las cepas mutantes son indistinguibles de las cepas salvajes correspondientes, tanto a nivel de la morfología como de densidad celular.

De igual forma, se procedió a la evaluación de los efectos de la ausencia de D-Glu en la morfología bacteriana utilizando para ello la microscopia de transmisión electrónica (TEM). Mediante esta técnica, observamos que los mutantes ATCC 17978 Δ*murI1* Δ*murI2*, PAO1 Δ*murI* y 132 Δ*murI* Δ*dat* sufren una degeneración progresiva en la ausencia de este compuesto como resultado del bloqueo de la síntesis del peptidoglicano. Se aprecian células con una conformación alterada que pierden su estructura semirrígida, células con varias rupturas y desplazamiento de las membranas, lisis celular y pérdida del contenido intracelular. Por lo tanto, el mecanismo de la lisis en las bacterias auxótrofas para D-Glu se puede resumir de la siguiente forma: primeramente, la inhibición de la formación de pared celular conlleva a que el protoplasma quede recubierto únicamente por la membrana

interna (caso de las bacterias Gram-negativas) o por la única membrana (caso de las bacterias Gram-positivas), dejándolo totalmente expuesto a las variaciones de tonicidad del medio. A continuación, ocurre la lisis celular por presión osmótica, dejándose vestigios de membranas citoplasmáticas que pueden formar agregados, o material intracelular. Estos fenómenos pueden ocurrir secuencialmente u en simultaneo.

Una de las características que hace con que los organismos genéticamente modificados sean especialmente útiles como vacunas es su grado de atenuación de la virulencia. Para testar la hipótesis de que las bacterias auxótrofas para D-Glu están atenuadas, medimos la supervivencia de ratones de la línea BALB/c después de la inyección intraperitoneal de estas cepas mimetizando una infección aguda letal. Con este modelo, pudimos determinar la DL_{100} (mínima dosis letal para el 100% de los ratones) tanto de los mutantes como de las cepas salvajes: *A. baumannii* ATCC 17978, DL_{100} = 2.5X; ATCC 17978 Δ*murI1* Δ*murI2*, DL_{100} = 6X; *P. aeruginosa* PAO1, DL_{100} = 0.4X; PAO1 Δ*murI*, DL_{100} > 40X; *S. aureus* 132, DL_{100} = 1X; 132 Δ*murI* Δ*dat*, DL_{100}>10X. Estos resultados indicaron que las cepas auxótrofas para D-Glu están atenuadas frente a sus homólogos salvajes.

Para evaluar la respuesta humoral generada con las cepas auxótrofas para D-Glu, cuantificamos la producción de anticuerpos en ratones inmunizados con estas cepas por ELISA. Efectivamente, los ratones inmunizados mostraron niveles significativos de las inmunoglobulinas IgM, IgG, IgG1, IgG2a, IgG2b y IgG3 específicos contra *A. baumannii* ATCC 17978, *P. aeruginosa* PAO1 y *S. aureus* 132 Δ*spa* al terminar los calendarios de vacunación. La producción de anticuerpos después de dos administraciones de vacuna fue significativamente superior que después de una sola toma, exceptuando el caso de las inmunoglobulinas IgM inducidas por PAO1 Δ*murI*. IgG1 fue el subtipo de IgG dominante en la respuesta humoral inducida por las tres cepas auxótrofas para D-Glu, consistente con una activación predominante de linfocitos de tipo Th2. Los títulos de IgG2a, IgG2b y IgG3 inducidos en respuesta a 132 Δ*murI* Δ*dat* fueron sustancialmente inferiores que en el caso de *A. baumannii* y *P. aeruginosa*, sin embargo, fueron significativos. Esto indica que las tres cepas mutantes estimulan también la diferenciación de linfocitos de tipo Th1.

Se observaron niveles significativos de IgM y IgG en ratones vacunados con diferentes dosis de las tres cepas mutantes, una vez terminados los calendarios de vacunación. Una dosis 0.05X de ATCC 17978 Δ*murI1* Δ*murI2* fue suficiente para estimular significativamente las inmunoglobulinas de los subtipos IgG1, IgG2a, IgG2b y IgG3. Los títulos más elevados de IgG se obtuvieron con una dosis 0.4X de PAO1 Δ*murI*. Con *S. aureus*

132 Δ*murI* Δ*dat*, fue necesaria una dosis de 5X o 10X para elevar significativamente todos los subtipos de IgG. En su conjunto, estos datos sugieren que las cepas bacterianas auxótrofas para D-Glu estimulan los anticuerpos de forma dosis- dependiente.

Se observó que la vacunación con una dosis 0.0001X de *A. baumannii* ATCC 17978 Δ*murI1* Δ*murI2* es suficiente para estimular significativamente la producción de anticuerpos IgM, IgG, IgG1, IgG2a, IgG2b y IgG3 en ratón, y que estos se mantienen por lo menos hasta 1 año después de la inmunización.

Una de las principales características de una vacuna es su capacidad para generar una respuesta inmune amplia; en el caso concreto de las vacunas bacterianas vivas atenuadas, esto significa que una preparación que contenga una única cepa debe ser suficiente para estimular una respuesta inmunológica que reconozca patrones comunes en otras cepas no incluidas en la composición de la vacuna. Los anticuerpos IgG generados por la cepa ATCC 17978 Δ*murI1* Δ*murI2* presentan un alto nivel de reactividad cruzada frente a otras cepas de *A. baumannii*, tales como ATCC 19606, AbH12O-A2 (MDR) y Ab307-0294 (posee capsula). Los anticuerpos IgG generados por la cepa PAO1 Δ*murI* presentan reactividad cruzada frente a otras cepas de *P. aeruginosa*, tales como PA21_ST175, PA14, PA51441321, LES400, LES431, PA28562, PA12142 y PA51442390. Destacar que las cepas PA28562 y PA51442390 presentan el fenotipo mucoide asociado a las infecciones crónicas en pacientes con CF y que la cepa PA14 se trata de un clon más virulento que la PAO1. A su vez, los anticuerpos IgG generados por la cepa 132 Δ*murI* Δ*dat* presentan un alto nivel de reactividad cruzada frente a otras cepas de *S. aureus*, tales como: CA-MRSA USA300 (clone de alto riesgo), RF122 (origen bovino), ED133 (origen ovino) y ED98 (pollos). En su conjunto, estos datos indican que las cepas ATCC 17978 Δ*murI1* Δ*murI2*, PAO1 Δ*murI1* y 132 Δ*murI* Δ*dat* inducen una respuesta inmunitaria amplia frente a una gran diversidad de cepas de *A. baumannii*, *P. aeruginosa* y *S. aureus,* respectivamente.

Para que una vacuna sea eficaz debe estimular también una respuesta inmunitaria de tipo celular. Para explorar la naturaleza de la respuesta de tipo T estimulada por la vacunación con *A. baumannii* ATCC 17978 Δ*murI1* Δ*murI2*, *P. aeruginosa* PAO1 Δ*murI* y *S. aureus* 132 Δ*murI* Δ*dat*, cuantificamos el número de linfocitos productores de las interleucinas IFN-γ, IL-4 y IL-17, estimulados después de un contacto *ex vivo* con las cepas ATCC 17978 Δ*murI1* Δ*murI2*, PAO1 Δ*murI* y 132 Δ*murI* Δ*dat*, en ratones previamente vacunados, con la técnica de ELISpot. Tanto la cepa *A. baumannii* ATCC 17978 Δ*murI1* Δ*murI2*, como *P. aeruginosa* PAO1 Δ*murI* y *S. aureus* 132 Δ*murI* Δ*dat* fueron capaces de

estimular significativamente linfocitos de tipo Th17, productores de IL-17. De hecho, los linfocitos Th17 fueron la población mayoritaria de linfocitos T activada en respuesta a la vacunación con 132 Δ*murI* Δ*dat*. *S. aureus* 132 Δ*murI* Δ*dat* estimulo significativamente también la población de linfocitos Th1 (productores de IFN-γ). Se observó un incremento sustancial, aunque no significativo, de los linfocitos Th1 también con ATCC 17978 Δ*murI1* Δ*murI2* y PAO1 Δ*murI*. Se observó una población de linfocitos Th2 (productores de IL-4) activados en respuesta a la inmunización con ATCC 17978 Δ*murI1* ΔmurI2 y PAO1 Δ*murI*, pero no en respuesta a la inmunización con 132 Δ*murI* Δ*dat*. Estos datos indican que la inmunización activa con ATCC 17978 Δ*murI1* Δ*murI2* y PAO1 Δ*murI* desencadena una respuesta consistentemente de tipo Th2, mientras que 132 Δ*murI* Δ*dat* induce una respuesta de tipo Th1.

Para averiguar si tanto las respuestas inmunitarias de tipo humoral y celular se corresponden a un efecto protector de estas vacunas, evaluamos su eficacia en ratón efectuando un desafío experimental con una infección aguda letal. Aplicando un calendario de vacunación de 2 tomas separadas por 14 días, la vacunación con las tres cepas auxótrofas resultó en un efecto protector frente a la carga bacteriana de la cepa utilizada en el desafío, en los tejidos de los ratones vacunados. Además, la vacunación con la cepa 132 Δ*murI* Δ*dat* evitó la pérdida de peso de los ratones después del desafío con *S. aureus* 132. *A. baumannii* ATCC 17978 Δ*murI1* Δ*murI2* tuvo un efector protector frente al desafío con las cepas ATCC 17978, AbH12O-A2 y Ab307-0294. *P. aeruginosa* Δ*murI* fue eficaz en proteger a los ratones frente a las cepas PAO1, PA28562 y PA14, para esta última se aplicó un calendario de vacunación con 3 tomas intramusculares separadas por 14 días. *S. aureus* 132 Δ*murI* Δ*dat* tuvo un efecto protector frente a las cepas *S. aureus* 132, CA-MRSA USA300, RF122 y ED98. Estos resultados ponen de manifiesto que *A. baumannii* ATCC 17978 Δ*murI1* Δ*murI2*, *P. aeruginosa* PAO1 Δ*murI* y *S. aureus* 132 Δ*murI* Δ*dat* son vacunas eficaces contra cepas multirresistentes, virulentas y epidémicas, algunas incluso de origen animal. Además, verificamos que este efecto protector no es exclusivo del fondo genético de los ratones BALB/c, considerando que observamos que estas vacunas son eficaces también en ratones de la línea C57BL/6.

Se observó también que los anticuerpos generados por *A. baumannii* ATCC 17978 Δ*murI1* Δ*murI2*, *P. aeruginosa* PAO1 Δ*murI* y *S. aureus* 132 Δ*murI* Δ*dat* se pueden transferir a un recipiente en riesgo de contraer la enfermedad causada por cualquier uno de estos microrganismos, para conferirles una inmunidad pasiva protectora.

A. Resumo

El grado de atenuación de una bacteria debe ser suficiente para minimizar su patogenicidad pero no debe debilitar su capacidad invasiva, por el riesgo de dificultar la generación de una respuesta inmune fuerte y de larga duración, y tampoco debe conducir al individuo vacunado a un estado de portador crónico. La solución a este problema puede derivar de la capacidad de las cepas auxótrofas para colonizar y replicarse en el individuo vacunado durante un periodo limitado de tiempo, antes de sufrir una lisis, o ser eliminadas del organismo sin llegar a causar la enfermedad. Esta eliminación rápida de la sangre fue observada después de administradas las cepas *A. baumannii* ATCC 17978 Δ*murI1* Δ*murI2*, *P. aeruginosa* PAO1 Δ*murI* y *S. aureus* 132 Δ*murI* Δ*dat* al ratón, lo cual sugiere que estas cepas no presentan un riesgo potencial de causar enfermedad o dispersarse descontroladamente en el ambiente.

Para que un organismo genéticamente modificado sea seguro como un componente de una vacuna sus mutaciones y sus características derivadas deberán ser irreversibles. Para evaluar la irreversibilidad de la auxotrofia nutricional de *A. baumannii* ATCC 17978 Δ*murI1* Δ*murI2*, *P. aeruginosa* PAO1 Δ*murI* y *S. aureus* 132 Δ*murI* Δ*dat*, se crecieron estas cepas con D-Glu durante 8 días y se evaluó su viabilidad en placas con y sin D-Glu. En el caso hipotético de una reversión de fenotipo, observaríamos el mismo número de colonias bacterianas en las placas con y sin D-Glu, a partir del cultivo con D-Glu. Sin embargo, observamos recuentos sustancialmente superiores en las placas suplementadas con D-Glu, tanto al inicio de la incubación, como en los días posteriores, lo que indica que estas cepas mantienen la auxotrofia nutricional a lo largo del tiempo.

Además, una cepa bacteriana viva atenuada que constituya un ingrediente activo de una vacuna debe ser incapaz de replicar y persistir en el medio ambiente si hipotéticamente se dispersa a través del individuo vacunado. Así que evaluamos la persistencia de las cepas auxótrofas para D-Glu en comparación con sus homólogos salvajes. De hecho, observamos que las cepas ATCC 17978 Δ*murI1* Δ*murI2* y PAO1 Δ*murI* presentan una capacidad de resistir a la osmolisis sustancialmente inferior a la de sus homólogos salvajes, cuando mantenidas en agua durante varios días. Observamos también una reducción sustancial en la capacidad de la cepa *S. aureus* 132 Δ*murI* Δ*dat* para resistir a la desecación frente a su homologo salvaje *S. aureus* 132.

En conclusión, en el presente trabajo presentamos tres microorganismos genéticamente modificados, denominados $MurI^{-}$ y/o $MurI^{-}Dat^{-}$, incapaces de replicarse en el húesped debido a la inexistencia de concentraciones suficientes de D-Glu para la correcta

formación del peptidoglicano. Estas cepas bacterianas, auxótrofas para D-Glu, son vacunas prometedoras frente a los patógenos *A. baumannii*, *P. aeruginosa* y *S. aureus*, ya que presentan un nivel de eficacia y seguridad muy elevado en ratón. Más importante, esta estrategia para la atenuación es una plataforma que puede ser ampliamente aplicada a otras bacterias Gram-negativas y Gram-positivas de interés, y las composiciones vacunales individuales pueden ser reforzadas con la introducción de múltiples cepas para la profilaxis tanto de humanos como de animales en el futuro.

B. CURRICULUM VITAE

First name(s) / Surname(s): Maria Clara Póvoa Cabral
Address: Calle Habitat, 19 3º izq. 15172 Perillo (A Coruña) - Spain
☎ **Telephone:** (+34) 698153692
E-mail: ma.clara.povoa.cabral@sergas.es, clara.mcc15564@gmail.com
Nationality: portuguese
Date of birth: 15/06/1984
Gender: female

EDUCATION AND TRAINING

• **Vaccines Specialist, postgraduate certificate**	III Curso de Especialización Universitario en Vacunas. Facultade de Medicina. Departamento de Psiquiatría, Radioloxía e Saúde Pública. Universidade de Santiago de Compostela (USC), **SPAIN. 2013-2014**
• **Categories B and C in animal experimentation (recognized by the Spanish Authority). Training in animal protection and experimentation for scientists responsible for the design and conduction of experiments with animals.**	ANIMALARIA, Formación y Gestión S.L. Duration: 40 hours (Category B) + 80 hours (Category C). **SPAIN. 2014**
• **Course of R statistical software**	Complejo Hospitalario Universitario A Coruña (CHUAC). **SPAIN. 2014**
• **Course of drafting Patent applications**	Vicerreitoría de Investigación e Transferencia e o Centro Universitario de Formación e Innovación Educativa (CUFIE). Universidade da Coruña (UDC). **SPAIN. 2nd-3rd October 2013**
• **Masters Degree on Health Care and Research – Speciality: Fundamentals of Biomedical Research**	Facultad de Ciencias de la Salud. Universidade da Coruña (UDC). **SPAIN. 2008-2009**
• **Masters Degree on Medical Microbiology (not completed)**	Instituto de Higiene e Medicina Tropical (IHMT), Faculdade de Ciências e Tecnologia (FCT), Faculdade de Ciências Médicas (FCM), Instituto de Tecnologia Química e Biológica (ITQB). Universidade Nova de Lisboa (UNL). **PORTUGAL. 2008**

• **Degree on Molecular and Cellular Biology**	Faculdade de Ciências e Tecnologia (FCT). Universidade Nova de Lisboa (UNL). **PORTUGAL. 2003-2007**
• **Training in Research and Control of Nosocomial Infections. Epidemiological surveillance and study of susceptibility profiles of nosocomial bacteria. Study of incidence of bloodstream infections, urinary tract infections and multi-resistant bacteria**	Infection Control Committee of Hospital Nossa Senhora do Rosário, E.P.E. Barreiro. **PORTUGAL. 2007**
• **Training in Scientific Research. Degree dissertation entitled: "Characterization and Prevalence of Different Species of Beta-hemolytic *Streptococcus* Responsible for Nasopharyngeal Colonization of Preschool Children in Oeiras, Portugal, During 2006"**	Instituto de Tecnologia Química e Biológica (ITQB) (Laboratório de Epidemiologia Microbiana); Faculdade de Ciências e Tecnologia (FCT). Universidade Nova de Lisboa (UNL). **PORTUGAL. 2006-2007**
• **Ettan™ DIGE System Training Course, 2-D Fluorescence Difference Gel Electrophoresis, GE HEALTHCARE LIFE SCIENCES**	Faculdade de Ciências e Tecnologia (FCT). Universidade Nova de Lisboa (UNL). REQUIMTE (Rede de Química e Tecnologia), Fundação para a Ciência e Tecnologia, FCT-MCTES. **PORTUGAL. 2008**
• **Course of real-time PCR. Basics and applications of real-time PCR**	Faculdade de Ciências Médicas (FCM). Universidade Nova de Lisboa (UNL). Lisbon, **PORTUGAL. 2007**

LIST OF PUBLICATIONS

Articles in international journals with peer review

- Rumbo-Feal, S., Gómez, M. J., Gayoso, C., Alvarez-Fraga, L., **CABRAL, M. P.**, Aransay, A. M., Rodríguez-Ezpeleta, N., Fullaondo, A., Valle, J., Tomás, M., Bou, G., and Poza, M. Whole transcriptome analysis of *Acinetobacter baumannii* assessed by RNA-sequencing reveals different mRNA expression profiles in biofilm compared to planktonic cells. PLoS One. 2013 (vol 8(8):e72968).
PMID:24023660

- Pérez, A., Poza, M., Fernández, A., Fernández, M. del C., Mallo, S., Merino, M., Rumbo-Feal, S., **CABRAL, M. P.**, and Bou, G. Involvement of the AcrAB-TolC efflux pump in the resistance, fitness, and virulence of *Enterobacter cloacae*. Antimicrobial Agents and Chemotherapy. 2012 (vol. 56, 2084-2090). **PMID:22290971**

- Aranda J., Bardina C., Beceiro A., Rumbo S., **CABRAL M. P.**, Barbé J., Bou G. The *Acinetobacter baumannii* RecA protein in the repair of DNA damage, antimicrobial

resistance, general stress response, and virulence. Journal of Bacteriology. 2011 (vol. 193(15):3740-3747). **PMID: 21642465**

- **CABRAL M. P.**, Soares N. C., Aranda J., Parreira J. R., Rumbo C., Poza M., Valle J., Calamia V., Lasa I., Bou G. Proteomic and functional analyses reveal a unique lifestyle for *Acinetobacter baumannii* biofilms and a key role for histidine metabolism. Journal of Proteome Research. 2011 (vol. 10(8):3399-3417). **PMID: 21612302 (see attached document)**

- Soares, N. C.*, **CABRAL, M. P.***, Gayoso, C., Mallo, S., Rodriguez-Velo, P., Férnandez-Moreira, E., and Bou, G. Associating growth-phase-related changes in the proteome of *Acinetobacter baumannii* with increased resistance to oxidative stress. Journal of Proteome Research. 2010 (vol. 9(4):1951-1964). **PMID: 20108952 (*CO-AUTHORS) (see attached document)**

- Soares, N. C., **CABRAL, M. P.,** Parreira, J. R., Gayoso, C., Barba, M. J., and Bou, G. 2-DE analysis indicates that *Acinetobacter baumannii* displays a robust and versatile metabolism. Proteome Science. 2009 (vol. 28, 7-37). **PMID:19785748 (see attached document)**

Oral communications by invitation

- Aranda J., Bardina C., Beceiro A., Tomás M., Rumbo S., **CABRAL M. P.**, Barbé J., Bou G. The *Acinetobacter baumannii* RecA protein is atypically regulated and contributes to antibiotic resistance and stress survival. Interscience Conference on Antimicrobial Agents and Chemotherapy (51st ICAAC). American Society of Microbiology (ASM). 17th - 20th September (2011). Chicago, USA. (oral communication by Bou, G.)

Oral communications

- **CABRAL, M. P.,** Rumbo, C., Aranda, J., Poza, M., Bou, G. Glutamate racemase is a critical gene for *Acinetobacter baumannii* biofilm formation and attachment to eukaryotic cells. 22nd European Congress of Clinical Microbiology and Infectious Diseases (ECCMID), The European Society of Clinical Microbiology and Infectious Diseases (ESCMID). 31 March - 3 April (2012). London, UNITED KINGDOM. (oral communication by CABRAL, M. P.)

- Pérez A., Poza M., Fernández M., López A., Fernández A., Mallo S., Merino M., Rumbo-Feal S., **CABRAL M. P.,** Bou G. Reducción de la "fitness" en *Enterobacter cloacae* debido a la pérdida de un componente estructural de bomba de expulsión AcrAB-TolC. XV Congreso de la Sociedad Española de Enfermedades Infecciosas y Microbiología Clínica. Sociedad Española de Enfermedades Infecciosas y Microbiología Clínica (SEIMC). 1st – 4th July (2011). Málaga, SPAIN. (oral communication by Pérez, A.)

- Aranda J., Bardina C., Beceiro A., Rumbo S., **CABRAL M. P.,** Llagostera M., Barbé J., Bou G. Implicación de la proteína RecA en la reparación del DNA, la resistencia a antimicrobianos, la respuesta general a estrés y la virulencia en *Acinetobacter baumannii*. XV Congreso de la Sociedad Española de Enfermedades Infecciosas y

Microbiología Clínica. Sociedad Española de Enfermedades Infecciosas y Microbiología Clínica (SEIMC). 1st – 4th July (2011). Málaga, SPAIN. (oral communication by Aranda J.)

- Soares, N. C., **CABRAL, M. P.,** Aranda, J., Rumbo, C., Bou, G. Mechanisms of biofilm formation in *Acinetobacter baumannii* – a proteomic perspective. 8th International Symposium on the Biology of *Acinetobacter*. Federation of European Microbiological Societies (FEMS), European Society of Clinical Microbiology and Infectious Diseases (ESCMID), Doctoral School of Biology (Università di Roma Tre). 1st - 3rd Septiembre (2010). Rome, ITALY. (oral communication by Soares, N. C.)

Poster Communications

- **M. P. CABRAL,** C. Rumbo, M. Merino, A. Beceiro, M. Poza, A. Pérez, G. Bou. Blockade of glutamate racemisation during cell wall formation prevents biofilms and proliferation of *Acinetobacter baumannii in vivo*. 23rd European Congress of Clinical Microbiology and Infectious Diseases (ECCMID). The European Society of Clinical Microbiology and Infectious Diseases (ESCMID). 27-30 April (2013). Berlin, GERMANY

- Poza M., Gayoso C., Gómez M. J., Rumbo-Feal S., Aransay A. M., Rodríguez-Ezpeleta N., Fullaondo A., Tomás M., Fernández-Banet J., **CABRAL M. P.,** Valle J., Lasa I., Bou G. Comparative transcriptome analysis of the *Acinetobacter baumannii* biofilm vs. planktonic cells. Interscience Conference on Antimicrobial Agents and Chemotherapy (51st ICAAC). American Society of Microbiology (ASM). September 17-20 (2011). Chicago, USA

- Poza, M., Gayoso, C., Gómez, M. J., Rumbo-Feal, S., Aransay, A. M., Rodríguez-Ezpeleta, N., Fullaondo, A., Tomás, M., Fernández-Banet, J., **CABRAL, M. P.,** Valle, J., Lasa, I., Bou, G. Obtención del transcriptoma del biofilm de *Acinetobacter baumannii* mediante técnicas de secuenciación masiva. XXIII Congreso Nacional de Microbiología. Sociedad Española de Microbiología (SEM). 11-14 July (2011). Salamanca, SPAIN

- **M. P. CABRAL,** J. R. Parreira, N. C. Soares, J. Aranda, M. Poza and G. Bou. Proteome analysis of *Acinetobacter baumannii* reveals a key role for histidine metabolism in biofilms. 4th EuPA Meeting and 6th ProCura Meeting. October 23-27 (2010). Estoril, PORTUGAL

- **M. P. CABRAL,** J. R. Parreira, N. C. Soares, M. Poza, J. Aranda, G. Bou. Novel proteins involved in formation of *Acinetobacter baumannii* biofilms. 50th ICAAC. September 12-15 (2010). Boston, USA

- N. C. Soares, **M. P. CABRAL,** J. Aranda, C. Rumbo, and G. Bou. Proteomics unveals mechanisms of biofilm development in *Acinetobacter baumannii*. 4th EuPA Meeting and 6th ProCura Meeting. October 23-27 (2010). Estoril, PORTUGAL

- Nelson C. Soares, **M. P. CABRAL,** Carmen Gayoso, Esteban Fernández-Moreira, Susana Mallo, Patricia Rodriguez-Velo and Germán Bou. Associating in vitro growth changes in the proteome of *Acinetobacter baumannii* with resistance to oxidative stress. 3rd EuPA Congress. June 14-17 (2009). Stockholm, SWEDEN

- **CABRAL, MARIA C.;** Soares, Nelson C.; Parreira, José R.; Bou, Germán. The effects of sodium salicylate on *Acinetobacter baumannii* – a proteomic view. 5th Congress of the Portuguese Proteomics Network - ProCura and 1st International Congress on Analytical Proteomics - ICAP. September 30th - October 3rd (2009). Caparica, PORTUGAL

- I. Santos-Sanches, R. Pires, D. Rolo, **C. CABRAL,** P. Diogo, e R. Mato. Nasopharyngeal Colonization of Children by Beta-hemolytic Streptococci (BHS). Congresso Nacional MICRO-BIOTEC. Sociedade Portuguesa de Microbiologia e Sociedade Portuguesa de Biotecnologia. November 30th – December 2nd (2007). Faculdade de Ciências da Universidade de Lisboa. Lisbon, PORTUGAL

- **CABRAL M. C.,** Santos P.E., Ferreira M. E., Lopes J. J. and Clemente J.A. Trends in Antimicrobial Activity Against Bacteria Isolated From Hospital Nossa Senhora do Rosário, Portugal. 4th Congress of the European Society for Emerging Infections. The European Society for Emerging Infections. September 30th - October 3rd (2007). Hotel Tivoli Tejo. Lisbon, PORTUGAL

Conferences and Meetings

• **3rd ESCMID Conference on Vaccines. Vaccines for Mutual Protection.**	6-8th March. The European Society of Clinical Microbiology and Infectious Diseases (ESCMID). Lisbon, **PORTUGAL. 2015**
• **BIOSPAIN 2014. 7th INTERNATIONAL MEETING ON BIOTECHNOLOGY**	24-26th September. Santiago de Compostela, **SPAIN. 2014**
• **23rd European Congress of Clinical Microbiology and Infectious Diseases (ECCMID)**	The European Society of Clinical Microbiology and Infectious Diseases (ESCMID). Berlin, **GERMANY. 2013**
• **VIII Scientific Conference of REIPI (The Spanish Network for Research in Infectious Diseases)**	26-27th November. Hospital Universitario Vall d'Hebrón (Barcelona). **SPAIN. 2013**
• **22nd European Congress of Clinical Microbiology and Infectious Diseases (ECCMID)**	The European Society of Clinical Microbiology and Infectious Diseases (ESCMID). London, **UNITED KINGDOM. 2012**
• **VII Scientific Conference of REIPI (The Spanish Network for Research in Infectious Diseases)**	Instituto de Biomedicina de Sevilla, IBiS. **SPAIN. 2012**
• **18th Lilly Scientific Symposium entitled Microbiome: "Discovering The Last Body Organ"**	EUROFORUM Infantes de San Lorenzo de El Escorial, Madrid. **SPAIN. 2010**
• **6th EuPA Meeting and 4th ProCura Meeting**	The Portuguese Proteomics Network - ProCura and the Organizing committee of EuPA (European Proteomics Association). Estoril, **PORTUGAL. 2010**

• **5th ProCura Congress and 1st International Congress on Analytical Proteomics – ICAP**	The Portuguese Proteomics Network – ProCura. Caparica, **PORTUGAL. 2009**
• **Scientific Meeting on Clinical Proteomics: "From the peptide fingerprint image to the tissue"**	Instituto de Investigación Biomedica de A Coruña. **SPAIN. 2009**
• **4th Congress of the European Society for Emerging Infections**	The European Society for Emerging Infections. Hotel Tivoli Tejo, Lisbon. **PORTUGAL. 2007**

Title, category or activity	
	From 2014 to the actuality
MAGIC BULLET	• MAGIC BULLET european project (participant)
	From 2008 to 2013
PhD student, Instituto de Investigación Biomedica de A Coruña (INIBIC). Complejo Hospitalario Universitario a Coruña. SPAIN	• Doctoral degree grant holder (SFRH/BD/6474/2009) from FCT-MCTES, PORTUGAL • Thematics: "Searching for proteins involved in biofilm formation, antibiotic resistance and persistence of *Acinetobacter baumannii*: a proteomics and genetics approach" • PhD Director: Germán Bou Arévalo • Group of Microbiology and Infectious Diseases., Complejo Hospitalario Universitario A Coruña (CHUAC) and Instituto de Investigación Biomédica (INIBIC). SPAIN
	From 2014 to the actuality
Former member of SEIMC (The Spanish Society for Emerging Infections and Clinic Microbiology)	• SEIMC: Sociedad Española de Enfermedades Infecciosas y Microbiología Clínica, member ID: 4226. SPAIN
	From 2010 to the actuality
Former member of REIPI (The Spanish Network for Research in Infectious Diseases)	• RETICS – REIPI, Instituto de Salud Carlos III. Ministerio de Ciencia e Innovación. SPAIN • Expedient number (RD): RD006/0008/0025 • Principal Investigador: Germán Bou Arévalo • Center: Complejo Hospitalario Universitario A Coruña (CHUAC)

Participation in Projects

	PI15/00860
Development of a platform for the generation of live bacterial vaccines auxotrophic for D-glutamate	**Principal Investigator:** Germán Bou Arévalo **Funding Entity:** Instituto de Salud Carlos III (FIS). Ministerio de Economía y Competitividad. SPAIN **Total Funding:** 261.723€ **Duration (Period of funding):** 2016-2018 **Team Member**
	Grant agreement 278232
MAGIC BULLET: Optimization of off-patent antimicrobials for the treatment of ventilator-associated pneumonia	**Principal Investigator:** Michael McConnell, José Miguel Cisneros **Funding Entity:** European Commision, 7th Programme Framework **Total Funding:** 5.998.018€ **Duration (Period of funding):** 2012-2015 **Team Member**
	PI061368
Preclinical Studies with D-amino acids to Attenuate the Virulence of Acinetobacter baumannii and Other Multiresistant Pathogens: A New Strategy to Eradicate Infections	**Principal Investigator:** Germán Bou Arévalo **Funding Entity:** Instituto de Salud Carlos III (FIS). Ministerio de Economía y Competitividad. SPAIN **Total Funding:** 261.723€ **Duration (Period of funding):** 2013-2015 **Team Member**
	PS07/90
Genomics and Transcriptomics of Acinetobacter baumannii biofilms	**Principal Investigator:** Margarita Poza Domínguez **Funding Entity:** Instituto de Salud Carlos III (FIS). Ministerio de Ciencia e Innovación. SPAIN **Total Funding:** 125.729€ **Duration (Period of funding):** 2012-2014 **Team Member**
	PI081613
Adaptation of the Pathogen Acinetobacter baumannii at Different Stress Conditions: Searching for New Therapeutic Targets	**Principal Investigator:** Germán Bou Arévalo **Funding Entity:** Consellería de Innovación, Industria y Comercio, Xunta de Galicia. SPAIN **Total Funding:** 71.282€ **Duration (Period of funding):** 2008-2011 **Team Member**
	08CSAO064916PR
Mechanisms of Antibiotic Resistance Regulation and	**Principal Investigator:** Germán Bou Arévalo **Funding Entity:** Instituto de Salud Carlos III (FIS). Ministerio de

Virulence in the Nosocomial Pathogen Acinetobacter baumannii	Sanidad y Consumo. SPAIN **Total Funding:** 90.387€ **Duration (Period of funding):** 2008-2011 **Team Member**
	PI11/01034
Study of Antimicrobial Resistance in the Nosocomial Pathogen Acinetobacter baumannii by a Proteomic Approach	**Principal Investigator:** Germán Bou Arévalo **Funding Entity:** Consellería de Sanidade, Xunta de Galicia. SPAIN **Total Funding:** 88.429€ **Duration (Period of funding):** 2007-2010 **Team Member**
	PI12/00552
Implication of The Bacterial Outer Membrane Permeability In Resistance To Carbapenem Antibiotics: The Nosocomial Pathogen Acinetobacter baumannii as a Model	**Principal Investigator:** Germán Bou Arévalo **Funding Entity:** Instituto de Salud Carlos III (FIS). Ministerio de Sanidad y Consumo. SPAIN **Total Funding:** 178.475€ **Duration (Period of funding):** 2006-2008 **Team Member**

Grants and prizes

2015 **Free Registration**	3rd Conference on Vaccines. Vaccines for Mutual Protection. **European Society of Clinical Microbiology and Infectious Diseases (ESCMID)**
2013 **Travel Grant and Free Registration**	23rd European Congress of Clinical Microbiology and Infectious Diseases (ECCMID). Grants were awarded to those with outstanding abstracts **European Society of Clinical Microbiology and Infectious Diseases (ESCMID)**
2012 **Travel Grant and Free Registration**	22nd European Congress of Clinical Microbiology and Infectious Diseases (ECCMID). Grants were awarded to those with outstanding abstracts **European Society of Clinical Microbiology and Infectious Diseases (ESCMID)**
2011 **1st prize for Aranda, J., for the best oral communication**	Aranda J., Bardina C., Beceiro A., Rumbo S., **CABRAL M. P.,** Llagostera M., Barbé J., Bou G. Implicación de la proteína RecA en la reparación del DNA, la resistencia a antimicrobianos, la respuesta general a estrés y la virulencia en *Acinetobacter baumanii* **Sociedad Española de Enfermedades Infecciosas y Microbiología Clinica (SEIMC), SPAIN**

2010-2013 **Doctoral degree grant**	Doctoral degree grant (SFRH/BD/6474/2009) obtained in December 2009 on the subject "Biological sciences" from Fundação para a Ciência e a Tecnologia, MCTES. **FCT – MCTES, PORTUGAL**

Patents or Utility Models

Title: Live attenuated vaccines

PCT Application number: PCT/EP2014/071926
Date of receipt: 13th October, 2014 17:43 (CEST)
Applicant: Servicio Galego de Saúde (SERGAS), Fundación Profesor Novoa Santos
Receptor: European Patent Office (EPO) (RO/EP)
Inventors: Germán Bou Arévalo, **Maria Clara Póvoa Cabral**, Astrid Pérez Gómez, María Merino Carballeira, Alejandro Beceiro Casas
Agents: Gustavo Fúster, code 1039/1

Title: Live bacterial attenuated vaccines auxotrophic for D-glutamate ("Vacunas bacterianas vivas atenuadas auxótrofas para D-glutamato")

Application number: P201331504
Priority Date: 11th October, 2013 17:52 (CEST)
Applicant: Servicio Galego de Saúde (SERGAS), Fundación Profesor Novoa Santos
Receptor: OEPM Madrid, Spain
Inventors: Germán Bou Arévalo, **Maria Clara Póvoa Cabral**, Astrid Pérez Gómez, María Merino Carballeira, Alejandro Beceiro Casas
Agents: Gustavo Fúster, code 1039/1

Languages

Portuguese	High level, native
Spanish	High level
English	High level

Proteome Science

BioMed Central

Research

Open Access

2-DE analysis indicates that *Acinetobacter baumannii* displays a robust and versatile metabolism

Nelson C Soares, Maria P Cabral, José R Parreira, Carmen Gayoso, Maria J Barba and Germán Bou*

Address: Servicio de Microbiologia-Unidad de Investigacion, Complejo Hospitalario Universitario A Coruña, 15006 La Coruña, Spain

Email: Nelson C Soares - ncrusoa@canalejo.org; Maria P Cabral - Maria.Clara.Povoa.Cabral@sergas.es; José R Parreira - Jose.Dias.Parreira@sergas.es; Carmen Gayoso - Maria.Carmen.Gayoso.Babio@sergas.es; Maria J Barba - Maria.Jose.Barba.Miramonte@sergas.es; Germán Bou* - germanbou@canalejo.org

* Corresponding author

Published: 28 September 2009

Proteome Science 2009, **7**:37 doi:10.1186/1477-5956-7-37

Received: 29 June 2009
Accepted: 28 September 2009

This article is available from: http://www.proteomesci.com/content/7/1/37

Abstract

Background: *Acinetobacter baumannii* is a nosocomial pathogen that has been associated with outbreak infections in hospitals. Despite increasing awareness about this bacterium, its proteome remains poorly characterised, however recently the complete genome of *A. baumannii* reference strain ATCC 17978 has been sequenced. Here, we have used 2-DE and MALDI-TOF/TOF approach to characterise the proteome of this strain.

Results: The membrane and cytoplasmatic protein extracts were analysed separately, these analyses revealed the reproducible presence of 239 and 511 membrane and cytoplamatic protein spots, respectively. MALDI-TOF/TOF characterisation identified a total of 192 protein spots (37 membrane and 155 cytoplasmatic) and revealed that the identified membrane proteins were mainly transport-related proteins, whereas the cytoplasmatic proteins were of diverse nature, although mainly related to metabolic processes.

Conclusion: This work indicates that *A. baumannii* has a versatile and robust metabolism and also reveal a number of proteins that may play a key role in the mechanism of drug resistance and virulence. The data obtained complements earlier reports of *A. baumannii* proteome and provides new tools to increase our knowledge on the protein expression profile of this pathogen.

Background

Acinetobacter baumannii is a Gram-negative, nonmotile, aerobic coccobacillus that is often found in health care settings. There is increasing concern as regarding the prevalence of this bacterium in hospital environments, especially in intensive care units, where it has been associated with different types of infections such as pneumonia, meningitis, bacteraemia, urinary tract infections and others [1-3]. In addition, *A. baumannii* has a remarkable capacity to acquire resistance to most antibiotics used in clinical practice and to cause outbreaks throughout cities, countries and even continents [4-6]. Despite the emerging awareness of the potential hazards of this bacterium, little is known about the mechanisms that operate during antibiotic resistance, virulence, or persistence strategies of *A. baumannii*.

Genomic approaches have recently been successfully applied for *A. baumannii*. For instance, genomic comparison between SDF and AYE strains with the soil-living *A. baylyi* strain ADP1 revealed important exclusive features of each strain, which may partly explain their existence in different ecological niches [7,8]. The recently described sequence of *A. baumannii* ATCC 17978 isolate revealed that its genome is composed by 3,976,746 base pairs (bp) and that it has 3,830 open reading frames (ORFs), of which nearly 17% are situated in 28 putative alien islands [9], which suggests that the genome has acquired a significant amount of foreign DNA.

Nevertheless, it is widely accepted that most ORFs are expressed under different conditions and/or states of growth and environmental stress [10]. Moreover, the identification of proteins via MS/MS analyses validate predicted genes, correct erroneous gene annotation and reveal some completely missed genes [10,11]. Therefore as pointed out by Brötz-Oesterhelt *et al.* (2005) [12], the application of further techniques such as proteomics is required in order to establish the protein composition of a given cell under certain conditions, independently of its linear gene sequence.

Proteomics analysis has been applied to fractions enriched with *A. baumannii* cell membranes, and a group of 22 proteins, composed by ribosomal proteins, chaperones elongation factors and outer membrane proteins identified [13]. A total of 135 proteins (inner and outer membrane) and 23 periplasmic proteins were identified in *A. baumannii* in another study [14]. More recently, it was characterise the proteome of outer membrane vesicles from a clinical *A. baumannii* isolate [15]. These studies provide important data regarding the proteome of *Acinectobacter*, nevertheless as far as we are aware, the cytoplasmatic proteome of *A. baumannii* remains to be characterised. In the current study, we used 2-DE and MALDI-TOF/TOF to analyse the membrane and cytoplasmatic proteome of *A. baumannii*, and the data obtained confirms the results of previous genomic studies showing that *A. baumannii* displays a robust and versatile metabolism capable of exploiting a variety of carbon sources and energy.

Materials and methods

Bacterial strain and growth conditions

A. baumannii ATCC 17978 was grown overnight in Mueller Hinton broth (Fluka, Madrid, Spain) at 37°C under constant shaking. Fresh nutrient media (500 mL) was inoculated with a 1:100 dilution of the overnight culture and grown to OD_{600} = 0.4-0.6, at 37°C with vigorous shaking.

Protein extraction

The cell were harvested by centrifugation at 3,500 g for 15 min at 4°C and washed twice with 10 mL 0.9% (w/v) NaCl. The resultant pellet was resuspended in 3 or 5 mL of disintegration buffer [13] (7.8 g/L NaH_2PO_4, 7.1 g/L Na_2HPO_4, 0.247 g/L MgSO4 7.H_2O + protease inhibitor mix (GE Healthcare, USA) + nuclease mix (GE Healthcare, USA)) and sonicated on ice for 3 periods of 5 min. The unbroken cells were separated by centrifugation at 1,500 *g*. The supernatant was centrifuged for 30 min at 4°C at 4,500 rpm and was then clarified through a 0.45 μM filter (Milipore, USA) to remove the cell debris. Finally, the extract was processed with a 2-DE Cleanup Kit (GE Healthcare, USA).

The same extraction method was used to extract cell surface membrane. However, after the separation of unbroken cells, the lysate was treated as described by Molly *et al.* (2000) [16]. Briefly, an equal volume of ice-cold 0.1 M sodium carbonate (pH 11) was added to the resulting supernatant and the mixture was stirred slowly overnight, on ice. The carbonate treated membranes were then collected by ultracentrifugation at 100,000 *g* for 45 min at 4°C, and the membranes were then re-suspended in 500 μl H_2O. Finally, as with the soluble fraction, the extract was processed with a 2-DE Cleanup Kit (GE Healthcare, USA).

Two-dimensional gel electrophoresis (2-DE)

Protein concentration in the extracts was determined with a Biorad protein assay kit (Biorad, Germany), by a modified Bradford assay [17] as suggested by Ramagli *et al.* (1999) [18].

For isoelectric focusing (IEF), the IPGphor III system was used (GE Healthcare, USA) with 3-10 non-linear (NL), 4-7 (L) or 6-11(L) pH gradient strips (IPG strips, GE Healthcare, Sweden). Proteins were solubilised in 8 M urea, 2% (w/v) CHAPS, 40 mM DTT and 0.5% (v/v) corresponding IPG buffer (GE Healthcare, Sweden). IEF was carried out at 30 V for 12 h, followed by 250 V for 1 h, 500 V for 1.5 h, 1,000 V for 1.5 h, a gradient to 8,000 V over 1.5 h and maintenance at 8,000 V for a further 4 h, all at 20°C. Note, for 6-11 (L) pH gradient strips, IEF was carried out at 30 V for 12 h, followed by 500 V for 1 h, 1,000 V for 1 h, a gradient to 8,000 V for 2.5 h and maintenance at 8,000 V for 0.5 h. Prior to the second dimension (SDS-PAGE), the focused IPG strips were equilibrated for 2 × 15 min in buffer containing 50 mM Tris-HCl (pH 8.8), 6 M urea, 30% (v/v) glycerol, 2% (w/v) SDS and a trace of Bromophenol Blue. DTT at 1% (w/v) was added to the first equilibration step and 2.5% (w/v) iodoacetamide to the second. SDS-PAGE was performed on 12% or 15% polyacrylamide gels [19]. For analytical 2-DE gels, silver

staining was performed according to Blum *et al.* (1987) [20] and gels were loaded with 25 to 40 μg of total protein. For preparative gels, MS-compatible silver staining [21] was used and the gels were loaded with at least 350 μg of total protein.

Image acquisition and 2-DE analyses

Gels were scanned with an Image Scanner v3.3 densitometer (GE Healthcare) and analysed with Image Master Platinum software, V.6.0, as described by the manufacturer (GE Healthcare). Briefly, a matched set consisting of three images was created. In order to confirm reproducibility, at least three biological replicates were processed. For spot detection, the parameters were adjusted in the following order: smooth 2; MinArea 5; Saliency 1.00000, and only spots observed on all three gels of a replicated group were considered for further analyses. Numerical data for individual spots were generated automatically and expressed as % of spot volume.

Trypsin digestion of proteins and characterisation by MALDI-TOF/TOF

Selected spots were manual excised from the gels and transferred to microcentrifuge tubes. Samples were then destained with a solution containing 20% (w/v) sodium thiosulphate and 1% (w/v) potassium ferricyanide for 5 min. Destained spots were then in-gel reduced, alkylated and digested with trypsin as suggested be Sechi and Chait 1998 [22]. Briefly, spots were washed twice with 25 mM ammonium bicarbonate in 50% (v/v) acetonitrile (ACN) for 20 min. The gel spots were then shrunk with 100% (v/v) in acetonitrile and dried in a speed-vac (Savant, USA). The samples were reduced with DTT and subsequently alkylated with iodoacetamide. Samples were digested with 20 ng/μl sequencing grade trypsin (Roche Applied Science, USA), overnight at 37°C. After digestion the supernatant was collected and 1 μl was spotted onto a MALDI target plate (384-spot Teflon®-coated plates) and allowed to air dry at room temperature. Where necessary, tryptic peptides were passed through C18 Zip-Tips (Millipore, USA) and mixed with 3 mg/ml of an α-cyano-4-hydroxycinnamic acid in 0.1% (v/v) TFA and 50% (v/v) ACN was added to the dried peptide digest spots and allowed to air dry. The samples were analyzed using a MALDI-TOF/TOF mass spectrometer 4800 Proteomics Analyzer (Applied Biosystems). MALDI-TOF spectra were acquired in reflector positive ion mode using 1000 laser shots per spectrum. Data Explorer version 4.2 (Applied Biosystems) was used for spectra analyses and generating peak picking list. All mass spectra were internally calibrated using autoproteolytic trypsin fragments and externally calibrate using standard peptide mixture (Sigma-Aldrich). TOF/TOF fragmentation spectra were acquired by selecting the 10 most abundant ions of each MALDI-TOF peptide mass map (excluding trypsin autolytic peptides and other background ions) and averaging 2,000 laser shots per fragmentation spectrum. The parameters used to analyze the data were a signal to noise threshold of 20, minimum area of 100 and a resolution higher than 10,000 with a mass accuracy of 20 ppm.

Database queries and protein identification

The monoisotopic peptide mass fingerprinting data obtained from MS and the amino acid sequence tag obtained from each peptide fragmentation in MS/MS analyses were used to search for protein candidates using Mascot version 1.9 from Matrix Science http://www.matrixscience.com. Peak intensity was used to select up to 50 peaks per spot for peptide mass fingerprinting and 50 peaks per precursor for MS/MS identification. Tryptic autolytic fragment-, keratin-, and matrix-derived peaks were removed from the data set utilised for data-based search. The search for peptides mass fingerprints and tandem MS spectra were performed in NCBInr database without any taxonomy restriction. Fixed and variable modifications were considered (Cys as S-carbadiomethyl and Met as oxidised methionine, respectively), allowing one trypsin missed cleavage. MS/MS ions search were conducted with a mass tolerance of ± 1.2 Da on the parent and 0.3-0.8 Da on fragments, in all cases the peptide charge was +1. Decoy search was done automatically by Mascot on randomized database of equal composition and size. Mascot scores for all protein identifications were higher than the accepted threshold for significance (at the $p < 0.050$ level, positive rate measured to be 0.047). For protein subcellular localisation prediction it was utilised PSORTb v.2.0.4, available free online at http://www.psort.org/psortb/index.html.

Results and Discussion

Bimodal distribution of Acinetobacter baumannii proteome

In the current study, a 2-DE based proteomic analyses of *A. baumannii* ATCC 17978, grown under rich medium conditions and harvested during exponential phase were performed. The study was based on the analysis of two distinct protein fractions, a fraction enriched in membrane proteins and a fraction enriched in cytoplasmatic proteins; for convenience, these are referred in the text as membrane and cytoplasmatic fractions respectively. Analysis of three biological replicates revealed that at least 239 spots were reproducibly detected in the membrane fraction, whereas the cytoplasmatic fraction contained a total of 511 reproducible spots.

As a first approach, both the membrane and the cytoplasmatic protein fractions were analysed by use of 2-DE gels with immobilized pH gradient (IPG) strips (pH 3-10) (see Fig. 1A and 1B, respectively). However, for the cytoplasmatic fraction, these analyses revealed a clear predomi-

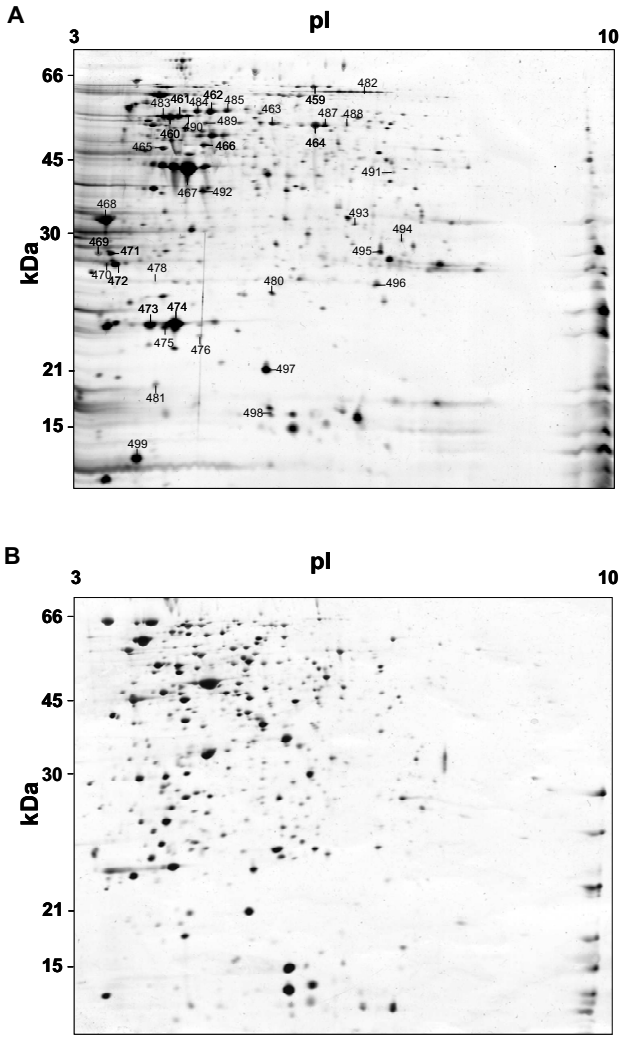

Figure 1
2-DE gels showing *A. baumannii* proteins. (A) membrane proteins, (B) cytoplasmatic proteins. Numbered spots (in A) indicate membrane proteins identified by MALDI-TOF/TOF. All gels (12% SDS) were silver stained and loaded with 25 μg total protein.

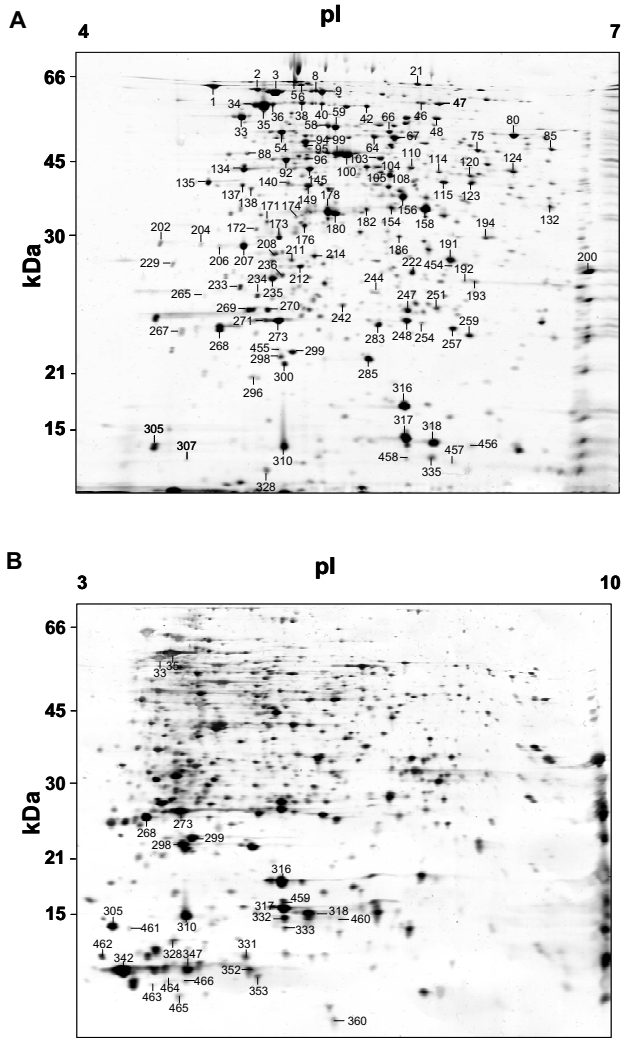

Figure 2
The cytoplasmatic fraction was analysed with IPG strips of various pH range and silver stained gels with different concentrations of acrylamide. 2-DE (12% SDS) gels containing proteins within a range pH 4-7 (A), 2-DE (15% SDS) gel containing proteins within a range pH 3-10 (B), gels were loaded with 25 μg, total protein. Numbered spots indicate proteins identified by MALDI-TOF/TOF.

nance of acidic proteins, although a number of highly basic proteins remained unresolved close to the cathode (p*I* > 9) (see Fig. 1B). Therefore, in an attempt to overcome the intrinsic under-representation of the alkaline proteins [12,23], the acidic and basic cytoplasmatic subproteomes were analysed using immobilized pH gradient strips of various pH range (see Fig. 2 and 3). Use of 2-DE 12% polyacrylamide (p*I* ranges of 4-7) silver stained gels revealed 390 spots that could be reproducibly detected on the acidic range (Fig. 2A). Additionally, complementary analyses using 15% polyacrylamide silver stain gels in the range pH 3-10 revealed the presence of further 30 protein spots of low molecular weight (between 9 and 12 kDa) (Fig. 2B). Use of 2-DE gels 12% polyacrylamide (p*I* ranges of 6-11) added a further 91 reproducible alkaline protein spots (nearly 21% of the total soluble protein spots) (Fig. 3).

In concordance with previous reports referring other bacteria species [23], the 2-DE gels analysis revealed that the spot pattern of this pathogen is characterised by clear predominance of high molecular protein spots and in terms of pI there is visible a bimodal distribution of protein spots, where the most crowded regions is found between pI 4-7 and 9-11 (Fig. 4).

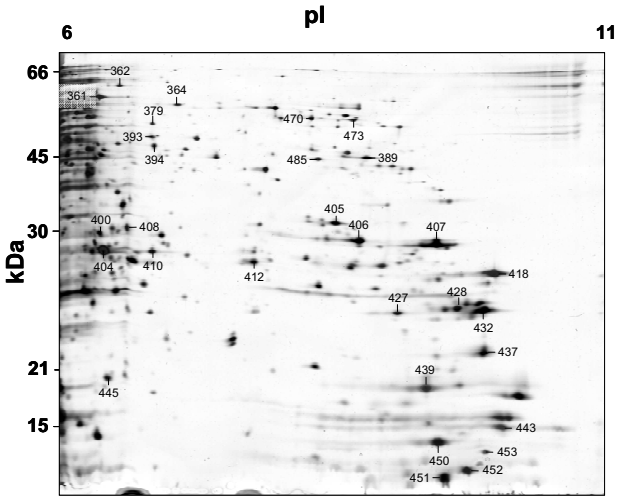

Figure 3
2-DE (12% SDS) gel containing basic proteins within a pH range of 6-11. Gel was loaded with 40 μg, total protein. Numbered spots indicate proteins identified by MALDI-TOF/TOF.

Characterisation of the Acinetobacter baumannii proteome

In the current study we wished to identify the most abundant proteins spots, since these are likely to play a relevant role in bacterial biology. A total of 192 protein spots were identified 37 and 155 from membrane and cytoplasmatic protein fractions respectively. The list included proteins within a p*I* range of 4.3-10.5 and a Mw from 9.2 - 73.8 kDa (table S1, Additional file 1 and table S2, Additional file 2), indicating that the 2-DE analyses provided a representative view of the *A. baumannii* proteome. Most of the identifications were based on multiple peptide matches (table S3, Additional file 3), although in some cases protein identification was based on a single peptide sequence (namely spot # 36, 110, 134, 172, 242, 248, 459 - see table S1, Additional file 1 and table S2, Additional file 2, table S3, Additional file 3,). However, the scores for all proteins identified here were higher than the significance threshold (determined at the 95% confidence level) calculated by Mascot (table S1, Additional file 1 and table S2, Additional file 2) and in all cases the data was search against an Mascot decoy database in order to check for false positive (additional identification data for all spots is provided as supplementary material). Furthermore, all the proteins identified belong to *A. baumannii* proteome, and from the 192 spots, 172 were in fact matched with proteins belonging to *A. baumannii* ATCC 17978 proteome. This criterion, together with the fact that in most of the cases the theoretical molecular weights and/or p*I* of the identified proteins were very close to that observed in gel (table S1, Additional file 1 and table S2, Additional file 2) provided additional confidence in the identification.

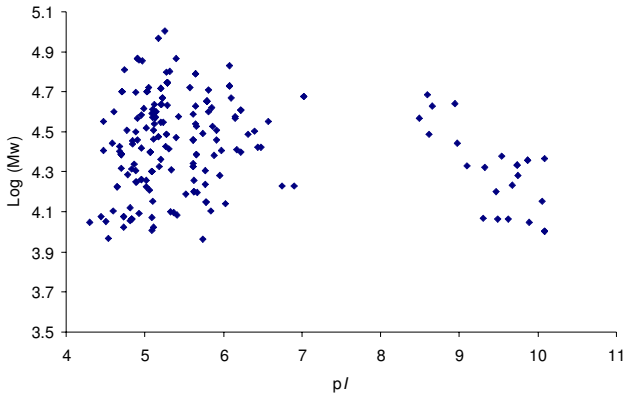

Figure 4
Representation of the bimodal distribution of the all identified proteins, according to the predicted p*I* and molecular weight. The most crowded regions are found at pH range of 4-7 and 9-11.

Occasionally, protein spots with only small shifts in molecular weight and/or pI were identified with the same sequence in the data base (e.g. spots; 34, 35 & 36, 64 & 67; spots 94 & 95, spots 271 & 273, 469 & 472; 473 & 474 among others, see also table S1, Additional file 1 and table S2, Additional file 2). These observations are a common feature of 2-DE gels [14,24], and possibly arise from the heterogeneity in post-translation modifications. Therefore within this context, membrane and cytoplasmatic fractions together contained 153 unique proteins. Other spots shared homology with the same protein families (e.g. spot # 1, spot # 2 and spot # 35), but with different corresponding gene sequences, indicating the presence of multi-gene families in the A. baumannii proteome.

The results demonstrate that the *A. baumannii* proteome is diverse in nature, and can be conveniently divided into at least 16 distinct functional groups, namely: amino acid transport and metabolism; carbohydrate transport and metabolism; cell division and chromosome partitioning; coenzyme metabolism; cell envelope and outer membrane biogenesis (transport); defence; energy production and conversion; general function predicted only; multifunctional; nucleotide transport and metabolism; post-translation modification, protein turnover, chaperones; redox reactions; RNA and protein synthesis; signalling; translation, ribosomal structure and biogenesis and transcription (see Fig. 5), in addition there was further 4 hypothetical proteins with unknown function. Whenever possible the proteins were classified according to the clusters of orthologous groups (COG) [25].

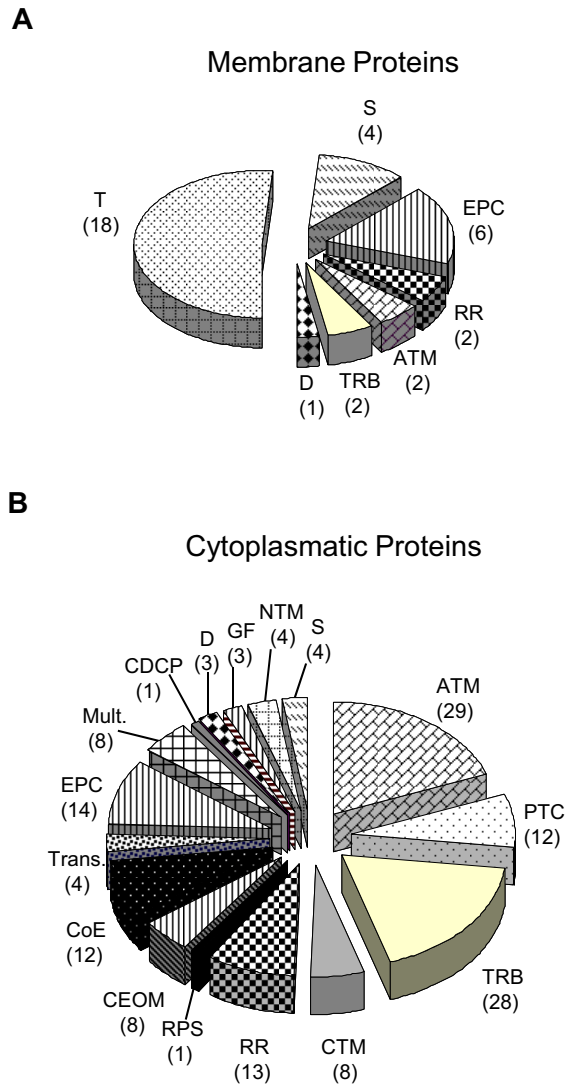

Figure 5
A functional classification of the 37 most abundant protein spots in the membrane fraction (A) and of the 155 most abundant protein spots in the cytoplasmatic fraction (B). The protein class was abbreviated as follows: ATM, amino acid transport and metabolism; CDCP, cell division and chromosome partitioning; CTM, carbohydrate transport and metabolism; CEOM, cell envelope biogenesis and outer membrane; CoE, coenzyme metabolism; D, Defence; EPC, energy production and conversion; GF, general function predicted only; Mult., multifunctional; NTM, nucleotide transport and metabolism; PTC, postranslation modification, protein turnover, chaperones; RPS, RNA and protein synthesis; RR, proteins involved in redox reactions; S, signalling; TRB, translation, ribosomal structure and biogenesis; Trans., transcription; T, transport. Note: Hypothetical proteins (3) with unknown function are not included in this classification.

Membrane extract

MALDI-TOF/TOF analyses of 37 selected membrane spots revealed that 12 were identified as outer membrane proteins (Omps) (*e.g.* spot # 459, 465, 466, 467, 468, 469, 470, 471, 472, 473, 474, and 496) and 7 proteins spots (spot # 462, 483, 484, 485, 488, 490 and 499) were identified as subunits of membrane-bound complex F(1)F(0)-ATP synthase (see table S2, Additional file 2). In addition, further analyses using PSORTb v.0.4 (a program for bacterial protein subcellular localisation prediction) [26] indicated that there are several other proteins which could be located in the membrane, for instance: spot # 460 (localisation (L): outer membrane; localisation score (LS): 9.49), spot # 461 (L: outer membrane; LS: 9.52), spot # 463, 464, 487 and 488 (L: outer membrane, LS: 9.49), spot # 478 (L: periplasmic, LS: 4.48), spot # 481 (L: Cytoplasmic membrane; LS: 0.51), spot # 493 (L: Cytoplasmic membrane; LS: 0.51), spot # 494 (L: Cytoplasmic membrane; LS: 0.51), spot # 495 (L: Cytoplasmic membrane; LS: 0.51).

Curiously, when comparing the data here presented with previous reports, it become visible that several proteins here identified are also present in the membrane proteome of other *A. baumannii* strains, including clinical isolates [13-15] (see table S2, Additional file 2). It is therefore tempting to propose that these proteins are constitutively present in the membrane of *A. baumannii* and if that so, then this valuable information can be utilised for development of new drugs, vaccines and/or diagnostic.

A number of Omps associated with the transport across the membrane of several compounds were identified in the present study. Including proteins such as putative copper receptor (OprC, spot # 459), which allows the penetration of small cations, a putative Omp (OprD, spot # 465) that in *Pseudomonas aeruginosa* has been demonstrated to be involved in the uptake of basic amino acids, small peptides and of imipenem [27]; putative glucose-sensitive porin (OprB-like spot # 466), this porin is often referred to as carbohydrate selective porin, since it acts as a central component of glucose, mannitol, glycerol, and fructose transport across the outer membrane [28]; Omp 38 precursor (spot # 467) belonging to the OmpA family, which has been suggested to be involved with the transport of β-lactams and saccharides up to approximately 800 Da [29,30]; an Omp (with homology with Omp 33-36 kDa, spot # 468) involved in the transport of water and carbapenems [31]; Omp CarO (spot # 469 & spot # 472), which is essential for the uptake of L-ornithine and participates in the selective uptake of carbapenems and other basic amino acids in *A. baumannii* [32].

Hence, the results indicate that the most abundant membrane proteins were those involved in the transport of dif-

ferent components (amino acid, sugars, and fatty acids), which suggests that *A. baumannii* have an adaptable metabolism that utilises a wide range of carbon sources.

Cytoplasmatic extract

MALDI-TOF/TOF analyses of cytoplasmatic extract revealed that of the 155 identified spots, 12 were identified as hypothetical proteins (see table S1, Additional file 1) and of those 9 could be functionally classified according COG (information obtained by MASCOT analyses). The three most representative groups are those related to amino acid and transport metabolism (29), translation, ribosomal structure and biogenesis (28) and energy production and conversion (14). Also there are other important groups (see table S1, Additional file 1 and Fig. 5). Analyses of the cytoplasmatic proteins revealed that much of the *A. baumannii* proteome is dedicated to the metabolism of a wide range of components. One of the most highly represented classes of proteins was that involved in amino acid transport and metabolism. This comprised proteins involved in the metabolism of amino acid such as glutamine (spot # 8), serine (spot # 64 & 67), aspartate (spot # 103), methionine (spot # 104), cysteine (spot # 182 & 186), trypthophan (spot # 233), lysine (spot # 95; 176 & 211), glutamate (spot # 85), proline (spot # 75), threonine (spot # 108), and histidine (spot # 120; 182 & 234). In addition, the multifunctional proteins included proteins such as branched-chain amino acid transferase, which catalyses the transamination of the branched-chain amino acids (spot # 132) leucine, isoleucine and valine to their respective alpha-keto acids [33]. Taking into consideration the number, level of expression (in a population with an average of % spot volume of 0.21 there was: spot # 67 0.6 ± 0.04; spot # 123 0.55 ± 0.03; spot # 285 1.13 ± 0.36; see also Fig. 2) and the diversity of proteins within this group, it is reasonable to conclude that the amino acid metabolism is in fact a major pillar of the overall *A. baumannii* metabolism.

Interestingly, a phospho-2-dehydro-3-heoxyheptonate aldolase (spot # 123) was identified; in *E. coli* this type of synthetase catalyses the first step in aromatic amino acid biosynthesis from chorismate [34]. Earlier studies have demonstrated that species of the genus *Acinetobacter* are capable of degrading aromatic compounds [24,35-37]. The capacity of *Acinetobacter* spp. to degrade aromatic compounds is of particular interest for bioremediation studies [38] and also for the development of new antibiotics [24]. Therefore, the protein here identified and its possible involvement in aromatic compound degradation may be subject of further investigation.

As mentioned above, a low molecular weight protein named nitrogen assimilation regulatory protein P-II 2 (spot # 352) was identified. In *E. coli* this protein regulates the assimilation of nitrogen by modulating the activity of glutamase synthase [39], this regulatory mechanism allows the cell to adjust the glutamase synthase activity quickly - in response to alterations in the abundance of the preferred nitrogen source, ammonia [39]. Although further investigation is required, this suggests that nitrogen is another source of energy utilised by this microorganism.

In concordance with previous genomic studies [8,9,40] that indicated the inability of *A. baumannii* to catabolise glucose, the current proteomic analysis did not detect any enzymes such as hexokinase, glucosekinase or proteins of the phosphotransferase transport system essential for glycolysis. However, it has to be referred the already mentioned presence of the putative glucose porin sensitive outer membrane (OprB-like) suggests the uptake of glucose from *A. baumannii*. Hence, this information supports the existence of a route passing through the Entner-Doudoroff pathway [41], in which the oxidation of glucose in the periplasm leads to pyruvate formation. Moreover, the presence of both fructose-1,6-bisphosphatase (spot # 138) and fructose-1,6-bisphosphate aldolase (spot # 156), shows that the bacterium in question is capable of catabolising fructose. Hence, it would be interesting to investigate further the capability of these and other sugars to support growth of this bacterium.

Identification of the selected alkaline spots revealed that most were ribosomal proteins (see table S1, Additional file 1) as previously described in other microbe studies [42]. In addition, to ribosome-associated proteins, several other proteins of the translational machinery were also detected. For instance, translation elongation factors EF-G (spot # 5), EF-Tu (spot # 100), EF-Ts (spot # 178), EF-P (spot # 235) and ribosome releasing factor (spot # 248). Ribosomes, ribosome-associated proteins and proteins associated with translation are targets for many antibiotics, which interfere with translation through different molecular mechanisms of action [12]. As far as we know, this is the first proteomic study that has identified such a large number of ribosomes and ribosome-associated proteins in the *A. baumannii* proteome, and we believe that the data provided here can serve as preliminary data for further studies on this bacterium, including studies of antibiotic drug action.

Proteins with potential role in drug resistance, stress response and in virulence

A recent description of the *A. baumannii* ATCC 17978 genome revealed that this strain has acquired several genes from its environment, these foreign genes are clustered in small (>10 kb) regions called putative alien islands (pAs) [9]. In addition, it was reported that ATCC 17978 genome have a total of 28 pAs and some of these

are associated with drug resistance, virulence, iron uptake, metabolism and others [9]. Of the identified proteins, only 26 out of 192 were encoded by genes mapped in these pAs (see table S1, Additional file 1 and table S2, Additional file 2). This led us to conclude that most of the expressed proteins correspond to genes located in the native *A. baumannii* chromosome. Hence, it is tempting to speculate that those pAs are mainly expressed under specific conditions, *e.g.* stress.

Although for the most cases it was not clear the association between the protein and its respective pAs function, there were a few examples where it was possible to establish a more direct association. For instance, heat-shock proteins (Hsps) namely chaperone Hsp60 (spot # 35), and Co-chaperonin GroES (spot # 347), are encoded by genes situated in drug resistance pA 23 [9]. Many of the Hsps are chaperones and are important for protection against environmental stress and provide tolerance to high temperature [43,44], nutrient deprivation [45], salinity and osmotic stress [46]. Moreover, taking into account that Hsp60 chaperones were by far one of the most abundant protein spot (spot # 35 1.13 ± 0.8); and considering the presence of other Hsps (spot # 1, 2 and 393), it appears reasonable to suggest that these Hsps play a relevant role in the responses of *A. baumannii* to environmental changes and in the survival and adaptation to stress conditions. At this respect, a recent report have shown downregulation of Hsp60 proteins associated with resistance to colistin concomitantly to a decrease in bacterial fitness in an *A. baumannii* isolate [47]. In addition to Hsps, the Universal stress proteins (Usps) here identified (spot # 332, 333 and 498) are encoded by genes located in pA 18, which is associated with drug resistance [9]. In *E. coli* the expression level of these small cytoplasmatic proteins increase when cells are exposed to stress including $CdCl_2$, H_2O_2, DNP, CCCP and osmotic stress [48], moreover Usp enhances the rate of cell survival during prolonged exposure to stress conditions [48]. In *A. baumannii*, the function of Usps remain elusive, recently we have observed that the expression of these proteins increase at late phases of *in vitro* growth (data not published), therefore Usps can be an attractive target for further studies concerning drug resistance.

Within the stress response context it is worthy to refer the presence of proteins known to play a relevant role in response to oxidative stress such as alkyl hydroperoxide reductase (spot # 271 and 273), superoxide dismutase (spot # 247), and glutathione peroxidase (478).

Here we have identified several proteins encoded by genes situated in pAs with a predicted role in virulence, however again it is not straightforward the association of those proteins with virulence. Nevertheless, amongst the proteins identified in this report, a few may be more directly related to virulence. For example, a protein blast alignment (data not shown) of the here identified OmpW revealed that this protein shares a high homology with putative virulence-related OmpW (gi|188591914) from *Cupriavidus taiwanensis*. Also, it has been suggested that Omp 38 (spot # 467) may act as a potential virulence factor inducing apoptosis of epithelial cells in the early stage of *A. baumannii* infection [[49], Choi, 2008 #392]. In addition, a recently publication describing the proteome of OMVs of a clinical *A. baumannii* presented evidence that virulence-associated proteins such as Omp38 (gi|126642864), OmpW (gi|126640380) and bacterioferritin (gi|126640856) are transported in OMVs, where they have been suggested to play an important role during *in vivo* infection [15]. It is of interest that whereas Kwon *et al.* (2009) [15] identified proteins such as 30S ribosomal protein S1 (spot # 3), Glutamine synthetase (spot # 8), Malic enzyme (spot # 21), Chaperone Hsp60 (spot # 35) and others (see table S1, Additional file 1) associated to the OMVs, we find these proteins exclusively in the cytoplasmatic fraction. In the referred study, the authors do not rule out the possibility of the entrapment of these proteins by unknown mechanism. If this is the case, then the data gathered here, together with that presented in the referred study provide a list of potential candidate cytoplasmatic proteins that can be transported in OMVs.

Furthermore, in the current study a putative type III effector (spot # 353) was identified, and the interactions between *Pseudomonas synringae*-host interaction is mediated in great part by effector proteins, which are injected into plant cells by type III secretion [50]. In *A. baumannii* the function of type III effector has yet to be elucidated, although it probably participates in bacterium-host interactions.

The specific virulence factors or pathogenic mechanisms of this bacterium remain elusive [51]. In light of the present results, it would be interesting to use a proteomic approach to investigate the expression of these and other proteins with a potential role in virulence, in the presence of virulence-induced stimuli or in the process of host-bacteria interactions (experiments are currently in progress).

Conclusion

Here we report for the first time a 2-DE based analysis, of both membrane and cytoplasmatic fraction of the opportunistic pathogen *A. baumannii*. Analysis of the most abundant proteins of this microorganism indicates that *A. baumannii* has a versatile and robust metabolism capable of utilising a wide range of nutrient sources. In addition, this study revealed the presence of highly expressed proteins such as porins (membrane fraction) and chaperones or heat-shock proteins and others, which are likely to play

a crucial role not only in mechanisms of virulence and drug resistance, but also in adaptive environmental responses, which are probably related to the persistence in hospital settings, one of the hallmark of this microorganism. Thus, this proteomic approach provides us with new molecular tools to investigate the complexity of mechanisms operating during virulence and adaptive responses of this pathogen, which has been recently outlined by the Infectious Diseases Society of America as one of six important highly dangerous drug resistant microbes in hospitals worldwide.

Abbreviations

2-DE: two-dimensional gel electrophoresis; Hsp: heat-shock protein; MALDI: matrix-assisted laser desorption ionisation; Omp: outer membrane protein; pAs: putative alien islands; TOF: time of flight.

Competing interests

The authors declare that they have no competing interests.

Authors' contributions

NCS, MPC and GB have made substantial contributions to conception and design of the experiments. NCS and MPC carried out the 2-DE gels experiments and performed the MALDI-TOF/TOF acquisition and interpretation of data. NCS and JRP carried out the Image Master data analysis and interpretation. MPC, CG and MJB were responsible for cell culture and protein sample. NCS, CPC and GB have been involved in drafting the manuscript or revising it critically for important content. All authors read and approved the final manuscript.

Additional material

Additional file 1

Table S1 - MALDI-TOF/TOF identification of* Acinetobacter baumannii *cytoplasmatic protein spots. *Identified proteins are listed with 2-DE spot numbers, protein description, theoretical Mr and* pI*, in gel Mr and* pI*, accession numbers, functional class, values resulting from Mascot data (score, number of matched peptides and percentage coverage) and information concerning the respective pAs.*
Click here for file
[http://www.biomedcentral.com/content/supplementary/1477-5956-7-37-S1.PDF]

Additional file 2

Table S2 - MALDI-TOF/TOF identification of* Acinetobacter baumannii *membrane protein spots. *Identified proteins are listed with 2-DE spot numbers, protein description, theoretical Mr and* pI*, in gel Mr and* pI*, accession numbers, functional class, values resulting from Mascot data (score, number of matched peptides and percentage coverage) and information concerning the respective pAs.*
Click here for file
[http://www.biomedcentral.com/content/supplementary/1477-5956-7-37-S2.PDF]

Additional file 3

Table S3 - MALDI-TOF/TOF identification of* Acinetobacter baumannii *proteins with the respective matched peptide sequences. *Complementary results of the MALDI-TOF/TOF and MASCOT analyses. For each protein the number and the sequences of matched peptides and corresponding NCBI identifier are provided.*
Click here for file
[http://www.biomedcentral.com/content/supplementary/1477-5956-7-37-S3.PDF]

Acknowledgements

NCS was supported by the Ministerio de Sanidad y Consumo, Instituto de Salud Carlos III-FEDER, Spanish Network for the Research in Infectious Diseases (REIPI RD06/0008). This work was also funded by FIS PI061368, PI081613; and 08CSA064916PR and SERGAS PS07/90 from Xunta de Galicia

References

1. Charnot-Katsikas A, Dorafshar AH, Aycock JK, David MZ, Weber SG, Frank KM: **Two Cases of Necrotizing Fasciitis Due to *Acinetobacter baumannii*.** *J Clinical Microbiol* 2009, **47:**258-263.
2. Fournier P, Richet H: **The epidemiology and control of *Acinetobacter baumannii* in health care facilities.** *Clin Infect Dis Dis* 2006, **42:**692-699.
3. Katsaragakis S, Markogiannakis H, Toutouzas K, Drimousis P, Larentzakis A, Theodoraki E-M, Theodorou D: ***Acinetobacter baumannii* infections in a surgical intensive care unit: predictors of multi-drug resistance.** *World J Surg* 2008, **32:**1194-1202.
4. Bou G, Cervero G, Dominguez MA, Quereda C, Martinez-Beltran J: **Characterization of a nosocomial outbreak caused by a multiresistant *Acinetobacter baumannii* strain with a carbapenem-hydrolyzing enzyme: high-level carbapenem resistance in *A. baumannii* is not due solely to the presence of beta-lactamases.** *J Clin Microbiol* 2000, **38:**3299-3305.
5. Jones M, Draghi D, Thornsberry C, Karlowsky J, Sahm D, Wenzel R: **Emerging resistance among bacterial pathogens in the intensive care unit - a European and North American Surveillance study (2000-2002).** *Ann Clin Microbiol Antimicrob* 2004, **3:**14.
6. Vila J, Marti S, Sanchez-Cespedes J: **Porins, efflux pumps and multidrug resistance in *Acinetobacter baumannii*.** *J Antimicrob Chemother* 2007, **59:**1210-1215.
7. Fournier P-E, Vallenet D, Barbe V, Audic S, Ogata H, Poirel L, Richet H, Robert C, Mangenot S, Abergel C, *et al.*: **Comparative genomics of multidrug resistance in *Acinetobacter baumannii*.** *PLoS Genet* 2006, **2:**e7.
8. Vallenet D, Nordmann P, Barbe V, Poirel L, Mangenot S, Bataille E, Dossat C, Gas S, Kreimeyer A, Lenoble P, *et al.*: **Comparative analysis of *Acinetobacters*: three genomes for three lifestyles.** *PLoS ONE* 2008, **3:**e1805.
9. Smith MG, Gianoulis TA, Pukatzki S, Mekalanos JJ, Ornston LN, Gerstein M, Snyder M: **New insights into *Acinetobacter baumannii* pathogenesis revealed by high-density pyrosequencing and transposon mutagenesis.** *Genes Dev* 2007, **21:**601-614.
10. Keller M, Hettich R: **Environmental proteomics: a paradigm shift in characterizing microbial activities at the molecular level.** *Microbiol Mol Biol Rev* 2009, **73:**62-70.
11. Gupta N, Tanner S, Jaitly N, Adkins JN, Lipton M, Edwards R, Romine M, Osterman A, Bafna V, Smith RD, Pevzner PA: **Whole proteome analysis of post-translational modifications: applications of mass-spectrometry for proteogenomic annotation.** *Genome Res* 2007, **17:**1362-1377.
12. Brötz-Oesterhelt H, Bandow JE, Labischinski H: **Bacterial proteomics and its role in antibacterial drug discovery.** *Mass Spectrom* 2005, **24:**549-565.
13. Martí S, Sánchez-Céspedes J, Oliveira E, Bellido D, Giralt E, Vila J: **Proteomic analysis of a fraction enriched in cell envelope proteins of *Acinetobacter baumannii*.** *Proteomics* 2006, **6:**S82-S87.

14. Siroy A, Cosette P, Seyer D, Lemaitre-Guillier C, Vallenet D, Van Dorsselaer A, Boyer-Mariotte S, Jouenne T, De E: **Global comparison of the membrane subproteomes between a multidrug-resistant *Acinetobacter baumannii* strain and a reference strain.** *J Proteome Res* 2006, **5:**3385-3398.
15. Kwon S-O, Gho YS, Lee JC, Kim SI: **Proteome analysis of outer membrane vesicles from clinical *Acinetobacter baumannii* isolate.** *FEMS Microbiol Lett* 2009, **297:**159-156.
16. Molloy MP, Herbert BR, Slade MB, Thierry R, Nouwens AS, Williams KL, Gooley AA: **Proteomics analysis of the *Escherichia coli* outer membrane.** *Eur J Biochem* 2000, **267:**2871-2881.
17. Bradford M: **A rapid and sensitive method for the quantification of microgram quantities of protein utilizing the principle of protein-dye binding.** *Anal Biochem* 1976, **72:**248-254.
18. Ramagli L: **Quantifying protein in 2-D PAGE solubilisation buffers.** *Methods Mol Biol* 1999, **112:**99-103.
19. Laemmli UK: **Cleavage of structural proteins during the assembly of head proteins of bacteriophage T4.** *Nature* 1970, **227:**680-685.
20. Blum H, Beier H, Gross H: **Improved silver staining of plant proteins, RNA and DNA in polyacrylamide gels.** *Electrophoresis* 1987, **8:**93-99.
21. Pandey A, Andersen J, Mann M: **Use of mass spectrometry to study signalling pathways.** *Sci STKE* 2000, **2000:**PL1.
22. Sechi S, Chait BT: **Modification of cysteine residues by alkylation. A tool in peptide mapping and protein identification.** *Anal Chem* 1998, **70:**5150-5158.
23. Lamberti C, Pessione E, Giuffrida MG, Mazzoli R, Barello C, Conti A, Giunta C: **Combined cup loading, bis(2-hydroxyethyl) disulfide, and protein precipitation protocols to improve the alkaline proteome of *Lactobacillus hilgardii*.** *Electrophoresis* 2007, **28:**1633-1638.
24. Park S-H, Kim J-W, Yun S-H, Leem S-H, Kahng H-Y, Kim SI: **Characterization of beta-ketoadipate pathway from multi-drug resistance bacterium, *Acinetobacter baumannii* DU202 by proteomic approach.** *J Microbiol* 2006, **44:**632-640.
25. Tatusov RL, Koonin EV, Lipman DJ: **A genomic perspective on protein families.** *Science* 1997, **278:**631-637.
26. Gardy JL, Laird MR, Chen F, Rey S, Walsh CJ, Ester M, Brinkman FS: **PSORTb v.2.0: Expanded prediction of bacterial protein subcellular localization and insights gained from comparative proteome analysis.** *Bioinformatics* 2005, **21:**617-623.
27. Nikaido H: **Molecular basis of bacterial outer membrane permeability revisited.** *Microbiol Mol Biol Rev* 2003, **67:**593-656.
28. Wylie JL, Worobec EA: **The OprB porin plays a central role in carbohydrate uptake in *Pseudomonas aeruginosa*.** *J Bacteriol* 1995, **177:**3021-3026.
29. Gribun A, Nitzan Y, Pechatnikov I, Hershkovits G, Katcoff DJ: **Molecular and structural characterization of the HMP-AB gene encoding a pore-forming protein from a clinical isolate of *Acinetobacter baumannii*.** *Curr Microbiol* 2003, **47:**434-443.
30. Nitzan Y, Pechatnikov I, Bar-El D, Wexler H: **Isolation and characterization of heat-modifiable proteins from the outer membrane of *Porphyromonas asaccharolytica* and *Acinetobacter baumannii*.** *Anaerobe* 1999, **5:**43-50.
31. del Mar Tomas M, Beceiro A, Perez A, Velasco D, Moure R, Villanueva R, Martinez-Beltran J, Bou G: **Cloning and functional analysis of the gene encoding the 33- to 36-kilodalton outer membrane protein associated with carbapenem resistance in *Acinetobacter baumannii*.** *Antimicrob Agents* 2005, **49:**5172-5175.
32. Mussi MA, Relling VM, Limansky AS, Viale AM: **CarO, an *Acinetobacter baumannii* outer membrane protein involved in carbapenem resistance, is essential for L-ornithine uptake.** *FEBS Let* 2007, **581:**5573-5578.
33. Harper AE, Miller RH, Block KP: **Branched-Chain Amino Acid Metabolism.** *Annual Review of Nutrition* 1984, **4:**409.
34. Shumilin I, Kretsinger R, Bauerle R: **Crystal structure of phenylalanine-regulated 3-deoxy-D-arabino-heptulosonate-7-phophate synthase from Escherichia coli.** *Structure* 1999, **7:**865-875.
35. Giuffrida MG, Pessione E, Mazzoli R, Dellavalle G, Barello C, Conti A, Giunta C: **Media containing aromatic compounds induce peculiar proteins in *Acinetobacter radioresistens*, as revealed by proteome analysis.** *Proteomics* 2001, **22:**1705-1711.
36. Pessione E, Giuffrida MG, Barello C, Mazzoli R, Fortunato D, Conti A, Giunta C: **Membrane proteome of *Acinetobacter radioresistens* S13 during aromatic exposure.** *Proteomics* 2003, **3:**1070-1076.
37. Kim E-A, Kim JY, Kim S-J, Park KR, Chung H-J, Leem S-H, Kim SI: **Proteomic analysis of *Acinetobacter lwoffii* K24 by 2-D gel electrophoresis and electrospray ionization quadrupole-time of flight mass spectrometry.** *J Microbio Methods* 2004, **57:**337-349.
38. Kim SI, Choi J-S, Kahng H-Y: **A proteomics strategy for the analysis of bacterial biodegradation pathways.** *OMICS* 2007, **11:**280-294.
39. Jiang P, Zucker P, Atkinson MR, Kamberov ES, Tirasophon W, Chandran P, Schefke BR, Ninfa AJ: **Structure/function analysis of the PII signal transduction protein of *Escherichia coli*: genetic separation of interactions with protein receptors.** *J Bacteriol* 1997, **179:**4342-4353.
40. Iacono M, Villa L, Fortini D, Bordoni R, Imperi F, Bonnal RJ, Sicheritz-Ponten T, De Bellis G, Visca P, Cassone A, Carattoli A: **Whole genome pyrosequencing of an epidemic multidrug resistant *Acinetobacter baumannii* strain belonging to the European clone II group.** *Antimicrob Agents Chemother* 2008. ACC.01643-01607
41. Taylor WH, Juni E: **Pathways for biosynthesis of a bacterial capsular polysaccharide II.: Carbohydrate metabolism and terminal oxidation mechanisms of a capsule-producing Coccus.** *J Bacteriol* 1961, **81:**694-703.
42. Kolker E, Purvine S, Galperin MY, Stolyar S, Goodlett DR, Nesvizhskii AI, Keller A, Xie T, Eng JK, Yi E, *et al.*: **Initial proteome analysis of model microorganism *Haemophilus influenzae* strain Rd KW20.** *J Bacteriol* 2003, **185:**4593-4602.
43. Lu Q, Han J, Zhou L, Coker JA, DasSarma P, DasSarma S, Xiang H: **Dissection of the regulatory mechanism of a heat-shock responsive promoter in *Haloarchaea*.** *Nucleic Acids Res* 2008, **36:**3031-3042.
44. Plesofsky-Vig N, Brambl R: **Heat shock response of *Neurospora crassa*: protein synthesis and induced thermotolerance.** *J Bacteriol* 1985, **162:**1083-1091.
45. Spence J, Cegielska A, Georgopoulos C: **Role of *Escherichia coli* heat shock proteins DnaK and HtpG (C62.5) in response to nutritional deprivation.** *J Bacteriol* 1990, **172:**7157-7166.
46. Bhagwat AA, Apte SK: **Comparative analysis of proteins induced by heat shock, salinity, and osmotic stress in the nitrogen-fixing cyanobacterium *Anabaena* Csp. strain L-31.** *J Bacteriol* 1989, **171:**5187-5189.
47. Fernández-Reyes M, Rodríguez-Falcón M, Chiva C, Pachón J, Andreu D, Rivas L: **The cost of resistance to colistin in *Acinetobacter baumannii*: a proteomic perspective.** *Proteomics* 2009, **9:**1632-45.
48. Nystrom T, Neidhardt FC: **Expression and role of the universal stress protein, UspA, of *Eschrichia coli* during growth arrest.** *Mol Microbiol* 1994, **11:**537-544.
49. Choi CH, Lee EY, Lee YC, Park TI, Kim HJ, Hyun SH, Kim SA, Lee S-K, Lee JC: **Outer membrane protein 38 of *Acinetobacter baumannii* localizes to the mitochondria and induces apoptosis of epithelial cells.** *Cell Microbiol* 2005, **7:**1127-1138.
50. Lindeberg M, Stavrinides J, Chang JH, Alfano JR, Collmer A, Dangl JL, Greenberg JT, Mansfield JW, Guttman DS: **Proposed guidelines for a unified nomenclature and phylogenetic analysis of type III Hop effector proteins in the plant pathogen *Pseudomonas syringae*.** *Mol Plant Microbe Interact* 2005, **18:**275-282.
51. Choi CH, Hyun SH, Lee JY, Lee JS, Lee YS, Kim SA, Chae J-P, Yoo SM, Lee JC: ***Acinetobacter baumannii* outer membrane protein A targets the nucleus and induces cytotoxicity.** *Cell Microbiol* 2008, **10:**309-319.

research articles Journal of proteome research

Associating Growth-Phase-Related Changes in the Proteome of *Acinetobacter baumannii* with Increased Resistance to Oxidative Stress

Nelson C. Soares,[#] Maria P. Cabral,[#] Carmen Gayoso, Susana Mallo, Patricia Rodriguez-Velo, Esteban Fernández-Moreira, and Germán Bou*

Servicio de Microbiologia-INIBIC, Complejo Hospitalario Universitario La Coruña, As Xubias s/n, 15006 La Coruña, Spain

Received December 4, 2009

Acinetobacter baumannii is an opportunistic pathogen that has been associated with severe infections and outbreaks in hospitals. At present, very little is known about the biology of this bacterium, particularly as regards mechanisms of adaptation, persistence and virulence. To investigate the growth phase-dependent regulation of proteins in this microorganism, we analyzed the proteomic pattern of *A. baumannii* ATCC 17978 at different stages of *in vitro* growth. In this study, proteomics analyses were conducted using 2-DE and MALDI-TOF/TOF complemented by iTRAQ LC-MS/MS. Here we have identified 107 differentially expressed proteins. We highlight the induction of proteins associated with signaling, putative virulence factors and response to stress (including oxidative stress). We also present evidence that ROS (O_2^- and OH^-) and RNI ($ONOO^-$) accumulate during late stages of growth. Further assays demonstrated that stationary cells survive at high concentrations of H_2O_2 (30 mM), the O_2^- donor menadione (500 μM) or the NO donor sodium nitroprusside (1 mM), and showed a higher survival rate against several bactericidal antibiotics. The growth phase-dependent changes observed in the *A. baumannii* proteome are discussed within a context of adaptive biological responses, including those related to ROS and RNI stress.

Keywords: Proteomics • Growth curve • *Acinetobacter baumannii* • Oxidative stress • Antibiotic resistance • 2-DE • iTRAQ • MALDI-TOF/TOF

Introduction

Acinetobacter baumannii is a Gram-negative, nonmotile, aerobic coccobacillus that is often found in health care settings, where it has been associated with several types of infections that mostly affect debilitated hospitalized patients in the ICUs.[1,2] Recently, this pathogen has been related with fatal cases of necrotizing fasciitis.[3] *A. baumannii* is often referred as a successful pathogen, not only due to its epidemiological characteristics, but also due to its outstanding ability to acquire resistance to most antibiotics used in clinical practice.[1,4,5] Despite the attention given to this bacterium over the last 10 years,[2] so far little is known about the mechanisms operating during adaptation, virulence and persistence of *A. baumannii*. Hence, as pointed out by Dijkshoorn et al.,[1] the employment of further approaches such as genomics, proteomics and fitness studies might contribute insights into the mechanisms behind the remarkable adaptability of this pathogen to variable conditions and selective pressures.

Recent studies have revealed some pertinent aspects of the *A. baumannii* proteome.[6−8] For instance, a 2-DE -based analysis demonstrated that this microorganism has a robust and versatile metabolism[8] and a comparative study between a drug-susceptible and multidrug-resistant strains revealed that the latter showed significant differences in the membrane protein pattern.[7] In addition, a comparison between a colistin-resistant and a susceptible strain demonstrated that the induced resistance was associated with the down-regulation of several proteins.[9] However, with the exception of the latter study, changes in the *A. baumannii* proteome in response to changes in environmental conditions and/or in response to stress have not been investigated in any detail. Analysis of the changes that occur during *in vitro* growth culture is a suitable mean for obtaining useful information regarding bacterial adaptation. Throughout *in vitro* growth, bacteria are exposed to several different conditions in the surrounding medium. For instance, during the exponential phase, all nutrients are present in excess and there is scarce accumulation of waste products; these nearly optimal conditions favor bacterial growth and this stage is characterized by doubling of the population.[10] There then follows a period during which the growth rate of bacteria slows down owing to nutrient limitation and/or accumulation of an end product, and the organisms must respond accordingly to such limitations. During the stationary phase of growth, the bacteria are exposed to a much more hostile environment as the culture reaches its maximum cell density, so that individuals face strong competition and a lack of nutrients,

* To whom correspondence should be addressed. Dr. Germán Bou. Phone: +34-981176087. Fax: +34-981176097. E-mail: German.Bou.Arevalo@sergas.es.
[#] These authors have contributed equally to this work.

10.1021/pr901116r

Published on Web 01/28/2010

changes in pH, induction of several virulence factors, oxygen depletion and accumulation of toxic products.[11] Thus, as mentioned by Lee et al.,[12] proteins that undergo significant changes in the level of expression throughout the growth curve are likely to play a relevant role in central intermediary metabolism, amino acid synthesis, nucleotide, and fatty acid metabolism, cell wall synthesis, protein degradation and stress responses.

Reactive oxygen species (ROS) and reactive nitrogen intermediates (RNI) are potentially highly reactive molecules that are continuously produced in organisms as byproduct of aerobic respiration metabolism and under hypoxic conditions, respectively. Previous reports have demonstrated that late phases of growth are often associated with the induction of stress responsive proteins, including those specifically associated with oxidative stress.[12−15] Moreover, in other bacterial species, it has been demonstrated that late stationary cells support higher concentrations of ROS.[13,16,17] Similarly, it has been demonstrated that during stationary phase there is an increase in the expression of proteins associated with responses to nitric oxide (NO) and RNI stress.[18,19]

Understanding bacterial adaptation to oxidative and nitrosative stress is of particular interest, as during infection microbial pathogens are literally engulfed by phagocytic cells, such as macrophages, and are then exposed to lethal levels of both ROS and RNI.[20,21] Moreover, further interest has been recently focused in bacterial resistance to oxidative stress following the demonstration that the production of ROS is in fact a common mechanism of cell death initiated by bactericidal antibiotics.[22,23] Furthermore, it has been recently demonstrated that, in *Escherichia coli*, this mode of action of ROS can be extended to include other bacteriostatic antibiotics.[24]

Herein, we present a report that for the first time provides a dynamic view of the *A. baumannii* proteome during adaptation to different environmental conditions. In addition, changes observed are discussed within the context of adaptive biological responses, including those related to ROS and RNI stress.

Materials and Methods

Bacterial Strain and Growth Conditions. *A. baumannii* ATCC 17978 was grown overnight in Mueller Hinton (MH) broth (Fluka, St. Louis, MO) at 37 °C with constant shaking. Fresh nutrient medium (500 mL) was inoculated with a 1:100 dilution of the overnight culture and grown at 37 °C with vigorous shaking. Cells were harvested at exponential ($OD_{600\ nm} = 0.4$), early stationary ($OD_{600\ nm} = 1.4$) and late stationary phases of growth, approximately 48 h after inoculation ($OD_{600\ nm} = 2.0$).

Protein Extraction. Cytoplasmatic Protein Fraction. The cells were harvested by centrifugation at 3500*g* for 15 min and washed twice with 10 mL of 0.9% (w/v) NaCl. The resultant pellet was resuspended in 3−5 mL of disintegration buffer[6] (7.8 g/L NaH_2PO_4, 7.1 g/L Na_2HPO_4, 0.247 g/L $MgSO_4 \cdot 7H_2O$ + protease inhibitor mix (GE Healthcare, Piscataway, NJ)) + nuclease mix (GE Healthcare) and sonicated on ice for 3 periods of 5 min. Unbroken cells were separated by centrifugation at 1500*g*. The supernatant was centrifuged for 30 min at 4 °C at 3395*g* and then clarified through a 0.45 μm filter (Millipore, Billerica, MA) to remove cell debris. Finally, the extract was processed with a 2-DE Cleanup Kit (GE Healthcare).

Membrane Protein Fraction. The same extraction method was used to extract the cell surface membrane. However, after separation of unbroken cells, the lysate was treated as described by Molloy et al.[25] Briefly, an equal volume of ice-cold 0.1 M sodium carbonate (pH 11) was added to the resulting supernatant and the mixture was stirred slowly overnight, on ice. The carbonate-treated membranes were then collected by ultracentrifugation at 100 000*g* for 45 min at 4 °C, and then resuspended in 500 μL of H_2O. The extract was processed with a 2-DE Cleanup Kit.

Two-Dimensional Gel Electrophoresis (2-DE). In this study, cell extracts were harvested at three time points of the *in vitro* growth curve (see above), and the membrane and cytoplasmatic fractions were analyzed separately. In addition, for cytoplasmatic protein, fractions were subject to isoelectric focusing (IEF) using IPG strips of pH 4−7 and pH 6−11 to obtain further resolution of acidic and basic proteins, respectively. The protein concentration in the extracts was determined with a Biorad protein assay kit (Biorad, Munich, Germany), by a modified Bradford assay[26] as suggested by Ramagli.[27]

For IEF, an IPGphor III system was used (GE Healthcare), with 3−10 nonlinear (NL), 4−7 linear (L) pH or 6−11 (L) pH gradient strips (13 cm IPG strips, GE Healthcare, Uppsala, Sweden). Proteins were solubilized in 8 M urea, 2% (w/v) CHAPS, 40 mM DTT and 0.5% (v/v) corresponding IPG buffer (GE Healthcare, Sweden) and 3 μL of DeStreak solution (GE Healthcare, Sweden). For 3−10 (NL) and 4−7 (L) pH gradient strips, IEF was carried out at 30 V for 12 h, followed by 250 V for 1 h, 500 V for 1.5 h, 1000 V for 1.5 h, a gradient to 8000 V for 1.5 h and maintenance at 8000 V for a further 4 h, all at 20 °C. For 6−11 (L) pH gradient strips, IEF was carried out at 30 V for 12 h, followed by 500 V for 1 h, 1000 V for 1 h, a gradient to 8000 V for 2.5 h and maintenance at 8000 V for 0.5 h. Prior to the second-dimension (SDS-PAGE), the focused IPG strips were equilibrated for 2 × 15 min in buffer containing 50 mM Tris-HCl (pH 8.8), 6 M urea, 30% (v/v) glycerol, 2% (w/v) SDS and a trace of bromophenol blue. One percent (w/v) DTT was added to the first equilibration step and 2.5% (w/v) iodoacetamide to the second. SDS-PAGE was performed on 12% or 15% polyacrylamide gels.[28] For analytical 2-DE gels, silver staining was performed according to Blum et al.,[29] and gels were loaded with 25−40 μg of total protein. For preparative gels, MS-compatible silver staining[30] was used and the gels were loaded with at least 250 μg of total protein.

Image Acquisition and 2-DE Analyses. Gels of at least three biological replicates were scanned with an Image Scanner version (v).3.3 densitometer (GE Healthcare, Sweden) and analyzed with Image Master Platinum software, v.6.0, as described by the manufacturer (GE Healthcare, Sweden). Briefly, a matched set consisting of three images was created for each time point on the curve, which allowed intercomparative analyses between three matched sets consisting of nine images. For spot detection, the parameters were adjusted in the following order: smooth 2; MinArea 5; Saliency 1.00000, and only spots observed on all three gels of a replicated group were considered for further analyses. Numerical data for individual spots were generated automatically and expressed as % of spot volume. A minimum fold-change of two and Student *t*-test ($p < 0.050$) was used to select for significant changes in protein levels between growth phases.

Trypsin Digestion of Proteins and Characterization by MALDI-TOF/TOF. Selected spots were excised from the gels and destained in 20% (w/v) sodium thiosulphate and 1% (w/v) potassium ferricyanide for 5 min. Destained spots were then in-gel reduced, alkylated and digested with trypsin as suggested by Sechi and Chait.[31] Briefly, spots were washed

twice with 25 mM ammonium bicarbonate in 50% (v/v) acetonitrile (ACN) for 20 min. The gel spots were then incubated with 100% (v/v) ACN and dried in a Speed-Vac (Savant, Ramsey, MN). The samples were reduced with DTT and subsequently alkylated with iodoacetamide. Samples were digested overnight with 20 ng/μL sequencing grade trypsin (Roche Applied Science, Mannheim, Germany) at 37 °C. After digestion, the supernatant was collected and 1 μL was spotted onto a MALDI target plate (384-spot Teflon-coated plates) and allowed to air-dry at room temperature. Where necessary, tryptic peptides were passed through C18 Zip-Tips (Millipore) prior to spotting. The dried peptide digests were mixed with 3 mg/mL of an α-cyano-4-hydroxycinnamic acid in 0.1% (v/v) TFA and 50% (v/v) ACN and allowed to air-dry. The samples were analyzed using a MALDI-TOF/TOF mass spectrometer 4800 Proteomics Analyzer (Applied Biosystems, Farmingham, MA) and 4000 Series explorer software (Applied Biosystems). MALDI-TOF spectra were acquired in reflector positive ion mode using 1000 laser shots per spectrum. Data Explorer v.4.2 (Applied Biosystems) was used for spectra analyses and generating peak picking list. All mass spectra were internally calibrated using autoproteolytic trypsin fragments and externally calibrate using standard peptide mixture (Sigma-Aldrich, St. Louis, MO). TOF/TOF fragmentation spectra were acquired by selecting the 10 most abundant ions of each MALDI-TOF peptide mass map (excluding trypsin autolytic peptides and other background ions) and averaging 2000 laser shots per fragmentation spectrum. The parameters used to analyze the data were a signal-to-noise threshold of 20, minimum area of 100 and a resolution higher than 10 000 with a mass accuracy of 20 ppm. For database queries and protein identification, the monoisotopic peptide mass fingerprinting data obtained from MS and the amino acid sequence tag obtained from each peptide fragmentation in MS/MS analyses were used to search for protein candidates using Mascot v.1.9 from Matrix Science (www.matrixscience.com). Peak intensity was used to select up to 50 peaks per spot for peptide mass fingerprinting and 50 peaks per precursor for MS/MS identification. Tryptic autolytic fragment-, keratin-, and matrix-derived peaks were removed from the data set utilized for database search. The search for peptides mass fingerprints and tandem MS spectra were performed in NCBInr database without any taxonomy restriction. Fixed and variable modifications were considered (Cys as S-carbamidomethyl and Met as oxidized methionine, respectively), allowing one trypsin missed cleavage. MS/MS ions search were conducted with a mass tolerance of ±1.2 Da on the parent and 0.3−0.8 Da on fragments. Decoy search was done automatically by Mascot on randomized database of equal composition and size. Mascot scores for all protein identifications were higher than the accepted threshold for significance (at the $p < 0.050$ level, positive rate measured to be 0.047).

iTRAQ Analysis. Protein Label. Total proteins samples were submitted to W.M. Keck Foundation Biotechnology resource laboratory at Yale University (New Haven, CT). To accurately determine the protein concentration, each sample was subject to AAA (amino acid analysis). Sample labeling with isobaric tagging reagents was carried out according to the manufacturer's instructions (Applied Biosystems). Briefly, 50 μg was dissolved in 20 μL of dissolution buffer and 2 μL of denaturant (2% SDS) from iTRAQ kit. Two microliters of reducing reagent (50 mM TCEP) was added followed by incubation at 60 °C for 1 h. After centrifugation, 1 μL of cysteine-blocking (200 mM MMTS) agent was added and incubated at room temperature for 10 min. This was followed by addition of 5 μL of Lys C which was incubated for 5 h at 37 °C and then 5 μL of Trypsin (Promega grade, Madison, WI) incubated overnight at 37 °C. Digested samples were labeled with eight different iTRAQ reagents dissolved in 50 μL of isopropanol and left at room temperature for 2 h. The samples were labeled with iTRAQ tag as follows: exponential1, iTRAQ 113; exponential2, iTRAQ 114; Late stationary1, iTRAQ 115; Late stationary2, iTRAQ 116. The differentially labeled digests were mixed and analyzed by LC-MS/MS.

Cation-Exchange Chromatography and LC-MS/MS Analyses. After digestion, 180 μL of the combine peptide mixture was loaded onto an off-line strong cation exchange chromatography (SCX) using an Applied Biosystems Vision Workstation with a 2.1 mm × 200 mm PolySulfethyl A column (5 μm 300 Å bead, from PolyLC, Inc., 2.1 × 200 mm, PN 202SE0503). The PolySulfethyl A column is equilibrated with Buffer A (10 mM KH_2PO_4, 25% ACN, pH 3.0). Peptides are then separated into 20 fractions using a 90 min linear salt gradient from 0−98% Buffer B (10 mM KH_2PO_4, 25% ACN, 1 M KCl, pH 3.0). All 20 collected fractions from the SCX chromatography were dried and reconstituted with 5 μL of 70% Formic acid and 15 μL of 0.1% TFA. LC-MS/MS was performed on a QSTAR Elite mass spectrometer interfaced with a Waters nanoAcquity UPLC system running Analyst QS 2.0 software. Peptides were resolved for LC-MS/MS by loading 5 μL of sample onto a Symmetry C18 nanoAcquity trapping column (180 μm × 20 mm, 5 μm) with 2% ACN/0.1% FA at 15 μL/min for 3 min. After trapping, peptides were resolved on a BEH130 C18 nanoAcquity column (75 μm × 250 mm, 1.7 μm) with a 60 min, 2−40% ACN/0.1% FA linear gradient (0.3 μL/min flow rate).

Electrospray ionization was performed using a Nanospray II interface (Applied Biosystems) equipped with the Microionspray source and FS360-75-15-D-20 PicoTip Emitter (New Objective, Inc., Woburn, MA). Data dependent acquisition with each cycle consisted of 0.2 s MS spectrum and MS/MS acquisition using Smart CE and Smart Exit functionality on three highest peptide peaks.

Data Analysis and Statistics. Each of the QSTAR Elite mass spectrometer spectra files (*.wiff) was processed with MASCOT Distiller v.2.3.1 and the resulting peak lists were combined and database searched using MASCOT Server 2.2.06 and Swiss-Prot 57.0 (released March 24, 2009 and contained 428 650 sequences). The search parameters included trypsin with one miscleavage, static modifications carbamidomethyl (cys) and iTRAQ reagents (N-term, K), and variable modifications for oxidation (met). iTRAQ Quantiation and secondary protein identification was performed using the Paragon search algorithm[32] in ProteinPilot v.3.0 software using Swiss-Prot 57.0 database with "thorough search". The "iTRAQ 8plex peptide labeled" sample type and a "biological modification ID focus" were selected in the analysis method. Trypsin was selected as the digestion enzyme with cysteine alkylation by methyl methane thiosulfonate as a modification. Raw data that included, but was not limited to, reporter ion peak areas, reporter ion peak area error, and peptide assignment, and confidence was exported from ProteinPilot (tab-delimited) without ProteinPilot's auto bias correction applied (non-normalized data) so we could perform quantile normalization as described below. The tab delimited ProteinPilot results was then uploaded into our Yale Protein Expression Database (YPED). For secondary protein identification, each protein had to have also been

identified by Paragon and had two or more identified peptides and a ProteinPilot Confidence Score >2 (99% confidence level). To ensure that we only compared data that ProteinPilot includes in its quantitation analysis, peptides had to be classified as "used", which requires the presence of an iTRAQ label and at least one valid iTRAQ reporter ion ratio. Additionally, ProteinPilot only uses high-quality reporter ions for the peak area measurements to calculate iTRAQ peptide ratios. To remove low-intensity reporter ion ratios from the exported raw data sets, we used ProteinPilot's nonmodifiable criterion, which requires that valid iTRAQ reporter ion ratios must contain two iTRAQ reporter ions with a summed S/N ratio >9 to be included in the analysis. The data was then merged and loaded onto the Yale Protein expression database (YEPD, http://yped.med.yale.edu), which allows the view data online and perform downstream data analysis.

Real Time Reverse Transcription (QRT-PCR) Analysis. The samples were collected as described above. Total RNA was isolated from harvested bacteria with the RNeasy Mini Kit (Qiagen, Huntsville, AL), according to the manufacturer's instructions. Each preparation was incubated with RNase-free DNase (Promega) at room temperature for 45 min, extracted with phenol/chloroform (1:1 v/v) and precipitated with ethanol. Purified RNA was resolved on an ethidium bromide-containing agarose gel to check integrity. Reverse transcription (RT) was carried out according to the instructions for Transcriptor First strand cDNA synthesis kit (Roche).

The RNA in each sample (at exponential, early stationary and late stationary phases of growth) was analyzed independently, three times by QRT-PCR. For each pair of primers (designed to amplify 90−100 pb and described in Table 3 of Supporting Information), different amounts of cDNA were used as template with a constant cycle number of 20.

Briefly, the following QRT-PCR conditions were set: denaturing step of 5 min at 94 °C, followed by 45 amplification cycles of 94 °C for 10 s, 60 °C for 10 s, and 72 °C for 10 s using the kit LightCycler 480SYBR Green I Master (Roche). PCR products were tested for melting temperature with a temperature ramp of 2.2 °C/s from 65 to 95 °C and shown to correspond to the expected amplicons. Overexpression was considered for genes whose expression was 2-fold that of the control (in this case, expression values obtained at exponential phase). Similarly, the value 0.5-fold was used to identify underexpression.

Detection of ROS and RNI. For the detection of exogenous ROS, growth medium was harvested at the above-mentioned three time points on the curve and the supernatant was then centrifuged for 5 min at 27 000*g*. For detection of O_2^-, 250 μL of each supernatant was incubated with 6 mM nitroblue tetrazolium (NBT; Fluka) for 4 h. Note that in all cases the results presented are mean values of 3 replicates. For detection of H_2O_2, 500 μL of 500 μM ferrous ammonium sulfate; 50 mM H_2SO_4, 200 μM xylenol and 200 mM sorbitol was added to 500 μL of culture medium after removing the bacteria. After 45 min incubation, the respective absorbance was measured at 560 nm in a UV/Visible Nicolete Evolution (Thermo) spectrophotometer.[33]

To measure the endogenous production of ROS and RNI, a series of reactive fluorescent dyes were used for the detection of specific ROS and RNI produced during *A. baumanni* growth: dihydrorhodamine 123 (DHR) (Sigma-Aldrich) for detection of peroxynitrite ($ONOO^-$); 5-(and-6)carboxy-2′,7′-dichlorodihydrofluorescein diacetate (H_2DCF-DA) (Fluka) for detection of hydrogen peroxide (H_2O_2); hydroethidine (HEt) (Sigma-Aldrich) for detection of superoxide radicals (O_2^-) and 3′-(*p*-hydroxyphenyl) fluorescein (HPF) (Invitrogen, Molecular Probes, Eugene, OR) for detection of hydroxyl radical (OH^-). Procedures were followed as indicated by the manufacturers for each fluorophore. All data were collected using a Becton Dickinson FACSCalibur flow cytometer with a 488 nm argon laser and a 515−545 nm emission filter (FL1) at low flow rate. At least 50 000 cells were collected for each sample.

Antioxidant Activity Assay. To remove small molecules that could interfere with the measurement of protein antioxidant activity, all samples were in advance subject to gel-filtration with PD-10 columns (GE Healthcare, Buckinghamshire, U.K.). To measure the total antioxidant capacity (TAA) of the protein extracts, the Antioxidant Assay Kit (Sigma-Aldrich) was utilized according to the manufacturer's instructions. Briefly, we used the manual spectrophotometric assay to determine the TAA of experimental samples, and a reference antioxidant, the water cytoplasmatic analogue of vitamin E, Trolox (6-hydroxy-2,5,7,8-tetramethylchroman-2-carboxylic acid). The kinetics of the quenching of the 2,2-azino-*bis*-(3-ethylbezothiazoline-6-sulfonic acid; ABTS) radical cation was followed at 405 nm, using a visible spectrophotometer. TAA values were calculated from a Trolox standard curve that showed a linear relationship (r^2 = 0.99) between concentration (0−0.42 mM). Here we have measured the TAA from protein extract (containing a total protein concentration of 4 μg) obtained from both exponential and late stationary phases of growth. Note: this was based in three biological replicates and the protein extracts were obtained as described for cytoplasmatic protein fraction (see above).

Survival Studies of *A. baumannii* in the Presence of H_2O_2, O_2^-, and $ONOO^-$ and Antibiotics. Bacterial cells collected at exponential phase of growth ($OD_{600\ nm}$ = 0.4) or late stationary phases of growth (approximately 48 h after inoculation; $OD_{600\ nm}$ = 2.0) were incubated in either 30 mM hydrogen peroxide (H_2O_2, Sigma-Aldrich), 500 μM menadione (Sigma-Aldrich) as a supply of O_2^-, 1 mM of the NO donor sodium nitroprusside (SNP, Sigma-Aldrich) or several bactericidal antibiotics such as β-lactams (ceftazidime, imipenem), quinolones (levofloxacin) and colistin.

After addition of hydrogen peroxide/menadione/SNP, aliquots of bacteria at both exponential and stationary phases of growth were removed and the viability analyzed after 15, 30, 45, and 60 min. Cells were collected at the indicated time points, diluted accordingly and plated onto MH agar plates. After 24 h incubation at 37 °C, colonies were counted. The data correspond to three independent biological experiments. Each biological experiment is the result of three independent measurements.

The bactericidal effect of ceftazidime, imipenem, levofloxacin and colistin with cells at two different phases of growth curve was measured by counting colonies or CFU (colony-forming unit). Briefly, cells were obtained from both growth phases and washed twice with 0.9% NaCl. After centrifugation at 3500*g* for 10 min, cell pellets were then resuspended in 5 mL of fresh MH broth, adjusted to 0.4 (exponential cells) and 1.0 (late stationary cells) Mc Farland units and inoculated into 15 mL of MH broth with adjusted volume of antibiotic stock solutions. After 0, 2, and 4 h of incubation at 37 °C with shaking, aliquots of cells were taken, diluted in 0.9% NaCl and plated onto McConkey agar plates. After 24 h incubation at 37 °C, cells were counted and CFU was determined according to each dilution factor. Each experiment was repeated at least three times.

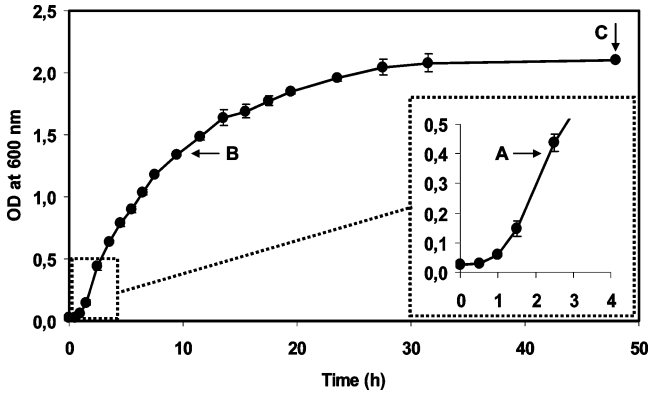

Figure 1. *In vitro* growth of *A. baumannii* ATCC 17978 in MH broth. The figure shows the ±SD of values obtained from three independent cultures. The arrows indicate time points at which the cells were collected for proteomic analysis. (A) Exponential phase ($OD_{600\ nm} = 0.4$); (B) early stationary phase ($OD_{600\ nm} = 1.4$); (C) late stationary phase ($OD_{600\ nm} \approx 2.0$ at 48 h).

A Student's *t*-test was used for two-group comparisons and ANOVA followed by an unpaired Student's *t*-test with Bonferroni's correction was used for multiple group comparisons.

Results and Discussion

Proteome Profiles of *A. baumannii* in Different Growth Phases. Characterization of the Growth Phase Dependent Proteins. In the present study, a 2-DE and MALDI-TOF/TOF coupled with iTRAQ approach was used to establish a proteome profile for *in vitro* cultured *A. baumannii* strain ATCC 17978. To obtain an overview of the temporal regulation of protein expression, cells were harvested at exponential, early stationary and late stationary phases of growth (Figure 1) and analyzed using 2-DE based approach. Time-dependent changes in the proteome of *A. baumannii* strain ATCC 17978 during *in vitro* culture are summarized in Table 1 and 2 (see also Figure 2).

2-DE analyses of three biological replicates and Student's paired *t* test (95% confidence interval) was performed and a minimum fold-change of 2 was used to select protein spots which suffered significant changes in intensity during *in vitro* growth. Using this gel-based proteomic approach, we have identified a total of 76 proteins that were differentially expressed during *in vitro* growth. The differentially expressed proteins consisted of 13 membrane and 63 cytosolic proteins (Table 1 and Supporting Information).

To further increase confidence of assigning protein expression level, we also performed an iTRAQ coupled with LC-MS/MS analyses. In this case, we have analyzed protein extracts from both cells harvested during exponential and late stationary phases of growth (Figure 1). iTRAQ analyses of the two biological replicates were performed. To be considered with significant altered expression, its representative peptides must have met the following criteria: (i) protein score should be more than 2 (99% confidence); (ii) the protein had to be represented by at least two peptides of differing amino acid sequence; and (iii) to be considered a differentially regulated protein the protein ratio should be greater than 1.2 or less than 0.8. Through iTRAQ analyses we have identified 31 differentially expressed proteins (Table 2) and of these, there are a number of proteins identified by both iTRAQ and 2-DE gel approach which show the same tendency of change throughout the *in vitro* growth (e.g., spots nos. 178 and i16; 432 and i62; 437 and i49; E23 and i5; 54 and i14; L10 and i158, and IL11 and i242, see Tables 1 and 2). Therefore, our results support the concept that these two techniques complement each other[34] and that in this case combining the two methods not only allowed a validation of some results, but also to obtain a wider view of the proteome changes occurring during *in vitro* growth of *A. baumannii*.

The results regarding the pattern of protein expression throughout the growth phases (resumed in Tables 1 and 2) revealed a clear tendency for the down-regulation of proteins functionally related with cell division, such as trigger factor septum formation molecular chaperones (spot no. 33, Figure 2A) and cell division protein FtsZ (spot no. 88, Figure 2B). Similarly, there was a reduced expression of several proteins associated with translation, ribosomal structure and biogenesis (Tables 1 and 2).

As stated earlier in the text, during the stationary phase, bacteria are exposed to a rather hostile environment, and therefore, survival of bacteria at this stage will largely rely on the promptness and suitability of the bacterial response to external stimuli. Many of such adaptive responses are mediated by the activation of complex signal transduction systems, that are sensitive to changes in the external environment and that coordinate cellular events accordingly. Within this context, the present results revealed the *de novo* appearance of a lipoprotein (spot no. L17, Figure 2C) in the late stationary phase. This lipoprotein, which belongs to the NlpE superfamily, is apparently required for signaling by the Cpx pathway. The Cpx two-component signal transduction pathway responds specifically to stress caused by envelope disturbances, and increases the expression of periplasmic protein folding and degradation factors.[35] Thus, NlpE together with the other sensing and signaling proteins identified here (e.g., spot nos. L22, Figure 2D; BL2, Figure 2E; IL6, IL7, Figure 2F; IL17 and protein no. i280, see Tables 1 and 2) are attractive targets for future studies aimed at a better understanding of signal transduction systems mediating environmental adaptation in *A. baumannii*.

Furthermore, previous studies in other species have demonstrated a correlation between the entry into stationary phase and the induction of virulence factors.[36,37] The present results revealed that proteins with adhesive surface properties, which are probably involved in biofilm formation, were up-regulated at late stages of growth, for example, the lipoprotein NlpE (spot no. L17, Figure 2C)[35] and putative peptidoglycan-binding LysM (spot nos. IL6 and IL7, Figure 2F).[38,39] These type of proteins may be considered to be virulence factors, since preliminary observations indicate that *A. baumannii* biofilm-forming strains could be associated with catheter-related urinary and bloodstream infections.[40,41] Regarding virulence factors, it is worth mentioning the presence of Omp38, as it has been demonstrated that this outer membrane protein may act as a potential virulence factor inducing apoptosis of epithelial cells in the early stage of *A. baumannii* infection.[42] Moreover, another known virulence mechanism is the ability of some pathogens, including *A. baumannii*, to acquire iron from their hosts.[43,44] Here, the present report indicate the induction of two proteins, namely, bacteroferritin (spot no. IL11, Figure 2G) and a heme containing protein flavohemoprotein (spot no. 172, Figure 2H), which may be involved in iron uptake and storage, respectively. Finally, it is worth mentioning that a putative protein belonging to the glyoxalase I family is greatly increased with the entry into the stationary phase (spot no. L23, Figure 2I); this is of particular interest considering that this type of protein may play a relevant role in the pathogenicity of *Mycobacterium tuberculosis*.[45]

Table 1. Functional Classification of Identified Differentially Expressed 2-DE Gels Protein Spots during *A. baumannii in vitro* Culture[a]

protein description	spot no.[b]	NCBInr accession no.	average % spot volume (MSD) exp.[c]	early[c]	late[c]	MALDI-TOF/TOF score	matched peptides	(%) cov.
Post-translation Modification, Protein Turnover, Chaperones								
Trigger factor septum formation molecular chaperone	33	gi|126640548	0.54 (0.08)	0.32 (0.12)	0.01 (0.01)	313	4	18
Chaperone Hsp60	35	gi|126642698	1.14 (0.28)	1.15 (0.49)	0.73 (0.15)	585	5	21
ATP-dependent protease Hsp 100	E20	gi|126641234	ND	0.25 (0.18)	ND	251	4	7
ATP-dependent protease Hsp 100	L2	gi|126641234	ND	ND	0.45 (0.05)	172	3	5
Translation, Ribosomal Structure and Biogenesis								
30S ribosomal protein S1	3	gi|126641617	0.71 (0.29)	0.19 (0.11)	0.02 (0.01)	167	3	7
Elongation factor Ts	178	gi|126642362	1.14 (0.42)	0.82 (0.29)	0.14 (0.13)	794	10	33
30S ribosomal protein S2	406	gi|126642363	2.15 (0.22)	0.66 (0.04)	ND	60	1	28
50S ribosomal protein L3	428	gi|126643095	0.77 (0.09)	0.09 (0.09)	ND	491	7	41
50S ribosomal protein L6	432	gi|169632365	3.50 (0.24)	2.46 (0.57)	ND	306	5	28
50S ribosomal protein L5	437	gi|126643084	1.78 (0.11)	1.06 (0.40)	ND	156	3	32
50S ribosomal protein L13	439	gi|126643019	2.13 (0.06)	ND	ND	161	4	42
30S ribosomal protein S8	443	gi|169632364	1.54 (0.21)	ND	ND	301	4	38
50S ribosomal protein L23	450	gi|126643093	2.58 (0.02)	ND	ND	139	2	35
30S ribosomal protein L25	451	gi|126643096	2.86 (0.31)	ND	ND	474	5	44
50S ribosomal protein L25	452	gi|126640884	1.94 (0.31)	0.53 (0.12)	ND	305	2	36
Elongation factor G	E23	gi|126640918	0.20 (0.01)	0.16 (0.01)	ND	72	2	4
Elongation factor Tu	L12	gi|162286746	0.05 (0.02)	0.04 (0.00)	0.62 (0.12)	255	4	10
Elongation factor Tu	L14	gi|162286746	0.05 (0.02)	0.04 (0.01)	0.62 (0.18)	189	4	10
Elongation factor G	L39	gi|126640918	0.09 (0.04)	ND	0.42 (0.02)	145	4	9
Elongation factor Tu	L44	gi|162286746	ND	0.41 (0.10)	0.30 (0.08)	288	7	24
Energy Production and Conversion								
F0F1 ATP synthase subunit β	54	gi|162286755	0.50 (0.14)	0.32 (0.07)	0.13 (0.02)	213	4	15
Phosphoglycerate kinase	135	gi|126641588	0.38 (0.03)	0.06 (0.08)	0.05 (0.07)	81	2	10
Putative flavohemoprotein	172	gi|126643100	0.20 (0.02)	0.52 (0.13)	0.47 (0.03)	57	1	7
Electron transferase flavoprotein α-subunit	L9	gi|169632682	ND	ND	0.64 (0.15)	575	7	48
Cell Division and Chromosome Partioning								
Cell division protein FtsZ	88	gi|126643338	0.32 (0.12)	0.21 (0.01)	ND	107	2	12
Amino Acid Transport and Metabolism								
Methionine adenosyltranferase	104	gi|126641564	0.28 (0.12)	0.16 (0.02)	0.01 (0.01)	184	4	16
Succinylornithine transaminase	110	gi|126643147	0.08 (0.01)	0.11 (0.03)	0.03 (0.03)	61	1	6
Xanthine phosphoribosyltransferase	259	gi|126643050	0.33 (0.05)	0.17 (0.01)	0.11 (0.02)	88	3	22
2,3,4,5-tetrahydropyridine-2-carboxylate N-succinyltransferase	300	gi|126642574	0.37 (0.05)	0.17 (0.01)	0.09 (0.02)	195	4	20
Aconitate hydratase 1	E21	gi|193076354	ND	0.18 (0.02)	ND	147	4	5
Putative intracellular/amidase	L3	gi|193078218	0.06 (0.01)	0.53 (0.06)	0.59 (0.01)	192	4	18
Putative protease	L15	gi|193078237	0.27 (0.15)	1.09 (0.40)	0.93 (0.30)	218	3	16
2,3,4,5-tetrahydropyridine-2-carboxylate N-succinyltransferase	L48	gi|126642574	0.32 (0.09)	0.17 (0.08)	0.83 (0.05)	201	4	19
Dihydrodipicolinate synthase	L49	gi|126642699	ND	ND	0.20 (0.06)	431	7	32
Coenzyme Metabolism								
Succinyl-CoA synthetase α chain	137	gi|126642750	0.36 (0.01)	0.19 (0.01)	0.13 (0.01)	64	2	14
Putative acetyl-CoA carboxylase, β subunit	194	gi|126642893	0.27 (0.05)	0.27 (0.08)	0.03 (0.01)	101	2	8
Acetoacetyl-CoA transferase α subunit	L5	gi|126641777	0.04 (0.03)	0.24 (0.05)	0.25 (0.07)	242	7	47
Putative enoyl-CoA hydratase II	L13	gi|193077017	ND	ND	0.39 (0.23)	576	11	48
Transcription								
DNA-directed RNA polymerase subunit α	145	gi|158513671	0.40 (0.06)	0.32 (0.05)	0.03 (0.07)	379	8	27
Carbohydrate Transport and Metabolism								
Inorganic pyrophosphatase	268	gi|126640295	0.79(0.08)	0.77(0.07)	0.76 (0.08)	181	3	23
Lipid Transport and Metabolism								
Biotin carboxyl carrier protein of acetyl-CoA carboxylase (BCCP)	310	gi|126642055	1.07 (0.23)	0.94 (0.45)	0.06 (0.03)	108	2	29
Multifunctional								
Putative lipoprotein	L17	gi|169633901	ND	ND	0.34 (0.05)	251	5	20
Putative lipoprotein	L41	gi|126641128	ND	ND	0.39 (0.05)	394	6	37
Possible Role in Signaling								
Putative signal peptide	BL2	gi|193077163	0.12 (0.02)	0.05 (0.00)	1.67 (0.31)	238	4	31
Putative signal peptide	IL17*	gi|126643195	ND	ND	2.33 (0.10)	435	7	43

Table 1 Continued

protein description	spot no.[b]	NCBInr accession no.	average % spot volume (MSD) exp.[c]	early[c]	late[c]	MALDI-TOF/TOF score	matched peptides	(%) cov.
Cell Envelope Biogenesis, Outer Membrane								
Outer membrane protein (Omp)38 precursor	140	gi|75438841	0.54 (0.11)	0.52 (0.09)	ND	364	6	17
Omp38 precursor	149	gi|75438841	1.40 (0.64)	1.34 (0.48)	ND	256	4	11
Putative outer membrane protein	202	gi|126643304	0.18 (0.03)	0.10 (0.08)	0.03 (0.01)	91	3	24
Putative peptidoglycan-binding LysM	298	gi|126640876	0.79 (0.27)	1.03 (0.28)	0.15 (0.07)	189	5	59
Putative outer membrane protein W	299	gi|126640380	0.88 (0.20)	0.91 (0.21)	1.02 (0.19)	97	2	15
Omp38	L8	gi|126642864	ND	ND	1.56 (0.23)	719	8	23
Putative peptidoglycan-binding LysM	L22	gi|126640876	ND	ND	1.19 (0.20)	183	3	24
Omp38	BL5	gi|126642864	ND	ND	4.2 (1.60)	306	6	16
Putative outer membrane protein	BL9	gi|126640934	0.42 (0.07)	ND	1.24 (0.09)	73	2	11
Omp38	467*	gi|126642864	2.45 (0.17)	5.8 (0.31)	5.9 (0.00)	690	9	30
Omp 33−36 kDa	468*	gi|193078641	3.56 (0.29)	1.25 (0.56)	0.56 (0.26)	465	5	28
Omp CarO precursor	469*	gi|126642573	0.38 (0.04)	0.85 (0.14)	0.79 (0.13)	145	3	20
Omp CarO precursor	472*	gi|126642573	1.60 (0.06)	4.05 (0.90)	4.10 (0.02)	308	4	35
Putative Omp W	474*	gi|126640380	3.01 (0.52)	4.26 (1.19)	3.6 (1.38)	356	6	44
Omp 38	IL3*	gi|126642864	ND	ND	1.03 (0.26)	112	2	10
Omp 38	IL4*	gi|126642864	ND	ND	0.32 (0.00)	108	2	6
Omp 38	IL5*	gi|126642864	ND	ND	0.44 (0.06)	98	2	6
Putative peptidoglycan-binding LysM	IL6*	gi|126640876	ND	2.83 (0.54)	2.27 (0.48)	120	3	24
Putative peptidoglycan-binding LysM	IL7*	gi|193076594	0.87 (0.13)	2.10 (0.11)	2.12 (0.03)	163	4	32
Outer membrane protein CarO precursor	IL18*	gi|126642573	0.48 (0.04)	0.61 (0.18)	0.95 (0.42)	187	2	13
Function Unknown								
Conserved hypothetical protein	204	gi|169797441	0.17 (0.02)	0.11 (0.06)	0.03 (0.01)	64	2	11
Hypothetical protein A1S_2728	L4	gi|126642759	ND	ND	0.39 (0.05)	149	4	29
Hypothetical protein A1S_2406	L45	gi|126642443	0.24 (0.03)	0.53 (0.16)	0.59 (0.10)	435	7	30
Proteins Involved in Redox Reactions								
Thioredoxin reductase	171	gi|193076628	0.22 (0.10)	0.16 (0.05)	0.15 (0.01)	174	2	7
Superoxide dismutase [Mn/Fe]	247	gi|126642383	0.47 (0.21)	0.31 (0.12)	0.49 (0.05)	138	2	9
Alkyl hydroperoxide reductase C22 subunit	271	gi|126641253	0.30 (0.03)	0.39 (0.05)	0.10 (0.03)	127	2	16
Alkyl hydroperoxide reductase C22 subunit	273	gi|126641253	1.37 (0.03)	1.05 (0.09)	0.57 (0.10)	197	3	26
NADH-dependent enoyl-ACP reductase	E6	gi|126640605	0.24 (0.19)	0.36 (0.08)	0.08 (0.06)	115	3	14
Alkyl hydroperoxide reductase C22 subunit	L10	gi|126641253	0.06 (0.04)	ND	1.05 (0.06)	433	6	38
Putative oxidoreductase	L16	gi|126641974	0.05 (0.01)	0.40 (0.11)	0.49 (0.06)	245	3	20
Putative antioxidant protein	L19	gi|126642887	ND	ND	0.46 (0.05)	75	2	18
Glyoxalase I super family protein (Hypothetical protein A1S_2863)	L23	gi|193078285	0.06 (0.02)	0.70 (0.19)	0.71 (0.11)	112	4	27
Glutathione peroxidase	IL1*	gi|126640260	ND	0.24 (0.07)	0.37 (0.01)	98	2	14
Bacterioferritin	IL11*	gi|126640856	0.23 (0.05)	1.39 (0.28)	1.40 (0.18)	150	4	26
Defense								
Universal stress protein	L25	gi|169795610	0.08 (0.02)	0.56 (0.26)	0.40 (0.07)	410	5	57
Universal stress protein	L26	gi|169795610	0.21 (0.03)	1.23 (0.08)	1.43 (0.18)	443	6	58
Universal stress protein	L27	gi|126642117	ND	0.45 (0.04)	0.32 (0.07)	388	4	49

[a] Some constitutive proteins (spots nos. 35, 171, 247, 268, 299, and 474*) are shown for comparison. [b] (*) Protein spots isolated by the method used to extract cell surface membranes. [c] Exp., early and late refer to exponential, early stationary and late stationary stages of growth, respectively. Student's test statistical significance of changes in percentage of spot volume. Levels $p \leq 0.05$ were considered significant. ND, protein spot not detected. MSD, the square root of the average difference of each sample value to the center location is calculated. Note: all the identifications were based on multiple peptide matches, although in three specific cases protein identification was based on a single peptide sequence (spot nos. 110, 172, and 406). However, the scores for all proteins identified here were higher than the significance threshold (determined at the 95% confidence level) calculated by Mascot and in all cases the data was searched against an Mascot decoy database in order to check for false positive (additional identification data for all spots is provided as supplementary material).

Interestingly, the results revealed that *A. baumannii* contains several proteins that may be directly associated with ROS metabolism (see Tables 1 and 2). In addition, it was seen that entry into stationary phase is associated with the induction of a number of oxidative stress responsive proteins, such as alkyl hydroperoxidase reductase (spot no. L10, Figure 2J), glutatione peroxidase (spot no. IL1, Figure 2K), catalase-peroxidase (protein no. i26), catalase HPII (protein no. i287) and antioxidant proteins (spot nos. L16 and L19, Figure 2L,M). In addition to these, there was the induction of proteins known to play an important role in the detoxification processes, such as bacteroferritin[46] (spot no. IL11, Figure 2G), putative glyoxalase I family protein (spot no. L23, Figure 2I)[47,48] and universal stress proteins (USPs) (spot no. L25, L26, Figure 2N and L27).[49] Moreover, a growth phase-dependent induction of proteins involved in DNA repair (e.g., integration host factor (IHF) (protein no. i96) and protein recA (protein no. i80), Table 2) was observed, as well as the induction of proteins implicated in protein repair (e.g., chaperone protein dnaK, 10 kDa and 60 kDa chaperonins (protein nos. i7, i8 and i270, respectively), Table 2).

Spot Pattern Indicating Oxidative Modification of the Late Stationary Proteome. Occasionally, protein-spots were identified as the same protein included in the database. Some

Table 2. Functional Classification of Differentially Expressed Proteins Identified by iTRAQ

protein description	protein no.[a]	NCBInr accession no.	(%) cov.	no. peptides	E2:E1[a]	L1:E1[b]	L2:E1[c]
Post-translation Modification, Protein Turnover, Chaperones							
Chaperone protein dnaK	i7	gil226738224	80.03	40	1.10 (0.12)[d]	2.38 (0.00)	2.13 (0.00)
60 kDa chaperonin	i8	gil226704107	82.35	33	0.99 (0.99)	2.38 (0.00)	1.75 (0.00)
10 kDa chaperonin	i270	gil166233974	54.17	2	1.12 (0.75)	2.50 (0.28)	3.10 (0.21)
Protein grpE	i144	gil226737248	55.40	4	0.95 (0.61)	2.14 (0.02)	1.50 (0.01)
Trigger factor	i21	gil226703990	72.97	24	0.85 (0.07)	0.46 (0.00)	0.52 (0.00)
Translation, Ribosomal Structure and Biogenesis							
Elongation factor G	i5	gil238685496	81.88	39	0.93 (0.40)	0.51 (0.00)	0.78 (0.00)
Elongation factor Ts	i16	gil166221178	89.00	18	0.83 (0.05)	0.58 (0.07)	0.52 (0.00)
50S ribosomal protein L2	i35	gil160419217	71.17	15	0.89 (0.33)	0.46 (0.00)	0.54 (0.00)
50S ribosomal protein L21	i168	gil226730509	48.54	4	0.82 (0.03)	0.51 (0.12)	0.54 (0.01)
50s ribosomal protein L5	i49	gil226731478	78.09	13	0.72 (0.21)	0.31 (0.00)	0.44 (0.01)
50s ribosomal protein L10	i74	gil226700243	70.24	6	0.80 (0.33)	0.50 (0.26)	0.51 (0.20)
50S ribosomal protein L6	i62	gil226731363	62.7	6	0.67 (0.05)	0.31 (0.00)	0.48 (0.03)
Energy Production and Conversion							
ATP synthase β-subunit	i14	gil226694415	69.4	19	0.87 (0.33)	0.33 (0.00)	0.58 (0.00)
Isocitrate lyase	i147	gil76364071	23.7	2	1.46 (0.26)	2.76 (0.35)	4.06 (0.18)
Amino Acid Transport and Metabolism							
2,3,4,5- tetrahydropyridine-2-carboxylate N-succinyltransferase	i64	gil166224190	56.78	10	0.94 (0.63)	1.36 (0.07)	1.14 (0.43)
Aconitate hydratase 1	i51	gil81622450	25.8	6	1.59 (0.07)	3.60 (0.01)	3.89 (0.02)
Lipid Transport and Metabolism							
Fatty acid oxidation complex α-subunit	i10	gil254788553	72.94	32	1.74 (0.00)	3.30 (0.00)	3.20 (0.00)
D-amino acid dehydrogenase small subunit	i76	gil226722637	32.07	8	1.61 (0.07)	3.00 (0.00)	4.54 (0.00)
Possible Role in Signaling							
Carbon storage regulator homologue	i280	gil226711125	57.1	2	0.86 (0.60)	2.68 (0.12)	1.25 (0.27)
Replication, Recombination and Repair							
Protein recA	i80	gil238685519	40.4	8	1.30 (0.01)	2.08 (0.00)	2.05 (0.00)
Integration host factor α-subunit	i96	gil226707551	62.2	4	1.38 (0.07)	4.43 (0.03)	4.26 (0.02)
Transcription							
DNA-directed RNA polymerase β-subunit	i6	gil212288355	62.78	46	0.87 (0.08)	0.49 (0.00)	0.65 (0.00)
DNA-directed RNA polymerase α-subunit	i38	gil158513671	68.66	18	0.83 (0.04)	0.65 (0.00)	0.59 (0.00)
Cell Envelope Biogenesis, Outer Membrane							
Omp38	i17	gil148839593	69.9	14	1.60 (0.00)	0.68 (0.12)	0.93 (0.63)
Dihydroorotate dehydrogenase	i185	gil226711019	33.53	6	0.86 (0.50)	2.46 (0.15)	1.69 (0.04)
Alanine racemase	i221	gil226711023	19.3	2	1.20 (0.42)	3.40 (0.22)	2.73 (0.26)
Proteins Involved in Redox Reactions							
Catalase-peroxidase	i26	gil215275637	52.2	15	1.50 (0.10)	3.02 (0.00)	3.34 (0.00)
Alkyl hydroperoxide reductase C22 subunit[e]	i158	gil83286947	21	1	1.87 (-)	7.59 (-)	2.98 (-)
Bacterioferrtin	i242	gil74599304	80.0	2	1.24 (0.65)	3.50 (0.41)	2.72 (0.33)
Superoxide dismutase [Fe][e]	i263	gil34098495	23.2	1	0.80 (-)	3.93 (-)	1.76 ± (-)
Catalase HPII	i287	gil81541033	12.0	2	0.86 (0.68)	2.59 (0.17)	2.92 (0.38)

[a] E2:E1, the ratio of different expression level between biological replicates of exponential cell. [b] L1:E1, the ratio of different expression level between exponential cell control (E1) and late stationary cell (L1). [c] L2:E1, the ratio of different expression level between exponential cell control (E1) and late stationary cell (L2). [d] *p*-value obtained from Protein pilot analyses. [e] Protein ID based on one peptide; however, these are shown for comparison with respective 2-DE generated data.

of these spots in which small shifts in spot p*I* were verified are probably isoforms of the same protein (e.g., spot nos. 34 and 35, see Figure 2A and Supporting Information). There were, however, several examples of protein isoforms in which the molecular weights of spots and/or the p*I* substantially differed, and which demonstrated differing regulation with growth phase progression (e.g., spot nos. 273 and L10 Figure 2J; L26 and L25 Figure 2N; 298 and L22, Figure 2D and also 149 and L8, BL5, Figure 2O, P and Q). For instance, during stationary phase, Omp38 (spot nos. L8 and BL5) and elongation factor G (EF-G) (spot no. L39, Figure 2R) migrated at masses much lower than expected. In fact, Omp38 peptides from one isoform (spot no. L8, Figure 2P) were found only from the N-terminal part of the protein, whereas peptides from a further isoform (spot no. BL5, Figure 2Q) were found only from the C-terminal (data not shown), suggesting cleavage of Omp38 into two halves (spot nos. L8 and BL5). In addition, the iTRAQ analysis revealed that Omp38 (protein no. i17, Table 2) in fact suffered a slight decreased in expression level during late stationary phase, which suggests that the *de novo* appearance of both spot nos. L8 and BL5 can only be explained by the proteolysis of this protein. Oxidation damage has been found to be a major limiting factor for bacterial cells in stationary-phase.[11] In addition, a recent study of protein oxidative damage in *E. coli* revealed that proteins such as Omp38, EF-G and F0F1 suffered major modification in their structure.[50] Therefore, it is possible

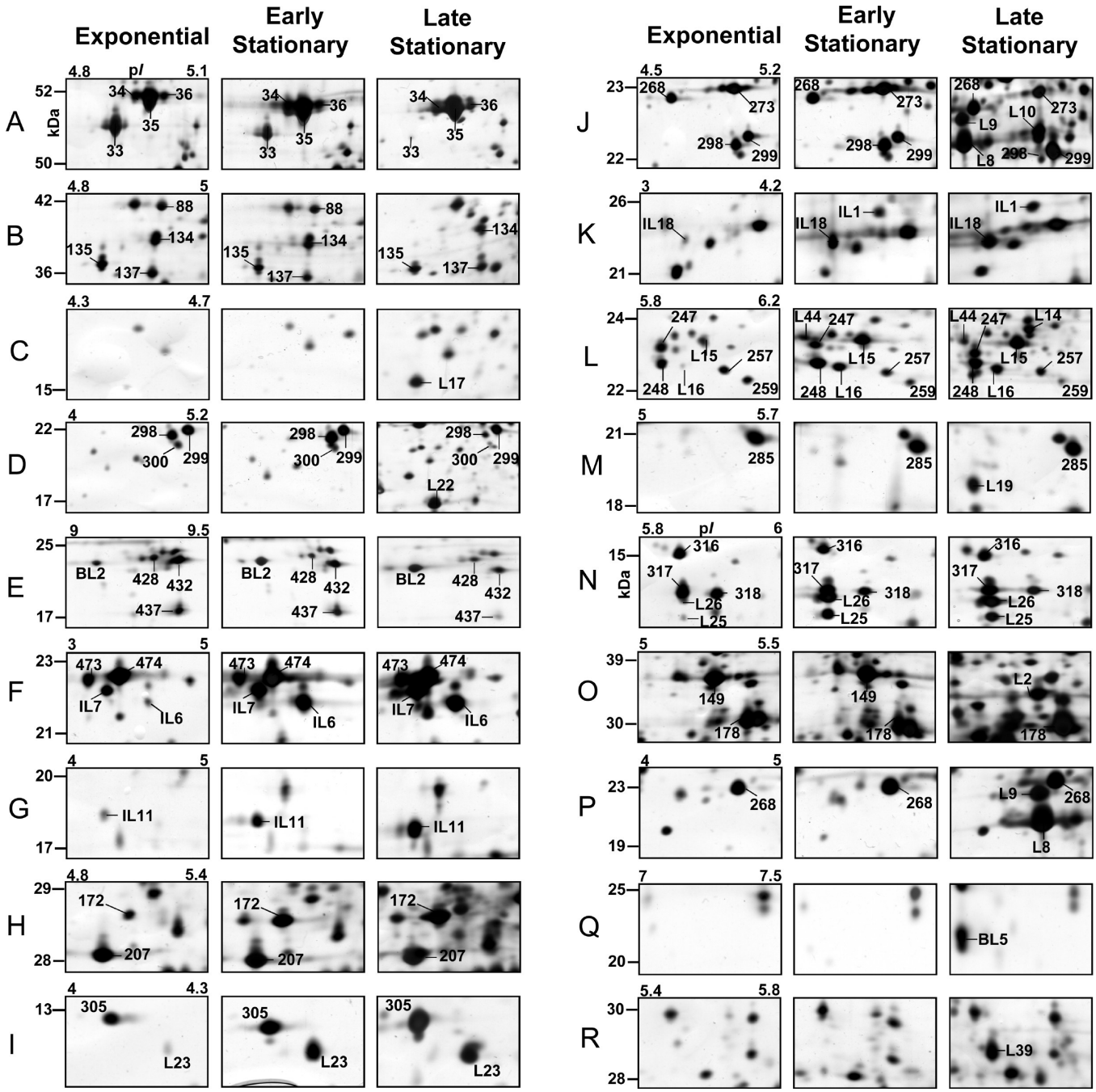

Figure 2. Representative protein spot images of differentially expressed proteins at each growth phases (exponential, early stationary and late-stationary panels). There are examples of spots that in terms of it intensity remained nearly unchanged throughout the growth curve, these are shown for comparison (e.g., spot nos. 34 and 35 {panel A}; spot no. 135 {panel B}; spot no. 285 {panel M} spot no. 268 {panel P}; for additional information concerning the protein identification of these type of spots please see Supporting Information). The figure shows examples of protein spots that suffered a visible decrease in spot intensity at the late stage of the growth curve (e.g., spot no. 33 {panel A}; spot no. 88 {panel B}, spot no. 437 {panel E}; spot# no. 259 {panel L} and spot no. 149 {panel O}). There are also several examples in which spot intensity increased clearly during early and stationary phases (e.g.; spot no. BL2 {panel E}; spot no. IL6 and IL7 {panel F}; IL11 {panel G}; spot no. 172 {panel H}; spot no. L23 {panel I}; spot no. IL1 and IL18 {panel K}; spot no. L15, L16 {panel L} and spot no. L25, L26 {panel N}). It is also indicated cases of the appearance of *de novo* spots at late stationary phase (e.g., spot no. L17 {panel C}; spot no. L22 {panel D} spot no. L10 {panel J}; L14 and L44 {panel L}; spot no. L19 {panel M}; spot no. L8, L9 {panel P}; spot no. BL5 {panel Q} and spot no. L39 {panel R}). Note that panel F, G and K represent areas from gels obtained from membrane protein fractions.

that, in the present study, late-stationary phase isoforms of Omp38 and EF-G are a consequence of oxidative damage.

Moreover, the analysis of 12 genes involved in ROS metabolism and stress response by real time reverse transcription (QRT-PCR) showed a poor correlation between the mRNA transcript and the protein pattern (Figure 3). These discrepancies are consistent with the suspicion that a considerable number of protein spot changes observed during the late stationary phase are due to possible post-translational modification and/or post-transcriptional regulation as pointed out by Choi et al. who made similar observations in *Helicobacter pylori*.[51]

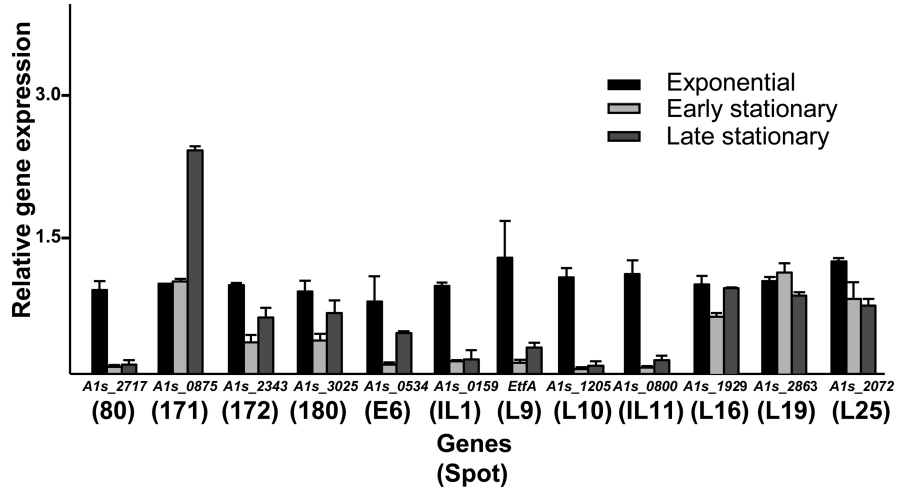

Figure 3. Real time RT-PCR (QRT-PCR) of genes involved in ROS metabolism and stress response. Expression was calculated by the ΔΔCt method with *gyrB* as internal control. Names refer to the identified protein spots as well genes in the annotated *A. baumannii* ATCC 17978 genome.

ROS and RNI Production during *in Vitro* Growth of *A. baumannii*. Our proteomic data strongly suggests that throughout *in vitro* growth, the ability of *A. baumannii* to respond to oxidative stress undergoes adaptive changes. To test for any correlation between late stationary phase and the accumulation of ROS in the medium, ROS production was measured during the three growth phases, as described in Material and Methods (Figure 4).

In a first approach, colorimetric assays were used to verify qualitative changes in exogenous ROS production. The incubation of samples of medium from exponential and early stationary phases with NBT indicated that there was no detectable production of O_2^- during these phases. However, a strong reaction with NBT was observed with medium from the late stationary phase (Figure 4.1), indicating production and accumulation of O_2^- in the late stationary phases of *in vitro* growth of *A. baumannii*. Xylenol orange was used to monitor production of H_2O_2, but no reaction was with medium from any phase of growth (data not shown).

On the basis of these results, we then proceeded to evaluate quantitative changes of endogenous ROS production. For this purpose, we used several fluorescent report dyes, 5-(and-6)carboxy-2′,7′-dichlorodihydrofluorescein diacetate (H_2DCF-DA), hydroethidine (HEt), and 3′-(*p*-hydroxyphenyl) fluorescein (HPF), which detect H_2O_2, O_2^-, and OH^-, respectively (see Material and Methods). Consistent with the colorimetric assays, flow cytometry/report dye analysis revealed that O_2^- accumulated during late stationary phase (Figure 4.2 (A) (data not shown)) and that the levels of H_2O_2 did not change throughout growth. Furthermore, as regards OH^- detection, it was verified that the level remained the same during exponential and early stationary phases and increased at the late stationary phase (Figure 4.2 (B)).

The apparent discrepancy between O_2^- and H_2O_2 accumulation was somewhat surprising, since that it is known that detoxification of O_2^- via scavenging enzymes, namely, superoxide dismutase and superoxide reductase (SOR) (in prokaryotic cells only),[52] results in the formation of H_2O_2. However, a recent study in *Pseudomonas aeruginosa*, which is closely related to *A. baumannii*, revealed that O_2^-, but not H_2O_2 accumulated during biofilm formation.[53] The authors justified this by the existence of high levels of catalases, enzymes that disproportionate and neutralize H_2O_2. An analogous explanation may be applied to the current results, since in later stages of the growth curve catalase-peroxidase and alkyl hydroperoxidase reductase increased (Tables 1 and 2), and both of these proteins have been referred to as major scavengers of H_2O_2.[54]

It is known that NO reacts with O_2^- to form a potential peroxynitrite ($ONOO^-$), which may damage cellular components in a similar way to other chemical oxidants.[55,56] Here it was demonstrated that O_2^- accumulated during growth. To determine whether O_2^- accumulation during growth was accompanied by NO formation and consequently $ONOO^-$ accumulation, we have used fluorescence DHR, which measures the accumulation of both $ONOO^-$ and H_2O_2. However, as mentioned earlier, we were unable to detect exogenous or endogenous production of H_2O_2 and we can therefore reasonably assume that assays involving DHR detected the accumulation of $ONOO^-$ alone. The results confirmed that as for O_2^-, $ONOO^-$ accumulates at the late stationary phase of growth (Figure 4.2 (C)).

A recent study in *Staphylococcus aureus* revealed that the addition of different oxidative stresses to exponentially growing cells resulted in complex changes in protein expression, including the induction of many proteins with a role in protection against oxidative stress.[57] Here, we also observe that ROS accumulation occurs in late stationary phase of *in vitro* growth and that this occurs with the induction of several proteins with a role in protection against oxidative stress. It is conceivable that throughout the growth curve, ROS act as signaling molecules activating pathways that regulate the induction of these proteins.

***A. baumannii* Stationary Cells Show a Constitutive Protection against ROS and RNI Related Stress.** To test the susceptibility of *A. baumannii* to ROS throughout *in vitro* growth, cells from exponential and late stationary phases were incubated with menadione (500 μM) as a source of O_2^- or H_2O_2 (30 mM).[13,57,58] As referred to above, O_2^- can be dismutated into H_2O_2, which in its turn decomposes into hydroxyl radicals (OH^-) through catalysis by low-valence-transition metal ions in a Fenton-Haber-Weiss reaction. These oxidizing agents react strongly with macromolecules, resulting in a variety of types of base damage.[59] The results obtained here revealed that when challenged with H_2O_2 the cell survival rates increased from 0%

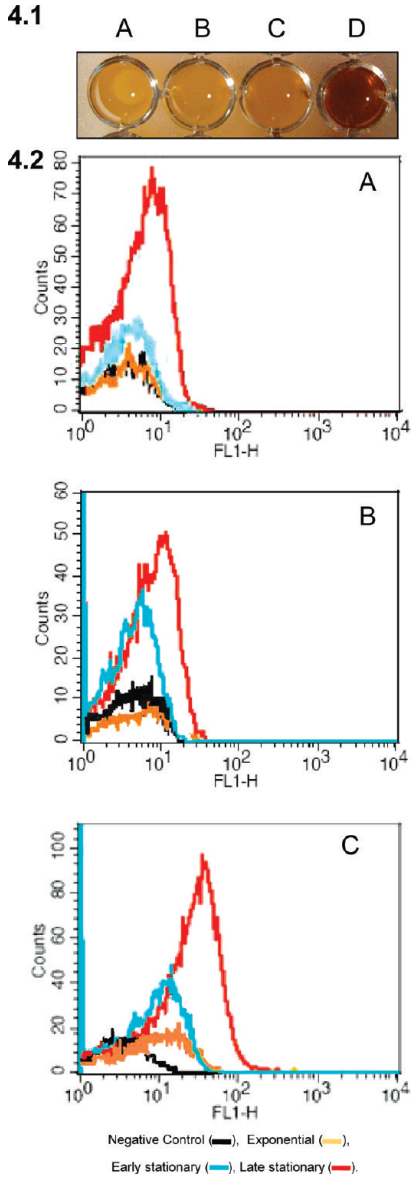

Figure 4. Accumulation of ROS during growth phases. **(4.1)** Detection of exogenous O_2^- accumulation with NBT. A change in color indicates accumulation of O_2^-. No color change was observed in the control wells (A), at exponential phase (B), and early stationary phase (C). The well corresponding to stationary phase medium was the only one in which incubation with NBT resulted in a change in color to deep red (D). The same result was obtained in three independent experiments. **(4.2)** Production of endogenous ROS and RNI at different phases of growth; (A) O_2^-, (B) OH^- and (C) $ONOO^-$. In each panel, black line represents the negative control, yellow line represents exponential cells, blue line represents the early stationary cells, and red represents the late stationary cells.

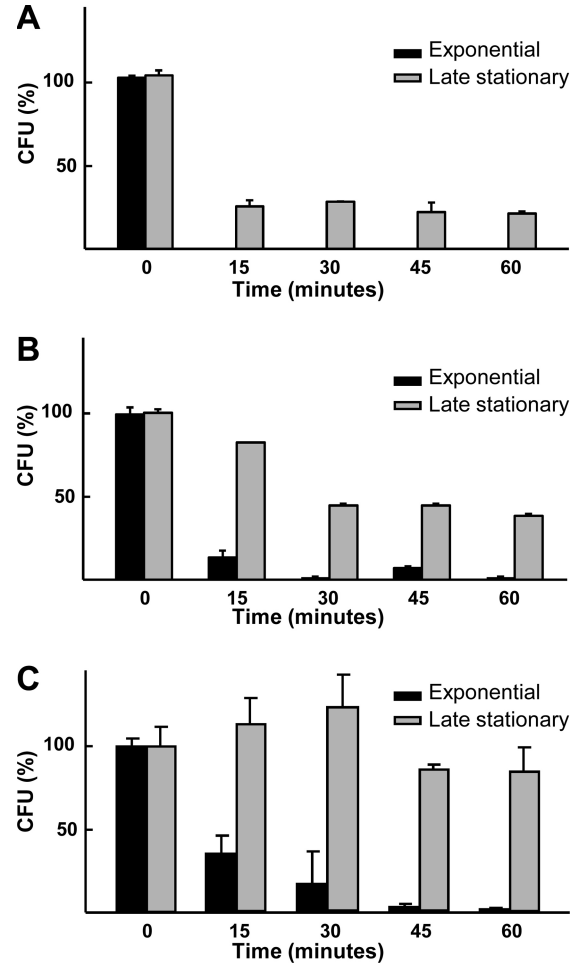

Figure 5. Effects of different oxidant stress on cells at different stages of growth. Exponential growing cells and late stationary cells were treated with 30 mM of H_2O_2. (A) Exponential growing cells and late stationary cells were treated with 500 μM of menadione (supply of O_2^-). (B) Exponential growing cells and late stationary cells were treated with 1 mM of a sodium nitroprusside (NO donor), (C). Error bars indicate the standard deviations for replicate samples. At least three replicate experiments were performed and each had results similar to those shown. Error bars indicate the standard deviations for replicate samples. At least three replicate experiments were performed and each had results similar to those shown ($p < 0.001$ in all cases).

(exponential cells) to approximately 25% (late stationary) (Figure 5A). Similarly, when incubated with menadione, the cell survival rates increased from approximately 5% (exponential cells) nearly to 40−85% (late stationary) (Figure 5B).

To determine if the increased resistance of late stationary cell to ROS could be associated with the induction of antioxidant proteins, we have compared the antioxidant capacities of cell lysates obtained from the exponential and late stationary phases of growth (see Materials and Methods). According to total antioxidant activity assay, the antioxidant capacity increased from 0 (exponential cells) to 80 240 ± 8300 μM/mg of protein extract of late stationary cells.

This report clearly indicates that late stationary cells are in fact more protected against oxidative stress and this can be associated with the induction of several enzymes that scavenge ROS, such as catalases (protein nos. i26 and i287), alkyl hydroperoxidase reductase (spot no. L10, Figure 2J), glutatione peroxidase (spot no. IL1, Figure 2K), antioxidant proteins (spot nos. L16 and L19, Figure 2L and 2M), but also with increased in the expression level of proteins related with protein repair, such as dnaK that minimize protein oxidative damage. In addition, the induction of DNA repair proteins, such as IHF, has been shown to play an important role against DNA OH^- cleavage.[60]

As referred to above, $ONOO^-$ accumulates at late stages of growth (Figure 4.2 (C)). On the basis of this, we wished to test the susceptibility of *A. baumannii* to RNI during *in vitro* growth.

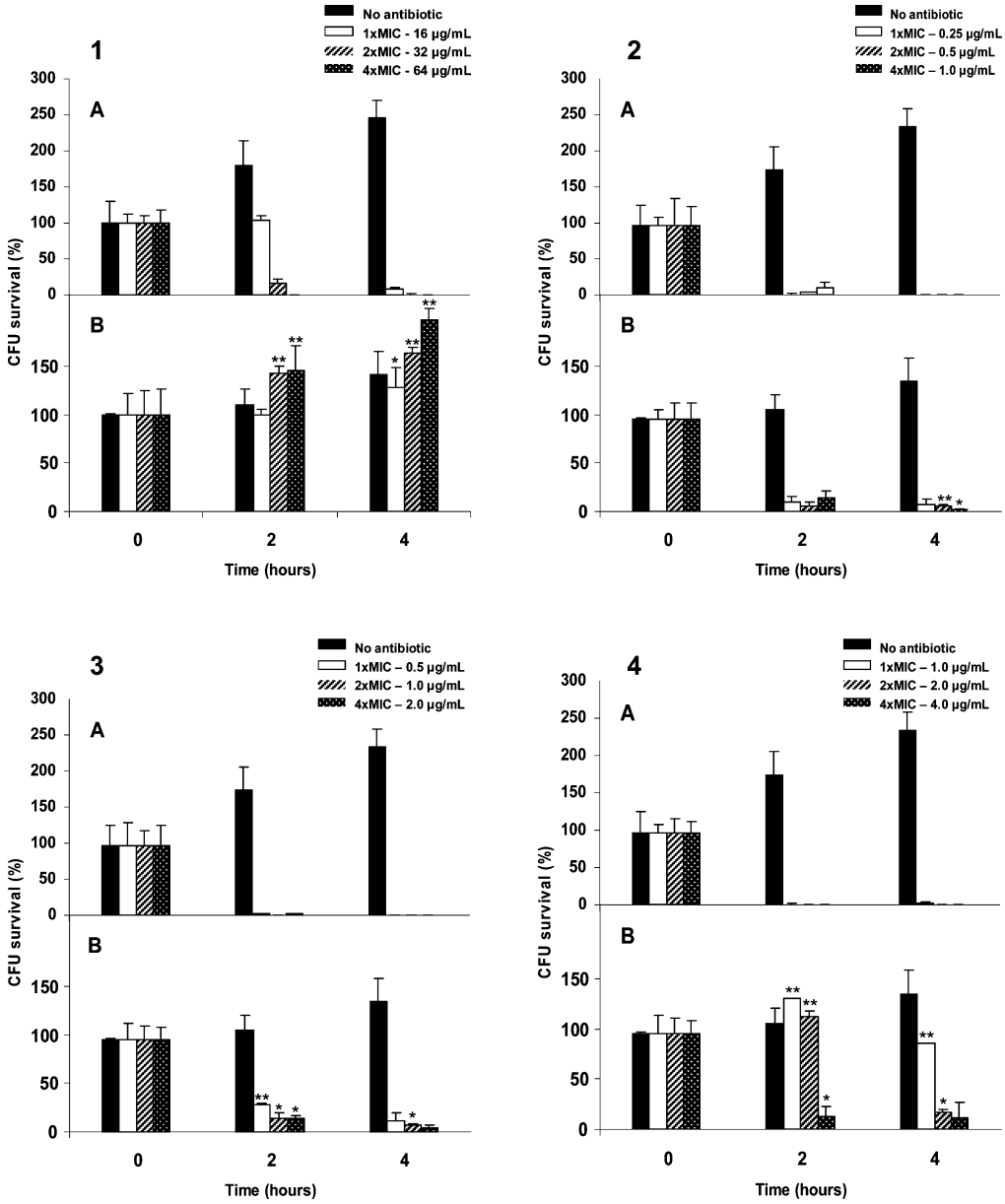

Figure 6. Survival rate of exponential growing *A. baumannii* cells and late stationary cells after treatment with different antibiotics: Ceftazidime **(1)**; Levofloxacin **(2)**; Imipenem **(3)**; Colistin **(4)**. In all cases the upper panel indicates the CFU of exponential cells (A) and lower panel indicates the cfu of cells at stationary phase of growth (B), after treatment with the respective antibiotics at the indicated minimal inhibitory concentrations (MIC). Error bars indicate the standard deviations for replicate samples. At least three replicate experiments were performed and each had results similar to those shown and statistical significant differences are indicated by $*p < 0.050$ and $**p < 0.010$.

Here the cells from both exponential and late stationary phase were incubated with 1 mM of a NO donor sodium nitroprusside (SNP).[53] Similar to the ROS assays, it was found that survival rates were higher among the late stationary cells when compared with exponential cells (Figure 5C). Interestingly, entry to stationary phase was associated with the induction of a flavohemoprotein (spot no. 172, Figure 2H). This correlation is of particular interest, since it was recently demonstrated that NO-inducible flavohemoproteins play an important role in protecting bacterial cells from nitrosative stress.[19,21,61] Hence, it is very likely that the up-regulation of this protein is part of an adaptive response of *A. baumannii* to the accumulation of RNI accumulation.

Several reports have shown evidence suggesting that an efficient defense mechanism against ROS and RNI damage enhances the ability of bacteria to survive macrophage attack.[62−65] We suggest that comparative analyses of the different phases of *in vitro* cultures can provide a convenient means of gaining new insights into the bacterial mechanism underlying during host interaction.

Stationary Cells Present a Higher Survival Rate to Antibiotics. It was recently demonstrated that the production of ROS is a common mechanism of cell death induced by bactericidal antibiotics.[22] As referred above, our observations indicate that late stationary cells are more protected against oxidative stress, which prompted us to investigate whether the susceptibility of *A. baumannii* to this type of antibiotics changed during the different growth phases of *in vitro* culture. Three major classes of bactericidal antibiotics were utilized, namely, β-lactams (ceftazidime and imipenem), quinolones (levofloxacin) and colistin.

The assays clearly showed that in all cases late stationary cells show higher survival rates to the action of bactericidal antibiotics (Figure 6). Whereas, in case of colistin, this is the first time that have been reported, in case of β-lactams and levofloxacin, this was some how expected, since that is widely accepted that the mode of action interferes with cell wall biosynthesis and DNA replication, respectively. However, it has to be mentioned that, for both β-lactams and quinolones, other toxicity mechanisms are implicated; for instance, it has been demonstrated that these types of antibiotics cause cell death by inducing ROS.[22,24,66]

Recent studies have demonstrated that ROS detoxifying enzymes such as catalases, superoxide dismutase and alkyl hydroperoxide reductase play an important role during response to antimicrobial stress.[24,67] Consistent with the concept that bacteria protection to ROS confers cross-protection against antibiotics, here we propose that throughout *in vitro* growth *A. baumannii* is exposed to adaptive doses of ROS, which in its turn leads to the induction of several oxidative stress responsive proteins and these are implicated in the protection not only against oxidative stress, but also against antibiotic stress.

Concluding Remarks

Herein, for first time, it was demonstrated that ROS and RNI accumulate during *in vitro* growth. This study indicates that *A. baumannii* contains a dynamic proteome, which responds accordingly to changes in the surrounding environment. Within this context, we highlight the induction of several oxidative-stress responsive proteins during the late stationary phase of growth, which may function in ROS and RNI detoxification, DNA repair and protein repair processes. Hence, it can be concluded that the *A. baumannii* proteome possesses robust machinery against oxidative stress. Moreover, it can be concluded that, throughout *in vitro* growth, *A. baumannii* undergoes important adaptive changes (including at the proteome level), that permitted late stationary phase cells to withstand levels of ROS, RNI and antibiotics considered to be lethal in other culture systems.

Acknowledgment. N.C.S. was supported by the Ministerio de Sanidad y Consumo, Instituto de Salud Carlos III-FEDER, Spanish Network for the Research in Infectious Diseases (REIPI RD06/0008). This work was also funded by FIS PI081613, PS09/00687 and PS07/90, PS07/51, and 08CSA064916PR from Xunta de Galicia. We gratefully acknowledge helpful advices from Dr. Cristina Romero Ruiz and Dr. Jesus Mateos Martín (INIBIC). For technical support, we would like to acknowledge our laboratory technician Maria Jose Barba Miramontes.

Supporting Information Available: Table 3, oligonucleotides used in RT-PCR experiments; Tables 4 and 5, MALDI-TOF/TOF characterization of *A. baumannii* proteins. This material is available free of charge via the Internet at http://pubs.acs.org.

References

(1) Dijkshoorn, L.; Nemec, A.; Seifert, H. An increasing threat in hospitals: multidrug-resistant *Acinetobacter baumannii*. *Nat. Rev. Microbiol.* **2007**, *5* (12), 939–951.

(2) Peleg, A. Y.; Seifert, H.; Paterson, D. L. *Acinetobacter baumannii*: emergence of a successful pathogen. *Clin. Microbiol. Rev.* **2008**, *21* (3), 538–582.

(3) Charnot-Katsikas, A.; Dorafshar, A. H.; Aycock, J. K.; David, M. Z.; Weber, S. G.; Frank, K. M. Two cases of necrotizing fasciitis due to *Acinetobacter baumannii*. *J. Clin. Microbiol.* **2009**, *47* (1), 258–263.

(4) Jones, M.; Draghi, D.; Thornsberry, C.; Karlowsky, J.; Sahm, D.; Wenzel, R. Emerging resistance among bacterial pathogens in the intensive care unit - a European and North American Surveillance study (2000−2002). *Ann. Clin. Microbiol. Antimicrob.* **2004**, *3* (1), 14.

(5) van den Broek, P. J.; van der Reijden, T. J. K.; van Strijen, E.; Helmig-Schurter, A. V.; Bernards, A. T.; Dijkshoorn, L. Endemic and epidemic *Acinetobacter* species in a university hospital, an eight years' survey. *J. Clin. Microbiol.* **2009**, *47* (11)), 3593–3599.

(6) Martí, S.; Sánchez-Céspedes, J.; Oliveira, E.; Bellido, D.; Giralt, E.; Vila, J. Proteomic analysis of a fraction enriched in cell envelope proteins of *Acinetobacter baumannii*. *Proteomics* **2006**, *6* (S1), S82–S87.

(7) Siroy, A.; Cosette, P.; Seyer, D.; Lemaitre-Guillier, C.; Vallenet, D.; VanDorsselaer, A.; Boyer-Mariotte, S.; Jouenne, T.; Dé, E. Global comparison of the membrane subproteomes between a multidrug-resistant *Acinetobacter baumannii* strain and a reference strain. *J. Proteome Res.* **2006**, *5* (12), 3385–3398.

(8) Soares, N. C.; Cabral, M.; Parreira, J.; Gayoso, C.; Barba, M.; Bou, G. 2-DE analysis indicates that *Acinetobacter baumannii* displays a robust and versatile metabolism. *Proteome Sci.* **2009**, *7* (1), 37.

(9) Fernández-Reyes, M.; Rodríguez-Falcón, M.; Chiva, C.; Pachón, J.; Andreu, D.; Rivas, L. The cost of resistance to colistin in *Acinetobacter baumannii*: a proteomic perspective. *Proteomics* **2009**, *9* (6), 1632–1645.

(10) Robin, A.; Joseleau-Petit, D.; D'Ari, R. Transcription of the ftsZ gene and cell division in *Escherichia coli*. *J. Bacteriol.* **1990**, *172* (3), 1392–1399.

(11) Nyström, T. Stationary-phase physiology. *Annu. Rev. Microbiol.* **2004**, *58*, 161–181.

(12) Lee, K. J.; Bae, S. M.; Lee, M. R.; Yeon, S. M.; Lee, Y. H.; Kim, K.-S. Proteomic analysis of growth phase-dependent proteins of *Streptococcus pneumoniae*. *Proteomics* **2006**, *6* (4), 1274–1282.

(13) Dowds, B. C.; Murphy, P.; McConnell, D. J.; Devine, K. M. Relationship among oxidative stress, growth cycle, and sporulation in Bacillus subtilis. *J. Bacteriol.* **1987**, *169* (12), 5771–5775.

(14) Gonzalez-Flecha, B.; Demple, B. Role for the oxyS gene in regulation of intracellular hydrogen peroxide in *Escherichia coli*. *J. Bacteriol.* **1999**, *181* (12), 3833–3836.

(15) von Ossowski, I.; Mulvey, M. R.; Leco, P. A.; Borys, A.; Loewen, P. C. Nucleotide sequence of *Escherichia coli* katE, which encodes catalase HPII. *J. Bacteriol.* **1991**, *173* (2), 514–520.

(16) Eisenstark, A.; Calcutt, M. J.; Becker-Hapak, M.; Ivanova, A. Role of *Escherichia coli* rpos and associated genes in defense against oxidative damage. *Free Radical Biol. Med.* **1996**, *21* (7), 975–993.

(17) Fernandez, J. L.; Cartelle, M.; Muriel, L.; Santiso, R.; Tamayo, M.; Goyanes, V.; Gosalvez, J.; Bou, G. DNA fragmentation in microorganisms assessed in situ. *Appl. Environ. Microbiol.* **2008**, *74* (19), 5925–5933.

(18) Ouellet, H.; Ouellet, Y.; Richard, C.; Labarre, M.; Wittenberg, B.; Wittenberg, J.; Guertin, M. Truncated hemoglobin HbN protects *Mycobacterium bovis* from nitric oxide. *Proc. Natl. Acad. Sci. U.S.A.* **2002**, *99* (9), 5902–5907.

(19) Svensson, L.; Marklund, B. I.; Poljakovic, M.; Persson, K. Uropathogenic *Escherichia coli* and tolerance to nitric oxide: the role of flavohemoglobin. *J. Urol.* **2006**, *175* (2), 749–753.

(20) Hassett, D. J.; Cohen, M. S. Bacterial adaptation to oxidative stress: implications for pathogenesis and interaction with phagocytic cells. *FASEB J.* **1989**, *3* (14), 2574–2582.

(21) Poole, R. K.; Hughes, M. N. New functions for the ancient globin family: bacterial responses to nitric oxide and nitrosative stress. *Mol. Microbiol.* **2000**, *36* (4), 775–783.

(22) Kohanski, M. A.; Dwyer, D. J.; Hayete, B.; C, A. L.; Collins, J. J. A common mechanism of cellular death induced by bactericidal antibiotics. *Cell* **2007**, *130* (5), 797–810.

(23) Wright, D. G. On the road to bacterial cell death. *Cell* **2007**, *130* (5), 781–783.

(24) Kolodkin-Gal, I.; Sat, B.; Keshet, A.; Kulka, H. E. The communication factor EDF and the toxin-antitoxin module mazEF determine the mode of action of antibiotics. *PLoS Biol.* **2008**, *6* (12), e319.

(25) Molloy, M. P.; Herbert, B. R.; Slade, M. B.; Thierry, R.; Nouwens, A. S.; Williams, K. L.; Gooley, A. A. Proteomics analysis of the *Escherichia coli* outer membrane. *Eur. J. Biochem.* **2000**, *267* (10), 2871–2881.

(26) Bradford, M. A rapid and sensitive method for the quantification of microgram quantities of protein utilizing the principle of protein-dye binding. *Anal. Biochem.* **1976**, *72*, 248–254.

(27) Ramagli, L. Quantifying protein in 2-D PAGE solubilization buffers. *Methods Mol. Biol.* **1999**, *112*, 99–103.
(28) Laemmli, U. K. Cleavage of structural proteins during the assembly of head proteins of bacteriophage T4. *Nature* **1970**, *227* (5259), 680–685.
(29) Blum, H.; Beier, H.; Gross, H. Improved silver staining of plant proteins, RNA and DNA in polyacrylamide gels. *Electrophoresis* **1987**, *8* (2), 93–99.
(30) Pandey, A.; Andersen, J.; Mann, M. Use of mass spectrometry to study signalling pathways. *Sci. STKE* **2000**, *2000* (37), PL1.
(31) Sechi, S.; Chait, B. T. Modification of cysteine residues by alkylation. A tool in peptide mapping and protein identification. *Anal. Chem.* **1998**, *70* (24), 5150–5158.
(32) Shilov, I. V.; Seymour, S. L.; Patel, A. A.; Loboda, A.; Tang, W. H.; Keating, S. P.; Hunter, C. L.; Nuwaysir, L. M.; Schaeffer, D. A. The Paragon Algorithm, a Next Generation Search Engine That Uses Sequence Temperature Values and Feature Probabilities to Identify Peptides from Tandem Mass Spectra. *Mol. Cell. Proteomics* **2007**, *6* (9), 1638–1655.
(33) Jiang, Z. Y.; Woollard, A. C.; Wolf, S. P. Hydrogen peroxide production during experimental protein glycation. *FEBS Lett.* **1990**, *268* (1), 69–71.
(34) Kolkman, A.; Dirksen, E. H. C.; Slijper, M.; Heck, A. J. R. Double standards in quantitative proteomics: direct comparative assessment of difference in gel electrophoresis and metabolic stable isotope labeling. *Mol. Cell. Proteomics* **2005**, *4* (3), 255–266.
(35) Otto, K.; Silhavy, T. J. Surface sensing and adhesion of *Escherichia coli* controlled by the Cpx-signaling pathway. *Proc. Natl. Acad. Sci. U.S.A.* **2002**, *99* (4), 2287–2292.
(36) Hammer, B. K.; Swanson, M. S. Co-ordination of *Legionella pneumophila* virulence with entry into stationary phase by ppGpp. *Mol. Microbiol.* **1999**, *33* (4), 721–731.
(37) Swanson, M. S.; Fernández-Moreira, E. A microbial strategy to multiply in macrophages: the pregnant pause. *Traffic.* **2002**, *3* (3), 170–177.
(38) Downer, R.; Roche, F.; Park, P. W.; Mecham, R. P.; Foster, T. J. The elastin-binding protein of *Staphylococcus aureus* (EbpS) is expressed at the cell surface as an integral membrane protein and not as a cell wall-associated protein. *J. Biol. Chem.* **2002**, *277* (1), 243–250.
(39) Heilmann, C.; Thumm, G.; Chhatwal, G. S.; Hartleib, J.; Uekotter, A.; Peters, G. Identification and characterization of a novel autolysin (Aae) with adhesive properties from *Staphylococcus epidermidis*. *Microbiology* **2003**, *149* (10), 2769–2778.
(40) Rodríguez-Baño, J.; Martí, S.; Soto, S.; Fernández-Cuenca, F.; Cisneros, J. M.; Pachón, J.; Pascual, A.; Martínez-Martínez, L.; McQueary, C.; Actis, L. A.; Vila, J. Biofilm formation in *Acinetobacter baumannii*: associated features and clinical implications. *Clin. Microbiol. Infect.* **2008**, *14* (3), 276–278.
(41) Tomaras, A. P.; Dorsey, C. W.; Edelmann, R. E.; Actis, L. A. Attachment to and biofilm formation on abiotic surfaces by *Acinetobacter baumannii*: involvement of a novel chaperone-usher pili assembly system. *Microbiology* **2003**, *149* (12), 3473–3484.
(42) Choi, C. H.; Lee, E. Y.; Lee, Y. C.; Park, T. I.; Kim, H. J.; Hyun, S. H.; Kim, S. A.; Lee, S.-K.; Lee, J. C. Outer membrane protein 38 of *Acinetobacter baumannii* localizes to the mitochondria and induces apoptosis of epithelial cells. *Cell. Microbiol.* **2005**, *7* (8), 1127–1138.
(43) Dorsey, C. W.; Beglin, M. S.; Actis, L. A. Detection and analysis of iron uptake components expressed by *Acinetobacter baumannii* clinical isolates. *J. Clin. Microbiol.* **2003**, *41* (9), 4188–4193.
(44) Dorsey, C. W.; Tomaras, A. P.; Connerly, P. L.; Tolmasky, M. E.; Crosa, J. H.; Actis, L. A. The siderophore-mediated iron acquisition systems of *Acinetobacter baumannii* ATCC 19606 and *Vibrio anguillarum* 775 are structurally and functionally related. *Microbiology* **2004**, *150* (11), 3657–3667.
(45) Huard, R. C.; Chitale, S.; Leung, M.; Lazzarini, L. C. O.; Zhu, H.; Shashkina, E.; Laal, S.; Conde, M. B.; Kritski, A. L.; Belisle, J. T.; Kreiswirth, B. N.; Lapa e Silva, J. R.; Ho, J. L. The *Mycobacterium tuberculosis* complex-restricted gene cfp32 encodes an expressed protein that is detectable in tuberculosis patients and is positively correlated with pulmonary interleukin-10. *Infect. Immun.* **2003**, *71* (12), 6871–6883.
(46) Velayhudhan, J.; Castor, M.; Richardson, A.; Main-Hester, K. L.; Fang, F. C. The role of ferritins in the physiology of *Salmonella enterica* sv. *Typhimurium*: a unique ferritin B in iron-sulphur cluster repair and virulence. *Mol. Microbiol.* **2007**, *63* (5), 1495–1507.
(47) MacLean, M. J.; Ness, L. S.; Ferguson, G. P.; Booth, I. R. The role of glyoxalase I in the detoxification of methylglyoxal and in the activation of the KefB K^+ efflux system in *Escherichia coli*. *Mol. Microbiol.* **1998**, *27* (3), 563–571.
(48) Passalacqua, K. D.; Bergman, N. H.; Lee, J. Y.; Sherman, D. H.; Hanna, P. C. The global transcriptional responses of *Bacillus anthracis* Sterne (34F2) and a Delta sodA1 mutant to paraquat reveal metal ion homeostasis imbalances during endogenous superoxide stress. *J. Bacteriol.* **2007**, *189* (11), 3996–4013.
(49) Nachin, L.; Nannmark, U.; Nystrom, T. Differential roles of the universal stress proteins of *Escherichia coli* in oxidative stress resistance, adhesion, and motility. *J. Bacteriol.* **2005**, *187* (18), 6265–6272.
(50) Tamarit, J.; Cabiscol, E.; Ros, J. Identification of the major oxidatively damaged proteins in *Escherichia coli* cells exposed to oxidative stress. *J. Biol. Chem.* **1998**, *273* (5), 3027–3032.
(51) Choi, Y. W.; Park, S. A.; Lee, H. W.; Kim, D. S.; Lee, N. G. Analysis of growth phase-dependent proteome profiles reveals differential regulation of mRNA and protein in *Helicobacter pylori*. *Proteomics* **2008**, *8* (13), 2665–2675.
(52) Jenney, F. E. J.; Verhagen, M. F.; Cui, X.; Adams, M. W. Anaerobic microbes without superoxide dismutase. *Science* **1999**, *286* (5438), 306–309.
(53) Barraud, N.; Hassett, D. J.; Hwang, S.-H.; Rice, S. A.; Kjelleberg, S.; Webb, J. S. Involvement of nitric oxide in biofilm dispersal of *Pseudomonas aeruginosa*. *J. Bacteriol.* **2006**, *188* (21), 7344–7353.
(54) Imlay, J. A. Cellular defenses against superoxide and hydrogen peroxide. *Annu. Rev. Biochem.* **2008**, *77* (1), 755–776.
(55) Koppenol, W. H.; Moreno, J. J.; Pryor, W. A.; Ischiropoulos, H.; Beckman, J. S. Peroxynitrite, a cloaked oxidant formed by nitric oxide and superoxide. *Chem. Res. Toxicol.* **1992**, *5* (6), 834–842.
(56) Pryor, W. A.; Squadrito, G. L. The chemistry of peroxynitrite: a product from the reaction of nitric oxide with superoxide. *Am. J. Physiol.: Lung Cell Mol. Physiol.* **1995**, *268* (5), L699–722.
(57) Wolf, C.; Hochgräfe, F.; Kusch, H.; Albrecht, D.; Hecker, M.; Engelmann, S. Proteomic analysis of antioxidant strategies of *Staphylococcus aureus*: diverse responses to different oxidants. *Proteomics* **2008**, *8* (15), 3139–3153.
(58) Miyasaki, K. T.; Wilson, M. E.; Reynolds, H. S.; Genco, R. J. Resistance of *Actinobacillus actinomycetemcomitans* and differential susceptibility of oral *Haemophilus* species to the bactericidal effects of hydrogen peroxide. *Infect. Immun.* **1984**, *46* (3), 644–648.
(59) Cabiscol, E.; Tamarit, J.; Ros, J. Oxidative stress in bacteria and protein damage by reactive oxygen species. *Int. Microbiol.* **2000**, *3* (1), 3–8.
(60) Dhavan, G. M.; Chothers, D. M.; Chance, M. R.; Brenowitz, M. Concerted binding and bending of DNA by *Escherichia coli* intergration factor. *J. Mol. Biol.* **2002**, *315* (5), 1027–1037.
(61) Stevanin, T. M.; Read, R. C.; Poole, R. K. The hmp gene encoding the NO-inducible flavohaenoglobin in *Escherichia coli* confers a protective advantage in resisting killing within macrophages, but not in vitro: links with swarming motility. *Gene* **2007**, *398* (1−2), 62–68.
(62) Cosgrove, K.; Coutts, G.; Jonsson, I.-M.; Tarkowski, A.; Kokai-Kun, J. F.; Mond, J. J.; Foster, S. J. Catalase (KatA) and alkyl hydroperoxide reductase (AhpC) have compensatory roles in peroxide stress resistance and are required for survival, persistence, and nasal colonization in *Staphylococcus aureus*. *J. Bacteriol.* **2007**, *189* (3), 1025–1035.
(63) Hampton, M. B.; Kettle, A. J.; Winterbourn, C. Involvement of superoxide and myeloperoxidase in oxygen-dependent killing of *Staphylococcus aureus* by neutrophils. *Infect. Immun.* **1996**, *64* (9), 3512–3517.
(64) Nunoshiba, T.; DeRojas-Walker, T.; Tannenbaum, S. R.; Demple, B. Roles of nitric oxide in inducible resistance of *Escherichia coli* to activated murine macrophages. *Infect. Immun.* **1995**, *63* (3), 794–798.
(65) Nunoshiba, T.; deRojas-Walker, T.; Wishnok, J. S.; Tannenbaum, S. R.; Demple, B. Activation by nitric oxide of an oxidative-stress response that defends *Escherichia coli* against activated macrophages. *Proc. Natl. Acad. Sci. U.S.A.* **1993**, *90* (21), 9993–9997.
(66) Kolodkin-Gal, I.; Engelberg-Kulka, H. The stationary sigma factor σ^S is responsible for the resistance of *Escherichia coli* stationary cells to *mazEF*-mediated cell death. *J. Bacteriol.* **2009**, *191* (9), 3177–3182.
(67) Wang, X.; Zhao, X. Contribution of oxidative damage to antimicrobial lethality. *Antimicrob. Agents Chemother.* **2009**, *53* (4), 1395–1402.

PR901116R

Journal of proteome research

ARTICLE

pubs.acs.org/jpr

Proteomic and Functional Analyses Reveal a Unique Lifestyle for *Acinetobacter baumannii* Biofilms and a Key Role for Histidine Metabolism

Maria P. Cabral,[†,∥] Nelson C. Soares,[†,∥] Jesús Aranda,[†] José R. Parreira,[†] Carlos Rumbo,[†] Margarita Poza,[†] Jaione Valle,[‡] Valentina Calamia,[§] Íñigo Lasa,[‡] and Germán Bou*[,†]

[†]Laboratorio de Microbiología, Instituto de Investigación Biomédica de A Coruña (INIBIC), Servicio de Microbiología, Complejo Hospitalario Universitario A Coruña (CHUAC), As Xubias s/n; La Coruña, Spain

[‡]Laboratorio de Biofilms Microbianos, Instituto de Agrobiotecnología, Universidad Pública de Navarra-CSIC, Pamplona, Spain

[§]Unidad de Proteómica, INIBIC, As Xubias s/n; La Coruña, Spain

Supporting Information

ABSTRACT: Biofilm formation is one of the main causes for the persistence of *Acinetobacter baumannii*, a pathogen associated with severe infections and outbreaks in hospitals. Here, we performed comparative proteomic analyses (2D-DIGE and MALDI-TOF/TOF and iTRAQ/SCX-LC−MS/MS) of cells at three different conditions: exponential, late stationary phase, and biofilms. These results were compared with alterations in the proteome resulting from exposure to a biofilm inhibitory compound (salicylate). Using this multiple-approach strategy, proteomic patterns showed a unique lifestyle for *A. baumannii* biofilms and novel associated proteins. Several cell surface proteins (such as CarO, OmpA, OprD-like, DcaP-like, PstS, LysM, and Omp33), as well as those involved in histidine metabolism (like Urocanase), were found to be implicated in biofilm formation, this being confirmed by gene disruption. Although L-His uptake triggered biofilms efficiently in wild-type *A. baumannii*, no effect was observed in Urocanase and OmpA mutants, while a slight increase was observed in a CarO deficient strain. We conclude that Urocanase plays a crucial role in histidine metabolism leading to biofilm formation and that OmpA and CarO can act as channels for L-His uptake. Finally, we propose a model in which novel proteins are suggested for the first time as targets for preventing the formation of *A. baumannii* biofilms.

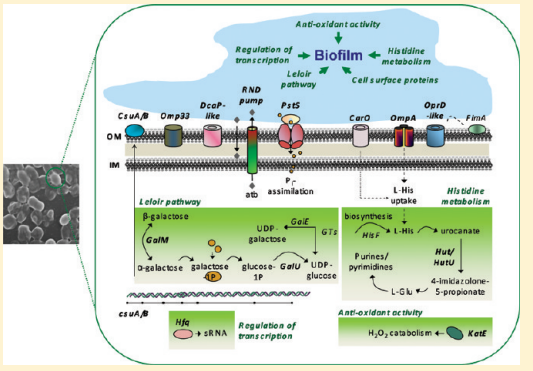

KEYWORDS: proteomics, *Acinetobacter baumannii*, biofilms, histidine, salicylate, 2DE, iTRAQ, MALDI-TOF/TOF

INTRODUCTION

Acinetobacter baumannii is a human pathogen that is often found in health care settings and is associated with a wide spectrum of infectious diseases, including pneumonia and bloodstream infections.[1,2]

Biofilms are assemblages of microorganisms characterized by cells that are irreversibly attached to a substratum and embedded in a matrix of self-produced extracellular polymeric substances, such as exopolysaccharides (EPS), proteins, nucleic acids and other substances; this type of sessile community−based existence is a critical characteristic for bacterial persistence.[3] Biofilm formation is frequent in clinical strains of *A. baumannii*,[4] and it is an important requirement for chronic colonization of human tissues and persistence in implanted medical devices. In addition, these structures are associated with multiple drug resistance,[5,6] being the microorganisms contained in the biofilm more resistant to desiccation, environmental stress (nutritional or oxidative stress), and UV light exposure. Although biofilm formation on abiotic surfaces contributes to the unique survival pattern of this pathogen in the hospital settings, little is known about this phenomenon. Therefore, the main goal of this study is to contribute insight into mechanisms behind the remarkable capacity of *A. baumannii* to form this type of structures.

Bacterial biofilm formation involves several complex molecular mechanisms in which some proteins are thought to play a major role during important events such as cell adhesion, maturation, signaling and others.[7−10] Biofilm initiation is mainly characterized by adhesion of cells to biotic or abiotic surfaces. Cell surface-attachment is mediated by proteins; some of which have already been described in *A. baumannii*. For instance, formation of biofilms on abiotic surfaces appears to depend on the expression of a CsuA/BABCDE chaperone-usher pili assembly system,[11] whereas the expression of the CsuA/BABCDE polycistronic operon is apparently not required for adhesion to biotic surfaces.[12,13] Instead, it is known that an outer membrane protein (OmpA) plays a crucial role during interaction with eukaryotic cells.[13]

Received: December 31, 2010
Published: May 26, 2011

Another example is a surface adhesin called Bap,[14] which is able to mediate primary attachment to both abiotic and biotic surfaces.[15] A Bap homologue has recently been described in *A. baumannii*,[16] and has been found to be directly involved in intercellular adhesion within mature biofilms, and to be conserved among a panel of 98 *Acinetobacter* strains.

The processes of cell surface attachment and subsequent biofilm formation/maturation involve complex regulatory networks, which coordinate the temporal expression of several mobility, adhesion, and exopolysaccharide genes.[17] Recently, the phosphoproteome was mapped over the course of biofilm development in *Pseudomonas aeruginosa*, and three novel two-component regulatory systems that are required for the development and maturation of biofilms were identified.[18] It has been suggested that in *A. baumannii*, an analogous two-component regulatory system comprising a sensor kinase encoded by bfmS and a response regulator encoded by bfmR, is involved in regulation of the CsuA/BABCDE chaperone-usher pili assembly system.[19]

Biofilm-associated microorganisms may grow in two different ways involving biofilms or planktonic (free-moving) lifestyles. The mechanism of biofilm development involves transition from planktonic cells to biofilm sessile cells, and the bacterium undergoes considerable changes during the transition. Comparison between these two states is therefore essential for obtaining further information about the biofilm lifestyle. At present, most of the available information regarding transition from planktonic lifestyle to biofilms is based on transcriptomic analyses. However, researchers have recently raised some concerns about the limitations of this technique for the identification of biofilm-regulated genes and, as pointed out by Sauer et al.,[9] proteomics is an essential complement to transcriptomic analyses. Taking this into account and that information concerning the transition of *A. baumannii* from planktonic to biofilms remains incomplete,[20] we propose a proteomic overview of this transition.

Recently, Shin et al.[21] used gels stained with Coomassie blue to compare the *A. baumannii* biofilm proteome with planktonic cells, and 17 differentially regulated proteins were detected of which 11 were up-regulated and 6 down-regulated in biofilms. In the above study, the biofilm protein extracts were recovered from 24 h-biofilm cultures grown in polystyrene Petri dishes for comparison with those obtained from a planktonic culture. However, as pointed out by Sauer et al.,[9] biofilms grown in beakers or microtiter plates are considered somewhat limited since mature biofilms cannot be studied under such experimental conditions. In the current study, we have attempted to complement this earlier work by comparing the proteome of biofilms obtained under flow conditions[22] with that of planktonic populations (at exponential and late stationary phases of growth). The respective protein extracts were subject to two-dimensional (2D) DIGE MALDI-TOF/TOF and iTRAQ analyses. We believe that the present study provides a more extensive and detailed description of the characteristics of the two bacterial lifestyles.

Several studies have indicated that salicylate (SA) affects the formation of biofilms in different bacterial species.[23,24] This compound is one member of a large group of pharmaceuticals referred to as nonsteroidal anti-inflammatories and it is the active component of the analgesic aspirin.[25] Moreover, salicylic acid produced by plants affects biofilm formation in a number of pathogenic bacteria, including *P. aeruginosa*,[26] *Staphylococcus aureus*,[27] *Staphylococcus epidermidis*,[28] and *Escherichia coli*.[29] In the present study, we show that SA effectively inhibits *A. baumannii* biofilm formation and that SA it is a useful tool for finding proteins that are directly or indirectly related to biofilm forming ability and even for obtaining further information about the mechanisms involved in biofilm formation.

A transcriptomic study comparing biofilm and planktonic cells in *E. coli* reported that biofilm development leads to up-regulation of amino acid metabolism[30] and in *Salmonella typhimurium*, a combination of transcriptomic and proteomic approaches revealed that genes involved in tryptophan biosynthesis and transport were up-regulated in the mature biofilm.[31] More recently, it has been reported that continuous-flow biofilms formed by many *E. coli* strains and other gram-negative bacteria accumulate high levels of valine, which inhibits the growth of *E. coli* K-12 and other isolates.[32] In a further report it was demonstrated that the presence of D-amino acids prevents biofilm formation in *S. aureus* and *P. aeruginosa*.[33] Overall, these studies illustrate the importance of amino acid metabolism during biofilm development. Moreover, evidence is provided here to support the idea that amino acid metabolism plays a pivotal role during biofilm formation in *A. baumannii*.

MATERIALS AND METHODS

Bacterial Strains and Plasmids

Bacterial strains and plasmids used in this study are listed in Table 1; see also refs 34−36. All strains were stored at −80 °C in Luria−Bertani broth (LB) containing 10% (v/v) glycerol. Kanamycin (50 μg/mL) and rifampicin (50 μg/mL; Sigma-Aldrich, St. Louis, MO) were used to select *E. coli* TG1 and *A. baumannii* mutant and complemented strains.

Growth Conditions for Obtaining *A. baumannii* Planktonic Cells and Biofilms

A. baumannii strain ATCC 17978 was grown overnight in Mueller-Hinton (MH) broth (Sigma-Aldrich) at 37 °C with constant shaking. To obtain SA-treated and nontreated cells, the resulting culture was diluted 100-fold in 500 mL of MH broth prepared with or without 16 mM SA (Sigma-Aldrich), respectively, and was incubated with shaking at 37 °C. Cells were harvested at exponential ($OD_{600\ nm}$ = 0.4) and late stationary ($OD_{600\ nm}$ = 2.0) phases of growth. The *A. baumannii* biofilm was obtained under a continuous flow culture system, consisting of 60-mL microfermentors (Pasteur Institute, Laboratory of Fermentation) with a continuous flow (40 mL/h) of MH broth and high constant aeration with sterile compressed air. Submerged Pyrex slides served as the growth substratum. A sample (with equivalent of $OD_{600\ nm}$ = 10) from an overnight culture of *A. baumannii* grown in MH broth was used to inoculate the microfermentors, which were then maintained at 37 °C for 24 h. Biofilms formed on the Pyrex slides were then removed with a cell scraper and frozen in liquid nitrogen.

Protein Extraction of Planktonic and Biofilm Cells

A. baumannii ATCC 17978 planktonic cells were harvested by centrifugation (3500*g*, 10 min, 4 °C) and washed twice with 0.9% (w/v) NaCl. The protein lysates of planktonic/biofilm cells were obtained by mechanical disruption. Briefly, total protein fractions were obtained from pellets were thawed in 3 or 5 mL lysis buffer [65 mM NaH_2PO_4, 50 mM Na_2HPO_4, 1 mM $MgSO_4 \cdot 7H_2O$, 30 or 50 μL of protease inhibitor mix (GE Healthcare) and 30 or

Table 1. Bacterial Strains and Plasmids Used in This Work

strain or plasmid	strain or plasmid	strain or plasmid
	Strains	
Acinetobacter baumannii		
ATCC 17978	wild-type strain	34
AbH12O-A2	clinical strain	35
CE1	clinical strain	laboratory stock
CE2	clinical strain	laboratory stock
CE3	clinical strain	laboratory stock
CE4	clinical strain	laboratory stock
urocanase protein mutant (Δhut)	derived from ATCC 17978. A1S_3407 locus mutant obtained by plasmid insertion. Kan^R, Zeo^R	this work
outer membrane protein CarO precursor mutant (ΔcarO)	derived from ATCC 17978. A1S_2538 locus mutant obtained by plasmid insertion. Kan^R, Zeo^R	this work
putative outer membrane protein mutant (ΔoprD-like)	derived from ATCC 17978. A1S_0201 locus mutant obtained by plasmid insertion. Kan^R, Zeo^R	this work
putative protein DcaP-like mutant (ΔdcaP-like)	derived from ATCC 17978. A1S_2753 locus mutant obtained by plasmid insertion. Kan^R, Zeo^R	this work
putative phosphate transporter protein mutant (ΔpstS)	derived from ATCC 17978. A1S_2448 locus mutant obtained by plasmid insertion. Kan^R, Zeo^R	this work
putative peptidoglycan-binding LysM protein mutant (ΔlysM)	derived from ATCC 17978. A1S_0820 locus mutant obtained by plasmid insertion. Kan^R, Zeo^R	this work
outer membrane protein OmpA mutant (ΔompA)	derived from ATCC 17978. A1S_2840 locus mutant obtained by plasmid insertion. Kan^R, Zeo^R	this work
outer membrane protein Omp33 mutant (Δomp33)	derived from ATCC 17978. A1S_3297 locus mutant obtained by gene replacement with an antibiotic resistance cassette flanked by regions homologous to the target locus. Kan^R	36
urocanase protein complemented mutant (Δhut-c)	derived from Δhut. Complemented with A1S_3407 locus gene cloned in pET-RA. Kan^R, Zeo^R, Rif^R	this work
outer membrane protein CarO precursor complemented mutant (ΔcarO-c)	derived from ΔcarO. Complemented with A1S_2538 locus gene cloned in pET-RA. Kan^R, Zeo^R, Rif^R	this work
putative outer membrane protein complemented mutant (ΔoprD-like-c)	derived from ΔoprD-like. Complemented with A1S_0201 locus gene cloned in pET-RA. Kan^R, Zeo^R, Rif^R	this work
putative protein DcaP-like complemented mutant (ΔdcaP-like-c)	derived from ΔdcaP-like. Complemented with A1S_2753 locus gene cloned in pET-RA. Kan^R, Zeo^R, Rif^R	this work
Escherichia coli		
TG1	supE thi-1 Δ(*lac-pro*AB) Δ(mcrB-hsdSM)5(rK− mK−) [F́ traD36 proAB lacIqZΔ*M15*]	laboratory stock
	Plasmids	
pCR-BluntII-TOPO	suicide plasmid for *A. baumannii*. Kan^R, Zeo^R	Invitrogen
pET-RA	*A. baumannii* replication origin. CTX-M14 β-lactamase gene promoter. Rif^R	HM219006[a]

[a] GenBank Accession Number.

50 μL of nuclease mix (GE Healthcare), depending on pellet mass] and sonicated for 3 × 5 min (0.5 cycle, 60 amplitude, 4 °C). Unbroken cells and cell debris were removed by centrifugation (1500*g* for 10 min and 3600*g* for 30 min, at 4 °C) and the supernatants were clarified through a 0.45 μm filter (Millipore, Billerica, MA). For gel-based analyses, the protein extracts were processed with a 2D Clean-up Kit (GE Healthcare), following the manufacturer's instructions and resuspended in rehydration buffer [8 M urea, 2% (w/v) CHAPS, 0.5% (v/v) IPG buffer pH 3.0−10.0 (GE Healthcare), 40 mM DTT]. The concentration of protein was measured by a modified Bradford assay[37] by use of a commercial kit (BioRad, Munich, Germany). In order to obtain the membrane-enriched protein fraction, the lysate was treated as described in Molloy et al.[38] and was modified as in Soares et al.[39] Briefly, an equal volume of 0.1 M Na_2CO_3 pH 11 was added to the *A. baumannii* protein lysate and was gently shaken overnight at 4 °C. The membrane-enriched fraction was obtained by ultracentrifugation (100 000*g*, 45 min, 4 °C) and the pellet was resuspended in 500 μL of double distilled water. The protein content was measured as above.

DIGE Experimental Design and Protein Labeling

The comparison of exponential cells, late stationary cells, and biofilms was performed across six DIGE gels (see Supporting Information Table S1.1), using 50 μg of total protein fraction per CyDye gel and two biological replicates for each condition (see Supporting Information Table S1.2). Cyanine dyes were reconstituted in 99.8% (v/v) anhydrous DMF and added to labeling reactions at a ratio of 400 ρmol CyDye/50 μg protein. To ensure that there were no dye-specific labeling artifacts, sample replicates in different gels were labeled with either Cy3 or Cy5, whereas the pooled standard sample was labeled with Cy2. The standard sample was prepared by pooling 50 μg of protein from each cell sample prior to labeling. Two samples of different replicates (Cy3 and Cy5) and an aliquot of internal standard pool (Cy2) were separated by two-dimensional gel electrophoresis (2DE) in each of the six gels (see Supporting Information Tables S1.1 and S1.2).

2DE and 2D DIGE

For DIGE analyses, total protein extracts from biofilm and planktonic cells were applied to 24 cm, nonlinear (NL) pH 3.0−11.0 IPG strips and treated as described in Ruiz-Romero et al.[40] For 2DE analysis of SA-treated and nontreated cells, solubilized protein extracts from planktonic cells (total and membrane-enriched fractions) were applied to 13 cm NL pH 3.0−10.0 IPG strips and treated as described in Soares et al.,[41] with some exceptions (described next). The 2DE experiments were performed with protein extracts obtained from three biological replicates of each condition. Standard continuous SDS-PAGE was performed on 15% (w/v) polyacrylamide gels. Analytical gels containing 25 μg of protein were stained with silver and used for image acquisition and gel analysis. Preparative gels were loaded with 500 μg of protein, stained with colloidal Coomassie staining,[42] and used for picking protein spots.

Image Acquisition and 2DE and 2D DIGE Gel Analyses

For DIGE, semiautomated image analysis was performed with Progenesis SameSpots V3.2 software (Nonlinear Dynamics). Image quality control was first performed to identify saturated spots. Multiplexed analysis was selected for DIGE experiments and a representative reference gel image was selected. The spots were detected in the subsequent segmentation. The normalized spot volumes were then ranked on the basis of ANOVA p-values, as well as fold changes.

Comparative analyses of 2DE silver-stained gels of SA-treated and nontreated cells were as described in Soares et al.[39] Images were acquired with an Image Scanner v3.3 densitometer (GE Healthcare). The 2DE gels were analyzed with Image Master Platinum 6.0 Software (GE Healthcare), according to the manufacturer's instructions. Spot detection parameters were adjusted to the following: smooth 2; MinArea 34, Saliency 10. For each protein fraction and growth phase, six image gels, three image gels for each growth condition (SA-treated cells compared with nontreated cells), were matched and combined to form a master gel, so that the same spot in different gels had the same identification number. Each matched spot was numbered, and the spot volumes were normalized by total spot volume. Intercomparative analyses between gels corresponding to SA-treated and nontreated cells were carried out for each growth phase and protein fraction. Differences between matched spots in both conditions were analyzed by Student's *t*-test, and considered significant at *p*-values <0.05. Results were expressed as change (*n*-fold) calculated using the ratio between the highest and lowest average spot volume between SA-treated and nontreated cells.

Trypsin Digestion of Proteins and Characterization by MALDI-TOF/TOF

Selected spots were excised from the gels, then treated and digested with trypsin (Roche Applied Science, Mannheim, Germany), as suggested in Sechi et al.[43] and detailed in Soares et al.[39] After digestion, the supernatant was collected and 1 μL was spotted onto a MALDI target plate (384-spot Teflon-coated plates) and allowed to air-dry at room temperature. The dried peptide digests were mixed with 3 mg/mL of an α-cyano-4-hydroxycinnamic acid in 0.1% (v/v) TFA and 50% (v/v) ACN and allowed to air-dry. The samples were analyzed using a MALDI-TOF/TOF mass spectrometer 4800 Proteomics Analyzer (Applied Biosystems, Framinghan, MA) and 4000 Series Explorer software (Applied Biosystems). MALDI-TOF spectra were acquired in reflector positive ion mode using 1000 laser shots per spectrum. Data Explorer version 4.2 (Applied Biosystems) was used for spectra analyses and generating peak picking list. All mass spectra were internally calibrated using autoproteolytic trypsin fragments and externally calibrate using standard peptide mixture (Sigma-Aldrich). TOF/TOF fragmentation spectra were acquired by selecting the 10 most abundant ions of each MALDI-TOF peptide mass map (excluding trypsin autolytic peptides and other background ions) and averaging 2000 laser shots per fragmentation spectrum. The parameters used to analyze the data were a signal-to-noise threshold of 20, minimum area of 100 and a resolution higher than 10000 with a mass accuracy of 20 ppm. For database queries and protein identification, the monoisotopic peptide mass fingerprinting data obtained from MS and the amino acid sequence tag obtained from each peptide fragmentation in MS/MS analyses were used to search for protein candidates using Mascot version 1.9 from Matrix Science (www.matrixscience.com). Peak intensity was used to select up to 50 peaks per spot for peptide mass fingerprinting and 50 peaks per precursor for MS/MS identification. Tryptic autolytic fragment-, keratin-, and matrix-derived peaks were removed from the data set utilized for database search. The search for peptides mass fingerprints and tandem MS spectra were performed in NCBInr database without any taxonomy restriction. Fixed and variable modifications were considered (Cys as S-carbamidomethyl and Met as oxidized methionine, respectively), allowing one trypsin missed cleavage. MS/MS ions searches were conducted with a mass tolerance of ±1.2 Da on the parent and 0.3−0.8 Da on fragments. Decoy search was done automatically by Mascot on randomized database of equal composition and size. Proteins and peptides scores were set up to maintain the false positive peptide ratio below 1%. Mascot scores for all protein identifications were higher than the accepted threshold for significance (at the $p < 0.05$ level, positive rate measured to be 0.047).

iTRAQ Analysis and Protein Label

The total protein fractions obtained from *A. baumannii* ATCC 17978 planktonic cells (exponential phase, late stationary phase, and SA-treated cells) and biofilms were submitted to the W.M. Keck Foundation Biotechnology resource laboratory at Yale University, U.S.A. Two biological replicates were obtained for each protein fraction and used in this analysis, based on the experimental design developed by Gan et al.[44] For accurate

determination of the protein concentration, each sample was subject to AAA (amino acid analysis). On the basis of the results of the AAA, 50 μg of each sample was digested with trypsin (Promega, Madison, WI) and subjected to 8plex iTRAQ labeling and strong Cation Exchange chromatography on the Yale University Vision workstation. Sample labeling with isobaric tagging reagents was carried out according to the manufacturer's instructions (Applied Biosystems). Briefly, 50 μg was dissolved in 20 μL of dissolution buffer and 2 μL of denaturant [2% (w/v) SDS] from iTRAQ kit. Two microliters of reducing reagent (50 mM TCEP) were added followed by incubation at 60 °C for 1 h. After centrifugation, 1 μL of cysteine-blocking (200 mM MMTS) agent was added and incubated at room temperature for 10 min. This was followed by addition of 5 μL of Lys C that was incubated for 5 h at 37 °C and then 5 μL of trypsin (Promega), followed by overnight incubation at 37 °C. Digested samples were labeled with eight different iTRAQ reagents dissolved in 50 μL of isopropanol and left at room temperature for 2 h. The samples were labeled with iTRAQ tags as follows: E1 (exponential phase), iTRAQ113; E2, iTRAQ114; L1 (late stationary phase), iTRAQ115; L2, iTRAQ116; Bio1 (biofilms), iTRAQ117; Bio2, iTRAQ118; SAexp (SA-treated samples, exponential phase), iTRAQ119; SAlate (SA-treated samples, late stationary phase), iTRAQ121.

Strong Cation Exchange Chromatography (SCX) and LC−MS/MS Analysis

After digestion, 180 μL of the combined peptide mixture was subjected to off-line SCX chromatography using an Applied Biosystems Vision Workstation with a 2.1 mm × 200 mm PolySulfethyl A column (5 μm 300 Å bead from PolyLC, Inc., 2.1 × 200 mm, PN 202SE0503). The column was equilibrated with Buffer A [10 mM KH_2PO_4, 25% (v/v) ACN, pH 3.0]. Peptides were then separated into 20 fractions using a 90 min linear salt gradient from 0−98% (v/v) Buffer B [Buffer A + 1 M KCl]. All 20 collected fractions from the SCX chromatography were dried and reconstituted with 5 μL of 70% (v/v) FA and 15 μL of 0.1% (v/v) TFA. LC−MS/MS was performed on a QSTAR Elite mass spectrometer interfaced with a Waters nanoAcquity UPLC system running Analyst QS 2.0 software. Peptides were resolved for LC−MS/MS by loading 5 μL of sample onto a Symmetry C18 nanoAcquity trapping column (180 μm × 20 mm, 5 μm) with 2% (v/v) ACN/0.1% (v/v) FA at 15 μL/min for 3 min. After trapping, peptides were resolved on a BEH130 C18 nanoAcquity column (75 μm tme250 mm, 1.7 μm) with a 60 min, 2−40% (v/v) ACN/0.1% (v/v) FA linear gradient (0.3 μL/min flow rate).

Electrospray ionization was performed using a Nanospray II interface (Applied Biosystems) equipped with the Microionspray source and FS360-75-15-D-20 PicoTip Emitter (New Objective Inc., Woburn, MA). Data dependent acquisition with each cycle consisted of 0.2 s MS spectrum and MS/MS acquisition using Smart CE and Smart Exit functionality on three highest peptide peaks.

Data Analysis and Statistics

Each of the QSTAR Elite mass spectrometer spectra files (*.wiff) was processed with MASCOT Distiller version 2.3.1 and the resulting peak lists were combined and database searched using MASCOT Server 2.2.06 and Swissprot 57.0 (released on March 24, 2009, containing 428 650 sequences). The search parameters included trypsin with one missed cleavage, static modifications carbamidomethyl (cys) and iTRAQ reagents (N-term, K), and variable modifications for oxidation (met). For the MS/MS acceptance criteria, protein identifications were accepted if they contained at least two peptide matches above identity threshold with a FRD of 0.28% and expectation >0.05. iTRAQ quantitation and secondary protein identification was performed using the Paragon search algorithm in ProteinPilot v.3.0 software using Swiss-Prot 57.0 database with "thorough search". The "iTRAQ 8plex peptide labeled" sample type and a "biological modification ID focus" were selected in the analysis method. Trypsin was selected as the digestion enzyme with cysteine alkylation by methyl methane thiosulfonate as a modification. Raw data that included, but was not limited to, reporter ion peak areas, reporter ion peak area error, peptide assignment, and confidence was exported from ProteinPilot (tab-delimited) without ProteinPilot's auto bias correction applied (non-normalized data) so we could perform quantile normalization as described below. The tab delimited ProteinPilot results were then uploaded into our Yale Protein Expression Database (YPED). For secondary protein identification, each protein had to have also been identified by Paragon and had two or more identified peptides and a ProteinPilot Confidence Score >2 (99% confidence level). To ensure that we only compared data that ProteinPilot includes in its quantitation analysis, peptides had to be classified as "used", which requires the presence of an iTRAQ label and at least one valid iTRAQ reporter ion ratio. Additionally, ProteinPilot only uses high-quality reporter ions for the peak area measurements to calculate iTRAQ peptide ratios. To remove low-intensity reporter ion ratios from the exported raw data sets, we used ProteinPilot's nonmodifiable criterion, which requires that valid iTRAQ reporter ion ratios must contain two iTRAQ reporter ions with a summed S/N ratio >9 to be included in the analysis. The data was then merged and loaded onto the Yale Protein expression database (YPED-http://yped.med.yale.edu), which allows viewing data online and performing downstream data analysis.

Quantitative Biofilm Assay

Biofilm formation was quantified using a protocol described previously[45] with some modifications. One colony of each strain of *A. baumannii* grown on agar media (37 °C, 18 h) was inoculated into 25 mL liquid media and incubated overnight (37 °C, shaking). Cells were harvested by centrifugation (3500*g*, 10 min, 4 °C) and the cell pellet was resuspended in fresh liquid media and adjusted to 0.7 McFarland units. From the adjusted culture, 200 μL were dispensed into each well of a 96 well flat-bottom polystyrene microtiter plate (excepting for the experiment presented in Figure 2, where U-bottom plates were used) and was incubated (37 °C, 48 h). The planktonic cells were then aspirated, and the wells were washed three times with sterile 0.9% (w/v) NaCl. The plate was then inverted and allowed to air-dry (room temperature, 1 h). Biofilms were stained with 0.2% (w/v) crystal violet solution (room temperature, 15 min), washed thrice as above, and quantified at 570 nm after solubilization with 200 μL of a 4:1 (v/v) mixture of absolute ethanol and acetone. All biofilm assays were performed with at least six replicates for each strain/condition (although the number of replicates was increased in some experiments, the absorbance values from six replicates are enough to determine an average and standard deviation for each strain or condition, providing a measure of the extent of biofilm formation).

Confocal Laser Scanning Microscopy (CLSM)

Bacterial biofilms were grown in chambered glass slides with polystyrene vessels (BD Falcon 8-well CultureSlides) for 48 h in MH broth containing different amounts of SA (0, 2, 4, 8, and 16 mM). The bacterial inoculum of *A. baumannii* ATCC 17978 was prepared and normalized as mentioned above for biofilm assay, and from the adjusted culture 500 μL was dispensed into each slide chamber. For imaging, the cell culture supernatant and planktonic cells were removed by aspiration with a pipet tip and the biofilms were washed thrice with sterile 0.9% (w/v) NaCl. The biofilms were stained with 200 μL of 1% (w/v) acridine orange solution (10 min) and subsequently washed twice with sterile 0.9% (w/v) NaCl. Confocal images were obtained in a Nikon A1R inverted microscope, and an argon laser (488 nm) was used for sample excitation. The images were viewed with NIS Elements (Nikon) software.

Scanning Electron Microscopy (SEM)

Biofilms formed by *A. baumannii* strains ATCC 17978, specific gene deletion mutants (ΔcarO, ΔdcaP-like, ΔoprD-like) and complemented (ΔcarO-c, ΔdcaP-like-c, ΔoprD-like-c) strains were analyzed by SEM. One colony of each strain grown on MH agar media (37 °C, 18 h) was inoculated into 2 mL of MH broth (supplemented with rifampicin in the case of complemented strains), dispensed into each well of a six-well polystyrene plate containing sterile coverslips, and incubated at 37 °C for 48 h. The coverslips were washed twice with 2 mL of PBS, fixed with 4% (v/v) paraformaldehyde in 0.1 M phosphate buffer pH 7.4 (30 min), and then washed twice with 2 mL of PBS. The coverslips were sequentially dehydrated for 10 min in 50, 70, 90, and 100% (v/v) ethanol and critical-point dried with CO_2 (Bal-Tec CPD 030). Finally, the coverslips were fixed to aluminum stubs with carbon tape and then coated with a layer of gold (Bal-Tec SCD 004 sputter coater) and examined with a Jeol JSM-6400 scanning electron microscope.

Construction of Specific Gene Mutants of *A. baumannii* and Gene Complementation

Gene inactivation was carried out as previously described in Héritier et al.[46] and Aranda et al.[36] with slight modifications. Briefly, kanamycin- and zeocin-resistant plasmid pCR-BluntII-TOPO (Invitrogen), unable to replicate in *A. baumannii*, was used as a suicide vector. An internal fragment (approximately 500 bp) of the target gene was amplified by PCR with the primers listed in Supporting Information Table S2, and genomic DNA from *A. baumannii* ATCC 17978 as template. The PCR product obtained was cloned into the pCR-BluntII-TOPO vector and the resulting plasmid was used to transform *E. coli* strain *TG1*. Recombinant plasmid (0.1 μg) was then introduced in the kanamycin- and zeocin-susceptible *A. baumannii* ATCC 17978 strain by electroporation. Mutants were selected on kanamycin-containing plates. Inactivation of the target gene by insertion of the plasmid via single crossover recombination was checked by sequencing the amplified PCR products with the primer pairs listed in Table S2.

In order to complement *A. baumannii* mutants, the wild-type gene was amplified from *A. baumannii* strain ATCC 17978 with the primers listed in Supporting Information Table S2 and cloned into the *XbaI* restriction site of the rifampicin-resistant pET-RA vector under the control of the β-lactamase CXT-M-14 gene promoter. *A. baumannii* mutants were transformed with the corresponding recombinant plasmid. Selection of transformants was made on rifampicin- and kanamycin-containing plates and confirmed by PCR.

Growth of *A. baumannii* Biofilms with Different Amino Acids and Isomers Supplied As the Only Carbon Source

To test the effect of given amino acids and specific L-His and D-His isomers on the biofilm formation process, *A. baumannii* strain ATCC 17978 was grown on MH agar and MH broth as made for the quantitative biofilm assay (see above). After harvesting, cells were washed thrice with sterile 0.9% (w/v) NaCl and resuspended in a solution of M9 minimal salts (42 mM Na_2HPO_4, 24 mM KH_2PO_4, 9 mM NaCl, and 19 mM NH_4Cl) supplemented with 0.1 mM $CaCl_2$, 2 mM $MgSO_4$ (M9 minimal media), and M9 minimal media containing 20 mM of different amino acids (L-His, L-Arg, L-Val, L-Asp, L-Glu, L-Ser, L-Thr, L-Cys, Gly), 20 mM D-His, and a combination of 20 mM L-His + (5, 10, and 20 mM) D-His. Adjusted cell suspensions were cultivated on polystyrene plates and concomitant biofilm formation was quantified as above. To test the specific effect of L-His, *A. baumannii* strains Δhut, ΔcarO, ΔoprD-like, ΔdcaP-like, ΔompA, and Δomp33 were also grown in M9 minimal media alone and supplemented with 20 mM of this amino acid. The biofilms formed were quantified as above. All L-amino acids and D-His were obtained from Sigma-Aldrich, excepting L-Glu, which was obtained from Merck−Calbiochem.

RESULTS AND DISCUSSION

Proteomics Evidence Showing That Biofilms Have a Unique Phenotype

There is an increasing controversy about whether biofilms are basically a mass of bacteria coexisting at various stages or if they present a specific phenotype. A transcriptome study of the biofilm and planktonic cells of *P. aeruginosa* revealed a difference of less than 1% in gene expression.[47] It can be argued that in such cases the biofilm phenotype appears to be regulated at translational and post-translational levels. In the present study, different proteomic approaches were used to verify whether *A. baumannii* biofilm cells have a unique protein pattern or are a mixture of exponential and stationary phase planktonic cells. Protein extracts were subjected to comparative DIGE-SameSpots analyses. Almost 1200 protein spots were detected across the three conditions. Gel images were analyzed, independent pair comparison was performed and a minimum fold change of 1.4 (p-value <0.05) was used to select protein spots, which suffered significant changes in intensity. Principal component analysis (PCA) was used to interpret variations in the mean quantity of spots in the context of the following question: Are biofilms composed of a mixture of cells at various phases of growth or do they display an exclusive proteome and therefore unique phenotype? The results of the analyses clearly indicate the presence of three different protein populations (Figure 1): biofilms, exponential phase, and stationary phase planktonic cells.

The comparison between biofilms and planktonic cells revealed 392 differential abundant protein spots [summarized in Table 2 as follows: 54 spots were exclusively up-regulated in the biofilm proteome (e.g., spots 369, 836, 860, and 1123), whereas 50 spots were exclusively down-regulated in biofilms cells]. Also, 129 of the protein spots were almost equally expressed both in exponential as well as in biofilms cells (e.g., spot 560) and 40 of the protein spots presented almost the same level of expression in

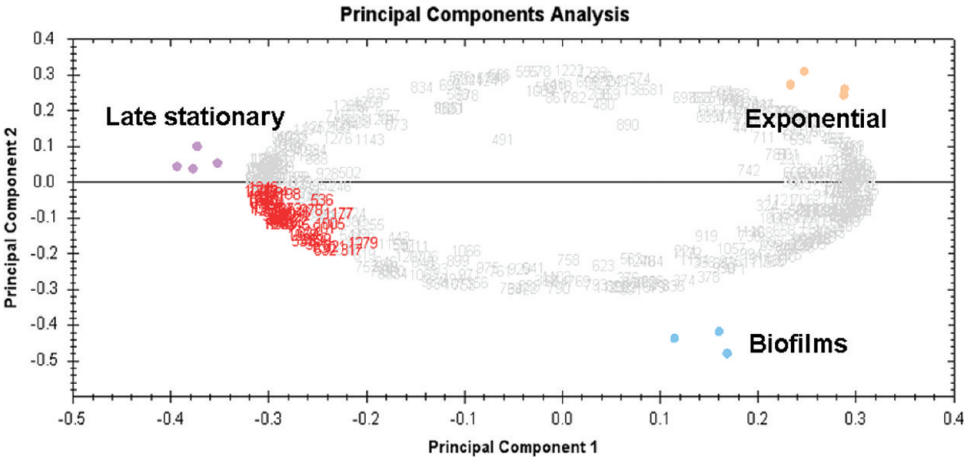

Figure 1. Principal component analysis provided by Samespots analyses, comparing the level of variance among biological replicates within the same sample and the level of variance among the three subproteomes (obtained from cells at exponential, late stationary phase, and biofilms).

both the biofilm and in late stationary phase cells (e.g., spots 463 and 605). Finally, 119 spots were exclusively up-regulated in late stationary phase cells.

Further gel-free analyses using SCX-LC−MS/MS 8plex iTRAQ labeling revealed that a total of 248 proteins were quantified with two or more peptides and with a protein score (PS) >2, and further 312 proteins were detected with single peptide and/or PS <2. The quantitative results of each sample are resumed in Table 3. Details as protein score, protein ratios, *p*-values, unique peptides, and percentage coverage are available at the Yale Protein expression database (YPED, http://yped.med.yale.edu). An acceptable biological variation level was found between the replicates; for example, replicates obtained from protein extracts of biofilms showed a correlation of $R^2 = 0.778$, a similar value to that found by Gan et al.[44] when comparing experimental replicates. Proteins with a ratio >1.2 or <0.8 (*p*-value <0.05) in two of the replicates were considered to be differentially expressed. The differences based on these criteria are summarized in Table 3. Of the 248 identified proteins, 41 were differentially regulated, for example, Orotate phosphoribosyltransferase (i134) and 29 kDa outer membrane protein (i213).

Although the three subproteomes share a constitutive expression of the majority of the proteins, iTRAQ and DIGE analyses provided here are consistent with the concept that the bacteria within biofilms display a different phenotype from their planktonic counterparts. Combining these proteomic approaches allowed us not only to validate results obtained by either techniques but also to gain information about unique features from each method. Hence, similar expression patterns were observed for F0F1 ATP synthase β-subunit (spot 605, Table 2; protein i14, Table 3), fatty acid oxidation complex α-subunit (spot 766, Table 2; protein i10, Table 3) and 29 kDa Omp (CarO) (spot 1071, Table 2; protein i213, Table 3), when comparing both techniques. Additionally, other proteins were found to be differentially expressed with only one of the referred methods. The number of specific biofilm proteins identified here is to some extent consistent with the proposed developmental model of biofilm formation, in which the transition from free-swimming lifestyle to biofilm involves a hierarchical network of genetic pathways leading to the differential regulation of biofilm-associated proteins.[48] Interestingly, the proteome of biofilm cells proteome is more similar to that of exponential cells rather than stationary cells, given the number of proteins that present similar expression patterns (see Tables 2 and 3). This was somewhat unexpected, since the results of previous transcriptomic studies in other bacterial species suggest that biofilm cells were more similar to a stationary phase mode of growth.[30,31] In the present study, the proteins that presented similar expression patterns in exponential phase and biofilms are related to bacterial growth and cell division, fo example, ribosomal subunits (e.g., spots 917 and 1181, Table 2; proteins i35 and i49, Table 3), elongation factors (spot 340, Table 2) and trigger factors (spot 560, Table 2; protein i19, Table 3). According to Stoodley et al.,[49] the biofilm developmental model is a temporal cycle comprised of five stages: planktonic, attachment, macrocolony formation, maturation, and dispersal. During the process of biofilm aging, nutrients become limiting, byproducts accumulate, and it may therefore be advantageous for biofilm-associated bacteria to dissemble and revert to initial planktonic existence.[49,50] One possible interpretation for these unexpected findings is that in order to ensure such versatility in lifestyle biofilm cells may conserve part of the required cell division machinery to behave promptly as exponential cells in case of reversion of biofilms to planktonic mode. Here, biofilms and late stationary proteomes showed distinct expression pattern for some proteins related to stress response and redox reactions. In the first case, a universal stress protein were found to be up-regulated in stationary phase but not in biofilm cells (spot 1196, Table 2, FC:3.3). In the last case, the expression pattern of some proteins involved in redox reactions indicates that late stationary cells could be more protected against oxidative stress, than biofilm cells. Examples are catalase-peroxidase (protein i26, Table 3), alkyl hydroperoxide reductase C22 subunit (spot 1017,Table 2), superoxide dismutase (spot 1027, Table 2) and a putative oxidoreductase (spot 1037, Table 2). These findings suggest that stationary phase planktonic and biofilms cells are subjected to different environmental pressures, which may result in different proteome patterns.

SA Inhibits Biofilm Formation and down-Regulates Biofilm-Related Proteins

As already mentioned, it has been reported that in species closely related to *A. baumannii*, such as *P. aeruginosa*, SA significantly

Table 2. Functional Classification of Identified and Differentially Expressed DIGE Protein Spots between *A. baumannii* Planktonic and Biofilm Culture

protein description	spot no.	Anova (p)	fold[a]	NCBInr acession no.	average spot volume exp[b]	late[c]	biofilm[d]
Post-translation Modification, Protein Turnover, Chaperones							
chaperon Hsp 70	403	9.344×10^{-5}	1.6	gi|126642981	0.810	1.312	0.886
trigger factor	560	5.133×10^{-7}	2.1	gi|169797268	1.254	0.591	1.044
Translation, Ribosomal Structure, and Biogenesis							
elongation factor G	340	3.729×10^{-4}	1.6	gi|50084094	1.131	0.690	1.022
30S ribosomal protein S1	447	9.201×10^{-6}	2.1	gi|50085438	1.376	0.670	1.115
30S ribosomal protein S1	463	7.837×10^{-5}	1.8	gi|126641617	1.249	0.712	0.886
50S ribosomal protein L1	892	8.237×10^{-6}	3.2	gi|126640372	2.117	0.812	2.582
30S ribosomal protein S2	917	2.082×10^{-4}	2.0	gi|50085372	1.540	0.772	1.391
50S ribosomal protein L6	1059	1.732×10^{-5}	2.5	gi|169632365	1.765	0.839	2.098
50S ribosomal protein L9	1181	0.003	1.7	gi|126642218	1.151	0.690	1.134
Energy Production and Conversion							
F0F1 ATP synthase β-subunit	605	0.006	1.7	gi|50083469	1.345	0.801	0.928
acetyl-coenzyme A carboxylase carboxyl transferase	944	6.227×10^{-5}	2	gi|126640675	1.432	0.703	0.706
Amino Acid Transport and Metabolism							
fumarate hydratase	619	9.018×10^{-4}	1.5	gi|169795668	0.748	1.097	1.072
Lipid Transport and Metabolism							
fatty acid oxidation complex α-subunit	766	1.074×10^{-5}	1.9	gi|150382987	0.745	1.438	0.954
Carbohydrate Transport and Metabolism							
quinoprotein glucose dehydrogenase B	630	3.980×10^{-6}	4.7	gi|118560	0.341	1.588	1.185
UTP-glucose-1-phosphate uridylyltransferase	805	2.460×10^{-4}	1.4	gi|169632096	0.900	0.945	1.255
mutarotase precursor	732	8.000×10^{-3}	1.6	gi|126641015	0.944	1.504	1.217
mutarotase precursor	749	1.580×10^{-7}	2.9	gi|126641015	0.529	1.305	1.543
Cell Envelope Biogenesis, Outer Membrane							
putative RND type efflux pump	860	4.052×10^{-4}	3.3	gi|126640124	0.840	0.829	2.755
outer membrane receptor FepA	369	2.740×10^{-4}	3.7	gi|169633929	0.645	0.705	2.392
putative protein (DcaP-like)	538	3.324×10^{-4}	2.6	gi|126642784	0.738	1.064	1.903
putative protein (DcaP-like)	702	0.003	1.6	gi|126642784	1.162	0.746	1.117
OmpA	760	2.500×10^{-5}	2.1	gi|126642864	0.699	0.961	1.475
OmpA	762	5.550×10^{-5}	1.6	gi|126642864	0.920	0.969	1.431
Cell Envelope Biogenesis, Outer Membrane							
OmpA	764	0.031	1.5	gi|126642864	1.021	0.986	1.468
putative phosphate transporter	836	2.831×10^{-7}	10.7	gi|126642484	0.526	0.461	4.926
Omp 33	876	9.043×10^{-7}	7.7	gi|193078641	1.632	0.284	2.180
Omp CarO precursor	984	3.426×10^{-6}	4.1	gi|126642573	0.454	1.136	1.870
putative peptidoglycan-binding LysM	1063	1.990×10^{-4}	1.7	gi|126640876	0.868	1.247	1.472
29 kDa Omp (CarO)	1071	2.529×10^{-6}	3.8	gi|55583803	0.495	1.063	1.901
CsuA/B	1123	6.231×10^{-5}	25.3	gi|126642263	0.160	0.288	4.045
Signaling							
two-component regulatory system	947	0.010	1.8	gi|50083946	1.245	0.744	1.321
putative signal peptide	1054	1.143×10^{-7}	6.5	gi|126641568	0.288	1.870	0.619
Transcription							
host factor I for bacteriophage Q beta replication	1156	2.455×10^{-7}	3.8	gi|169633286	1.360	0.415	1.579
transcription elongation factor GreA	1103	0.003	1.7	gi|126642719	0.837	0.975	1.412
Multifunctional							
2-keto-D-gluconate reductase	768	4.781×10^{-5}	1.5	gi|193077799	1.177	0.841	1.289

Table 2. Continued

protein description	spot no.	Anova (p)	fold[a]	NCBInr acession no.	average spot volume exp[b]	late[c]	biofilm[d]
Protein Involved in Redox Reactions							
catalase hydroperoxidase II	321	3.349×10^{-4}	2.0	gi|169796319	0.668	1.319	1.176
electron transfer flavoprotein α-subunit	859	2.867×10^{-5}	1.5	gi|169632682	0.827	1.264	0.971
electron transfer flavoprotein β-subunit	972	2.170×10^{-4}	1.8	gi|169632681	0.706	0.904	1.281
alkyl hyroperoxide reductase C22 subunit	1017	4.772×10^{-5}	2.1	gi|126641253	0.695	1.455	0.905
superoxide dismutase [Fe]	1027	1.063×10^{-5}	3.3	gi|169632935	0.460	1.511	0.678
alkyl hyroperoxide reductase C22 subunit	1031	5.380×10^{-4}	1.7	gi|126641253	0.832	1.375	0.897
putative oxidoreductase	1037	8.820×10^{-7}	4.8	gi|126641974	0.327	1.580	0.356
Defense							
universal stress protein	1196	9.315×10^{-9}	3.3	gi|169795610	0.515	1.606	0.484

[a] Fold indicates the ratio between the highest and lowest average spot volume detected among exponential, late stationary and biofilm proteomes. [b] Exp refers to the average spot volume determined for exponential proteomes. [c] Late refers to the average spot volume determined for exponential proteomes. [d] Biofilm refers to the average spot volume determined for biofilm proteomes.

compromises the ability of the bacteria to attach and form biofilms on abiotic surfaces.[26] In the present study, in order to evaluate the effects of SA on *A. baumannii* biofilm formation, we carried out an in vitro experiment in which several multiresistant epidemic *A. baumannii* strains were incubated in liquid media supplemented with or without SA. The impact of SA on biofilm formation was assessed by the crystal violet assay. In all cases, the presence of SA significantly reduced biofilm formation over a period of 48 h, relative to untreated cells (see Figure 2). Further microscopic confocal assays of treated and untreated cells, confirmed that SA significantly reduced biofilm formation (Supporting Information Figure S1). Taking into account that SA inhibits biofilm formation, we performed proteome analysis under SA treatment to obtain further information about proteins that are down-regulated in the presence of this compound. A total protein extract and membrane-enriched protein fractions of reference strain ATCC 17978 were analyzed by 2DE and MS/MS at two points of in vitro growth, exponential and late stationary phases, in the presence and absence of 16 mM SA. The 2DE maps and differentially expressed spots of *A. baumannii* under SA treatment relative to the control (no SA) for both protein fractions and growth phases are shown in Supporting Information Figure S2. Expression of a protein was considered to have changed if the percentage volume of its spot in the gels between bacteria cultured with and without SA showed a 2-fold or greater difference (p-value <0.05). For the exponential phase, this analysis resulted in identification of 34 and 21 nonunique proteins out of 55 and 45 gels spots differentially expressed in total and membrane-enriched fractions, respectively. Similarly, for the stationary phase, a total of 36 and 19 nonunique proteins were identified out of 81 and 61 gels spots investigated, respectively, in the same protein fractions. Altogether, 110 nonunique proteins were identified (corresponding to 109 spots) from the 242 differentially expressed spots obtained with SA treatment (see Supporting Information Tables S3 and S4).

Given the inhibitory effect of SA over *A. baumannii* biofilms, special attention was dedicated to those proteins that either suffered significant down-regulation in the presence of this compound and/or were induced in biofilm proteome, as a mean of identifying a clear association with inhibition of biofilms.

Cell Surface Proteins Play an Important Role in Biofilms

Among the proteins identified in this study, some of those previously described as *A. baumannii* biofilm-associated proteins were found to be up-regulated in biofilms, for example, CsuA/B[11] [spot 1123, Table 2, maximum fold change (FC) in biofilms: 25.3], OmpA[13] (spots 760/762/764, Table 2, maximum FC in biofilms: 2.1 for spot 760), outer membrane receptor FepA[21] (spot 369, Table 2, maximum FC in biofilms: 3.7) and putative DcaP-like protein[21] (spot 538, Table 2, maximum FC in biofilms: 2.6). DcaP-like protein was also negatively affected by SA treatment (spot 194, Table S3). We also suggest novel associations between some of the identified proteins and biofilms. This is the case of Omp33 (spot 876, Table 2, maximum FC in biofilms, 7.7), CarO (spots 984/1071, Table 2, maximum FC in biofilms, 4.1/3.8; protein i213, Table 3, ratio Bio2/E1 3.30), LysM (spot 1063, Table 2, maximum FC in biofilms, 1.7), putative phosphate transporter (PstS) (spot 836, Table 2, maximum FC in biofilms, 10.7) and others. In addition, we found a novel down-regulated protein in SA-treated cells (spot 190, Supporting Information Table S3, FC, −2.29) that contains an OprD domain. As this protein is predicted to interact with a fimbrial protein (STRING 8.3 interaction network, http://string-db.org; score 0.612) FimA, which is involved in cell adhesion, we considered this OprD-like protein for further analyses.

In order to confirm the relevance of some of the above proteins, molecular targets were selected for direct inactivation and evaluated for biofilm-forming ability. Selected mutants were constructed for OmpA (ΔompA), Omp33 (Δomp33), CarO (ΔcarO), OprD-like (ΔoprD-like) and DcaP-like (ΔdcaP-like) proteins. Also, complemented *A. baumannii* strains for some of these loci were constructed in order to confirm whether the results were caused by the specified locus mutation (ΔcarO-c, ΔoprD-like-c, and ΔdcaP-like-c strains). We compared biofilm formation between wild-type, mutant, and complemented *A. baumannii* strains by use of the quantitative crystal-violet assay and in some cases SEM. Significant differences in the pattern of biofilm formation between wild-type and the referred mutant strains were observed with crystal violet assay, as mutant strains showed reduced biofilm forming ability (Figure 3A). In contrast, complemented strains showed increased biofilm production

Publication Date (Web): June 17, 2011 | doi: 10.1021/pr101299j

Table 3. iTRAQ Identification of Differentially Expressed Proteins

protein description	protein no.	NCBInr acession no	(%) cov.	no. peptides	ratio of different expression level between samples[a] E2/E1[b]	L1/E1[c]	L2/E1[d]	Bio1/E1[e]	Bio2/E1[f]	SAexp/E1[g]	SAlate/E1[h]
Post-translation Modification, Protein Turnover, Chaperones											
chaperone protein dnaK	i7	gi|226738075	80.03	40	1.11(0.123)	**2.38(0.000)**	**2.13(0.000)**	1.06(0.632)	1.24(0.030)	**1.46(0.000)**	**1.44(0.000)**
60 kDa chaperonin	i8	gi|226704107	82.35	33	0.99(0.994)	**2.38(0.000)**	**1.76(0.000)**	1.14(0.319)	1.12(0.430)	1.15(0.180)	1.62(0.000)
trigger factor	i19	gi|226703990	72.97	24	0.85(0.075)	**0.46(0.000)**	**0.52(0.000)**	0.73(0.116)	0.68(0.141)	0.89(0.373)	0.68(0.000)
protein grpE	i141	gi|226737248	55.43	4	0.96(0.619)	**2.14(0.023)**	**1.50(0.012)**	1.34(0.058)	1.19(0.560)	**1.52(0.013)**	**1.24(0.033)**
Translation, Ribosomal Structure and Biogenesis											
elongation factor G	i5	gi|238685496	81.88	39	0.93(0.385)	**0.52(0.000)**	**0.78(0.015)**	**0.69(0.005)**	**0.76(0.035)**	0.79(0.075)	0.58(0.000)
elongation factor Ts	i15	gi|166221178	89.00	18	0.83(0.057)	0.58(0.072)	0.52(0.000)	**0.64(0.004)**	**0.56(0.002)**	0.79(0.061)	0.78(0.168)
ribosome-recycling factor	i65	gi|226703249	73.91	12	0.98(0.832)	1.83(0.000)	1.25(0.014)	1.35(0.019)	1.23(0.180)	**1.45(0.000)**	**1.51(0.000)**
50S ribosomal protein L2	i35	gi|22669930	71.17	15	0.87(0.338)	**0.46(0.000)**	**0.54(0.001)**	0.86(0.477)	0.69(0.085)	0.88(0.437)	0.47(0.000)
50S ribosomal protein L1	i47	gi|226724854	61.90	10	0.62(0.003)	0.66(0.070)	0.50(0.002)	**0.68(0.032)**	**0.63(0.019)**	0.66(0.08)	0.53(0.005)
50S ribosomal protein L5	i49	gi|226731453	78.09	13	0.72(0.215)	**0.31(0.000)**	**0.44(0.031)**	0.76(0.511)	0.65(0.312)	0.83(0.412)	0.38(0.008)
50S ribosomal protein L6	i61	gi|226731363	72.88	9	0.59(0.004)	**0.38(0.010)**	**0.43(0.001)**	0.55(0.076)	0.46(0.06)	0.68(0.013)	0.41(0.000)
50S ribosomal protein L14	i70	gi|226705065	76.23	9	0.69(0.118)	**0.46(0.007)**	**0.47(0.017)**	0.78(0.625)	0.62(0.203)	0.72(0.243)	0.28(0.001)
50S ribosomal protein L19	i78	gi|226723408	68.85	6	0.64(0.037)	**0.43(0.041)**	**0.43(0.011)**	0.52(0.098)	0.45(0.021)	0.69(0.285)	0.34(0.000)
50S ribosomal protein L15	i87	gi|226705097	70.55	9	0.73(0.099)	**0.48(0.000)**	**0.54(0.002)**	0.68(0.088)	0.53(0.012)	0.89(0.359)	0.49(0.000)
50S ribosomal protein L16	i90	gi|226710438	66.42	4	0.90(0.818)	**0.45(0.037)**	**0.53(0.017)**	0.50(0.118)	0.57(0.536)	0.73(0.497)	0.42(0.0.03)
50S ribosomal protein L18	i128	gi|266723574	74.14	6	0.78(0.114)	**0.52(0.001)**	**0.56(0.026)**	0.69(0.062)	0.67(0.029)	0.88(0.195)	0.49(0.009)
50S ribosomal protein L28	i190	gi|49529717	62.82	4	0.76(0.040)	**0.35(0.013)**	**0.55(0.021)**	**0.52(0.001)**	**0.34(0.014)**	0.82(0.457)	0.38(0.004)
30S ribosomal protein S3	i59	gi|226697655	80.00	14	0.93(0.682)	**0.20(0.000)**	**0.31(0.000)**	0.66(0.083)	0.63(0.067)	0.67(0.07)	0.51(0.000)
30S ribosomal protein S7	i64	gi|226705656	86.54	9	0.71(0.149)	**0.53(0.038)**	**0.61(0.05)**	**0.46(0.032)**	**0.39(0.005)**	0.85(0.565)	0.47(0.000)
30S ribosomal protein S12	i93	gi|226708443	48.39	4	0.53(0.029)	**0.22(0.000)**	**0.38(0.012)**	0.78(0.075)	0.71(0.058)	0.83(0.392)	0.27(0.004)
Energy Production and Conversion											
ATP synthase β-subunit	i14	gi|226739964	69.40	19	0.87(0.338)	**0.35(0.000)**	**0.55(0.002)**	0.79(0.290)	0.75(0.264)	0.58(0.030)	**0.46(0.003)**
ATP synthase α-subunit	i17	gi|226739833	57.98	18	0.76(0.007)	**0.41(0.000)**	**0.51(0.000)**	0.91(0.661)	0.73(0.020)	0.67(0.006)	**0.46(0.000)**
Amino Acid Transport and Metabolism											
urocanase hydratase	i11	gi|226707252	63.44	22	0.93(0.450)	1.03(0.820)	1.41(0.001)	**1.56(0.014)**	**1.48(0.033)**	**0.80(0.025)**	**0.71(0.006)**
GMP synthase	i41	gi|81393985	46.00	7	0.94(0.502)	**0.56(0.000)**	**0.69(0.031)**	**0.55(0.026)**	**0.52(0.025)**	0.91(0.576)	0.86(0.361)
gamma-glutamyl phosphate reductase	i43	gi|22671050	57.24	10	1.66(0.010)	**1.78(0.012)**	**1.67(0.009)**	1.23(0.401)	1.06(0.745)	1.34(0.275)	1.85(0.000)
leucyl-tRNA synthetase	i50	gi|226731222	34.44	11	0.95(0.685)	**0.61(0.002)**	**0.67(0.016)**	0.89(0.591)	0.84(0.392)	0.84(0.488)	0.89(0.246)
3-ketoacyl-CoA thiolase	i68	gi|150382987	47.18	10	1.47(0.022)	**1.91(0.010)**	**2.44(0.003)**	**1.72(0.001)**	**1.80(0.001)**	1.49(0.028)	1.92(0.013)
arginyl-tRNA synthetase	i74	gi|226701511	41.11	9	0.84(0.213)	**0.62(0.041)**	**0.70(0.04)**	0.79(0.183)	0.75(0.135)	0.85(0.386)	0.80(0.136)
D-amino acid dehydrogenase small subunit	i75	gi|226722637	32.07	8	1.61(0.08)	**3.00(0.001)**	**4.54(0.000)**	1.87(0.127)	2.34(0.022)	1.23(0.111)	0.81(0.125)
phosphoribosylglycinamide formyltransferase	i154	gi|172044080	24.63	6	1.43(0.085)	**1.89(0.008)**	**2.03(0.000)**	1.67(0.123)	1.5(0.213)	1.76(0.003)	1.73(0.003)

dx.doi.org/10.1021/pr101299j | J. Proteome Res. 2011, 10, 3399–3417

Publication Date (Web): June 17, 2011 | doi: 10.1021/pr101299j

Table 3. Continued

protein description	protein no.	NCBInr acession no	(%) cov.	no. peptides	ratio of different expression level between samples[a] E2/E1[b]	L1/E1[c]	L2/E1[d]	Bio1/E1[e]	Bio2/E1[f]	SAexp/E1[g]	SAlate/E1[h]
Lipid Transport and Metabolism											
fatty acid oxidation complex α-subunit	i10	gi|254788553	72.94	32	1.75(0.000)	**3.29(0.000)**	**3.19(0.000)**	2.08(0.000)	2.22(0.000)	1.59(0.000)	2.80(0.000)
Replication, Recombination, and Repair											
protein recA	i79	gi|238685519	40.40	8	1.30(0.011)	**2.08(0.001)**	**2.05(0.000)**	1.40(0.019)	1.59(0.081)	1.18(0.170)	1.27(0.105)
				8	1.30(0.011)	**2.08(0.001)**	**2.05(0.000)**	1.40(0.019)	1.59(0.081)	1.18(0.170)	1.27(0.105)
IHF integration host factor α-subunit	i95	gi|226707551	62.24	4	1.39(0.071)	**4.43(0.031)**	**4.26(0.024)**	1.39(0.344)	2.02(0.082)	1.95(0.155)	2.20(0.017)
Carbohydrate Transport and Metabolism											
phosphoenolpyruvate carboxykinase [GTP]	i21	gi|226739700	57.12	16	0.93(0.502)	**0.39(0.001)**	**0.40(0.000)**	0.56(0.070)	0.57(0.020)	0.69(0.188)	0.37(0.000)
Nucleotide Transport and Metabolism											
adenylate kinase	i46	gi|226722871	82.95	12	1.25(0.023)	1.77(0.005)	1.37(0.053)	**1.45(0.009)**	**1.41(0.002)**	**1.45(0.033)**	**1.55(0.004)**
putative nucleotide-binding protein	i104	gi|169632416	75.31	8	1.25(0.243)	**1.61(0.031)**	**1.46(0.029)**	1.24(0.071)	1.30(0.139)	1.21(0.390)	1.36(0.156)
orotate phosphoribosyltransferase	i134	gi|167011977	57.87	6	0.89(0.205)	0.85(0.167)	0.84(0.358)	**0.51(0.023)**	**0.58(0.044)**	0.80(0.468)	0.79(0.109)
Cell Envelope Biogenesis, Outer Membrane											
29 kDa outer membrane protein	i213	gi|55583803	91.67	2	2.05(0.189)	1.72(0.07)	2.32(0.125)	**2.76(0.012)**	**3.30(0.029)**	1.81(0.30)	3.89(0.127)
Transcription											
DNA-directed RNA polymerase ss-subunit	i3	gi|212288355	65.78	49	0.93(0.297)	**0.76(0.009)**	**0.73(0.000)**	0.95 (0.600)	0.97(0.767)	0.87(0.204)	0.68(0.000)
DNA-directed RNA polymerase α-subunit	i38	gi|226699358	68.66	18	0.83(0.047)	**0.65(0.007)**	**0.59(0.000)**	0.74(0.155)	0.83(0.439)	0.76(0.032)	0.81(0.019)
Protein Involved in Redox Reactions											
catalase-peroxidase	i26	gi|215275637	52.23	15	1.50(0.100)	**3.02(0.028)**	**3.34(0.003)**	1.32(0.194)	1.78(0.022)	1.29(0.210)	1.96(0.065)

[a] p-values obtained from Protein pilot analyses are shown between (); Protein ratios >1.2 or <0.8 (p-value <0.05) observed in two replicates are shown in bold. [b] E2/E1, the ratio of different expression level between biological replicates of exponential cells. [c] L1/E1, the ratio of the different expression level between late stationary cells (L1) and exponential cells control (E1). [d] L2/E1, the ratio of the different expression level between late stationary cells (L2) and exponential cells control (E1). [e] Bio1/E1, the ratio of the different expression level between biofilm cells (Bio1) and exponential cells control (E1). [f] Bio2/E1, the ratio of the different expression level between biofilm cells (Bio2) and exponential cells control (E1). [g] SAexp/E1, the ratio of different expression level between biological replicates of exponential SA-treated cells (SAexp) and exponential cells control (E1). [h] SAlate/E1, the ratio of different expression level between biological replicates of late stationary SA-treated cells (SAlate) and exponential cells control (E1).

dx.doi.org/10.1021/pr101299j | J. Proteome Res. 2011, 10, 3399–3417

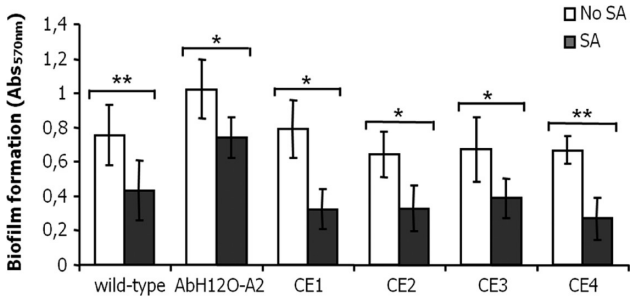

Figure 2. Quantitative biofilm formation in polystyrene wells by *A. baumannii* wild-type strain and AbH12O-A2, CE1, CE2, CE3, and CE4 clinical strains showing a general inhibitory effect of SA. Biofilms cultivated in MH (no SA) and MH supplemented with 16 mM of SA at 37 °C for 48 h were compared by use of the crystal violet assay. The bars indicate the means for six wells. Asterisks indicate significant differences (*p-value ≤0.05; **p-value ≤0.0001, t test) between supplemented and nonsupplemented MH broth.

when compared with mutant strains (Figure 3B). Using SEM, we also found that mutant strains formed simpler and smaller cell aggregates in contrast with wild-type strain, which formed a denser biofilm (Figure 4). Complemented strains formed biofilms with a structure similar to that displayed by wild-type strain, and all tested strains showed increased biofilm production relative to mutant strains.

Within the biofilm, bacterial cells are embedded in a self-produced extracellular matrix, and although this matrix protects bacteria against a number of environmental insults, it also limits bacterial access to fresh nutrients. Thus, the verified increase in expression of transmembrane channels appears to be an essential prerequisite for the entrance of important nutrient-containing fluid,[51] including amino acids, as discussed below. In addition, apart from acting as channels, porins may act as potential targets for adhesion to other cells and may mediate cell attachment through binding to the proteins released for biofilm formation.[52]

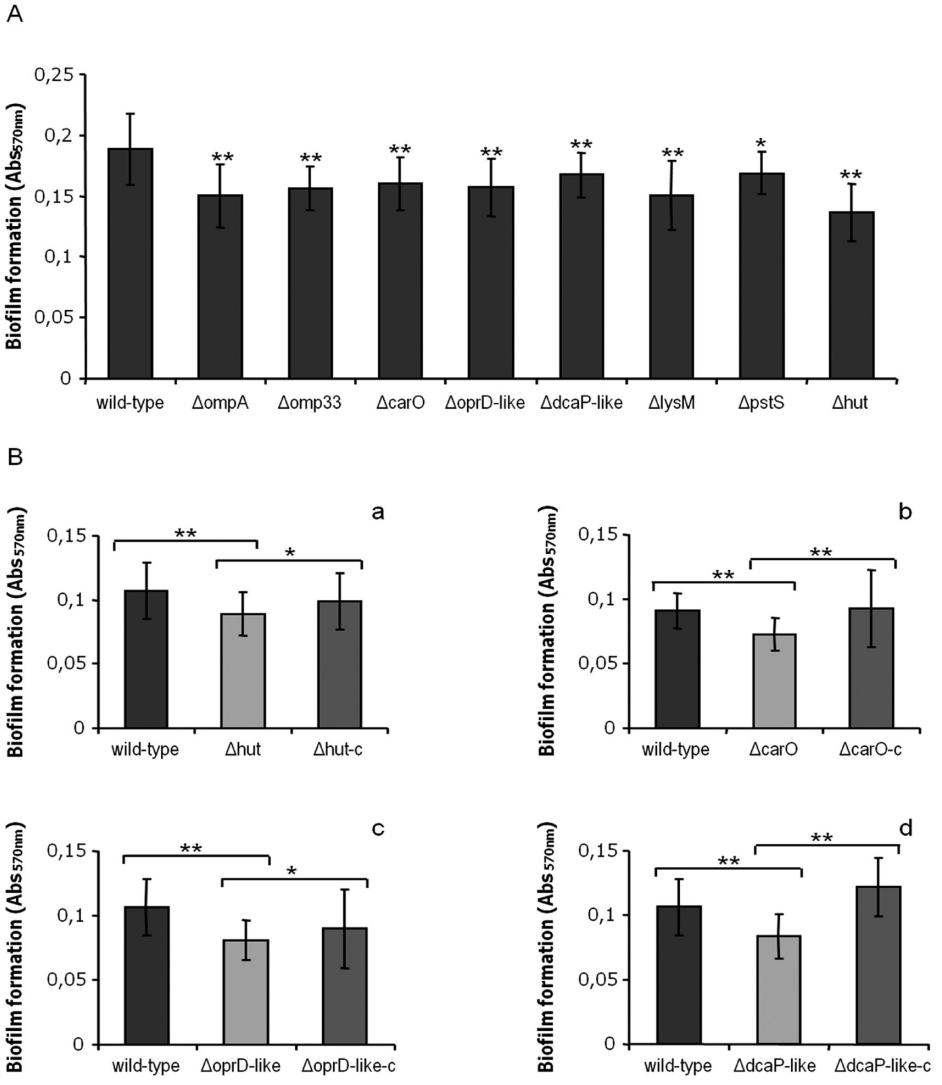

Figure 3. Quantification (crystal violet assay) of biofilm formation in polystyrene wells by multiple *A. baumannii* strains grown in MH broth at 37 °C for 48 h. (A) Biofilms formed by *A. baumannii* wild-type strain were compared with ΔompA, Δomp33, ΔcarO, ΔoprD-like, ΔdcaP-like, ΔlysM, ΔpstS, and Δhut mutant strains. (A) Biofilms formed by *A. baumannii* wild-type strain were compared with (a) Δhut strain; (b) ΔcarO strain; (c) ΔoprD-like strain; and (d) ΔdcaP-like strain. Comparisons were also made between mutant and complemented strains: (a) Δhut with Δhut-c strain, (b) ΔcarO with ΔcarO-c strain, (c) ΔoprD-like with ΔoprD-like-c strain, and (d) ΔdcaP-like with ΔdcaP-like-c strain. The bars indicate the means for at least 40 wells. Asterisks indicate significant differences (*p-value ≤0.05; **p-value ≤0.0001, t test) between means.

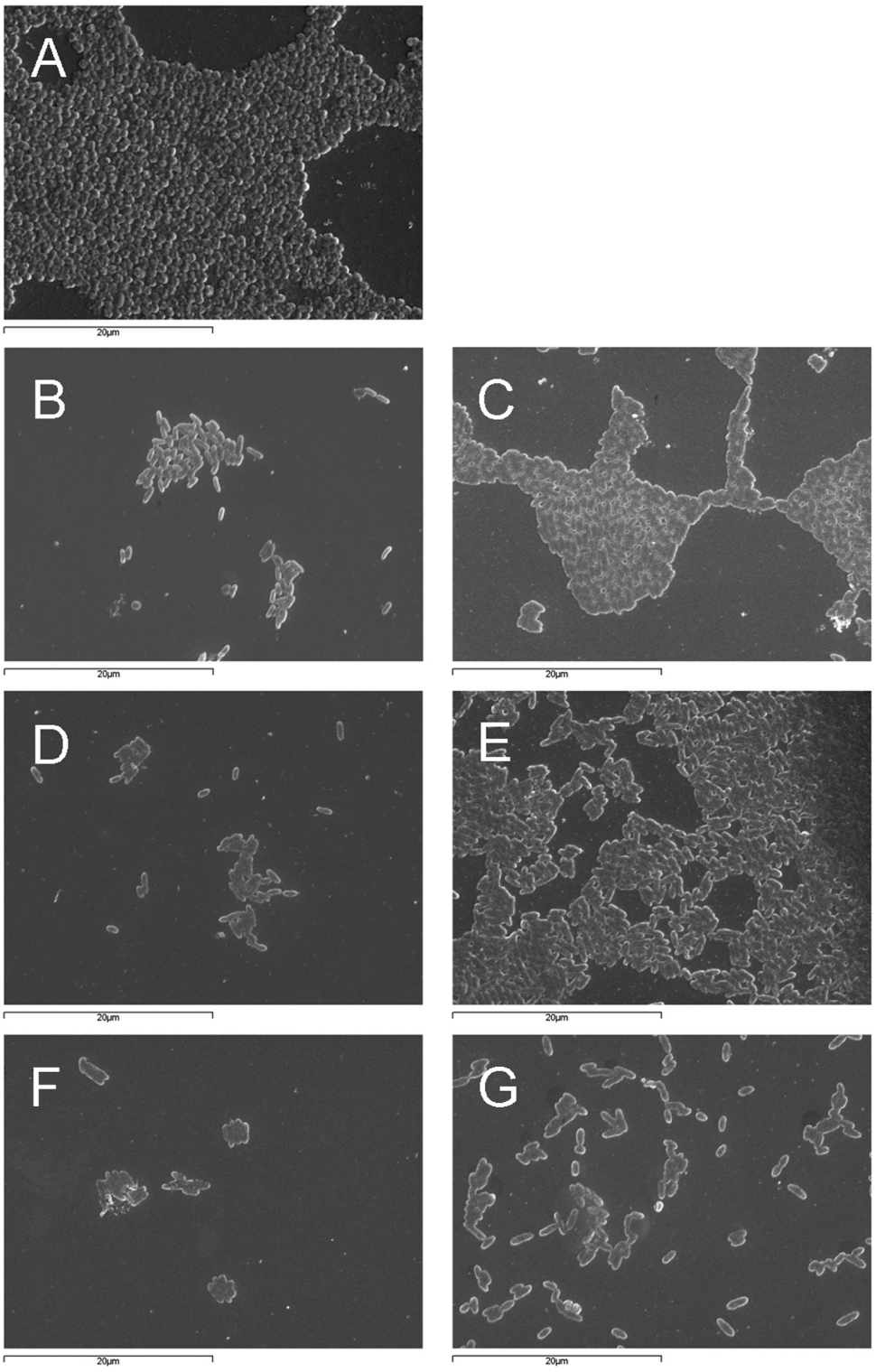

Figure 4. SEM images showing bacterial biofilms of *A. baumannii* formed on plastic coverslips. The morphology of biofilms was viewed at ×3000 magnification. Biofilms formed by (A) wild-type strain; (B) ΔcarO strain; (C) ΔcarO-c strain; (D) ΔdcaP-like strain; (E) ΔdcaP-like-c strain; (F) ΔoprD-like strain; and (G) ΔoprD-like-c strain. The scale magnification bar indicates 20 μm.

We were also interested in evaluating the impact of the gene mutation of other surface proteins with increased expression in biofilms, namely putative peptidoglycan-binding LysM (ΔlysM) and phosphate transporter (ΔpstS). These mutant strains also showed a reduced biofilm forming ability when compared with the wild-type strain (Figure 3A). Recently, a novel class of staphylococcal adhesins containing three N-terminal repetitive sequences that comprised features of a peptidoglycan-binding (the LysM domain) was proposed.[53,54] Apparently, autolysin/adhesins in *S. epidermidis* play an important role during biofilm

formation on polymer surfaces, being potentially involved in colonization. Although further investigation is necessary, it is likely that LysM protein here identified plays a similar role during cell attachment of *A. baumannii* to abiotic surfaces.

Interestingly, our results show for the first time that a phosphate transporter plays an important role in *A. baumannii* biofilm formation. Current research suggests that for many bacterial species, the concentration of external phosphate ion (P_i) is an important signal that regulates biofilm formation. Indeed, the activation of Pho regulon expression in the response of *Pseudomonas aureofaciens* to limiting concentrations of P_i resulted in inhibition of biofilm formation.[55] Furthermore, a recent study in *Pseudomonas fluorescens* has demonstrated that secretion of a large adhesin LapA (a critical component for biofilm formation) is inhibited by P_i limiting conditions.[56] Thus, it would be interesting to establish whether there is any relation with the concentration of external P_i and biofilm formation in *A. baumannii*.

Additionally, since specific gene mutations on individual membrane proteins reduced but did not abolish biofilm production completely, we can suggest that there are compensatory effects among these proteins during cell adhesion and biofilm formation, although further studies will be necessary to abrogate this hypothesis.

Biofilm Proteome Indicates the Induction of Proteins Related with Drug Resistance and the Response to Stress

Bacterial biofilms have been reported to be up to 1000 times more tolerant to specific antibiotics than their planktonic counterparts.[57] Here, we identified a putative resistance-nodulation-cell Division type efflux pump (RND pump), that increased in biofilms (spot 860, Table 2). Overexpression of this type of efflux pump in *A. baumannii* confers resistance to aminoglycosides, but also to other drugs, including fluoroquinolones, tetracyclines, chloramphenicol, erythromycin, trimethoprim, and ethidium bromide in *A. baumannii*.[58,59] The extent to which the inherent resistance of biofilms to antibiotics is due to the extracellular matrix or external influences such as low diffusion of compounds is not known. Here, the results indicate that changes in the *A. baumannii* proteome during biofilm formation may play an important role in the formation of acquired resistance to antibiotics. In addition, studies with planktonic *A. baumannii* cells showed a wide range of mechanisms of antibiotic resistance, for example, the down-regulation of porins.[60] In this study, however, we observed up-regulation of several membrane channels (as discussed above). Although many other antimicrobial resistance mechanisms operate in *A. baumannii*, it is tempting to suggest that the up-regulation of efflux pumps is a primary mechanism of antibiotic resistance operating in mature biofilms *of A. baumannii*.

Biofilm formation is also associated with antioxidative activity.[61] We previously demonstrated that defense against reactive oxygen species (ROS) is an important mechanism in the biology of *A. baumannii*.[39] As suggested by the up-regulation of Alkyl hydroperoxide reductase C22 subunit (spot 1017, Table 2) and catalase-hydroperoxidase II (KatE) (spot 321, Table 2), *A. baumannii* biofilm cells are more protected against the lethal effect of ROS than exponential phase planktonic cells. It is also worth noting that a Host factor I for bacteriophage Q beta replication protein (Hfq) appears to be involved in biofilm formation, according to the results presented here (spot 632, Supporting Information Table S4). This protein was shown to be negatively affected by SA, presenting an impressive fold change of −12.8 in the presence of this compound. In contrast, it was found to be up-regulated in biofilms relatively to stationary phase planktonic cells (spot 1156, Table 2). This bacterial RNA chaperone is involved in post-transcriptional regulation of many stress-inducible genes, via sRNAs. Although available information is scarce, there is evidence to indicate the possible effect of Hfq on biofilms. In one of these studies, an *E. coli* hfq mutant was found to be less prone to form biofilms.[62] Therefore, it is possible that biofilm formation depends to some extent on the regulatory activity of noncoding RNAs that adjust mRNA levels of target genes according to the environmental signals. Investigation into these specifically regulated mRNAs in *A. baumannii* appears to be an attractive future project.

Biofilm Proteome of *A. baumannii* Indicates That EPS Matrix Formation May Occur via the Leloir Pathway

It is widely accepted that biofilm formation is accompanied by the production of EPS production; however in *A. baumannii*, the underlying mechanisms of EPS formation remains yet to be elucidated. Recently, EPS precursors in *Acidithiobacillus ferrooxidans* were found to be formed via the Leloir pathway.[63] Another study in *Vibrio cholerae* shows that EPS constitutes the major bulk of biofilms and that galU and galE are essential for biofilm formation.[64] In the present study, we found two proteins that are up-regulated in biofilms that participate in this pathway, namely mutarotase (GalM) (spot 749, Table 2) (EC 5.1.3.3) and UTP-glucose1-phosphate uridylyltransferase (GalU) (spot 805, Table 2) (EC 2.7.7.9). Additionally, Shin et al.[21] reported another biofilm associated protein that in the Leloir pathway converts UDP-galactose to UDP-glucose (GalE). We suggest that EPS production in *A. baumannii* resembles the *A. ferrooxidans* Leloir pathway. According to this, interconversion between α- and β-galactose, and the formation of glucose-1-phosphate constitute intermediate steps for the biosynthesis of UDP-glucose, UDP-galactose and dTDP-rhamnose, the precursors of EPS,[63] which culminate in matrix formation via glycosyltransferases (GTs).

In addition, we found a putative phosphate transporter (PstS) that is up-regulated in biofilms (as mentioned above) and that may be indirectly involved in this pathway. This protein is a high-affinity phosphate-binding protein, part of the ABC transporter pstSACB complex involved in P_i transport. Because the Leloir pathway comprises a step in galactose phosphorylation (galactose-1P), we consider that this mechanism may function as a P_i-supplier for biofilm formation, as more EPS production will require more free P_i in the cell. In this sense, data here provided may represent initial steps to further understanding of the mechanism of EPS formation in *A. baumannii*.

Histidine Metabolism Plays an Important Role in Biofilm Formation

Further analysis of our results indicated that in the biofilm proteome there was a clear up-regulation of proteins that are directly or indirectly related to histidine metabolism, e.g. Urocanate hydratase (HutU) [(protein i11 − Table 3), which was also down-regulated with the presence of SA (Hut) (spots 65/75 − Table S3; spot 142 − Table S4)] and CarO (see above). Although this porin is not directly involved in histidine metabolism, it has been associated with L-His transport.[65] Taken together, these observations prompted us to investigate further the influence of L-His metabolism in the formation of biofilms. In order to clarify the importance of L-His, we first searched for differences in the pattern of biofilm formation in the presence of

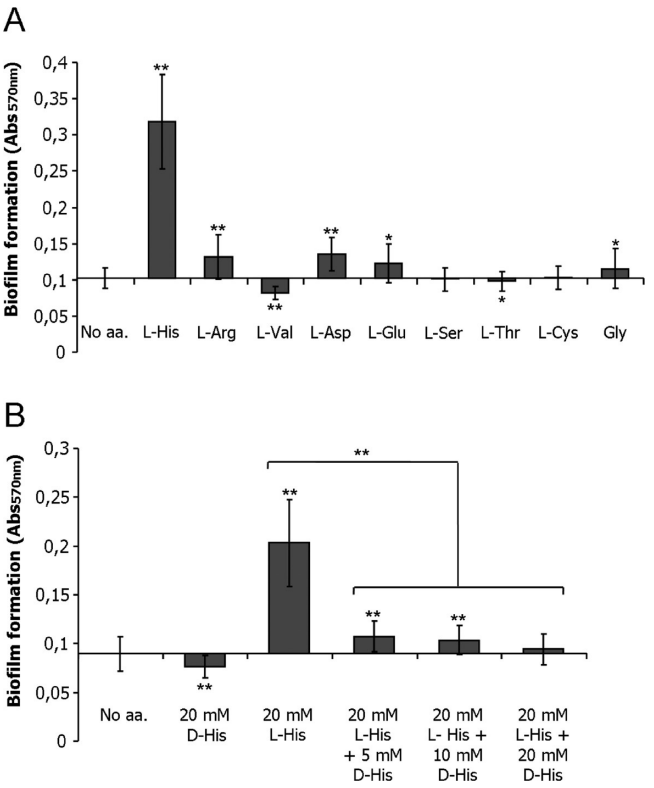

Figure 5. Quantification (crystal violet assay) of biofilm formation by *A. baumannii* in polystyrene wells. (A) Comparison between biofilms formed by *A. baumannii* wild-type strain in M9 minimal media (no aa) and M9 supplemented with 20 mM of different L-amino acids. Asterisks indicate significant differences (*p-value ≤0.05; **p-value ≤0.0001, t-test) between supplemented and nonsupplemented M9 media. The bars indicate the means for at least 30 wells. (B) Comparison between biofilms formed by *A. baumannii* wild-type strain in M9 minimal media (no aa) and M9 supplemented with D-His (20 mM), L-His (20 mM), and L-His (20 mM) plus D-His (5, 10, and 20 mM). Asterisks indicate significant differences (**p-value ≤0.0001, t-test) between supplemented and non supplemented M9 media and between L-His and L-His + D-His supplemented M9 media. The bars indicate the means for at least 50 wells.

different amino acids provided as the only carbon source. For this, the *A. baumannii* wild-type strain was cultivated in minimal media and minimal media supplemented with 20 mM of different L-amino acids, including positively charged (L-His and L-Arg), negatively charged (L-Asp and L-Glu) and finally neutral amino acids (L-Val, L-Ser, L-Thr, L-Cys and Gly). We found that L-His had the greatest effect on biofilm induction when compared with other amino acids (Figure 5A). These findings support the hypothesis that the effect on biofilm formation is somehow specific rather than due to a structural or charge effect.

A recent study has demonstrated that D-amino acids inhibit biofilm formation by *S. aureus* and *P. aeruginosa*.[33] Considering this and the above results, we were prompted to establish whether D-His had similar inhibitory effect on *A. baumannii* biofilm production, as well as to determine if D- and L-His isomers compete each other for the degradation pathway leading to biofilm formation. For instance, the *A. baumannii* wild-type strain was grown in the presence of L-His, D-His and a combination of L-His and various concentrations of D-His (Figure 5B). While L-His effectively induced biofilm formation, D-His was found to inhibit

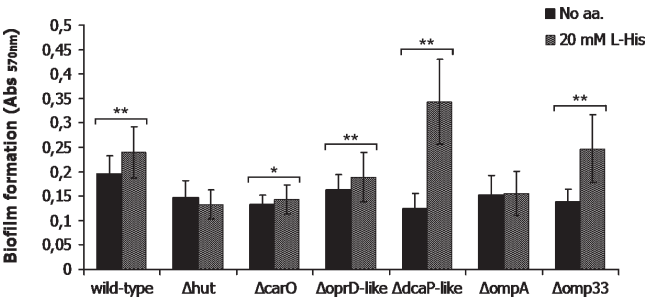

Figure 6. Quantitative biofilm formation in polystyrene wells by *A. baumannii* wild-type, Δhut, ΔcarO, ΔoprD-like, ΔdcaP-like, ΔompA, and Δomp33 strains in M9 minimal media (no aa) and M9 supplemented with 20 mM of L-His. The bars indicate the means for at least 30 wells. Asterisks indicate significant differences (*p-value ≤0.05; **p-value ≤0.0001, t-test) between supplemented and nonsupplemented M9 media.

this process. Notably, biofilm induction by L-His was progressively impaired in the presence of increasing concentrations of D-His, showing that D-His effectively weakened the effect of biofilm induction by L-His. These observations not only support the importance of histidine for biofilm formation, but also confirm that the D-isomer conformation inhibits biofilm formation and prevents the L-isomer effect.

We then wished to evaluate the importance of some biofilm-associated proteins with a hypothetical role in L-His metabolism. For this purpose, molecular targets were selected for direct inactivation, for further evaluation of their biofilm forming ability, as above. As Urocanase plays a central functional role in metabolism of histidine, both a mutant with target locus inactivation of this protein (Δhut) and a complemented strain (Δhut-c) of *A. baumannii* were constructed. Significant differences were observed with crystal violet assay, with the mutant strain showing reduced biofilm formation when compared with the wild-type strain (Figure 3A,B). Conversely, the complemented strain showed increased biofilm production when compared with the mutant strain (Figure 3B). In addition, we wished to investigate possible candidates at the membrane level for the uptake of L-His. In this case, ΔcarO, ΔoprD-like, ΔdcaP-like, ΔompA, and Δomp33 mutant strains were tested for their effect on biofilm forming ability in the presence and absence of this amino acid (for their possible implication as channels). The Δhut strain was also tested in this way due to its direct involvement in L-His metabolism; see Figure 6. The biofilm quantification assay clearly revealed that the presence of L-His had no effect on the production of biofilms by the Δhut and ΔompA strains. While the presence of L-His led to an increase in biofilm production by ΔoprD-like, ΔdcaP-like, and Δomp33 strains, only a slight increase in biofilm formation was observed the ΔcarO strain. These findings lead us to conclude that the Urocanase protein plays a crucial role in L-His degradation pathway, leading to biofilm formation and that, although not exclusively, OmpA may be one of the preferential (major) channels for L-His uptake by the cell, while CarO can be used as an alternative (minor) channel.

Although the mechanism whereby a signaling molecule such as an amino acid increases biofilm formation is rather complex, we can establish a comparison between our observations and those reported in a recent study in *Pseudomonas putida*.[66] The latter study describes a two-component global regulatory system

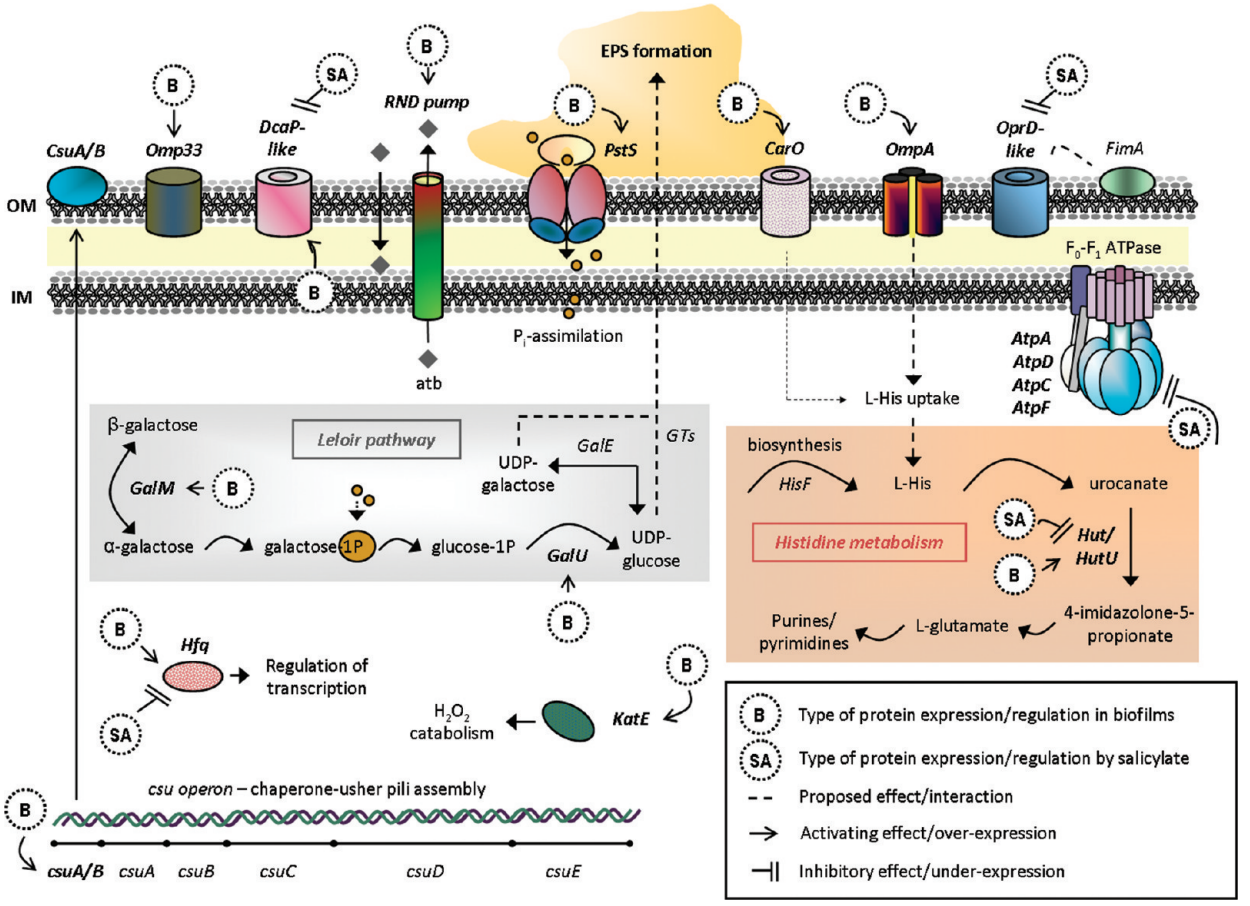

Figure 7. Schematic representation of SA effects on *A. baumannii* proteome, and type of protein expression occurring in biofilms, at the cellular level. The proteins identified in this study are shown in bold. Proposed pathways and potential genes intervening in biofilm formation are also shown. The model indicates possible connections between the Leloir pathway, EPS formation and P_i transport, and between histidine metabolism and uptake. Suggested interactions are also represented. GTs, glycosyltransferases; OM, outer membrane; IM, inner membrane; atb, antibiotics; P_i, phosphate ion.

required for assimilation of several amino acids including histidine as carbon or carbon and nitrogen sources. The authors observed that cbrB mutant was unable to use ornithine or tyrosine nitrogen and/or carbon sources, although it may use histidine when it is the only carbon and nitrogen source present in the medium. In addition (and more relevant to the present discussion), the transcriptomic profile of cbrB mutant showed significant changes in the expression levels of several genes encoding functions potentially involved in biofilm formation, such as signal transduction proteins, exopolysaccharide biosynthesis or transport and the adhesion protein LapF. Considering these observations together, it is reasonable to suggest that *A. baumannii* uses certain amino acids like L-His, thus reprogramming bacterial gene expression leading to biofilm formation, as in the model suggested for *P. putida*.

In several bacterial species, the histidine degradation pathway occurs via urocanase and leads to the production of purines and pyrimidines.[67] As extracellular DNA (eDNA) is also an important constituent of the biofilm matrix (along with EPS and proteins)[68] it is likely that histidine degradation may contribute to purine and pyrimidine synthesis for eDNA production. Also, as already mentioned, D-amino acids prevent biofilm formation via their incorporation into the cell wall in several bacteria species.[33] Similarly, we found that the inducible effect of L-His on biofilm formation was prevented by the presence of its D-isomer. Apparently, D-His interferes with the L-His degradation pathway leading to biofilm formation (rather than incorporation into the cell wall) and the two isomers may compete with each other for cell uptake and/or amino acid degradation.

CONCLUDING REMARKS

A. baumannii biofilm formation on abiotic surfaces is considered a major pathogenicity factor in foreign-body-associated infection. Through a multiapproach model superimposing proteomics and genetics analyses of cells exposed to SA and biofilms cultivated in vitro, we provide evidence about new mechanisms operating in *A. baumannii* biofilm formation (see Figure 7). Giving special emphasis to those proteins found to be down-regulated in SA-treated cells, and/or up-regulated in biofilms, we suggest a model in which membrane proteins and also intracellular pathways are involved and are often interconnected. The current report suggested that biofilms present a unique phenotype and allowed the identification of novel surface proteins with possible roles in biofilm formation and maintenance. Although further research is needed, the antibiofilm activity of D-His and/or the use of an urocanase inhibitor represent realistical tools for prevention/eradication of *A. baumannii* biofilms on abiotic surfaces.

Finally, although we have focused on cell surface proteins and histidine metabolism specifically, experiments are currently in

progress to demonstrate the implication of the remaining proteins identified here, such as like RND pump, KatE, Hfq, GalM/GalU, and the role of concomitant cellular processes including resistance to antibiotics, antioxidative activity, post-transcriptional regulation and the Leloir pathway in the physiology of *A. baumannii* biofilms.

■ ASSOCIATED CONTENT

Supporting Information

Additional information provided. This material is available free of charge via the Internet at http://pubs.acs.org.

■ AUTHOR INFORMATION

Corresponding Author

*Phone: +34 981176087. Fax: +34 981176097. E-mail: German.Bou.Arevalo@sergas.es.

Author Contributions

‖These authors contributed equally to this work.

■ ACKNOWLEDGMENT

MPC was supported by a doctoral degree grant (SFRH/BD/6474/2009) from FCT-MCTES. NCS acknowledges Xunta de Galicia postdoctoral program Angeles Alvariño (Dez, 2009). JA and CR were supported by a postdoctoral (Sara Borrell) and doctoral grants, respectively, from Instituto de Salud Carlos III. MP was supported by the Isidro Parga Pondal program from Xunta de Galicia. We acknowledge helpful assistance from Cristina Ruiz-Romero (ProteoRed), Jesús Mateos (ProteoRed), Mª del Carmen Fernández (technician), Nelson Espinosa Vergara (UDC), Ada Castro Couceiro (UDC) and Catalina Sueiro López (UDC). We also thank Phil Jackson from ITQB/UNL for the language revision and technical advice. This work was funded by the Spanish Network for the Research in Infectious Diseases (REIPI RD06/0008), FIS PI081613, PS09/00687, PS07/90, PS07/51, and 08CSA064916PR from Xunta de Galicia.

■ REFERENCES

(1) Dijkshoorn, L.; Nemec, A.; Seifert, H. An increasing threat in hospitals: multidrug-resistant *Acinetobacter baumannii*. *Nat. Rev. Microbiol.* **2007**, *5* (12), 939–951.

(2) Peleg, A. Y.; Seifert, H.; Paterson, D. L. *Acinetobacter baumannii*: emergence of a successful pathogen. *Clin. Microbiol. Rev.* **2008**, *21* (3), 538–582.

(3) Davey, M. E.; O'Toole, G. A. Microbial biofilms: from ecology to molecular genetics. *Microbiol. Mol. Biol. Rev.* **2000**, *64* (4), 847–867.

(4) Rodríguez-Baño, J.; Martí, S.; Soto, S.; Fernández-Cuenca, F.; Cisneros, J. M.; Pachón, J.; Pascual, A.; Martínez-Martínez, L.; McQueary, C.; Actis, L. A.; Vila, J. Biofilm formation in *Acinetobacter baumannii*: associated features and clinical implications. *Clin. Microbiol. Infect.* **2008**, *14* (3), 276–278.

(5) Lee, H. W.; Koh, Y. M.; Kim, J.; Lee, J. C.; Lee, Y. C.; Seol, S. Y.; Cho, D. T.; Kim, J. Capacity of multidrug-resistant clinical isolates of *Acinetobacter baumannii* to form biofilm and adhere to epithelial cell surfaces. *Clin. Microbiol. Infect.* **2008**, *14* (1), 49–54.

(6) Rao, R. S.; Karthika, R. U.; Singh, S. P.; Shashikala, P.; Kanungo, R.; Javachandran, S.; Prashanth, K. Correlation between biofilm production and multiple drug resistance in imipenem resistant clinical isolates of *Acinetobacter baumannii*. *Indian J. Med. Microbiol.* **2008**, *26* (4), 333–337.

(7) Gaddy, J. A.; Actis, L. A. Regulation of *Acinetobacter baumannii* biofilm formation. *Future Microbiol.* **2009**, *4*, 273–278.

(8) Latasa, C.; Solano, C.; Penadés, J. R.; Lasa, I. Biofilm-associated proteins. *C. R. Biol.* **2006**, *329* (11), 849–857.

(9) Sauer, K. The genomics and proteomics of biofilm formation. *Genome Biol.* **2003**, *4* (6), 219.

(10) Beloin, C.; Rou, A.; Ghigo, J. M. *Escherichia coli* biofilms. *Curr. Top. Microbiol. Immunol.* **2008**, *322*, 249–289.

(11) Tomaras, A. P.; Dorsey, C. W.; Edelmann, R. E.; Actis, L. A. Attachment to and biofilm formation on abiotic surfaces by *Acinetobacter baumannii*: involvement of a novel chaperone-usher pili assembly system. *Microbiology* **2003**, *149* (12), 3473–3484.

(12) De Breij, A.; Gaddy, J.; van der Meer, J.; Koning, R.; Koster, A.; van den Broek, P.; Actis, L.; Nibbering, P.; Dijkshoorn, L. CsuA/BABCDE-dependent pili are not involved in the adherence of *Acinetobacter baumannii* ATCC19606(T) to human airway epithelial cells and their inflammatory response. *Res. Microbiol.* **2009**, *160* (3), 213–218.

(13) Gaddy, J. A.; Tomaras, A. P.; Actis, L. A. The *Acinetobacter baumannii* 19606 OmpA protein plays a role in biofilm formation on abiotic surfaces and in the interaction of this pathogen with eukaryotic cells. *Infect. Immun.* **2009**, *77* (8), 3150–3160.

(14) Latasa, C.; Roux, A.; Toledo-Arana, A.; Ghigo, J. M.; Gamazo, C.; Penadés, J. R.; Lasa, I. BapA, a large secreted protein required for biofilm formation and host colonization of *Salmonella enterica* serovar Enteritidis. *Mol. Microbiol.* **2005**, *58* (5), 1322–1339.

(15) Cucarella, C.; Solano, C.; Valle, J.; Amorena, B.; Lasa, I.; Penadés, J. R. Bap, a *Staphylococcus aureus* surface protein involved in biofilm formation. *J. Bacteriol.* **2001**, *183* (9), 2888–2896.

(16) Loehfelm, T. W.; Luke, N. R.; Campagnari, A. A. Identification and characterization of an *Acinetobacter baumannii* biofilm-associated protein. *J. Bacteriol.* **2008**, *190* (3), 1036–1044.

(17) Southey-Pillig, C. J.; Davies, D. G.; Sauer, K. Characterization of temporal protein production in *Pseudomonas aeruginosa* biofilms. *J. Bacteriol.* **2005**, *187* (23), 8114–8126.

(18) Petrova, O. E.; Sauer, K. A novel signaling network essential for regulating *Pseudomonas aeruginosa* biofilm development. *PLoS Pathog.* **2009**, *5* (11), e1000668.

(19) Tomaras, A. P.; Flagler, M. J.; Dorsey, C. W.; Gaddy, J. A.; Actis, L. A. Characterization of a two-component regulatory system from *Acinetobacter baumannii* that controls biofilm formation and cellular morphology. *Microbiology* **2008**, *154* (Pt 11), 3398–3409.

(20) Dallo, S. F.; Weitao, T. Insights into *Acinetobacter* war-wound infections, biofilms, and control. *Adv. Skin Wound Care.* **2010**, *23* (4), 169–174.

(21) Shin, J. H.; Lee, H. W.; Kim, S. M.; Kim, J. Proteomic analysis of *Acinetobacter baumannii* in biofilm and planktonic growth mode. *J. Microbiol.* **2009**, *47* (6), 728–735.

(22) Vergara-Irigaray, M.; Valle, J.; Merino, N.; Latasa, C.; García, B.; Ruiz de Los Mozos, I.; Solano, C.; Toledo-Arana, A.; Penadés, J. R.; Lasa, I. Relevant role of fibronectin-binding proteins in *Staphylococcus aureus* biofilm-associated foreign-body infections. *Infect. Immun.* **2009**, *77* (9), 3978–3991.

(23) Kunin, C. M.; Hua, T. H.; Guerrant, R. L.; Bakaletz, L. O. Effect of salicylate, bismuth, osmolytes, and tetracycline resistance on expression of fimbriae by *Escherichia coli*. *Infect. Immun.* **1994**, *62* (6), 2178–2186.

(24) Muller, E.; Al-Attar, J.; Wolff, A. G.; Farber, B. F. Mechanism of salicylate-mediated inhibition of biofilm in *Staphylococcus epidermidis*. *J. Infect. Dis.* **1998**, *177* (2), 501–503.

(25) Price, C. T.; Lee, I. R.; Gustafson, J. E. The effects of salicylate on bacteria. *Int. J. Biochem. Cell Biol.* **2000**, *32* (10), 1029–1043.

(26) Prithiviraj, B.; Bais, H. P.; Weir, T.; Suresh, B.; Najarro, E. H.; Dayakar, B. V.; Schweizer, H. P.; Vivanco, J. M. Down regulation of virulence factors of *Pseudomonas aeruginosa* by salicylic acid attenuates its virulence on *Arabidopsis thaliana* and *Caenorhabditis elegans*. *Infect. Immun.* **2005**, *73* (9), 5319–5328.

(27) Herrmann, M. Salicylic acid: an old dog, new tricks, and staphylococcal disease. *J. Clin. Invest.* **2003**, *112* (2), 149–151.

(28) Teichberg, S.; Farber, B. F.; Wolff, A. G.; Roberts, B. Salicylic acid decreases extracellular biofilm production by *Staphylococcus*

epidermidis: electron microscopic analysis. *J. Infect. Dis.* **1993**, *167* (6), 1501–1503.

(29) Kang, G.; Balasubramanian, K. A.; Koshi, R.; Mathan, M. M.; Mathan, V. I. Salicylate inhibits fimbriae mediated HEp-2 cell adherence of and haemagglutination by enteroaggregative *Escherichia coli*. *FEMS Microbiol. Lett.* **1998**, *166* (2), 257–265.

(30) Domka, J.; Lee, J.; Bansal, T.; Wood, T. K. Temporal gene-expression in *Escherichia coli* K-12 biofilms. *Environ. Microbiol.* **2007**, *9* (2), 332–346.

(31) Hamilton, S.; Bongaerts, R. J.; Mulholland, F.; Cochrane, B.; Porter, J.; Lucchini, S.; Lappin-Schott, H. M.; Hinton, J. C. The transcriptional programme of *Salmonella enterica* serovar Typhimurium reveals a key role for tryptophan metabolism in biofilms. *BMC Genomics* **2009**, *10*, 599.

(32) Valle, J.; Da Re, S.; Schmid, S.; Skurnik, D.; ÒDAri, R.; Ghigo, J. M. The animo acid valine is secreted in countinous-flow bacterial biofilms. *J. Bacteriol.* **2008**, *190* (1), 264–274.

(33) Kolodkin-Gal, I.; Romero, D.; Cao, S.; Clardy, J.; Kolter, R.; Losick, R. D-amino acids trigger biofilm disassembly. *Science* **2010**, *328* (5978), 627–629.

(34) Smith, M. G.; Gianoulis, T. A.; Pukatzki, S.; Mekalanos, J. J.; Ornston, L. N.; Gerstein, M.; Snyder, M. New insights into *Acinetobacter baumannii* pathogenesis revealed by high-density pyrosequencing and transposon mutagenesis. *Genes Dev.* **2007**, *21* (5), 601–614.

(35) Merino, M.; Acosta, J.; Poza, M.; Sanz, F.; Beceiro, A.; Chaves, F.; Bou, G. OXA-24 carbapenemase gene flanked by XerC/XerD-Like Recombination sites in different plasmids from different *Acinetobacter* species isolated during a nosocomial outbreak. *Antimicrob. Agents Chemother.* **2010**, *54* (6), 2724–2727.

(36) Aranda, J.; Poza, M.; Pardo, B. G.; Rumbo, S.; Rumbo, C.; Parreira, J. R.; Rodríguez-Velo, P.; Bou, G. A rapid and simple method for constructing stable mutants of *Acinetobacter baumannii*. *BMC Microbiol.* **2010**, *10*, 279.

(37) Ramagli, L. Quantifying protein in 2D PAGE solubilization buffers. *Methods Mol. Biol.* **1999**, *112*, 99–103.

(38) Molloy, M. P.; Herbert, B. R.; Slade, M. B.; Thierry, R.; Nouwens, A. S.; Williams, K. L.; Gooley, A. A. Proteomics analysis of the *Escherichia coli* outer membrane. *Eur. J. Biochem.* **2000**, *267* (10), 2871–2881.

(39) Soares, N. C.; Cabral, M. P.; Gayoso, C.; Mallo, S.; Rodriguez-Velo, P.; Férnandez-Moreira, E.; Bou, G. Associating growth-phase-related changes in the proteome of *Acinetobacter baumannii* with increased resistance to oxidative stress. *J. Proteome Res.* **2010**, *9* (4), 1951–1964.

(40) Ruiz-Romero, C.; Calamia, V.; Mateos, J.; Carreira, V.; Martínez-Gomariz, M.; Fernández, M.; Blanco, F. J. Mitochondrial dysregulation of osteoarthritic human articular chondrocytes analyzed by proteomics: a decrease in mitochondrial superoxide dismutase points to a redox imbalance. *Mol. Cell Proteomics* **2009**, *8* (1), 172–189.

(41) Soares, N. C.; Cabral, M. P.; Parreira, J. R.; Gayoso, C.; Barba, M.; Bou, G. 2DE analysis indicates that *Acinetobacter baumannii* displays a robust and versatile metabolism. *Proteome Sci.* **2009**, *7* (1), 37.

(42) Neuhoff, V.; Stamm, R.; Pardowitz, I.; Arold, N.; Ehrhardt, W.; Taube, D. Essential problems in quantification of proteins following colloidal staining with coomassie brilliant blue dyes in polyacrylamide gels, and their solution. *Electrophoresis* **1990**, *11* (2), 101–117.

(43) Sechi, S.; Chait, B. T. Modification of cysteine residues by alkylation. A tool in peptide mapping and protein identification. *Anal. Chem.* **1998**, *70* (24), 5150–5158.

(44) Gan, C. S.; Chong, P. K.; Pham, T. K.; Wright, P. C. Technical, experimental, and biological variations in isobaric tags for relative and absolute quantitation (iTRAQ). *J. Proteome Res.* **2007**, *6* (2), 821–827.

(45) Tendolkar, P. M.; Baghdayan, A. S.; Gilmore, M. S.; Shankar, N. Enterococcal surface protein, Esp, enhances biofilm formation by *Enterococcus faecalis*. *Infect. Immun.* **2004**, *72* (2), 6032–6039.

(46) Héritier, C.; Poirel, L.; Lambert, T.; Nordmann, P. Contribution of acquired carbapenem-hydrolyzing oxacillinases to carbapenem resistance in *Acinetobacter baumannii*. *Antimicrob. Agents Chemother.* **2005**, *49* (8), 3198–3202.

(47) Whiteley, M.; Bangera, M. G.; Bumgarner, R. E.; Parsek, M. R.; Teitzel, G. M.; Lory, S.; Greenberg, E. P. Gene expression in *Pseudomonas aeruginosa* biofilms. *Nature* **2001**, *413* (6858), 860–864.

(48) Monds, R. D.; O'Toole, G. A. The developmental model of microbial biofilms: ten years of a paradigm up for review. *Trends Microbiol.* **2009**, *17* (2), 73–87.

(49) Stoodley, P.; Sauer, K.; Davies, D. G.; Costerton, J. W. Biofilms as complex differentiated communities. *Annu. Rev. Microbiol.* **2002**, *56*, 187–209.

(50) Karatan, E.; Watnick, P. Signals, regulatory networks, and materials that build and break bacterial biofilms. *Microbiol. Mol. Biol. Rev.* **2009**, *73* (2), 310–347.

(51) Costerton, J. W.; Lewandowski, Z.; DeBeer, D.; Caldwell, D.; Korber, D.; James, G. Biofilms, the customized microniche. *J. Bacteriol.* **1994**, *176* (8), 2137–2142.

(52) Dallo, S. F.; Denno, J.; Hong, S.; Weitao, T. Adhesion of *Acinetobacter baumannii* to extracellular proteins detected by a live cell-protein binding assay. *Ethn. Dis.* **2010**, *20* (1 Suppl 1), S1-7–11.

(53) Heilmann, C.; Günther, T.; Chhatwal, G. S.; Hartleib, J.; Uekötter, A; Peter, G. Identification and characterization of novel autolysin (Aae) with adhesive properties from *Staphylococcus epidermidis*. *Microbiology.* **2003**, *149* (Pt 10), 2769–2778.

(54) Heilmann, C.; Hartleib, J.; Hussain, M. S.; Peter, G. The multifunctional *Staphylococcus aureus* autolysin Aaa mediates adherence to immobilized fibrinogen and fibronectin. *Infect. Immun.* **2005**, *73* (8), 4793–4802.

(55) Monds, R. D.; Silby, M. W.; Mahanty, H. K. Expression of the Pho regulon negatively regulates biofilm formation by *Pseudomonas aureofaciens* PA147−2. *Mol. Microbiol.* **2001**, *42* (2), 415–426.

(56) Monds, R. D.; Newell, P. D.; Gross, R. H.; O'Toole, G. A. Phosphate-dependent modulation of c-di-GMP levels regulates *Pseudomonas fluorescens* Pf0−1 biofilm formation by controlling secretion of the adhesion LapA. *Mol. Microbiol.* **2007**, *63* (3), 656–679.

(57) Costerton, J. W.; Lewandowski, Z.; Caldwell, D. E.; Korber, D. R.; Lappin-Scott, H. M. Microbial biofilms. *Annu. Rev. Microbiol.* **1995**, *49*, 711–745.

(58) Magnet, S.; Courvalin, P.; Lambert, T. Resistance-nodulation-cell division-type efflux pump involved in aminoglycoside resistance in *Acinetobacter baumannii* strain BM4454. *Antimicrob. Agents Chemother.* **2001**, *45* (12), 3375–3380.

(59) Coyne, S.; Couvalin, P; Périchon, B. Efflux-mediated antibiotic resistance in *Acinetobacter spp*. *Antimicrob. Agents Chemother.* **2011**, *55* (3), 947–953.

(60) del Mar Tomás, M.; Beceiro, A.; Pérez, A.; Velasco, D.; Moure, R.; Villanueva, R.; Martínez-Beltrán, J.; Bou, G. Cloning and functional analysis of the gene encoding the 33- to 36-kilodalton outer membrane protein associated with carbapenem resistance in *Acinetobacter baumannii*. *Antimicrob. Agents Chemother.* **2005**, *49* (12), 5172–5175.

(61) Seneviratne, C. J.; Wang, Y.; Jin, L.; Abiko, Y.; Samaranayake, L. P. *Candida albicans* biofilm formation is associated with increased anti-oxidative capacities. *Proteomics* **2008**, *8* (14), 2936–2947.

(62) Kulesus, R. R.; Diaz-Perez, K.; Slechta, E. S.; Eto, D. S.; Mulvey, M. A. Impact of the RNA chaperone Hfq on the fitness and virulence potential of uropathogenic *Escherichia coli*. *Infect. Immun.* **2008**, *76* (6), 3019–3026.

(63) Barreto, M.; Jedlicki, E.; Holmes, D. S. Identification of a gene cluster for the formation of extracellular polysaccharide precursors in the chemolithoautotroph *Acidithiobacillus ferrooxidans*. *Appl. Environ. Microbiol.* **2005**, *71* (6), 2902–2909.

(64) Nesper, J.; Lauriano, C. M.; Klose, K. E.; Kapfhammer, D.; Kraiss, A.; Reidl, J. Characterization of *Vibrio cholerae* O1 EI tor *galU* and *galE* mutants: influence on lipopolysaccharide structure, colonization, and biofilm formation. *Infect. Immun.* **2001**, *69* (1), 435–445.

(65) Mussi, M. A.; Relling, V. M.; Limansky, A. S.; Viale, A. M. CarO, an *Acinetobacter baumannii* outer membrane protein involved in carbapenem resistance, is essential for L-ornithine uptake. *FEBS Lett.* **2007**, *581* (29), 5573–5578.

(66) Amador, C. I.; Canosa, I.; Govantes, F.; Santero, E. Lack of CbrB in *Pseudomonas putida* affects not only amino acids metabolism but

also different stress responses and biofilm development. *Environ. Microbiol.* **2010**, *12* (6), 1748–1761.

(67) Kapatral, V.; Campbell, J. W.; Minnich, S. A.; Thomson, N. R; Matsumura, P.; Prüss, B. M. Gene arrays analysis of *Yersinia enterocolitica* FlhD and FlhC: regulation of enzymes affecting synthesis and degradation of carbamoylphosphate. *Microbiology* **2004**, *150* (Pt7), 2289–2300.

(68) Flemming, H. C.; Wingender, J. The biofilm matrix. *Nat. Rev. Microbiol.* **2010**, *8* (9), 623–633.